GEOLOGY AND GENESIS OF URANIUM MINERALIZATION IN SUBAERIAL FELSIC VOLCANIC ROCKS OF THE BYERS BROOK FORMATION AND THE COMAGATIC HART LAKE GRANITE, WENTWORTH AREA, COBEQUID HIGHLANDS, NOVA SCOTIA

DAVID PATRICK GOWER

NOTICE

The quality of this microform is heavily dependent upon the quality of the original thesis submitted for microfilming. Every effort has been made to ensure the highest quality of reproduction possible.

If pages are missing, contact the university which granted the degree.

Some pages may have indistinct print especially if the original pages were typed with a poor typewriter ribbon or if the university sent us an inferior photocopy.

Reproduction in full or in part of this microform is governed by the Canadian Copyright Act, R.S.C. 1970, c. C-30, and subsequent amendments.

AVIS

La qualité de cette microforme dépend grandement de la qualité de la thèse soumise au microfilmage. Nous avons tout fait pour assurer une qualité supérieure de reproduction.

S'il manque des pages, veuillez communiquer avec l'université qui a conféré le grade.

La qualité d'impression de certaines pages peut laisser à désirer, surtout si les pages originales ont été dactylographiées à l'aide d'un ruban usé ou si l'université nous a fait parvenir une photocopie de qualité inférieure.

La reproduction, même partielle, de cette microforme est soumise à la Loi canadienne sur le droit d'auteur, SRC 1970, c. C-30, et ses amendements subséquents

Geology and Genesis of Uranium Mineralization in Subaerial Felsic Volcanic Rocks of the Byers Brook Formation and the Comagatic Hart Lake Granite, Wentworth Area, Cobequid Highlands, Nova Scotia.

by

David Patrick Gower, B.Sc.

A Thesis Submitted in
Partial Fulfillment of the
Requirements for the Degree of
Master of Science

Department of Earth Sciences
Memorial University of Newfoundland

August, 1988

ISBN 0-315-50461-7

ABSTRACT

The Byers Brook Formation and the Hart Lake Granite are situated in the Cobequid Highlands of northern Nova Scotia. The anorogenic granite and bimodal volcanic rocks are comagmatic and are suggested to be products of extensional tectonism. The granite has an Rb/Sr whole-rock age of 339 ± 4 Ma and the rhyolites 343 ± 5 Ma.

The Byers Brook Formation is a generally east-west (110-120 az.) striking, steeply dipping (70° N) sequence of rhyolitic pyroclastic, flow and volcaniclastic rocks intercalated with a relatively minor volume of basalt flows. All units are cut by an abundance of diabase and composite dikes with the highest density of dikes associated with rhyolite dome/flow complexes. Rhyolite dikes are restricted to these complexes.

Two periods of bimodal volcanism were separated by a brief hiatus represented by a 50-100 m thick conglomerate unit which grades eastward into laminated to thickly bedded lacustrine? siltstones. Both stages of volcanism are characterized by early pyroclastic eruptions which grade upwards into rhyolite and basalt flows. The base of the early sequence is intruded by the Hart Lake Granite. The

later sequence is approximately 2200 m thick and grades into the dominantly basaltic Diamond Brook Formation.

Geochemically, the granite and rhyolites are subalkaline, metaluminous, except for a discrete suite of peralkaline rhyolite and composite dikes. All rocks are generally enriched in Fluorine. Strong alkali metasomatism is pervasive throughout the extrusive rocks, however, late subvolcanic rhyolite and composite dikes are unaltered.

The largest and highest grade concentrations of uranium occur in breccia zones in and adjacent to rhyolite dome/flow complexes. It is hypothesized that these complexes were areas of high thermal gradient caused by the injection of late composite and rhyolite dikes, and thus the locus for the very large hydrothermal system which caused the pervasive alkali metasomatism. This large hydrothermal system leached uranium liberated during devitrification of the volcanic pile and concentrated it into permeable structures, such as lithophysae-rich zones, faults and breccia zones.

Other associated mineralization includes; cassiterite in amygdules of basalt flows, massive pyrite beds with up to 276 grams per ton silver in the lacustrine siltstones, and fluorite-zircon-sphene-calcite-allanite veins with highly anamalous rare earth element

concentrations hosted by the granophyric margin of the Hart Lake Granite.

Although the Byers Brook Formation in the Wentworth area has been subject to extensive exploration in the past, the data presented here suggest that perhaps the most prospective parts of the Formation are the dome/flow complexes, and these have not been adequately tested. In light of this the Byers Brook Formation and the Fountain Lake Group in general should be considered good prospects to host lithophile element mineralization.

ACKNOWLEDGEMENTS

Guidance provided by Dr. Dave Strong in all aspects of this thesis is gratefully acknowledged.

Gulf Minerals Canada Limited generously provided me with geochemical data, thin sections and base maps for which I am very grateful. Whole-hearted thanks are extended to the exploration crews of Gulf Minerals, and especially Neil Downey for introducing me to mineral exploration. H.C. Teng and Dr. A.K. Chatterjee provided stimulating discussions early in the course of this project. Thanks are extended to Colin McKenzie of BP-Selco for allowing me to use a company vehicle for running to the field area. Special thanks are extended to Dave Press for modifying his geochem programs to handle a very large, awkward data base. Pat O'Neil and Jim Maloney are thanked for numerous discussions and for critically reading early versions of the manuscript. I am indebted to Jim Langille at the N.S.D.M.E. core storage facility in Stellarton N.S. for many hours spent moving core boxes around and running the fork-lift, during the cold of winter.

Financial support for this thesis was provided by a Memorial University scholarship and grant A7975 to Dr. Dave Strong.

TABLE OF CONTENTS

	page
ABSTRACT	ii
ACKNOWLEDGEMENTS	v
TABLE OF CONTENTS	vi
LIST OF FIGURES	viii
LIST OF PLATES	x
LIST OF TABLES	xii
LIST OF APPENDICES	xii
CHAPTER 1 - INTRODUCTION	1
1.1 General	1
1.2 Purpose of the Study	1
1.3 Physiography	3
1.4 Previous Work and Exploration History	4
1.5 Regional Geology	9
1.5.1 Tectono-stratigraphic Position	9
1.5.2 Stratigraphy of the Cobequid Highlands	12
1.5.3 Magmatic History of the Cobequid Highlands	21
1.5.4 Structural Geology of the Cobequid Highlands	23
1.6 Devono-Carboniferous Geochronology	27
CHAPTER 2 - GEOLOGICAL SETTING OF THE WENTWORTH PROSPECT	30
2.1 Summary	30
2.2 General Geology of the Wentworth Map Area	32
2.2.1 Lower Byers Brook Formation	37
2.2.2 Upper Byers Brook Formation	41
2.2.3 Structure of the Byers Brook Formation	44
2.3 Geology of the J-zone	45
2.4 Geology of the DF-zone	48
2.5 Geology of the DL-zone	53
2.6 Petrographic Descriptions of the Map Units	57
2.6.1 Crystal Lithic Tuffs	57
2.6.2 Basalt Flows	59
2.6.3 Rhyolite Flows and Dome	63
2.6.4 Rhyolite Tuffs	70
2.6.5 Conglomerate	73

page

2.6.6 Laminated Siltstones---------- 74
2.6.7 Welded Ash Flow Tuffs, Ignimbrites--------- 79
2.6.8 Hart Lake Granite---------- 84
2.6.9 Diabase Dikes---------- 87
2.6.10 Rhyolite and Composite Dikes---------- 88

CHAPTER 3 - GEOCHEMISTRY AND ALTERATION---------- 97

3.1 Introduction---------- 97
3.2 Summary---------- 97
3.3 Alteration---------- 99
3.4 Geochemistry---------- 114
3.5 Geochemical Classification of the Byers Brook Formation---------- 138
3.5.1 Agpaiitic Index---------- 138
3.5.2 Alkaline vs Subalkaline---------- 140

CHAPTER 4 - MINERALIZATION---------- 149

4.1 Introduction---------- 149
4.2 DF-zone Mineralization---------- 150
4.2.1 East DF-zone Showing---------- 151
4.2.2 West DF-zone Showing---------- 159
4.3 J-zone Mineralization---------- 164
4.4 DL-zone REE Occurrence---------- 166
4.5 Geochemistry of Uranium Occurrences---------- 173
4.5 Discussion---------- 175
4.5.1 Alteration and Mineralization---------- 175
4.5.2 Mineral Stability and Uranium Solubility--- 179
4.5.3 Uranium Depositional Model---------- 205

CHAPTER 5 - SUMMARY AND CONCLUSIONS---------- 212

5.1 Summary---------- 212
5.2 Considerations for Exploration---------- 217

REFERENCES---------- 220

APPENDIX 1 - Diamond Drill Hole Data---------- 233

APPENDIX 2 - Analytical Methods, Whole Rock and Trace Element Analyses---------- 239

APPENDIX 3 - Geochemical Sample Locations---------- 241

APPENDIX 4 - Geochemical Analyses---------- 254

LIST OF FIGURES

		page
Figure 1.	Map of Nova Scotia, Location Map.	2
Figure 2.	Geology map of the Cobequid Highlands.	13
Figure 3.	Avalon Zone stratigraphic column.	20
Figure 4.	Geology map of the Wentworth area.	appended
Figure 4a.	Stratigraphic column of the Fountain Lake Group, Wentworth area.	35
Figure 5.	Schematic plan, J-zone.	46
Figure 6.	Diamond drill section, J-zone.	appended
Figure 7.	Schematic plan, DF-zone.	50
Figure 8.	Diamond drill section, DF-zone.	appended
Figure 9.	Schematic plan, DL-zone.	54
Figure 10.	Diamond drill section, DL-zone.	appended
Figure 11.	Igneous spectrum diagram.	100
Figure 12.	K_2O versus Na_2O plot.	110
Figure 13.	Harker diagrams for volcanic rocks and diabase, Byers Brook Formation.	115
Figure 14.	Harker variation diagrams for Hart Lake Granite and high-Zr dikes.	128
Figure 15.	Agpaiitic index diagrams.	139
Figure 16.	SiO_2 versus $Na_2O + K_2O$ plot.	141
Figure 17.	SiO_2 versus Zr/TiO_2 plot.	144
Figure 18.	East DF-zone uranium occurrence.	152
Figure 19.	West DF-zone uranium occurrence.	160
Figure 20.	Rare earth element plot, DL-16 zone.	167

page

Figure 21.	Stability relations among minerals as a function of cation activities.	182
Figure 22.	Temperature versus K activities aqueous chloride solutions in equilibrium with hypersolidus granodiorite magma.	185
Figure 23.	Calculated stability fields of minerals as a function of temperature and cation activity ratios.	187
Figure 24.	Distribution of uranyl complexes versus pH for typical ligand concentrations in ground water, Wind River Formation.	193
Figure 25.	Distribution of uranyl complexes at 100° C.	195
Figure 26.	Distribution of uranyl complexes at 200° C.	196
Figure 27.	Distribution of uranyl complexes at 300° C.	198
Figure 28.	Log fO2-pH diagram showing distribution of uranyl and uranous complexes and solubility of U-oxides at 200° C.	202
Figure 29.	Log fO2-pH diagram showing distribution of uranyl complexes, solubility of U-oxides, distribution of iron phases and relative stabilities of magnesium and potassium silicates at 200° C.	204
Figure 30.	Proposed genetic model for uranium mineralization.	208

List of Plates

		page
Plate 1:	Lapilli Tuff sample from drill core.	58
Plate 2:	Amygdaloidal basalt flow.	61
Plate 3:	Photomicrograph of amygdaloidal basalt.	61
Plate 4:	Lithophysae-rich zone in rhyolite flow.	67
Plate 5:	Spherulitic rhyolite flow.	67
Plate 6:	Autobrecciated flow banded rhyolite.	69
Plate 7:	Rhyolite crystal-lapilli tuff.	71
Plate 8:	Drill core sample of laminated siltstone.	78
Plate 9:	Photomicrograph of lacustrine siltstrone.	78
Plate 10:	Eutaxitic fabric in rhyolite ash flow.	83
Plate 11:	Devitrified glass shard.	83
Plate 12:	Drill core specimens showing different phases of the Hart Lake Granite.	85
Plate 13:	Drill core specimens of Zr-rich rhyolite dikes.	91
Plate 14:	Photomicrograph of peralkaline rhyolite dike.	93
Plate 15:	Felsic globules in diabase are characteristic along the margins of high-Z and subalkaline composite dikes.	93
Plate 16:	Photomicrographs showing various stages of alkali metasomatism in the Byers Brook Formation rhyolites.	104
Plate 17:	Porphyrytic rhyolite flow showing fracture controlled K-metasomatism.	108
Plate 18:	Pitchblende in drill core sample, DDH # DF-32.	154

page

Plate 19: Photomicrograph of east DF-zone uranium occurrence showing vein with epidote and garnet. 155

Plate 20: Photomicrograph of pitchblende, east DF-zone occurrence. 158

Plate 21: Autoradiograph showing pitchblende occupying fractures, east DF-zone occurrence. 158

Plate 22: Photomicrograph of uranium mineralized cataclasite, west DF-zone occurrence. 163

Plate 23: West Df-zone mineralized cataclasite. 163

Plate 24: Photomicrographs showing complex mineralogy associated with the zone of rare earth element concentration, DDH # DL-16. 169

List of Tables

		page
Table 1:	Comparative stratigraphic table.	6
Table 2:	Correlation of structural events of the Cobequid Highlands.	24
Table 3:	Summary of isotopic age data for the Fountain Lake Group and associated granites.	29
Table 4:	Analyses of samples characterizing various stages of alkali metasomatism.	106
Table 5:	Rare earth element analyses for samples of granaphyric granite, DDH # DL-16.	172
Table 6:	Average analyses of mineralized and adjacent unmineralized rhyolites.	174
Table 7:	Comparative classifications of porphyry copper assemblages.	180
Table 8:	List of uranyl and uranous complexes known to form with various anions.	191

List of Appendices

Appendix 1:	Diamond drilling data.	233
Appendix 2:	Analytical methods and sampling techniques.	239
Appendix 3:	Rock sample locations.	241
Appendix 4:	Geochemical analyses.	254

Chapter 1

1. Introduction:

1.1 General

The Wentworth uranium prospect is located between latitudes 45° 32'10" and 45° 37'30" and between longitudes 63° 34' and 63° 22'30", on the northeast flank of the Cobequid Highlands, northern Nova Scotia (Figure 1).

Geologic mapping and core logging were carried out by the writer in 1978-1981 while employed by Gulf Minerals Canada Ltd. and later during 1981-1983 while employed by Selco Inc. Gulf Minerals supplied thin sections and geochemical data which were used in this study.

1.2 Purpose of the Study

The purpose of this study is to investigate the mineralization, alteration and geochemistry of uranium occurrences in volcanic rocks of the Fountain Lake Group in an attempt to understand the processes responsible for their formation.

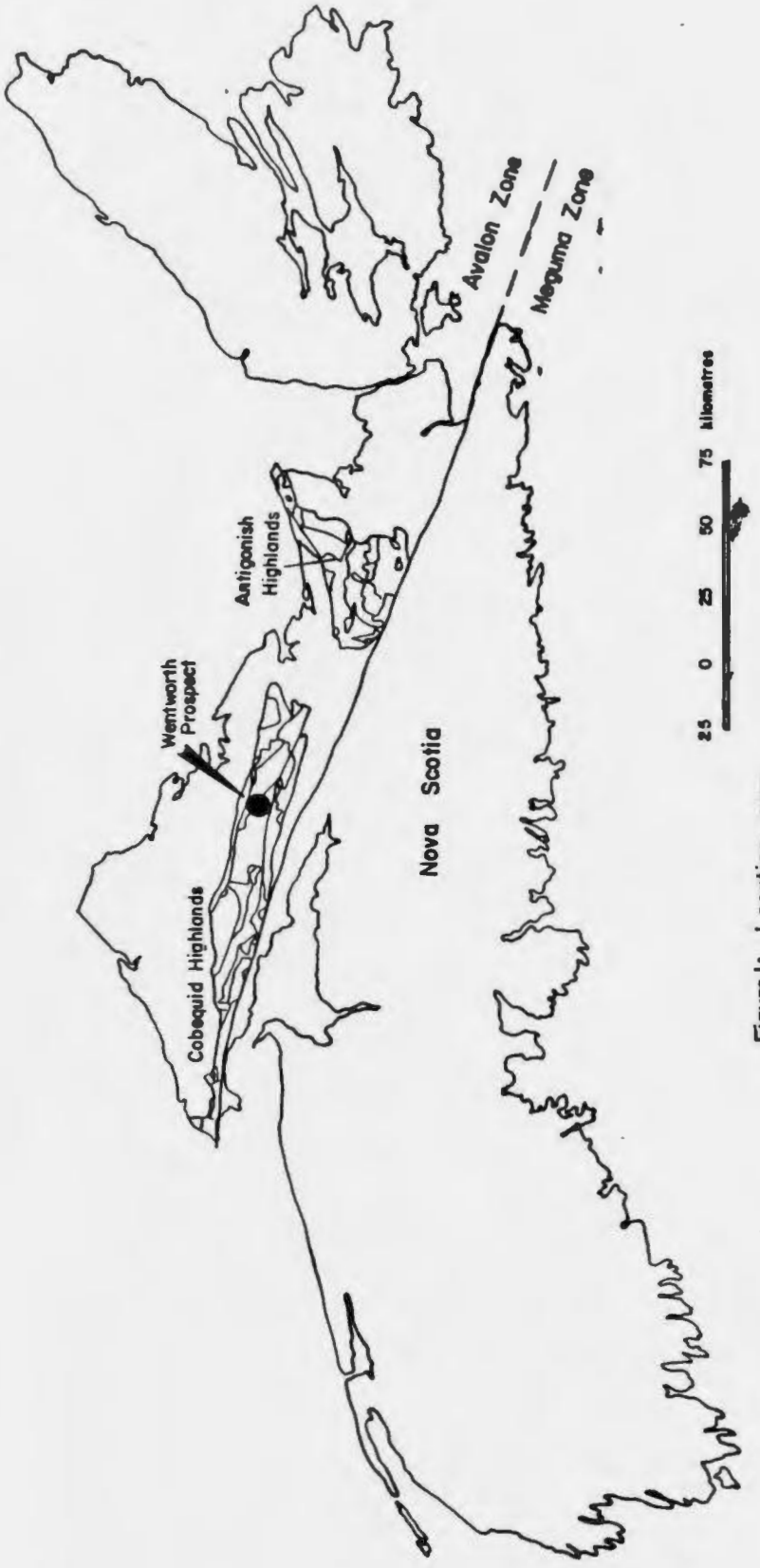

Figure 1: Location map.

This study has resulted in a major revision of the interpretation of the geological setting and controls of mineralization in the Fountain Lake Group volcanic rocks in the Wentworth area. The information gained from this research should be a useful aid to exploration for uranium and associated metals, both locally in the Cobequid Highlands and regionally in similar geological settings in the Appalachian orogen and elsewhere.

1.3 Physiography

The map area is situated on the top and flank of a highland plateau. The plateau reaches a maximum of elevation of approximately 350 meters and overlooks the Cumberland basin where the elevation is approximately 100 meters above sea level.

The plateau is dissected by numerous structurally controlled deep stream valleys. The area is is covered by mature softwood, hardwood and mixed forests with alder swamps and bogs occupying local depressions.

Bedrock is blanketed by a 0.5-3 meter Pleistocene cover, resulting in generally less than 10% bedrock exposure except in stream valleys and locally on ridges. Several esker-like features oriented approximately

north-south occur on the property. The glacial history of the area is complex, with up to three distinct ice movement directions recorded in till horizons. The latest ice movement was northerly, indicated by the provenance of Hart Lake Granite bouldersin the till up to 300 meters north of where the bedrock contact between the Hart Lake Granite and the Byers Brook Formation occurs (R. Snow, pers comm., 1981).

1.4 Previous Work and Exploration History

In 1836 Abraham Gesner published a map and geological report of Nova Scotia also based on lithological distinctions. He classified the Cobequid and Antigonish Highlands simply as slate and red sandstone.

In 1860 Dawson correlated the Cobequid mountains with the Gold Bearing Series (Meguma Group) which he considered to be of Silurian age. In 1868 he referred most of the rocks of the Cobequid Mountains to the Arisaig Series, based on fossils found at Earltown and New Annan. Dawson correlated the Arisaig Series with rocks in New Brunswick, Maine, Anticosti and New York State, and concluded that the Silurian of Arisaig and Anticosti did not compare directly with England or America and that the fossil assemblages were intermediate between Europe and

America. Dawson (1878) presented the most complete account of the geology of the Cobequid Highlands prior to the work of Kelly (1962-1968) and Donohoe and Wallace (1975-1980). He began his account with the observation that, "the great igneous outbursts, evidenced by masses and dykes of granite which cut the Lower Devonian rocks, make a strong line of distinction between later and older Palaeozoic." Based on intrusive relationships and studies of palaeontology, all of the Cobequid Highlands were assigned to the Silurian. Table 1 is an excerpt from Dawson's (1878) stratigraphic table and summarizes the geology of the Cobequid Highlands as understood at that time.

Much of the early palaeontological correlation, especially between the Cobequid Highlands, the Antigonish Highlands and England is attributable to Honeyman (1874). Gneissic rocks in the Cobequid Highlands were also first described by Honeyman (1874), and he noted they were at least pre-Silurian. Later he assigned the gneissic rocks of the Cobequid Highlands to the Archean (Honeyman, 1881).

Dawson (1888) reassigned the volcanic rocks of the Cobequid Highlands to the Ordovician, based on stratigraphic correlation with central and western New Brunswick. The fossiliferous beds at Wentworth were the only rocks considered to be of Silurian age in the Highlands after this reassessment.

TABLE 1: Comparative Stratigraphic Table (from Dawson 1878)

England (etc.)	Nova Scotia New Brunswick
Upper Silurian	
Ludlow, Wenlock, Llandovery Mascarene or Mayhill	Upper Arisaig Series, Series,, Lower Arisaig, Wentworth, New Canaan and Restigouche Series
Lower Silurian	
Caradoc and Bala with Snowdon Felsites and Ash Beds, Coniston and Knock Series	Upper Cobequid Series, slates, felsites, quartzites and greenstones
Great Felsite and Trap Ash Series of Barrowdale (Ward)	Lower Cobequid Series, Porphyrites, Agglomerates and Massive Syenite of Cobequids, Pictou and Cape Breton

Ami (1900) noted the uncertainty of assigning the volcanic rocks of the Cobequid Highlands to the Ordovician without supporting palaeontological evidence.

Williams (1914) stated that the Cobequid Series was clearly Ordovician but he did not cite evidence.

Stevenson (1958) includes good petrographic descriptions, providing an important link between the older and contemporary literature.

Kelly (1965, 1966, 1967) mapped the entire Cobequid Highlands, but his map was not published until it was included in a publication by Donohoe (1976).

In 1975 Donohoe began work to prepare Kelly's unpublished map for publication. Most of the pre-Carboniferous formation names currently in use are attributable to Kelly, however Donohoe (1975, 1976) and Donohoe and Wallace (1977, 1978, 1979, 1980) are responsible for the final definition of the map units and the introduction of some new units, including the Fountain Lake Group and its subdivisions the Byers Brook and Diamond Brook Formations.

The exploration program which provided much of the data for this study ran concurrently with Donohoe and Wallace's investigations and benefitted from numerous discussions with them.

The discovery of radioactive rhyolite boulders in 1976 initiated the interest of Gulf Minerals Canada Limited (G.M.C.L) in the volcanic assemblages underlying much of the core of the Cobequid Highlands. G.M.C.L. staked a large claim block, approximately 50 km. by 15 km., stretching from Earltown to Westchester Station (Figure 2). The most intensive exploration efforts were expended on Block III and this study concentrates on that block. Limited prospecting and diamond drilling were carried out before the end of 1976.

Follow-up exploration in 1977 consisted of regional helicopter-borne radiometric, magnetic and electromagnetic surveys over almost the entire Cobequid Highlands. Diamond drilling, prospecting, mapping and soil and lithogeochemical surveys were initiated.

Geological mapping, prospecting, soil geochemistry and diamond drilling were continued and a reverse circulation deep overburden sampling program was started in 1978. All surveys were continued in 1979 except diamond drilling. During the 1979 field season a major lithogeochemical survey was carried out for the purpose of defining alteration zones and ultimately drill targets. The reverse circulation drilling was completed in 1980 and the mapping and lithogeochemical surveys were continued. A

study of the Pleistocene geology was undertaken as an attempt to measure glacial displacement of radioactive boulders from their sources. The diamond drilling program was renewed.

During 1981 areas of specific interest were mapped in detail and diamond drilling was completed. A lithogeochemical survey of the diamond drill core was undertaken.

Due to a change in policy by the Nova Scotia Government regarding exploration for uranium, no exploration has been done on the G.M.C.L. claims since 1981.

1.5 Regional Geology

1.5.1 Tectono-stratigraphic Position

The Cobequid Highlands form an east-west trending upland, approximately 175 km. long, across northern Nova Scotia, within the Appalachian Orogen.

The Appalachian Orogen in Canada has been divided into five main tectonostratigraphic zones, each with independant pre-Silurian histories (Williams, 1969; Williams et al., 1972, 1974; Williams 1978, 1979; Williams

and Hatcher, 1983). The Cobequid Highlands are situated within the Avalon Zone (Williams, 1969) and are abruptly terminated against the Meguma Zone to the south along the Cobequid Fault System.

The Avalon Zone is the largest tectonostratigraphic terrane in the Appalachian Orogen, approximately twice as wide as all the rest of the orogen in Canada. It extends from eastern Newfoundland, through northern Nova Scotia and southern New Brunswick, continuing along the eastern seaboard of the U.S. as far south as Georgia (Williams, 1976, 1978; O'Brien et al., 1983; Williams et al., 1983). Correlatives of the Avalon Zone are thought to be present in the Caledonides of Britain, the Hercynian-Alpine Belts of Europe and the Pan-African Belts of northern Africa (Schenk, 1971; Hughes, 1972; Rast et al., 1976; Strong et al.,1978;, Strong, 1980; O'Brien et al., 1983; Williams et al., 1983).

All Avalon Zone boundaries are tectonic. In Newfoundland the Avalon Zone is juxtaposed against the Gander Zone of Williams (1978) along the Dover and Hermitage Faults (Blackwood and Kennedy, 1975; Blackwood and O'Driscoll, 1976; Blenkinsop et al., 1976; Dallmeyer et al., 1981; Elias and Strong, 1982). In Nova Scotia the northeast boundary of the Avalon Zone has been drawn at the

Aspy Fault in Cape Breton (Rast et al, 1976; Williams, 1978). Keppie (1979) interprets all of Cape Breton as being within his Avalon Composite Terrane. In southern New Brunswick, the northern boundary of the Avalon Zone is the Wheaton Brook Fault (McCutcheon, 1981). This boundary was formerly considered to be the Belleisle-Lubec Fault Zone (Kennedy, 1976; Williams, 1978).

The eastern boundary of the Avalon Terrane is seen only in northern Nova Scotia where it is truncated against the Meguma Terrane along the Cobequid Fault. The Cobequid Fault is part of the Glooscap Fault System of King et al., (1975). The Glooscap Fault System apparently extends eastward offshore across the edge of the Grand Banks, marked by a linear zone of magnetic and Bouger gravity anomalies (Haworth and MacIntyre, 1976). Geophysically the Avalon Zone has been projected under the Atlantic Continental Shelf, except off Nova Scotia where the Meguma Zone is postulated to underlie much of the continental shelf (Haworth and Le Fort, 1979).

1.5.2 Stratigraphy of the Cobequid Highlands

Donohoe (1976, 1977, 1983) and Donohoe and Wallace (1978, 1979, 1980) have defined the stratigraphy of the Cobequid Highlands (Figure 2). The rocks range in age from Middle(?) Proterozoic to Early Carboniferous.

The basement rocks of the Cobequid Highlands are represented by the Bass River and Mount Thom Complexes and are older than Late Hadrynian (Donohoe and Wallace, 1980; Donohoe, 1983). Donohoe and Cullen (1983) and Cullen (1984) have shown that the Bass River Complex comprises two lithotectonic units, an older gneissic basement and a younger metasedimentary and metavolcanic cover. The older Bass River Complex rocks (Great Village River Gneiss) and the Mount Thom Complex are thought to represent continental crust which was deformed at approximately 950 Ma (Donohoe, 1983). The Bass River Complex cover sequence (Folly River Schist, Gamble Brook Schist) not yet identified in the Mount Thom Complex, was deposited and deformed later in the Precambrian (Gaudette et al., 1983; Donohoe, 1983; Cullen,1984). The Great Village River Gneisses occur as biotite-muscovite granitoid gneisses in the eastern part of the complex and fine to coarse amphibolites west of Bass River (Donohoe, 1983). The Mount Thom Complex consists of

LEGEND

		STRATIFIED ROCKS		PLUTONIC ROCKS
PALEOZOIC	Carboniferous	25 26 — CANSO GROUP: (26) Londonderry Fm: green, grey quartz wacke, siltstone, shale; (25) West Bay Fm: grey, red, green siltstone, wacke, shale		
		24 — WINDSOR GROUP: grey limestone, red, grey siltstone, shale		
		22 — HORTON GROUP: grey, red siltstone, quartz wacke, shale	23	granite (syenogranite to alkali feldspar granite; granodiorite to monzogranite)
	Devono - Carboniferous	20 21 — Rapid Brook, Greville River Fms. (21): grey, tan siltstone, wacke, granite-clast conglomerate; (20) Nuttby Fm.: grey, red lithic wacke, siltstone, shale, conglomerate		
		17 — Falls Fm.: red-brown polymictic conglomerate, lithic wacke		
		UG 15 14 — FOUNTAIN LAKE GROUP (16): (15) Diamond Brook Fm.: basalt flows; red, grey siltstones; Byers Brook Fm.: rhyolitic, dacitic lava flows, ignimbrites, tuffs; siltstones, conglomerate; basalt flows	19	granite (monzogranite to alkali feldspar granite)
			18	diorite
	Devonian	13 — Murphy Brook Fm.: black, grey siltstone, wacke, polymictic conglomerate		
		12 — Portapique River Fm.: red, green siltstone, quartz and lithic wacke		
	Silurian	10 11 — Wilson Brook Fm. (11): grey siltstone, quartz wacke, shale, red siltstone, granite clast conglomerate; (10) Earltown Fm.: grey siltstone, wacke, calcareous siltstone; tan, green rhyolite flows, ignimbrite, tuffs; (11A) unamed black, grey siltstone, lapilli tuff; (11B) unnamed grey, tan, red siltstone, quartz arenite, wacke, granite clast polymictic conglomerate; may be younger		
	Cambro-Ordovician		9	McCallum Settlement Granite (syenogranite)
PROTEROZIC	age unknown		7 8	(8) granite (alkali feldspar granite; syenogranite) (?) diorite
	Hadrynian		6	Jeffers Brook Diorite
		4 5 — Warwick Mountain (5) and Jeffers Fm. (4): green, grey, mafic meta-volcanic rocks, meta-tuff, meta-wacke, marble		
	Pre-Hadrynian	2 — BASS RIVER COMPLEX: biotite schist, quartzite, chlorite schist, gneiss	3	granite gneiss
		1 — MT. THOM COMPLEX: biotite-garnet gneiss; granite gneiss; amphibolite		

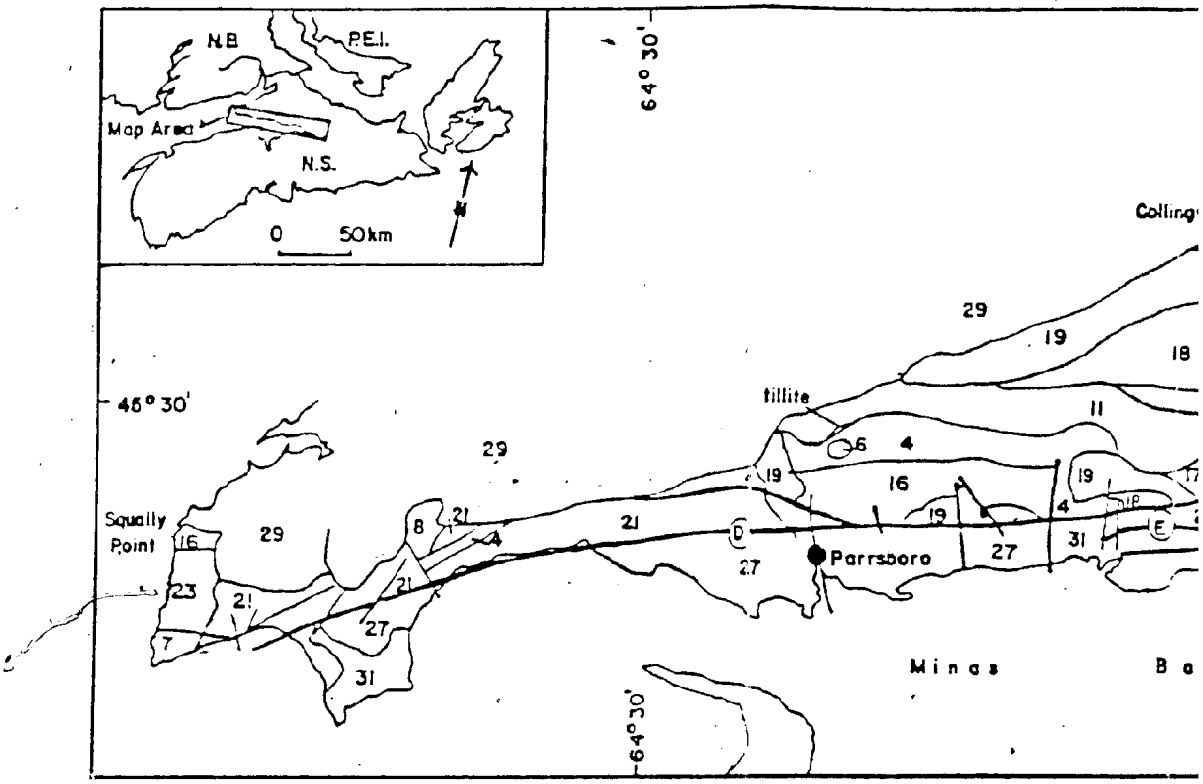

Figure 2: Geology map of the Cobequid Highlands (modified after Don

- Major Fault
- (A) East Wallace R. - Debert L. Lineament
- (B) Rockland Brook Fault
- (C) Londonderry Fault
- (D) Cobequid Fault
- (E) Portapique Fault
- (F) North River Fault
- (G) Economy Mountain Fault
- (H) Riversdale Fault

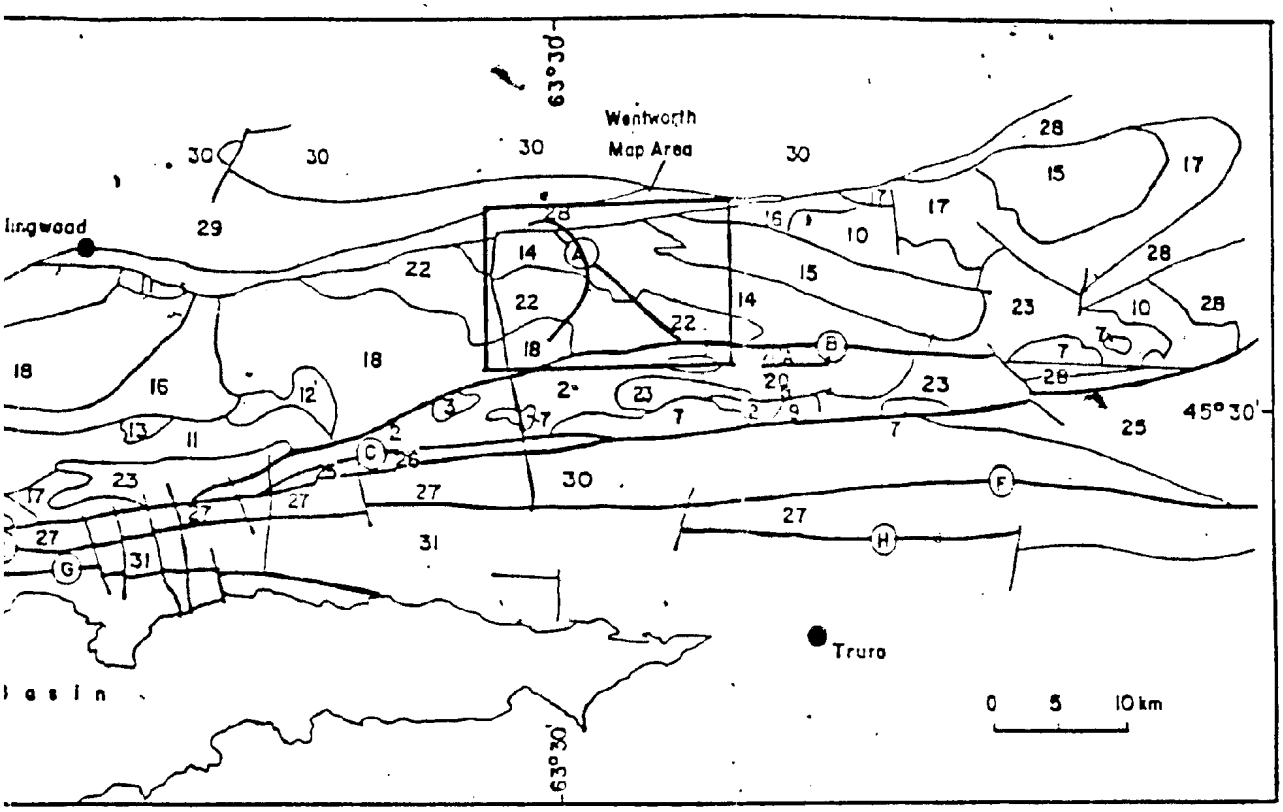

Donahoe and Wallace, 1981).

biotite-garnet-microcline gneiss, amphibolite and granitic gneiss. The Gamble Brook Schist comprises light greyquartzites interlayered with lesser amounts of biotite ± muscovite ± quartz schists. The Folly River Schists are more variable, represented by green mafic schists and mafic metavolcanic rocks. Red and maroon siliceous, hematitic iron formations are interlayered with the metavolcanic rocks. Some of the iron formations contain carbonate horizons. Quartzites are locally interlayered with the metavolcanic rocks, possibly resulting from structural mixing of the Folly River and Gamble Brook Schists (Donohoe, 1983).

Unconformably overlying the basement sequences are the Late Hadrynian Warwick Mountain and Jeffers Formations. These formations outcrop north of the Rockland Brook Fault (Figure 2). The strata comprise meta quartz wackes, volcanic wackes, meta siltstones, mafic metavolcanic rocks and minor marble, metamorphosed to greenschist facies (Donohoe and Wallace, 1979). The Jeffers Formation has been intruded by the Jeffers Pluton of probable Lower Cambrian age (Keppie et al., 1978; Wanless et al., 1973; Cormier, 1979). At the northern contact of the Jeffers Formation near Parrsboro (Figure 2), an exposure of tillite comprising unsorted clastic material ranging from fine sand to boulders up to 1 meter in

diameter was mapped by the author while employed by G.M.C.L. in 1979. This tillite has not been described in any publications that the author is aware of but its position at the top of the Jeffers Formation suggest that it is a correlative of the tillite marker horizon described by King (1982).

The oldest Palaeozoic rocks in the Cobequid Highlands are dark grey to black fossiliferous siltstones of Middle to Late Ordovician age as dated by brachiopods (R. Newman in Donohoe and Wallace, 1978). This unnamed unit outcrops south of the Rockland Brook Fault (Figure 2).

North of the Rockland Brook Fault the oldest strata are the Silurian Wilson Brook and Earltown Formations. The Wilson Brook Formation is dominantly quartz wacke and shale with minor felsic and mafic volcanic rocks near the base and top. The Earltown Formation is dominated by felsic pyroclastics and flows with rare beds of fossiliferous siltstone. Both of these formations have been penetratively deformed, and have resultant cleavage and folds (Donohoe and Wallace, 1980).

The Devonian Portapique River Formation conformably overlies the Wilson Brook Formation at Portapique River. Elsewhere the Murphy Brook Formation unconformably overlies the Wilson Brook Formation, and the

Portapique River Formation has been eroded off (Donohoe and Wallace, 1979). Both the Portapique River Formation and the Murphy Brook Formation have been penetratively deformed (Donohoe and Wallace, 1980).

The Devono-Carboniferous Fountain Lake Group (formerly Earltown Sequence) is a thick sequence of volcanic rocks which unconformably overlies the Silurian to Middle Devonian strata. In the eastern part of the Highlands the Fountain Lake Group has been divided into the older Byers Brook Formation and the younger Diamond Brook Formation. The Byers Brook Formation is a bimodal volcanic pile dominated by felsic pyroclastic rocks and lava flows. It grades into the Diamond Brook Formation, the base of which is dominantly basalt flows which grade upwards into redbeds.

The Fountain Lake Group is not penetratively deformed. In light of this several revisions of its outcrop area as mapped by Donohoe and Wallace (1980) are suggested. While employed by Selco Inc. during 1983 and 1984 the author aided M. Cullen mapping in the Cobequid Highlands, recognizing problems with the definition of the Fountain Lake Group in both the Simpson Lake and Parrsboro areas. On the Jeffers Brook tributary draining Cranberry Lake, dacitic to rhyolitic volcanic rocks have a tectonic

fabric distinct from any seen in the Fountain Lake Group. A northeast-striking low to moderately dipping cleavage marks at least some exposures in the area. Possibly part of the area between Jeffers Formation south boundary (Donohoe and Wallace, 1982) and the east-west break in topography north of MacAleese Lake is underlain by Silurian or older volcanic and sedimentary rocks (Cullen, 1983).

In the Simpson Lake area andesitic flows, dikes and pyroclastic rocks which outcrop between the Economy Lake forestry road and Sugarloaf Mountain are variably cleaved, distinguishing them from their correlatives to the south. This suggests that erosional levels in the northern part of the Highlands, at least in this area, are deep enough to have removed Fountain Lake Group lithologies and expose older cleaved volcanic sequences. It is suggested that these volcanic terranes are equivalent to Silurian volcanic rocks exposed elsewhere in the Highlands (Cullen, 1983).

The Fountain Lake Group is unconformably overlain by molasse, red brown polymictic conglomerates designated the Falls Formation (Donohoe and Wallace, 1980)

The Nuttby Formation, located south of the Rockland Brook Fault (Figure 2) was deposited in the Early Carboniferous as indicated by spores (S. Barss in Donohoe

and Wallace, 1980). The Rapid Brook and Greville River Formations of the western Highlands (Figure 2) are thought to be coeval with the Nuttby Formation, but the plant fossils observed in these formations are of indeterminate age (Donohoe and Wallace, 1980). All three formations consist of red and grey siltstones, wackes and polymictic conglomerates.

The Londonderry Formation which underlies part of the area between the Londonderry and Cobequid Faults (Figure 2) comprises the youngest strata in the Highlands. The grey and green quartz and feldspathic wackes have been dated by means of spores as Visean to Early Namurian (S. Barss in Donohoe and Wallace, 1980).

The stratigraphy of the Cobequid Highlands fits well into King's (1982) generalized stratigraphic column of the Avalon Zone (Figure 3).

The Cobequid Highlands are juxtaposed against Pennsylvanian and Triassic graben-filling redbeds to the south and onlapping, open folded redbeds to the north (Donohoe and Wallace, 1980).

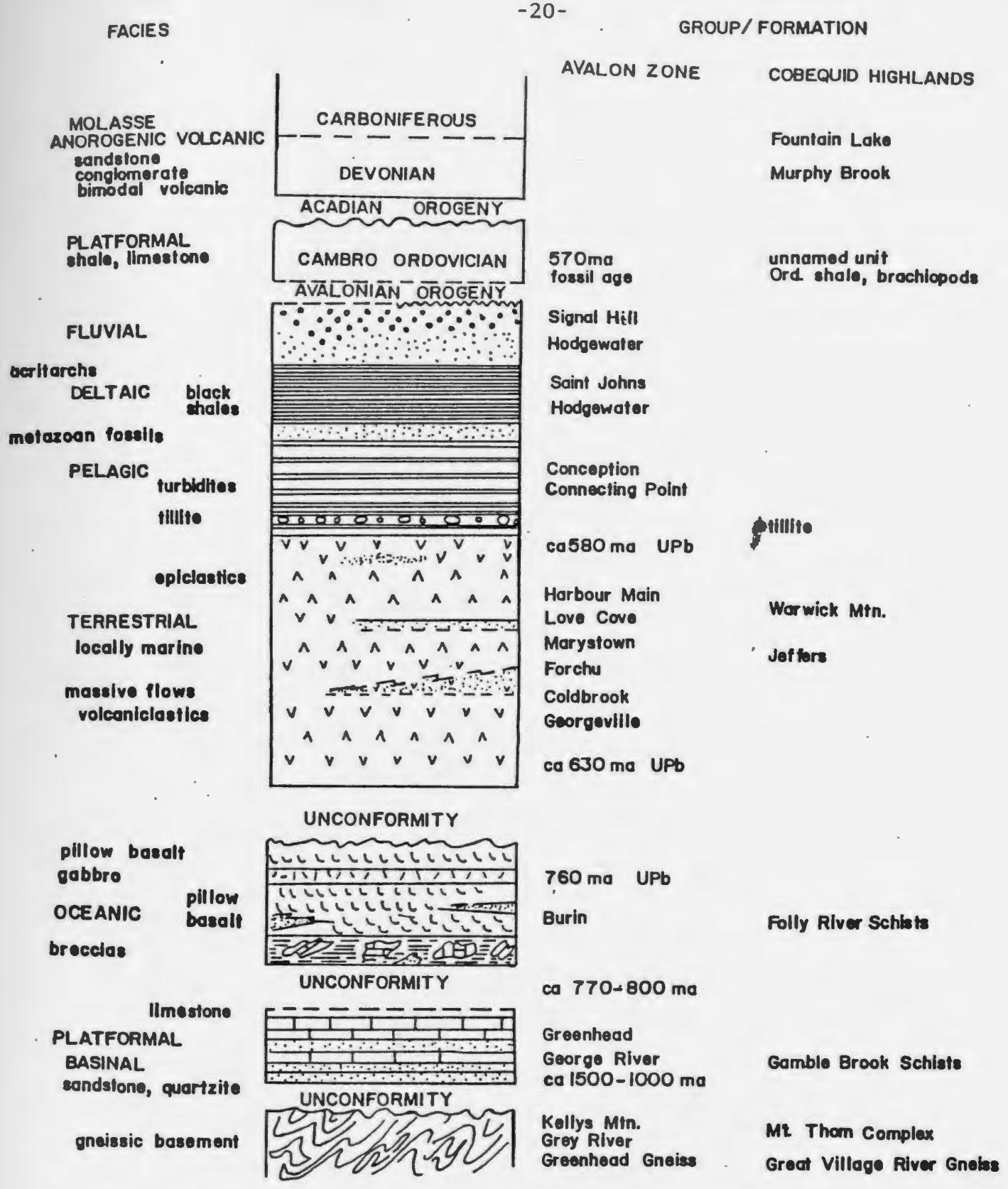

Figure 3: Major Avalon Zone facies and groups and corresponding units in the Cobequid Highlands. Precise stratigraphic correlations are not implied in the generalized column (modified after King, 1982).

1.5.3 Magmatic History of the Cobequid Highlands

Plutonic rocks of the Cobequid Highlands range from Proterozoic to Carboniferous in age. The oldest plutonic rocks are the granitic gneisses of the Mount Thom and Bass River Complexes. These have minimum Rb/Sr isotopic ages of 930 Ma and 839 Ma respectively (Gaudette et al., 1983; Donohoe, 1983). The granitic dikes are interleaved with amphibolite schists which are interpreted to be relict dikes.

The next magmatic episode recorded in the Cobequid Highlands is represented by the Folly River Schists. These amphibolite schists are mafic metavolcanic rocks (Donohoe, 1983) of the Bass River Complex cover sequence and were deformed later in the Precambrian than the first deformation of the basement granitic gneisses. They are a submarine mafic metavolcanic sequence as suggested by the intercalated iron formations and may be broadly correlative to the Burin Group of the Newfoundland Avalon Zone.

The Jeffers Formation represents the next period of magmatic activity in the Cobequid Highlands. This formation is correlated with the Forchu Group of Cape Breton (Murphy, 1977) and the Georgeville Group in the Antigonish Highlands (Keppie, 1979; Murphy et al., 1979)

and the Coldbrook Group near St. John, New Brunswick (Alcock,1938; Ruitenberg et al.,1979). The Jeffers Formation has been intruded by the Jeffers Brook Diorite which has been dated several times by K/Ar and Rb/Sr methods. Dates range from uppermost Hadrynian to Lower Cambrian (Keppie and Smith, 1978 after Wanless et al., 1973; Cormier, 1979), providing a minimum age for the Jeffers Formation.

The McCallum Settlement Granite has a Rb/Sr whole rock age of 504±27 Ma (Cormier in Donohoe and Wallace, 1980).

Silurian, dominantly felsic volcanism with a minor andesitic or basaltic component is recorded in the Wilson Brook and Earltown Formations. Silurian fossils are common in both formations, the oldest (Llandoverian A2) are in the Wilson Brook Formation (Donohoe and Wallace, 1980).

During the Devonian to Carboniferous large masses of diorite and alkali feldspar-hornblende granite to syenogranite intruded the Cobequid Highlands (Figure 2). Associated bimodal volcanism of Devono-Carboniferous age is represented by the Fountain Lake Group. These granites and associated volcanic rocks are the oldest rocks in the Highlands that were not affected by Acadian deformation and are considered anorogenic. For details concerning isotopic

and geochemical data refer to Clarke et al. (1980), Donohoe and Wallace (1980), Keppie (1979) and Cormier (1979).

1.5.4 Structural Geology of the Cobequid Highlands

Donohoe and Wallace (1980) described the structural history of the Cobequid Highlands, and this discussion is largely a precis of their work. The deformational history is summarized in Table 2.

Proterozoic crystalline rocks in the Cobequid Highlands have been deformed at least three times, although the actual timing of these deformations and their relationship to younger events is not clearly known.

The Jeffers and Warwick Mountain Formations have been deformed at least twice. The first deformation (D1) is a shallow to moderately dipping foliation parallel to the axial surfaces of reclined to recumbent isoclinal folds. The second deformation (D2) has produced open to tight, upright to inclined (F2) folds.

The earliest expression of the Acadian Orogeny in the Highlands is marked by the erosion of the Wilson Brook and Portapique River Formations. Continued Acadian uplift is recorded in the conglomerates of the Murphy Brook Formation. The Acadian deformation (D3) produced

Table 2: Correlation of structural events of the Cobequid Highlands (from Donohoe and Wallace, 1981).

ROCK UNIT (Map Unit)	AGE OF PENETRATIVE DEFORMATION			
	Proterozoic	Hadrynian	Acadian	Maritime
Londonderry Fm. (26)				D_4
Rapid Brook and Greville River Fms. (21), Nuttby Fm. (20)				D_4
Murphy Brook Fm. (13) Portapique River Fm. (12) Wilson Brook Fm. (11) Earltown Fm. (10)			D_3	
Unnamed unit (11A)			D_3 or	D_4
Warwick Mountain (5) and Jeffers (4) Fms.		D_1, D_2		
Bass River Complex (2)	$D_{\beta\alpha}, D_{B\beta}, D_{B\gamma}$			
Mt. Thom Complex (1)	$D_{T\alpha}, D_{T\beta}, D_{T\gamma}$			

development of fracture and slatey cleavage, and folds in Silurian and Devonian strata. The Fountain Lake Group is the oldest unit unaffected by (D3).

Volcanic rocks of the Fountain Lake Group unconformably overlie the older strata. The faults along which the uplift and resultant erosion of much Silurian and Early Devonian strata occurred are thought to have also facilitated the movement of magma through the crust.

The Maritime Disturbance (Poole, 1967) caused a single phase of folding (D4) and development of fracture and slatey cleavage in the Early Carboniferous strata which outcrops south of the Rockland Brook and Kirkhill Faults. The Maritime Disturbance in the Cobequid region was characterized by extensive vertical and horizontal fault movement, uplift and erosion (Donohoe and Wallace, 1980).

Granitoid plutons were emplaced north and south of the Rockland Brook Fault and in the western Cobequid Highlands during the Early to early Late Carboniferous. These plutons truncate and therefore postdate (D4) folds.

Major east-west trending faults of the Glooscap Fault System or the Minas Geofracture are the dominating structures of the Cobequid Highlands. In the eastern Highlands the Rockland Brook Fault is the northernmost member of this fault set. The Rockland Brook Fault is

marked over much of its length by a 50 meter to 300 meter wide mylonite zone. The system of major faults isolates stratigraphic units into separate fault blocks with distinct structural histories. Dip slip movement has occurred on many of the faults.

Movement on the east-west trending faults probably began during the Acadian Orogeny, in the Middle Devonian and continued into the Early Mesozoic. Donohoe and Wallace (1978) suggest a minimum dextral strike slip of 20 kilometers on the Cobequid Fault based on displacement of the Fountain Lake Group. Keppie (1979) suggests dextral movement of hundreds of kilometers based on palinspastic reconstructions of areas underlain by Proterozoic volcanic strata. This zone of movement, called the Minas Geofracture, does not include the Cobequid Fault which Keppie contends is a younger feature. The Cobequid Fault is the fundamental break between the Avalon Zone and the Meguma Zone (Keppie, 1979).

Movement on the Rockland Brook Fault had ceased by Middle Carboniferous time, but dextral movement on the Economy Mountain Fault offset basalt flows of Triassic to Jurassic age (Donahoe and Wallace, 1980).

The east-west trending faults are offset by three fault sets which trend northeast, northwest and

north-south. The north-south oriented faults offset all other faults and cut Early Jurassic strata of the Fundy Group. In the northern Cobequid Highlands the northeast and northwest oriented faults are overlain by Carboniferous strata but they do intersect the Devono-Carboniferous Fountain Lake Group. In the southern Highlands, Carboniferous and older strata are displaced along these faults.

This section is largely summarized from Donohoe and Wallace (1980).

1.6 Devono-Carboniferous Geochronology

R.F. Cormier has produced Rb/Sr whole rock dates for the Fountain Lake Group, the Byers Brook Formation and the Hart Lake Granite.

The Fountain Lake Group is dated at 341±4 Ma based on a seventeen point whole rock isochron. The seventeen samples were taken from across the Cobequid Highlands from Parrsboro to Scottsburn. Six samples from the Scottsburn area were from a petroleum well drilled by Chevron Canada, taken from depths of 1100m, 1250m, 1350m, 2198.5m, 2200m and 2633m (Cormier, pers comm 1982).

R.F. Cormier dated the Byers Brook Formation at 343±5 Ma

based on a ten point Rb/Sr whole rock isochron. These samples were taken from Gulf drill core.

Cormier also dated the Byers Lake Granite from samples of Gulf drill core. A ten point Rb/Sr whole rock isochron gives an age of 339±4 Ma for the granite.

Donohoe and Wallace (1976, 1977) published Rb/Sr whole rock dates of 331±27 and 331±17 Ma for the Hart Lake/Byers Lake pluton. The Cape Chignecto granite, which intrudes the Fountain Lake Group rhyolite flows and pyroclastic rocks at Squally Point in the western-most Highlands has a Rb/Sr whole rock age of 339±27 Ma. Table 3 summarizes the radiometric age data for the Fountain Lake Group and associated plutonic rocks. It demonstrates clearly that the Cobequid Highlands experienced a major episode of granitic intrusion and associated volcanic activity at approximately 340 Ma.

TABLE 3: Summary of Isotopic Age Data for Fountain Lake Group and Associated Granites.

Map Unit	Rb/Sr whole rock age	Initial 87Sr/86Sr	Reference
Fountain Lake Gp. (rhyolites)	341±4 Ma	0.7075±0.0012	Cormier, pers comm, 1984
Byers Bk. Fm. (rhyolites)	343±5 Ma	0.7087±0.0021	"
Byers Lake Granite	339±4 Ma	0.7083±0.0018	"
Hart Lake	331±26 Ma	0.708±0.010	Clarke et al, 1979
Hart Lake	331±17 Ma	0.710±0.009	"
Cape Chignecto Granite	339±27 Ma	0.706±0.007	"

CHAPTER 2

GEOLOGICAL SETTING OF THE WENTWORTH PROSPECT

2.1 Summary

The rock units in the map area (Fig. 4) are divisible into three age groups. The southernmost unit is the Proterozoic, Folly River Schist of the Bass River Complex. The Silurian Wilson Brook Formation underlies the northwest corner of the map area. All other rocks outcropping in the area are Devono-Carboniferous, including the Folly Lake Diorite, the Hart Lake Granite and the Fountain Lake Group.

The Fountain Lake Group in this area has been subdivided by Donohoe and Wallace (1980) into the older, dominantly felsic Byers Brook Formation which grades upwards into the dominantly basaltic Diamond Brook Formation. This study focuses on the Byers Brook Formation and its contacts with the Hart Lake Granite in the south and the Diamond Brook Formation in the northeast.

The Byers Brook Formation represents two discrete volcanic cycles separated by a conglomerate/siltstone marker horizon. In each cycle felsic pyroclastic rocks

dominate in the early part of the sequence and grade into dominantly bimodal assemblages at the top of the sequence.

Three areas within the Byers Brook Formation which contain Uranium mineralization and were subjected to extensive diamond drilling (J-zone, DF-zone, DL-zone) are described in detail. The J-zone, which is the westernmost of these straddles, the conglomerate/siltstone marker which separates the two volcanic cycles of the Byers Brook Formation. The DF-zone is situated approximately 1.5 km east of the J-zone and all except the northernmost DF-zone is below (south of) the conglomerate/siltstone marker. The DF-zone has been the focus of the most extensive diamond drilling and hosts the largest and highest grade mineralized zone discovered to date. A 20 m diamond drill intersection grading 4 lb/t U_3O_8 was discovered late in 1980 but follow-up drilling in 1981 failed to delineate a significant mineralized zone. The dominant feature of the DF-zone is a large rhyolite dome and flow complex which is considered to be the main eruptive center. The DL-zone is a 1.5 km long diamond drill cross section located approximately two km east of the DF-zone on the flank of the main dome complex.

2.2 General Geology of the Wentworth Map Area

The oldest unit in the map area is the Proterozoic Folly River Schist of the Bass River Complex. This unit outcrops south of the Rockland Brook Fault (Fig. 4). It comprises a polydeformed submarine mafic volcanic pile (Donohoe and Wallace, 1980). The mafic volcanic rocks are intercalated with minor red to maroon, jasper iron formations, which range from approximately 20 cm to 2.5 m in thickness and are locally associated with concordant carbonate bands which are 1 to 20 cm wide. The Folly River Schists are in fault contact along the Rockland Brook Fault with the Hart Lake Granite and the Folly Lake Diorite to the north. The igneous rocks and the schists are mylonitic in the fault, and the zone of mylonitization ranges from 10 to 150 m wide (Donohoe and Wallace, 1978).

The Silurian Wilson Brook Formation underlies the northeast corner of the map area, on the west side of the Wentworth Valley (Fig. 4). The Wilson Brook Formation in this area comprises grey, fossiliferous siltstone and shale underlain by felsic volcanic rocks. The Wilson Brook Formation is juxtaposed against the Byers Brook Formation to the east along a north-south fault which forms the Wentworth Valley.

The Folly Lake Diorite is suggested to be Devono-Carboniferous in age (Clarke et al., 1980; Donohoe and Wallace, 1980). It is interpreted by Donohoe and Wallace (1980) to predate the Hart Lake Granite, however field relations suggest that the two plutons may be coeval. The contact between the diorite and granite is sharp and very irregular with hypidiomorphic, medium grained quartz diorite making deep and abrupt indentations into medium grained, hypidiomorphic hornblende granite. The reverse relationship is just as common. There is no chilled margin on either the granite or the diorite at the contact. Pegmatite and aplite dikes from the granite vein the diorite and there is a higher density of veining near the contact. These veins also intrude the granite and are probably very late stage. Isotopic dating (Table 3) has shown that the Fountain Lake Group is coeval with the Hart Lake Granite. In the Wentworth area the Folly Lake Diorite does not intrude the Fountain Lake Group the base of which is everywhere intruded by the Hart Lake Granite, however, the diorite intrudes Fountain Lake Group volcanic rocks at its western contact near Simpson Lake (Fig. 2).

The focus of this study is on the Devono-Carboniferous Byers Brook Formation of the Fountain Lake Group and the associated Hart Lake Granite. Donahoe

and Wallace (1976-81) have subdivided the Fountain Lake Group in the Wentworth area into the older Byers Brook Formation and the younger Diamond Brook Formation (Figs. 2, 4 and 4a). These formations are generally poorly exposed in the map area and the crude stratigraphy is defined by interpolating between areas of adequate exposure. Detailed stratigraphy of the J-zone, DF-zone and DL-zone has been derived from diamond drill cross sections which supplement the limited bedrock exposure.

The Byers Brook and Diamond Brook Formations (Fig. 4) comprise bimodal volcanic and volcaniclastic strata which strike northwest-southeast (approximately 120°), and dip steeply (70-80°) north. The Byers Brook Formation is in gradational contact with the Diamond Brook Formation in the northeast corner of the map area.

The Byers Brook Formation is divided into two discrete volcanic packages by an east-west trending conglomerate/siltstone marker horizon. The conglomerate is 75 m to 130 m thick and has been traced from north of the Wentworth Ski Hill (Fig. 4) in the west, over 3 km eastward to the J-zone. In the J-zone the conglomerate intertongues with and is partly overlain by laminated to massive siltstone. The transition from conglomerate to siltstone is abrupt, occurring over 50 to 100 m. The siltstones

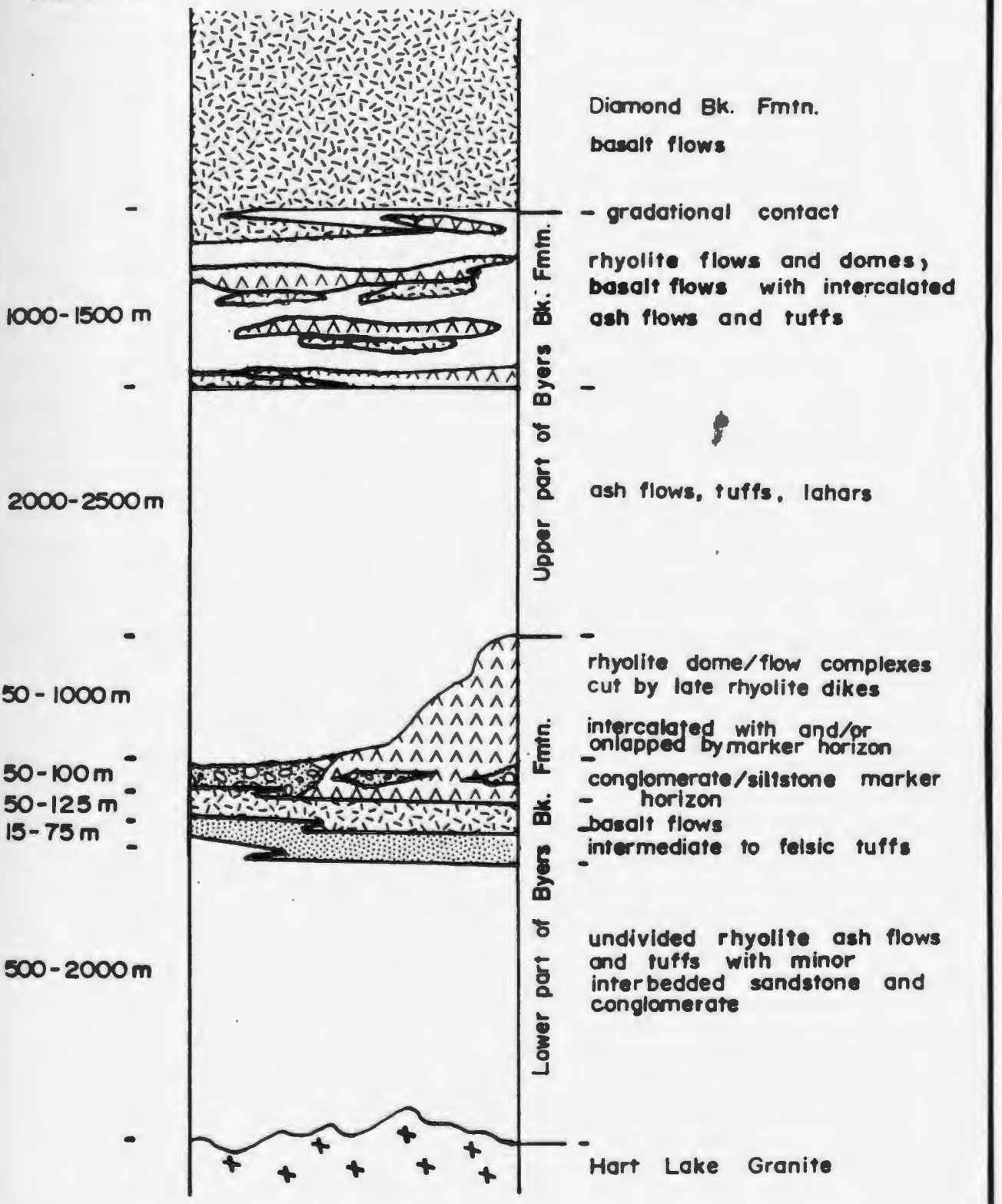

Figure 4a: Stratigraphic column of the Fountain Lake Group in the Wentworth area.

extend eastward along strike through the DF-zone to the east side of the DL-zone and are continuous except where interupted by a major dome/flow complex in the DF-zone. The siltstones range in thickness from 15 to 75 m. In the west, north of the ski hill the conglomerate is overlain by approximately 200 m of siltstones. These beds pinch out abruptly and are not continuous eastward to the J-zone. The siltstones and the conglomerate represent a period of volcanic quiescence and are time-stratigraphic equivalents.

The base of the Byers Brook Formation is everywhere intruded by the Hart Lake Granite. The Hart Lake granite is granophyric or micrographic with miarolitic cavities at the contact with the Byers Brook Formation volcanic rocks. It grades through fine to medium grained, hypidiomorphic, hornblende granite, southward, away from the contact. This southward transition from higher level to deeper level granitic textures suggests that the Hart Lake Granite and the Byers Brook Formation were rotated together as one block.

2.2.1 Lower Byers Brook Formation

The oldest rocks of the Byers Brook Formation are in the southwest since bedding faces north-northeast. The southernmost rocks consist of a thick (500 to 2000 meters) section of felsic tuffs and ash flows with minor conglomerate and sandstone interbeds. These rocks sparsely outcrop on the west side of the map area (Fig. 4), south of the Wentworth Ski Hill. This undivided succession of ash flows, tuffs, sandstones and conglomerates is juxtaposed to the west against the Wilson Brook Formation sedimentary and volcanic rocks along the north-south fault which forms the Wentworth Valley. These distal pyroclastic and epiclastic rocks are poorly exposed eastward along strike to the upper drainage of the Dotten Brook (Fig. 4) on the west side of the J-zone.

East from the J-zone in the lower Byers Brook Formation sequence (ie. below the conglomerate/siltstone marker) there is a marked change in the volcanic and clastic rocks. Immature conglomerate and sandstone interbedded with subaerial, felsic pyroclastic rocks comprise the sequence west of the Dotten Brook. East of the Dotten Brook, stratigraphically underlying the marker conglomerate/siltstone, rhyolite and basalt flows are

interbedded with subaqueous to subaerial pyroclastic rocks and lacustrine? siltstones or waterlain tuffs. This west to east transition from subaerial to subaqueous depositional environment is also reflected in the overlying marker bed in which there is an abrupt transition from conglomerate to laminated siltstone in the western J-zone.

Rhyolite flows typically overlie basalt flows and composite dikes occur in the vicinity of basalt/rhyolite flows. This phenomenon of composite flows fed by composite dikes has been documented by Gibson et al. (1963) in Iceland and Gamble (1979) in northeast Ireland.

Individual basalt flows are commonly separated by up to 30 cm of siltstone or thin (<20 cm) tuffaceous beds. The relatively thin pyroclastic units which occur in the eastern part of the lower sequence are lapilli or crystal tuffs in which bedding ranges from massive to graded. All units are variably veined by quartz, calcite, epidote, chlorite, fluorite and/or magnetite. The pyroclastic and sandstone sequences west of Dotten Brook are rarely veined except for minor quartz and epidote/chlorite veining associated with diabase dikes. Most intense veining is found in rocks nearest the large rhyolite dome/flow complex in the DF-zone.

The absence of lava flows west of Dotten Brook suggests that these rocks were deposited distal from the volcanic vent. The most westerly occurrence of rhyolite flows in the Lower Byers Brook Formation was observed in the J-zone. In the J-zone the single rhyolite flow is not voluminous. The large (1 km X 1.4 km) rhyolite dome and flow complex in the center and eastern DF-zone is suggested to be the main eruptive center. This complex interupts and partly overlies the siltstone marker and was probably a palaeotopographic high. DL-zone geology is characterized by smaller, composite rhyolite and basalt flows interbedded with laminated cherty siltstone beds and several ash flow sheets.

The lower Byers Brook Formation volcanic rocks are cut by diabasic, rhyolitic and composite dikes. Locally diabase dikes and sills are the dominant lithology within the volcanic pile. At least some of the dikes are feeders for the basalt and rhyolite flows. Cross-cutting mafic dikes indicate more than one intrusive event.

The composite dikes typically have a chilled diabasic margin and a rhyolitic core. Gibson and Walker (1963) suggest that to emplace a magma as viscous as rhyolite into cold country rock as a dike it is necessary to emplace it as a composite intrusion. The heat loss from

a sheet-like body, as opposed to a plug, prevents emplacement of rhyolite dikes without a less viscous hot blanket of diabase. The rhyolite is insulated from the cold country rock and gains the latent heat of crystallization from the diabase as it is chilled. Numerous case studies of composite dikes and composite flows have been documented (Rogers and Gibson, 1977; Buist, 1959; Rao, 1958; Gibson and Walker, 1963; McSween et al, 1979). The consensus of opinion of these authors is that composite dikes are emplaced in extensional tectonic regimes.

Rhyolite dikes are abundant in the DF-zone, associated with the large rhyolite dome/flow complex. Gibson and Walker (1963) observed that rhyolite dikes occurred only in the cores of central volcanoes in Iceland. The presence of rhyolite dikes intersecting the large rhyolite complex in the DF-Zone supports the interpretation that this was an eruptive center for the Byers Brook Formation albeit at a much smaller scale than the suggested Iceland correlative.

In summary the main volcanic center in the DF-zone is flanked by the J-zone to the west and the DL-zone to the east in which small fissure eruptions of composite flows were probably fed by composite dikes. West of the J-zone

the environment of deposition changes from subaqueous to subaerial and distal pyroclastic rocks are interbedded with unsorted conglomerates and sandstones.

2.2.2 Upper Byers Brook Formation

Above the conglomerate/siltstone marker horizon there is an abrupt change in volcanic rocks from lava flows and thin pyroclastic units which underlie the marker bed to thick felsic ash flow sheets with intercalated agglomerates, lahars and tuffs, suggesting a transition from relatively passive to explosive volcanism. Approximately 2200 m of ash flows were deposited before a second transition to more passive volcanism and effusion of rhyolite and basalt flows which grade into basalt flows of the Diamond Brook Formation in the northeast corner of the map area (Fig. 4). The ash flows are subaerial, generally pink to orange-red except near the base of the sequence. The earliest ash flows in the northern part of the J-zone and zones eastward are mottled red-green to dominantly green and were probably deposited in shallow water. There is an abundance of basaltic lithic fragments in the earliest ash flows but 250 meters up-section from

the marker bed, lithic fragments are almost entirely rhyolitic.

In the western part of the map area, (Fig. 4), north of the ski hill there are approximately 500 m of ash flows exposed, overlying the conglomerate/siltstone marker. These are juxtaposed against Carboniferous basinal sedimentary rocks, which generally unconformably onlap onto the Highlands. The ash flows can be traced approximately 2 km east to a large diabase dike (Fig. 4) and extend further along strike beyond the dike. The ash flows comprise sheets of 250 m thicknegs or greater, although exposure does not permit rigorous separation. These thicker sheets grade upwards into thinner welded ash flows (approximately 75 m) and more abundant unwelded tuffaceous horizons and ultimately become interlayered with rhyolite and basalt flows in the northeast part of the map area. These rocks are unconformably overlain by shallowly dipping, onlapping Carboniferous sandstones approximately 400 m north of the map area. The contact between the Fountain Lake Group and the Carboniferous sedimentary rocks forms the prominent scarp along Highway 248 from Wentworth to New Annan.

Reconnaissance mapping along the contact between the Byers Brook and Diamond Brook Formation in the northeast part of the map sheet, has delineated a

continuous zone of rhyolite flows along the contact (Fig. 4). The rhyolite flows are intercalated with basalt flows, ash to lapilli tuffs and rhyolitic agglomerates.

In the sequence immediately underlying the Diamond Brook Formation a lithic tuff forms an 80 to 120 m basal unit containing 0.1-2.0 cm rhyolite clasts occurring in 0.5 to 5 m thick beds separated by 10 cm fine ash horizons. This unit is overlain by a 20 to 30 m thick basalt flow with a strongly vesicular flow top which is in turn overlain by a 50 to 150 m thick rhyolite flow. The rhyolite flow is locally strongly silicified and contains abundant fluorite-filled vugs. Discordant zones contain 70-90% quartz and commonly fluorite-filled 2-15 mm lithophysae reminiscent of the lithophysae-rich zones observed in the DF-zone rhyolite complex. This is the transition zone between the Byers Brook and Diamond Brook Formations. Exposure is poor north of the rhyolite flow but intercalated basalts, rhyolites and lithic tuffs grade into the Diamond Brook Formation over approximately 300 m. Anomalous radioactivity is associated with the rhyolite flows but the economic potential of this area has not been tested .

Little work has been done on the easternmost Byers Brook Formation, east of Byers Lake (Fig. 4), and no marker

horizons for stratigraphic correlation have been discovered.

In summary, the Byers Brook Formation in the Wentworth area records two distinct volcanic cycles, separated by a conglomerate/siltstone marker horizon. Both cycles were initiated by explosive pyroclastic volcanism which waned to emplacement of rhyolite and basalt flows.

2.2.3 Structure of the Byers Brook Formation

Numerous north-south trending faults have caused minor offsets in the Byers Brook Formation stratigraphy. Offsets range from less than 1 meter to several tens of meters. The dominant structure in the Byers Brook Formation is the prominent East Wallace River-Debert Lake lineament which is oriented at approximately 140° azimuth (Fig. 4). This fault is marked by a deep stream valley and strong fracturing of the surrounding bedrock. Diamond drill hole JZ-13 attempted to probe the fault zone but 43 meters of diamond drill casing was pushed down without intersecting bedrock. The lineament is marked by a very pronounced airborne EM anomaly. Dip-slip displacement such that the southwest block was downthrown was accompanied by sinistral movement which juxtaposed Byers

Brook Formation volcanic rocks against granite to the northeast, near Debert Lake, and TL120+00S (Fig. 4).

2.3 Geology of the J-zone

The J-zone is located on the Cobequid Grid (Fig.4) between line 24+00 east and line 20+00 west and between line 12+00 south and 40+00 north (all grid coordinates are measured in feet). Overburden in the zone is generally less than 1 m, but bedrock is not well exposed. Stratigraphic units in the J-zone strike southeast (110^{o}) and dips steeply ($70\text{-}80^{o}$) north. The south margin of the J-zone is intruded by the Hart Lake/Byers Lake Granite. The stratigraphy of the J-zone is illustrated schematically in Figure 5 and in the diamond drill cross section (Fig. 6) which is included in the back pocket. The diamond drill hole location map and and diamond drill summary for the J-zone are included in Appendix 1.

The oldest unit mapped in the J-zone is a dark grey crystal-lithic tuff of intermediate composition, approximately 15 m thick. At least six basalt flows with an apparent total thickness of 125 m overlie the crystal tuff. Individual flows vary from 5 to 50 m in thickness.

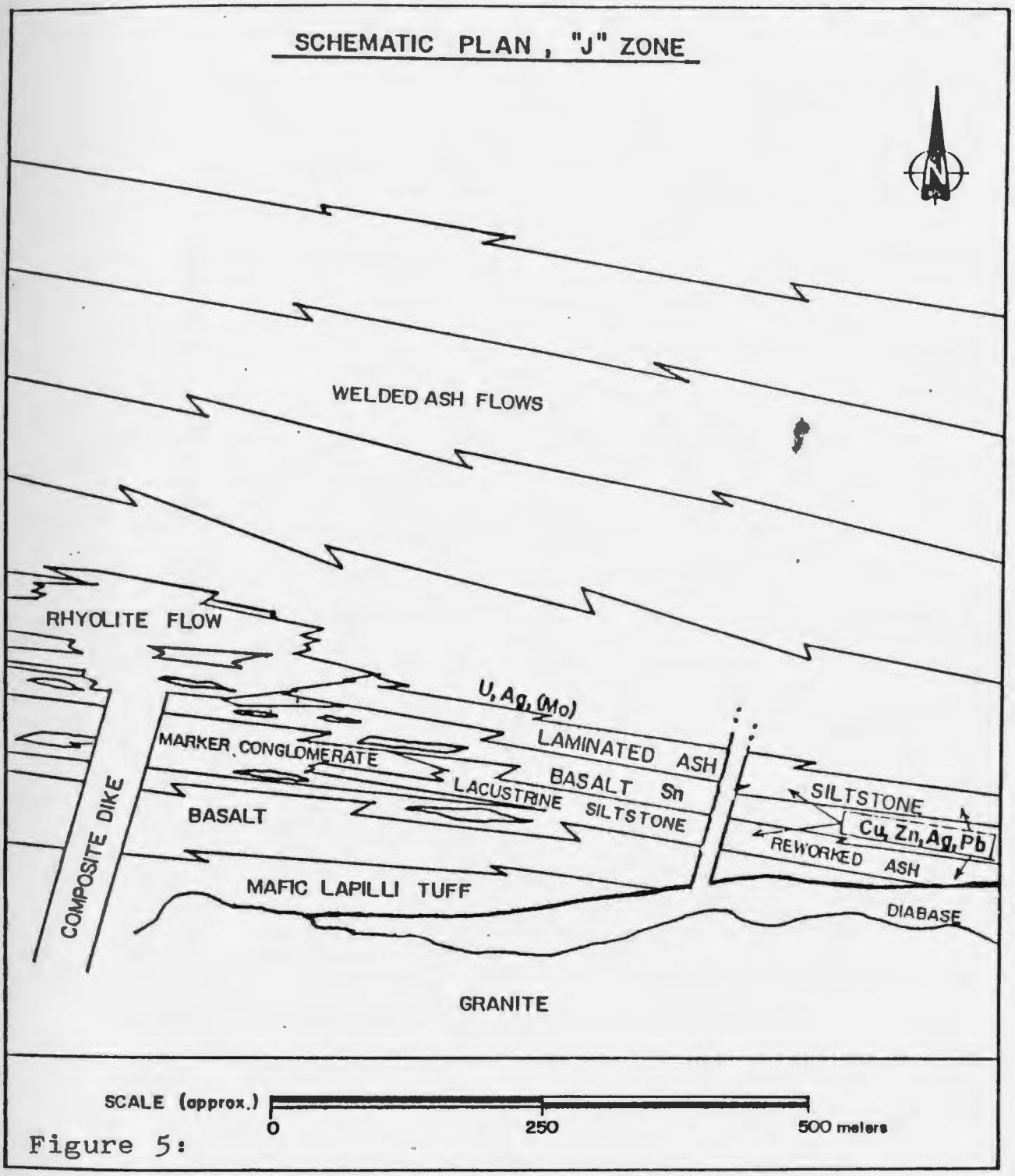
SCHEMATIC PLAN , "J" ZONE
N
WELDED ASH FLOWS
RHYOLITE FLOW
U, Ag, (Mo)
LAMINATED ASH
MARKER CONGLOMERATE
BASALT Sn
LACUSTRINE SILTSTONE
SILTSTONE
Cu, Zn, Ag, Pb
REWORKED ASH
BASALT
COMPOSITE DIKE
MAFIC LAPILLI TUFF
DIABASE
GRANITE
SCALE (approx.)
0
250
500 meters

Figure 5:

The uppermost basalt flows are intercalated with a rhyolite flow and the marker conglomerate. The eastward strike extension of the conglomerate is marked by a rapid transition into laminated to thickly bedded siltstones, composed of fine grey-green ash.

The period of relative volcanic quiescence during which the conglomerate and siltstone were deposited ended with the explosive eruption of ash flows. Four ash flow tuffs have been defined in the J-zone but the total thickness of ash flows extends well beyond the J-zone to the Byers Brook-Diamond Brook Formation transition zone. The earliest ignimbrite was erupted onto a palaeosurface littered with basaltic and felsic debris which has been incorporated into the base of the ash flow. The oldest ash flow tuff is divisible into two subunits; a lower subunit with an unwelded to weakly welded base which grades upwards into a strongly welded zone, the upper subunit is completely welded. This is typical of single eruptive ash flow sheets.

The overlying ash flows in the J-zone are simple cooling units in which unwelded lithic fragment-rich bases grade upward into welded ash flow tuff. The lithic fragment-rich zones gradually become more depleted in basaltic lithic fragments in each successive ash flow up

section. The colour of the groundmass in the two lowermost ash flows is grey to green, the youngest of these shows a transition from grey at the base to red near the top. It is suggested that the early ash flows were deposited in shallow water and grade upwards to subaerial ash flows because the early subaqueous ash flows are overlain by finely laminated, dark green to grey siltstones composed of ash whereas the later subaerial welded ash flow tuffs are overlain by a poorly preserved veneer of massive red-brown tuff. The siltstones are greenish grey and laminae are graded and exhibit load casts, flame structures and ripples, textures consistent with deposition in shallow water. The massive red brown tuffs are typical of subaerial depositional environments showing no sign of reworking by water.

The J-zone is intruded by numerous diabase dikes and composite dikes some of which may be the feeders for the basalt and rhyolite flows.

2.4 Geology of the DF-zone

The DF-zone lies between lines 40+00 east and 70+00 east and between line 50+00 south and the 0+00 base line on the southwest-side-down block along the prominent

East Wallace River/Debart Lake lineament (Fig. 4) within a large embayment in the Hart Lake/Byers Lake Granite. The DF-zone is almost entirely covered by alluvium, resulting in less than 5% bedrock exposure except in the northeast quadrant where there is approximately 30% exposure of the main rhyolite flow/dome complex. The stratigraphy of the DF-zone is illustrated schematically in Figure 7. Figure 8 shows diamond drill cross sections through the west and east DF-zone. The DF-zone diamond drill hole location map and drilling summary are in Appendix 1.

The southernmost (oldest) rocks in the DF-zone comprise unwelded grey tuffs, which outcrop immediately north of the Hart Lake/Byers Lake Granite. The tuffs are overlain by an approximately 15 m thick basalt which is covered by a veneer of angular vesicular basalt fragments in a brown tuffaceous matrix. A 20-50 m ash fall tuff unit overlies the basalt. The tuff comprises a lower fine ash zone overlain by a lapilli-ash zone which fines upwards into a second fine ash zone. The tuff is overlain by a 10-40 m rhyolite flow with an autobrecciated top and base and flow layering developed throughout the center.

Black to green, very fine grained, laminated to massive ash or siltstone overlie the rhyolite flow. These ash or siltstone beds are correlated westwards to the

Figure 7:

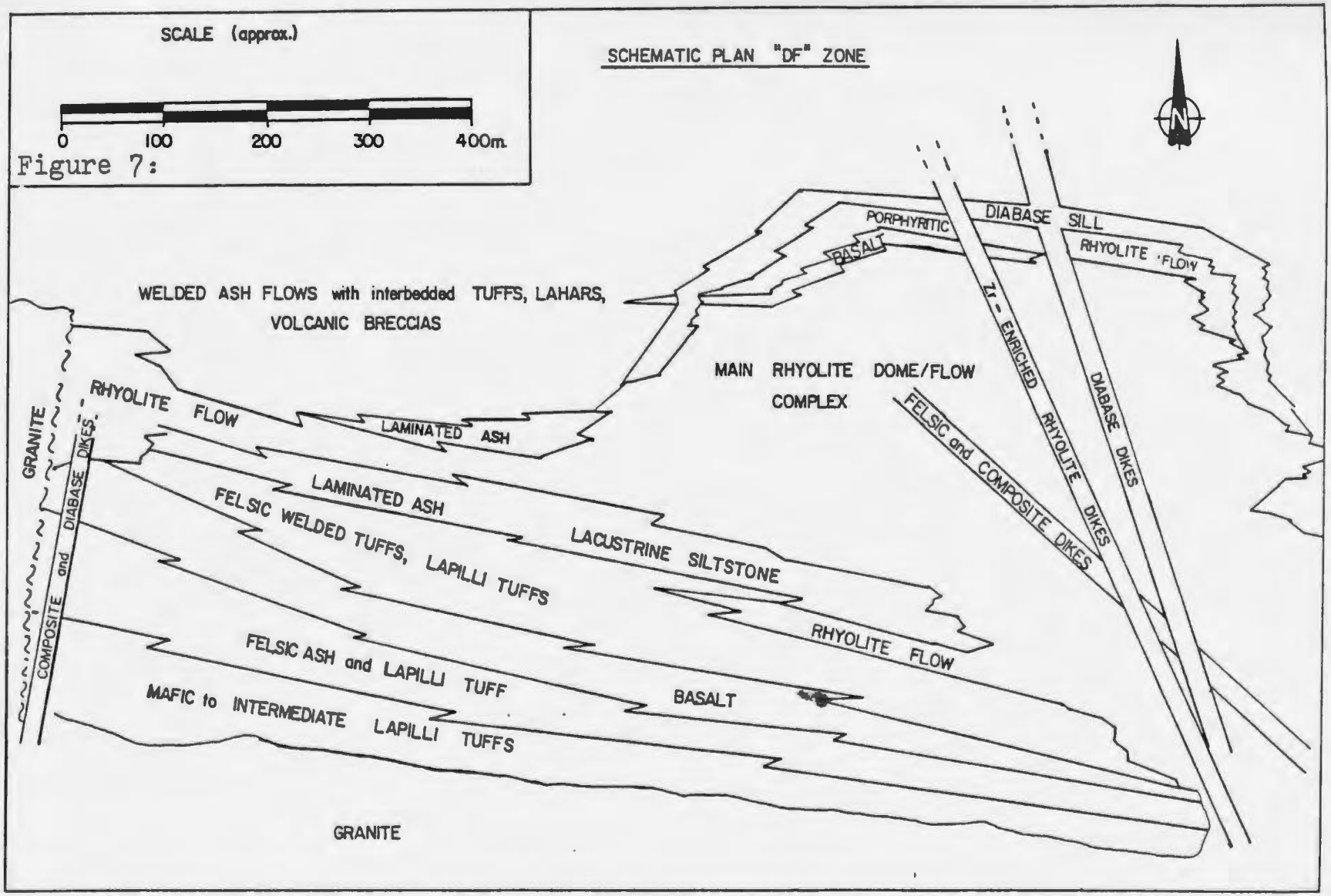
SCALE (approx.)
0
100
200
300
400m.
SCHEMATIC PLAN "DF" ZONE
N
PORPHYRITIC
BASALT
DIABASE SILL
RHYOLITE FLOW
WELDED ASH FLOWS with interbedded TUFFS, LAHARS,
VOLCANIC BRECCIAS
Zr - ENRICHED RHYOLITE DIKES
DIABASE DIKES
MAIN RHYOLITE DOME/FLOW
COMPLEX
FELSIC and COMPOSITE DIKES
GRANITE
RHYOLITE FLOW
LAMINATED ASH
COMPOSITE and DIABASE DIKES
LAMINATED ASH
LACUSTRINE SILTSTONE
FELSIC WELDED TUFFS, LAPILLI TUFFS
RHYOLITE FLOW
FELSIC ASH and LAPILLI TUFF
BASALT
MAFIC to INTERMEDIATE LAPILLI TUFFS
GRANITE

J-zone and are the strike extension of the conglomerate/siltstone marker horizon. These beds underlie and partly onlap the large rhyolite flow/dome complex which is the dominant feature of the DF-zone. The complex has been traced southeast to the west bank of Big Snare Lake (Fig. 4). Small radioactive showings have been found along this section. On the east bank of Big Snare Lake diamond drill hole DL-16 intersected a cupola of the Hart Lake/Byers Lake Granite which has a zone strongly enriched in rare earth elements, tin, tungsten and thorium. The morphology of the complex suggests that the cupola may be the feeder from the underlying magma chamber. This complex causes a break in the laminated ash or siltstone beds which are continuous on the east side of the dome complex in the DL-zone, and was probably a palaeotopographic high.

Overlying the laminated siltstone on the west side of the DF-zone (Fig. 7) is a series of several ash flows separated by thin tuffaceous horizons. Graphitic zones at the base of the earliest ash flow suggests the presence of organic material associated with the underlying lacustrine sediments. These ash flows are correlated with the ash flows which overlie the comglomerate and siltstone in the J-zone.

Overlying the large rhyolite flow/dome complex in the eastern DF-zone, and partly overlying the adjacent thin ash flows flanking the flow/dome complex in the western DF-zone, is a 15 m thick basalt flow which is in turn overlain by a strongly porphyritic rhyolite flow. The rhyolite flow comprises 30-40%, 0.5-1 mm K-feldspar and quartz crystals and 15-80%, 1 to 5 mm lithophysae. The base of the rhyolite flow has incorporated 1-15 cm basaltic and felsic lithic fragments. The rhyolite flow is overlain a by >1.5 km thickness of ash flows tuffs with rare agglomerate and laharic horizons.

The stratified units of the DF-zone are intruded by the Hart Lake Granite in the south. Numerous dikes and sills intrude all rock types and locally comprise up to 40% of the bedrock. Composite dikes and rhyolite dikes were intersected by nearly all drill holes in the DF-zone, with a higher density of dikes associated with the main flow/dome complex. Two texturally distinct rhyolite dikes are thought to represent the last felsic magmatism to have occurred in the DF-zone. These dikes are the most continuous features in the DF-zone and intersect the stratigraphy almost at right angles. Texturally the dikes are almost completely spherulitic with flow layering and axiolitic textures developed on dike margins. They are

chemically distinct in that they consistently contain between 1100 ppm and 1600 ppm zirconium.

2.5 Geology of the DL-zone

The DL-zone is on the east side of Big Snare Lake (Fig. 4), between lines 88+00 and 120+00 east and lines 12+00 and 84+00 south on the Cobequid grid. The DL-zone extends across approximately 1500 m stratigraphic thickness. Stratigraphy has been defined from a combination of bedrock mapping and a diamond drill core cross section through the zone. The stratigraphy of the DL-zone is presented schematically in Figure 9 and the actual diamond drill cross section (Fig. 10) is included in the back pocket. The DL-zone diamond drill hole locations and drilling data are given in Appendix 1.

The oldest unit in the DL-zone is a basalt flow which is approximately 20 m thick. The basalt flow is overlain by a lapilli, crystal tuff, which may correlate with the tuff overlying the lowermost basalt flow in the DF-zone. The tuff comprises 30-40% unsorted, 1-5 mm felsic and mafic lithic fragments in a light grey ash matrix. It is locally separated from the granite by an intervening 3-5 m diabase dike. The tuff is approximately 60 m thick.

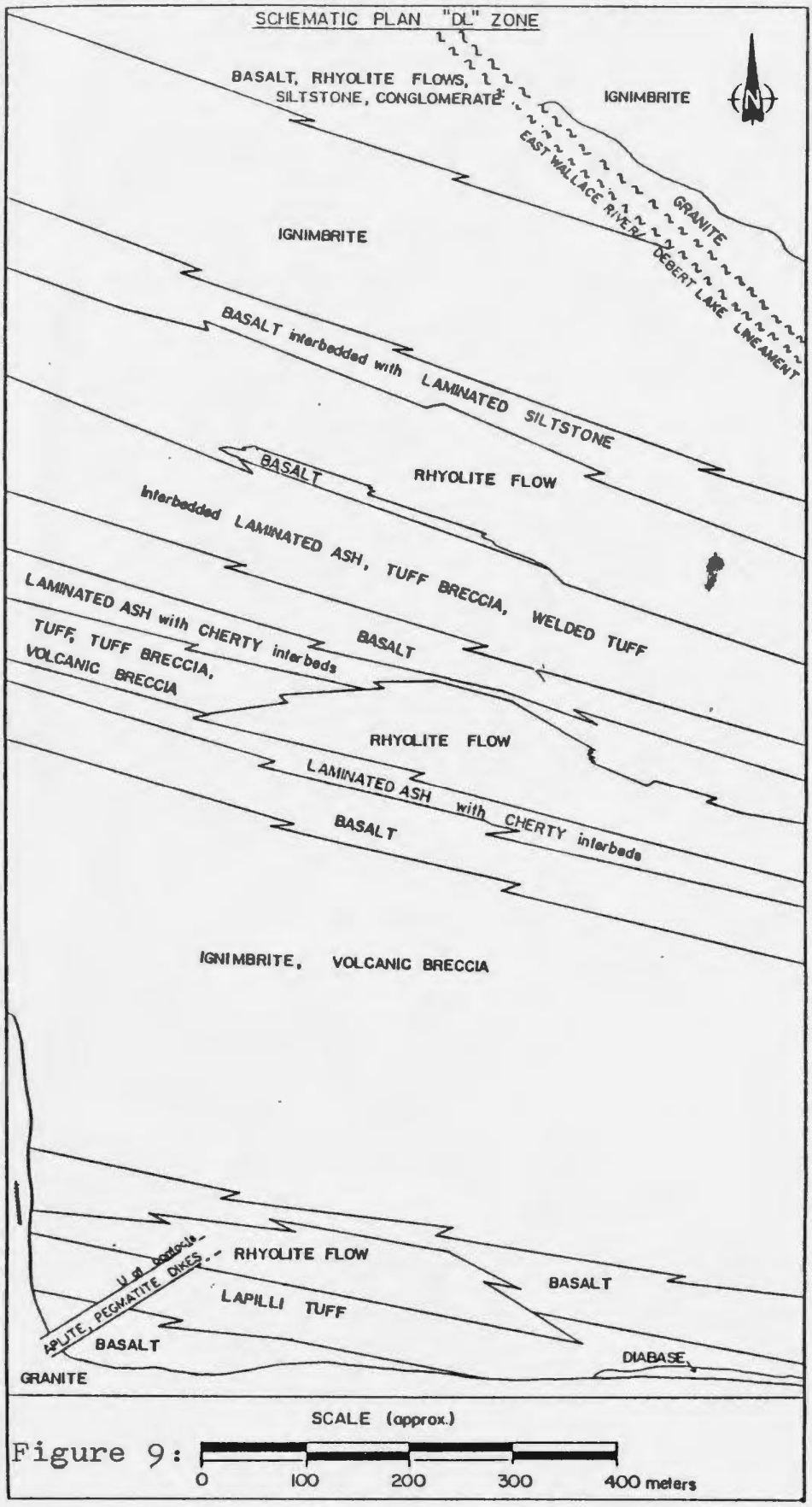
SCHEMATIC PLAN "DL" ZONE
BASALT, RHYOLITE FLOWS, SILTSTONE, CONGLOMERATE
IGNIMBRITE
N
EAST WALLACE RIVER
GRANITE
DEBERT LAKE LINEAMENT
IGNIMBRITE
BASALT interbedded with LAMINATED SILTSTONE
BASALT
RHYOLITE FLOW
Interbedded LAMINATED ASH, TUFF BRECCIA, WELDED TUFF
LAMINATED ASH with CHERTY interbeds
TUFF, TUFF BRECCIA, VOLCANIC BRECCIA
BASALT
RHYOLITE FLOW
LAMINATED ASH with CHERTY interbeds
BASALT
IGNIMBRITE, VOLCANIC BRECCIA
APLITE, PEGMATITE DIKES
RHYOLITE FLOW
BASALT
LAPILLI TUFF
BASALT
DIABASE
GRANITE
SCALE (approx.)
0
100
200
300
400 meters

Figure 9:

Overlying the crystal lithic tuff unit is a 50-60 m, grey weathering rhyolite flow which is strongly flow layered. The rhyolite flow is overlain by 20-40 m of basalt which is in turn overlain by approximately 400 m of ignimbrite with strongly welded pumice fragments (fiamme) and ash to lapilli size crystal and lithic fragments. The ash flow is overlain by a 50 m thick sequence of basalt flows. The basalt flows have irregular, vesicular flow tops and are locally intensely chloritized. A 100-200 m thick rhyolite flow overlies the basalt flows. The rhyolite flow has strongly developed millimeter-scale flow layering which is flow folded and autobrecciated. Although the flow is relatively thick it is laterally discontinuous. Degassing breccia dikes are abundant. The flow base has incorporated fragments from the underlying basalt flow. Laminated ash or siltstone interbedded with cherty horizons flank the rhyolite dome but do not overlie it. A zone of siliceous sinter, comprising massive, amorphous cherty material which outcrops east of DL-zone is 10 to 20 m thick. This sinter outcrops approximately along strike and is thought to be a strike extension of the cherty siltstone beds, but exposure is not good enough to make a definite correlation.

The rhyolite flows are overlain vertically and laterally by 30-40 m of basalt and approximately 100 m of tuffs and ash flows. The ash flows typically have lithic fragment rich bases, grade through a thin, spherulitic, devitrified zone into a strongly welded zone with abundant large fiamme. The ash flows are overlain by a sequence of massive to laminated ash to lapilli crystal tuffs. The laminated ash beds are graded and fine northwards. The base of these tuffs is thought to be subaqueous with an upwards (north) transition to subaerial near the top where the tuffs are massive and hematized, with stronger hematization between distinct tuff beds.

The subaqueous to subaerial tuffs are overlain by a 500 m thick section of ash flows, lithic tuffs and agglomerates intercalated with a 150 m flow-layered and spherulitic rhyolite flow and a 10-20 m thick basalt flow. Basalt flows, bedded crystal and lithic tuffs and rhyolite flows overlie the thick pyroclastic sequence. The individual rhyolite and basalt flows are 5-20 m thick and are overlain by ignimbrites.

The northernmost part of the section crosses the East Wallace River/Debert Lake fault (Fig. 9) where granite in the upthrown block (northeast) is juxtaposed against

Byers Brook volcanic and volcaniclastic rocks in the downthrown block (southwest).

The Hart Lake Granite intrudes the Byers Brook Formation in the south and west (Fig. 4), and the granite contact dips gently eastward in this zone.

Diabase and composite dikes intrude the DL-zone volcanic pile. In the southern DL-zone aplite and pegmatite dikes cut the granite and the rhyolites. Magnetite veins and anomalous radioactivity is associated with some of the aplite dikes

2.6 Petrographic Descriptions of the Map Units

2.6.1 Crystal Lithic Tuffs

Crystal and lithic tuffs range from brown to dark grey in colour. In the J-zone the fine grained ash matrix supports approximately 20%, 1-5 mm white to rusty red feldspar crystal fragments and up to 5% reddish to dark green angular to subrounded ash to lapilli size basaltic and rhyolitic lithic fragments. Bedding is weakly defined by alignment of lithic fragments. The mixture of felsic and mafic clasts give the tuff an intermediate composition.

Plate 1: Lapilli tuff, sample from drill core. This is the lowermost unit in the DF-zone stratigraphy, and has a significant mafic component.

In the southern DF-zone dark grey lapilli and ash tuffs of intermediate composition are poorly exposed in bedrock and have been intersected in diamond drill holes DF-36, DF-37 and DF-38, immediately north of the granite contact. The DF-zone tuffs are dark grey or black to dark brown in colour. Bedding is massive to thickly bedded (approximately 3 m thick beds). Lapilli tuffs comprise 50-70% basaltic and felsic lithic fragments (Plate 1) in a black ash groundmass. The lapilli-ash tuffs are rhythmic beds of lapilli tuff which fine upwards into fine black ash tuff. The beds are 0.5-3 m thick and only the top 10-50 cm is composed of fine ash. This bedded tuff zone ultimately grades into a 5-10 m thick massive, black ash tuff at the top. The base of this lapilli-ash tuff unit is intruded by the Hart Lake/Byers Lake Granite so the original thickness of the unit is not known.

2.6.2 Basalt Flows

The basalt flows are all megascopically similar in appearance (Plate 2 and Plate 3). The basalt flows are black to dark green and are aphanitic to very fine grained. They are generally aphyric but flows with 1-5%, 1-3 mm plagioclase crystals have been observed, especially

Plate 2: Amygdaloidal basalt flow.

Plate 3: Photomicrograph of amygdaloidal basalt, with calcite-chlorite filled amygdule in the lower left corner of the photograph.


PENTAX

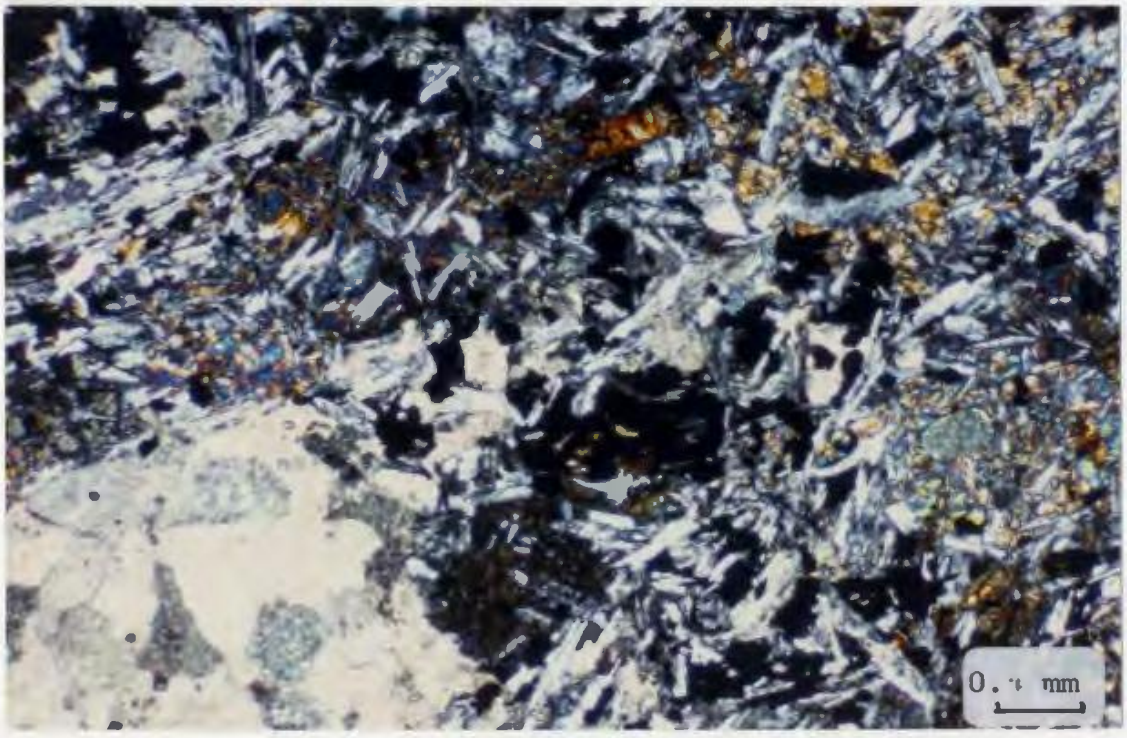
0.1 mm

in the J-zone. The flows are vesicular and/or amygdaloidal and the greatest concentration of vesicles occurs at flow tops. Cassiterite associated with fluorite has been observed in amygdules in one basalt flow in the J-zone (A.K. Chatterjee pers. com., 1983). Amygdules are commonly irregular and elongate near flow margins but are spheroidal in flow interiors.

In the J-zone there are at least six discrete basalt flows in the pile, separated by 10-50 cm grey or brown ash zones with an abundance of strongly amygdaloidal basalt fragments. Single basalt flows in other zones are usually overlain by a veneer of ash and basalt fragments similar to those observed between basalt flows in the J-zone.

Epidote veinlets from 0.1 to 5 cm wide are locally abundant and minor epidote veining is ubiquitous throughout the basalt flows. Calcite veinlets between 0.1 and 1 cm wide are rare to locally abundant, but ubiquitous in the basalts.

The basalts are moderately to strongly chloritized and may or may not be magnetic. Epidote, hematite and chlorite alteration selvages are common along veins and fractures.

In thin section the basalts show typical glomeroporphyritic texture of 0.1-0.75 mm euhedral plagioclase laths with interstitial anhedral mafic and opaque minerals. The mafic minerals may be strongly to completely altered to chlorite and epidote with accessory biotite. Relict pyroxenes are the only primary mafic minerals observed in some thin sections. Some basalt flows are only weakly chloritized.

Opaque minerals comprise 3-5% of the rock. Magnetite is the most abundant opaque mineral but pyrite has been observed in some flows.

Amygdules range from 0.2 mm to 2 cm in diameter and are filled with chlorite, calcite, epidote, fluorite, quartz and rarely barite. These same minerals are represented in veinlets which range from 0.1 mm to 2 cm wide.

2.6.3 Rhyolite Flows and Dome

The flow in the J-zone varies from reddish near the top to greyish-brown or pink near the bottom, and is best observed in the lower 40 meters of drill hole JZ-10. The flow contains 5-10% euhedral to subhedral, white to buff K-feldspar phenocrysts which are 1-4 mm long and

embayed, sometimes bipyramidal quartz phenocrysts which range from 1-3 mm. Crystals commonly are surrounded by a 1-2 mm hematized rim and are hosted by an aphanitic groundmass which is flow layered and completely microspherulitic to granophyric. Fewer crystals and thinner alteration rims are observed near the flow margins. Abundant mafic material from the underlying basalt flows has been incorporated into the base of the rhyolite flow and the base is strongly flow brecciated and epidote veined. The basaltic material is restricted to within approximately 1 meter of the rhyolite-basalt contact.

Rhyolite flows and domes are the dominating feature of the DF-zone. They are strongly flow layered and flow layers exhibit drag-folds and locally have been rolled into cylindrical structures. Flow layers range from 1 mm to approximately 1 meter wide. In the main dome/flow complex in the DF-zone the flow layering is contorted but oriented generally north-south. Flow layering in the earliest flow, which underlies the main dome complex and in the last flow which overlies the main dome complex is oriented approximately east-west.

Abundant zones in which lithophysae comprise 50-90% of the rock, discordantly and abruptly cut the flow

layers, or are dragged out concordantly along flow layering (Plate 4). Lithophysae range from 0.2-5 cm in diameter but are most commonly in the 1-2 cm range. The lithophysae are spheroidal to oblate or irregular and are commonly brecciated and overgrown by second and third generation lithophysae, attesting to more than one degassing episode. They have a characteristic concentrically banded shell and a radially banded interior which may be filled with quartz, K-feldspar, chlorite, epidote, rarely fluorite or are sometimes empty. Lithophysae-rich zones are usually strongly oxidized to red but are locally green. Devitrification textures are well developed in the rhyolite flows and domes. Axiolitic textures are observed along flow layers. Spherulites ranging from microscopic to 2 cm are abundant (Plate 5). Spherulites often form crude layers, occur in clusters and commonly nucleate on K-feldspar or quartz crystals. The groundmass of rhyolite flows is commonly completely micro-spherulitic.

Rhyolite flows are aphyric or weakly to strongly porphyritic, containing up to 30% K-feldspar and quartz crystals. The youngest flow in the DF-zone has the highest proportion of crystals comprising approximately 25% K-feldspar crystals and 5-10% quartz crystals.

Plate 4: Lithophysae-rich zone in which lithophysae are flattened and dragged along flow layering in flow layered rhyolite.

Plate 5: Spherulitic rhyolite flow.


PENTAX

The flows are autobrecciated especially near flow margin and degassing breccias are abundant (Plate 6). Minor felsic and basaltic debris are incorporated into some rhyolite flow bases. These clasts tend to be concentrated within a meter or two of the basal contact.

Pumice fragments are observed in the main flow/dome complex and small pumice fragments are sometimes stretched and flattened along flow layers. This is observed only in the main flow/dome complex. The main complex is intersected by abundant rhyolite, composite and diabase dikes.

Rhyolite flows in the DL-zone are texturally similar to those described in the J-zone and DF-zone. They are composite flows with flow layering, contain lithophysae zones with 10-70% lithophysae, are spherulitic or axiolitic and vary in colour from green to red. The flows have a 1-5 mm light grey weathered rind. Autobrecciation is common.

Flows in all zones are variably altered by the intrusion of numerous dikes and are strongly to weakly fractured. Fractures host veins of quartz, calcite, epidote, chlorite and fluorite. These veins range from 0.1 mm to 20 cm wide. Locally shearing and fracturing

Plate 6: Autobrecciated flow banded rhyolite.

accompanied by very strong hematite and chlorite alteration has destroyed all primary textures.

Accessory minerals identified in the rhyolites are zircon, sphene, magnetite, pyrite, barite and allanite.

2.6.4 Rhyolite Tuffs

Rhyolite crystal and lapilli tuff which is the stratigraphically lowermost unit in the DL-zone comprises 30-40% unsorted felsic and mafic lithic fragments which range in size from ash to lapilli, and approximately 10%, 1-3 mm K-feldspar and quartz crystal fragments in a light grey ash matrix. This unit is correlated westward to the DF-zone where the tuff has a fine ash base in sharp contact with a lapilli rich zone which is weakly graded and fines upwards into massive green fine ash with laminar bedding at the top of the unit. In the lapilli zone the lithic fragments are angular and are approximately 75% felsic. The lapilli zone comprises approximately 80% fragments and 20% matrix, and pyrite is disseminated throughout the matrix.

Rhyolite tuffs (Plate 7) are exposed at numerous levels in the stratigraphic column, generally as thin discontinuous beds. They commonly overlie rhyolite flows

Plate 7: Drill core sample of rhyolite crystal, lapilli tuff comprising quartz and K-feldspar crystal fragments and rhyolite lapilli in an aphanitic ash groundmass.

or occur as narrow tuffaceous zones locally preserved between ignimbrite sheets. In the pyroclastic sequence above the marker horizon tuffaceous beds in excess of 50 m thick have been observed. The tuffs range from unsorted and massive to graded beds which may be composed completely of fine ash to only approximately 20% ash as a matrix around lithic and crystal fragments. Except for the lowermost tuffs in the J-zone and DF-zone all other tuffs are rhyolitic to dacitic. Lapilli fragments are 75-95% felsic but there is always a minor basaltic component present. Strongly chloritized or sericitized pumice fragments are common. The groundmass of the tuffs may be green, red, white or grey. Lithic fragments range from ash through lapilli to block size (rarely up to 1 meter). Some tuffs contain up to 15-20% K-feldspar and quartz crystal fragments.

In thin section the tuffs are commonly hematized and or chloritized. The groundmass and felsic lithic fragments are variably sericitized, ranging from weak, patchy sericite alteration to complete sericitization of the groundmass. Mafic lithic fragments are usually strongly chloritized. Pyrite occurs in trace amounts in most tuffs with local concentrations of 2-3%. The tuffs

have abundant fractures which are filled by microveinlets of quartz and less abundant epidote, calcite, chlorite and fluorite.

2.6.5 Conglomerate

The polymictic conglomerate extends from north of the Wentworth Ski Hill (Fig. 4) to the J-zone. In the J-zone the conglomerate has a dark grey to black fine grained sandy matrix supporting subangular to very well rounded clasts which range up to 5 cm in diameter. West of the J-zone the matrix of the conglomerate varies from red to green or mottled red and green. The clasts consist of felsic and mafic volcanic rocks, quartz pebbles, siltstones and granite. Except for rare graded beds and rare coarse sandstone beds the conglomerate is unsorted, suggesting derivation from immature sediments close to their source. Pyrite and trace chalcopyrite range from approximately 1-5% and occur as disseminations in the matrix and as rims on clasts. The conglomerate is a lateral equivalent to laminated siltstones which occur at the same stratigraphic level, and partly overlie the conglomerate in the J-zone and north of the Ski Hill.

2.6.6 Laminated Siltstones

Laminated siltstones composed of fine ash extend from the center of the J-zone east to the DF-zone and are continuous on the east side of the main dome complex through to the DL-zone. This unit is thought to have been deposited in a lacustrine environment. The siltstone unit is best exposed in outcrop in the eastern J-zone but outcrops sparsely in the DF-zone and DL-zone also. It is best observed in drill core of the DF-zone and DL-zone.

The siltstones in the J-zone occur as 1-5 mm laminated beds of fine volcanic ash (Plate 8) with only rare horizons containing minor amounts of volcanic lapilli. In the laminated beds slump structures, load casts, flame structures and rippled bedding have been observed. Laminated siltstones in the J-zone drill core are intercalated with the earliest ash flows which also overlie the conglomerate marker. Pyrite is disseminated throughout the unit in the J-zone but has accumulated more abundantly in some beds, and concordant massive pyrite bands, 1-3 cm thick have been observed. Minor disseminated chalcopyrite is ubiquitous. Graphitic fault breccia zones in the siltstone unit in the J-zone locally host abundant

chalcopyrite, bornite, chalcocite, galena and sphalerite and have assayed up to 5 ounces per ton silver.

In the DF-zone bedding in the siltstone marker ranges from 1-5 mm laminations to massive, and colour varies from green to black. Normal grading can be seen in the thicker laminations with the aid of a hand lense and all the sedimentary structures observed in the J-zone are present in the DF-zone. In the DF-zone the beds are locally contorted possibly due to soft sediment slumping associated with volcanic activity in the adjacent dome complex.

The base of the siltstone marker in the DF-zone is a 10 cm thick massive pyrite bed which grades upwards through 40 cm of disseminated pyrite (5-20%) into another 5 cm massive (>50%) pyrite zone. Disseminated pyrite is ubiquitous throughout the unit and there are several beds which are up to 50 cm thick and contain up to 15% pyrite with accessory sphalerite, galena and chalcopyrite. Graphitic zones are common and there are local uranium concentrations.

Some of the beds are intensely epidotized. Epidote is deposited along the bedding laminae and in discordant veinlets. Siliceous beds are locally observed.

Near the top of the unit magnetite veins up to 2cm wide are observed, at the base pyrite veins are common. Fluorite veins up to 5 mm wide cut the siltstone, but they are rare.

The equivalent siltstones in the DL-zone have a green to grey or brown groundmass. Beds are slightly coarser grained in the DL-zone with fine lapilli grading upward into fine ash. Beds range from approximately 3 cm to 1 m thick. Cherty beds are interlayered with the graded beds and range from 1 to 20 cm in thickness. The cherty beds are thought to represent chemically precipitated silica, possibly from fumarolic fluids. East of DL-zone approximately along strike a discontinuous chert body approximately 10-20 m thick is thought to represent a siliceous sinter. Although lack of outcrop prevents definite correlation, it may be the source of the siliceous beds in the siltstones.

In thin section the laminations show micro-graded bedding and segregation of opaque minerals (Plate 9). Sedimentary features such as flame structures and load casts also occur on a microscopic scale. Crystals of quartz, K-feldspar and pyrite with trace muscovite range up to 0.5 mm in the laminated beds, consolidated in an aphanitic ashy matrix which is pervasively sericitized and

Plate 8: Sample of laminated siltstone from drill core. The siltstone comprises fine ash interpretted to have been deposited in a lacustrine environment.

Plate 9: Photomicrograph of lacustrine siltstone, note the graded bedding and flame structure.


0.4 mm

locally strongly epidotized. Quartz and K-feldspar crystal fragments up to 4 mm and lithic fragments up to 2 cm have been observed in the graded beds in the DL-zone. Lithic fragments include flow-layered rhyolite, ignimbrite and basalt.

2.6.7 Welded Ash Flow Tuffs, Ignimbrites

By far the largest volume of ash flow tuffs overlie the conglomerate/siltstone marker. The ignimbrites underlying the marker are thinner but texturally similar to those overlying it. Ash flows in the Wentworth area have red, pink, grey and/or green groundmass. They range in thickness from approximately 20-75 m with some ash flow sheets up to 500 m thick. The ignimbrites are not well exposed but appear to be of very irregular thickness, possibly reflecting rugged palaeotopography.

The base of the ash flows typically comprises an unwelded fine ash layer with pumice and lithic fragments. This layer is absent in some ash flows. Where present it is overlain by an unwelded lithic fragment-rich section in which fragments are 70-90% rhyolitic and 10-30% basaltic, depending on the ash flow. There is a general decrease in the proportion of basaltic fragments up-section from the

marker bed. The lithic fragments are angular to subangular, ash to block size (up to 1.5 meters) and consist of flow-banded rhyolite, ignimbrite, basalt, spherulitic rhyolite pumice and tuffs. The larger block size fragments are rhyolitic. Lithic fragments commonly have 1-3 mm reaction rims. Distribution of fragment sizes is highly irregular but crystal fragments increase in abundance toward the top of some ash flows with up to 15%, 1-4 mm euhedral to subhedral K-feldspar crystals and 3-5%, 1-3 mm embayed quartz crystals.

Flattened pumice fragments (fiamme) are green to dark brown in colour and comprise 5-40% of the welded portion of ignimbrite sheets. Fiamme are lens-shaped, typically with bifurcated edges, and often show reverse grading (coarsening upwards). They range from 1-40 mm on the short axis and 1-40 cm on the long axis. In intensely welded zones fiamme are so highly flattened they become wispy and are commonly indented by crystal or lithic fragments during compaction. The abundance of fiamme results in a strong eutaxitic fabric (Plate 10) which is locally contorted, possibly indicating rheomorphic flow or prelithification slumping. Spherulites and lithophysae are locally abundant and glass shards, although indistinct, are common, ranging from approximately 0.1-2 cm. Rhyolite

lithic fragments in strongly welded zones commonly have indistinct edges, probably due to partial melting at the fragment boundary. Trace pyrite is disseminated throughout most ash flows, and occurs in higher concentrations locally along bedding surfaces and as infilling of pumice fragments. With a few exceptions slightly higher concentrations of pyrite occur in grey or green ash flows than in hematized ones.

In thin section the welded ash flows comprise abundant crystal and lithic fragments, glass shards and flattened pumice which define a fabric which developed during compaction and welding. The groundmass comprises very fine (±0.0075 mm) crystals of K-feldspar and quartz or very finely devitrified glass. Cavities in the groundmass range from 1-4 mm and are filled with quartz, epidote or chlorite. Pyrite is disseminated throughout the groundmass and is locally concentrated along fragment boundaries or in fractures.

Shards are completely devitrified, commonly partly chloritized and are typically cuspate (Plate 11).

Quartz crystals are anhedral to subhedral and embayed. K-feldspar crystals are euhedral to subhedral and are sometimes weakly sericitized. Both crystal types are generally strongly micro-fractured.

Plate 10: The abundance of fiamme commonly results in a strong eutaxitic fabric in the ash flows of the Byers Brook Formation.

Plate 11: Devitrified glass shard with typical cuspate shape.


PENTAX

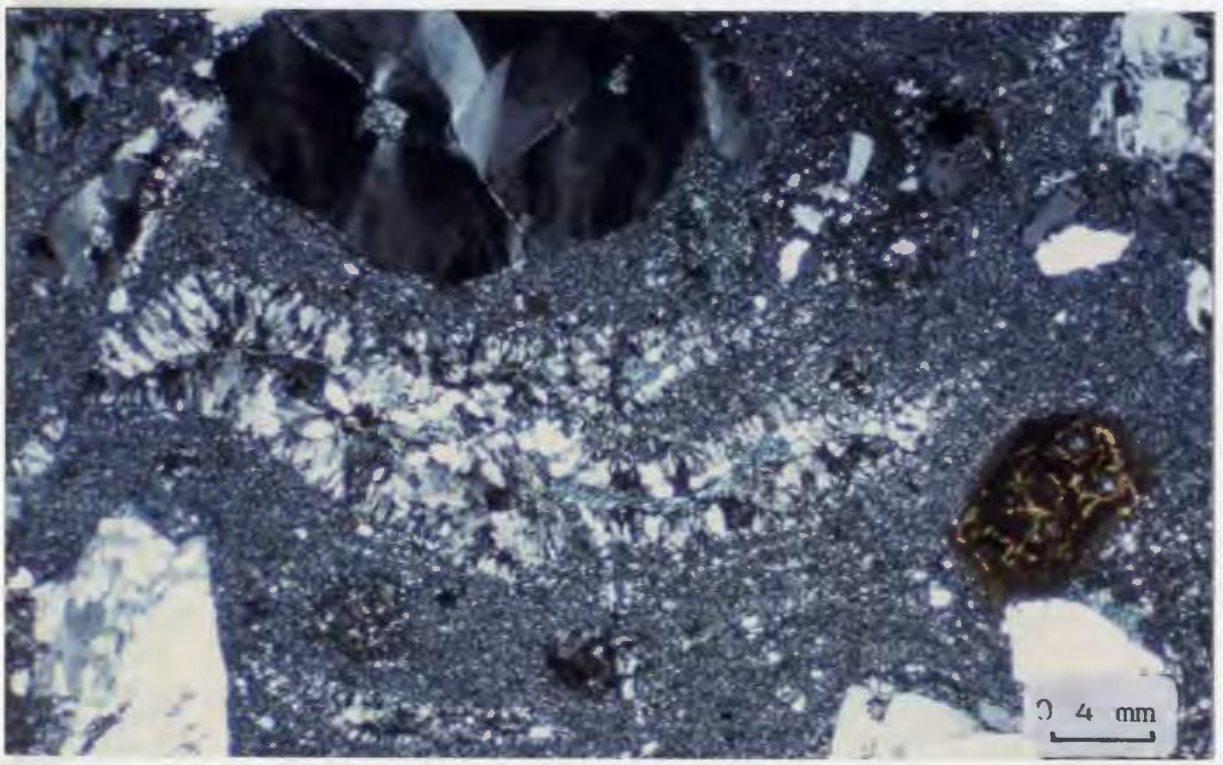
0 4 mm

Fiamme are roughly lensoid. They have completely devitrified axiolitic rims with spherulitic to aphanitically crystalline interiors and sometimes contain phenocrysts of quartz. They are often wrapped around crystal or lithic fragments during compaction and welding. Chlorite and/or pyrite commonly mark the spines of the fiamme.

Rhyolite lithic fragments in welded zones typically have ragged edges possibly indicating partial resorption. This is not observed in ash fall tuffs or unwelded parts of ignimbrite sheets. Mafic clasts are always strongly chloritized and epidotized.

2.6.8 Hart Lake Granite

The granite has intruded along the southern contact of the Byers Brook volcanic rocks and is intersected in drill core in the northern DF-zone on the edge of the main dome/flow complex. In the northern DL-zone the granite is faulted against the volcanic rocks along the East Wallace River/Debert Lake Fault. The pink hornblende granite ranges from granophyric through fine grained to medium grained (Plate 12). It is comprised of approximately 35% quartz, 30% K-feldspar, 30% plagioclase

Plate 12: Drill core specimens of the Hart Lake Granite illustrating the transition from granophyric through fine grained to medium grained (from left to right) moving progressively away from the contact with the Byers Brook Formation.

and 0.5-2% Hornblende. Biotite, ilmenite, magnetite, zircon, sphene allanite and barite are accessory minerals. Graphic and micrographic intergrowths of quartz and K-feldspar are common especially near the contact with the volcanic rocks. Pegmatite pods of quartz and K-feldspar from 5 to 20 cm wide and miarolitic cavities from 1 to 5 cm but generally less than 2cm, suggest high level emplacement. Miarolitic cavities are filled with quartz, chlorite, epidote, fluorite and/or calcite or are void with only a thin coating of quartz crystals lining the cavity. Fine grained aplite dikes and pegmatite dikes ranging from 1-30 cm wide intrude the Byers Brook Formation and the Hart Lake/Byers Lake Granite near the contact. The granite is abundantly veined along the contact with the volcanic pile by quartz, calcite, epidote, fluorite and chlorite, and in one section in drill hole DL-16 calcite - fluorite veins containing sphene, allanite, zircon and ilmenite are abundant and have elevated rare earth elements (REE), tin, tungsten and thorium values (discussed further in Chapter 4) associated with them.

2.6.9 Diabase Dikes

Diabase dikes are common and intrude all rock types in the volcanic pile and the granite. Crosscutting diabase dikes suggest episodic intrusion. The diabase dikes typically have black, aphanitic chill margins which grade into a fine grained black to dark green interior. Some dikes are porphyritic with up to 5%, 1-10 mm plagioclase phenocrysts and rarely up to 5%, 1-4 mm pyroxene phenocrysts. The plagioclase are greenish white in hand specimen and have saussuritized cores which impart their slight greenish tint. The pyroxene crystals are partly to completely altered to chlorite. The dikes are comonly magnetic, and disseminated pyrite or magnetite are ubiquitous. They have diabasic or ophitic textured groundmass except in chill margins which are 2-10 cm wide. The dikes range from 10 cm to greater than 10 m wide. Locally large areas are underlain by diabase (Fig. 4) but this is not representative of the total volume of diabase in the volcanic pile. Diabase dikes have been rotated into the horizontal, effectively increasing their outcrop area. This is especially evident on the flanks of Dotten Brook where the hilltop is underlain by diabase and the stream valley, which is a sharp topographic depression is

dominated by outcrops of felsic tuffs and ash flows. The maximum thickness of diabase dikes in the area is unknown for this reason. There is strong chloritization and epidote veining of the host rock near dike contacts, and usually hematization of rhyolite or granite. Locally strong fracturing and minor shearing has occurred along dike contacts as indicated by brecciation and slickensides. Epidote, calcite and chlorite veins are common in the dikes. The diabase dikes are moderately to strongly chloritized. They comprise 50-60% plagioclase, 30% chloritized pyroxene, 3-10% opaque minerals (magnetite and pyrite) and accessory quartz, hornblende, biotite and sphene.

2.6.10 Rhyolite Dikes and Composite Dikes

Rhyolite dikes are restricted to the main dome flow complex in the DF-zone. Composite dikes are more abundant and widespread and have been observed spatially associated with composite flows in the DF-zone, J-zone and DL-zone. Rhyolite dikes are defined as dikes of rhyolitic composition which do not have diabase on both margins. Composite dikes have diabase margins which are either in sharp contact with a rhyolitic core or grade into an

intermediate or rhyolitic core. Rhyolitic cores in composite dikes are identical in appearance to some rhyolitic dikes and in many cases there may be a transition from composite dikes to rhyolitic dikes, or the diabasic margin of some composite dikes may locally be absent. These dikes are seen only in drill core so their morphology is not easily observed. There is a marked increase in the abundance of rhyolite and composite dikes in the vicinity of the main dome complex. The dikes range from approximately 1.5-10 m thick.

There are several texturally distinct rhyolite and composite dikes which intrude the Byers Brook Formation. The most common type of rhyolite dike has 10-15% euhedral to subhedral, 1-5 mm K-feldspar phenocrysts and 5-15%, 0.5-2 mm quartz phenocrysts in a purplish to reddish brown groundmass. These dikes have sharp contact with their host rock whether it be rhyolite or diabase. They commonly have diabase on one margin and rhyolite flow on the other, suggesting that they have intruded along fissures already occupied by diabase. Emplacement of these dikes commonly caused brecciation in the adjacent country rock. Near the contacts the dikes are often green and aphyric, probably due to quenching. This chill zone is less than 10cm wide. There is locally a faint banded texture developed inside

the chill margin, similar to flow banding along the dike margins. In thin section the K-feldspar crystals and groundmass are weakly sericitized and quartz crystals are resorbed. The groundmass comprises 1-2% opaque crystallites and much less than 1% fine disseminated chlorite which represents the mafic component in the dikes. Iron oxide staining is pervasive. The groundmass ranges from granophyric to irregular shaped very fine grained (0.025-0.05 mm) quartz and K-feldspar crystals with rare spherulites.

There is a chemically distinct suite of peralkaline rhyolite dikes, which are different from all other rhyolitic rocks in the area. They consistently contain between 1100 ppm and 1600 ppm zirconium in abundant zircons (Plate 13 and 14). These dikes are very continuous in the DF-zone, associated with the main dome complex and cut all other stratigraphy and dikes. They are thought to represent the last magmatic event in the DF-zone. They are texturally distinct from all other rhyolitic rocks in the map area. The peralkaline dikes have been rotated with the stratified units such that they are now subhorizontal. Two texturally distinct peralkaline dikes occur in the DF-zone dome complex. One set of dikes is strongly porphyritic with 5-10%, 0.5-2 mm euhedral to subhedral K-feldspar

Plate 13: The zircon-rich rhyolite dikes (on the right) are characterized by either a strongly porphyritic rhyolite dike,comprising 30-40% K-feldspar phenocrysts, or a completely divitrified dike comprising dominantly spherulites, with generally less than 3% K-feldsar phenocrysts. The sample with the coin has developed riebeckitic oikocrysts, indicating deutiric metasomatism of the dikes. The high-Zr composite dikes (on the left) are characterized by an intermediate core with K-feldspar phenocrysts and either grade outwards into or are in sharp contact with a diabasic margin.

Plate 14: Photomicrograph showing the strongly devitrified, but relatively unaltered groundmass of a peralkaline rhyolite dike. Note the very fine zircons (circled).

Plate 15: Rhyolitic globules in a mafic groundmass cause the banded appearance which characterizes the contacts of the late rhyolitic and composite peralkaline and subalkaline dikes.

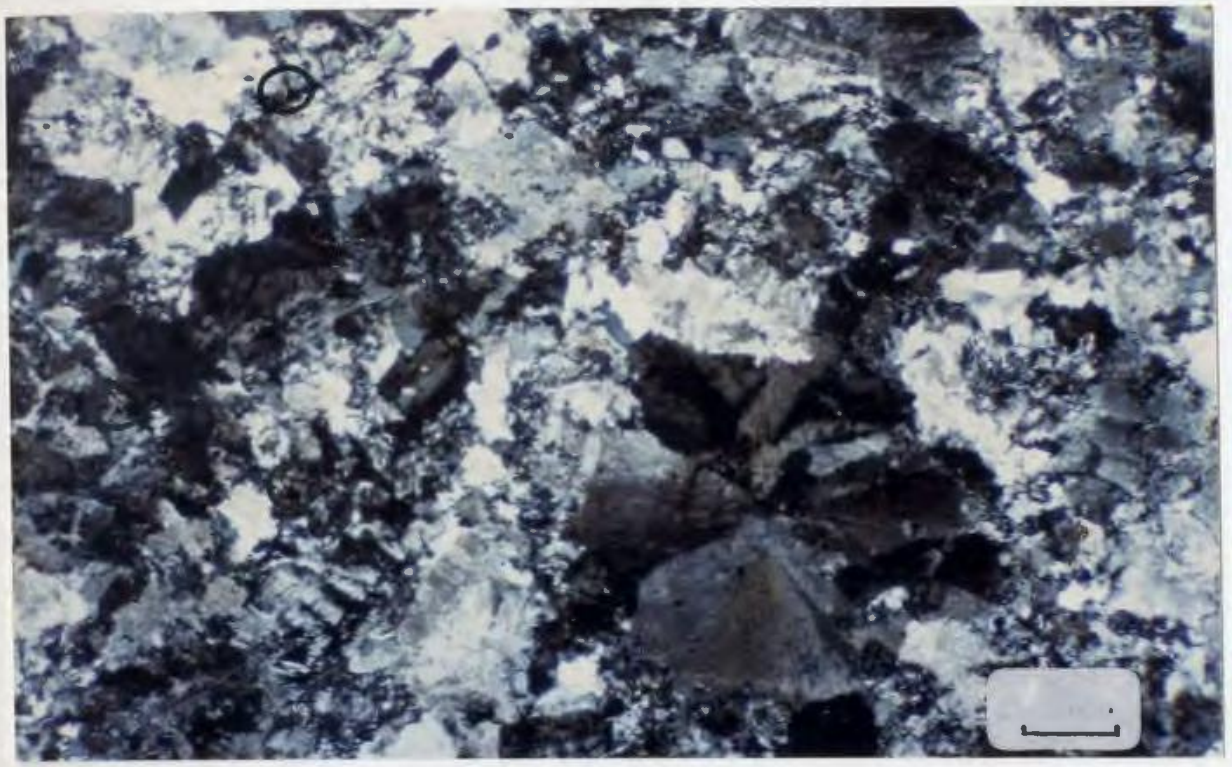

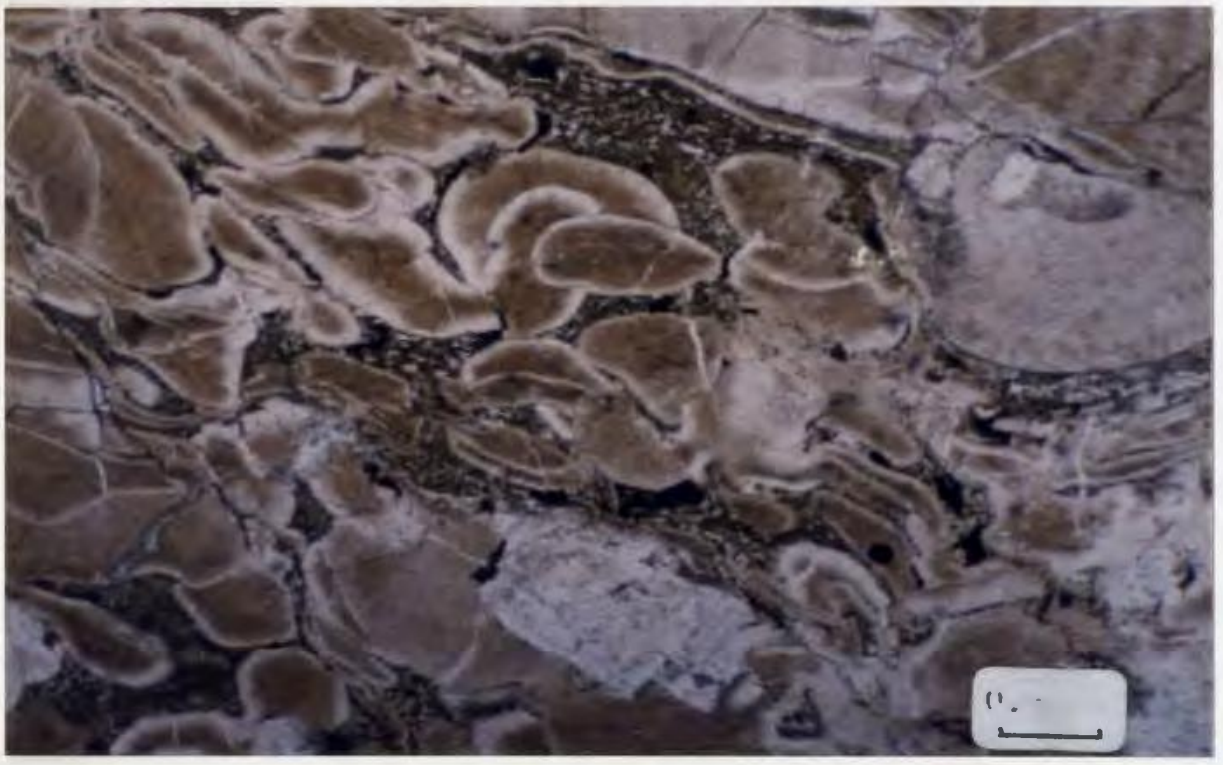

crystals, 2-5% 0.5 mm quartz phenocrysts and approximately 1% biotite in a microspherulitic groundmass. The other set comprises less than 1-3% K-feldspar phenocrysts in a groundmass of microscopic to 2 cm diameter spherulites. In thin section, spherulites commonly grade into narrow granophyric zones which in turn grade into very fine grained irregular shaped crystals of quartz and K-feldspar. This second set of peralkaline rhyolite dikes characterized by the larger spherulites, locally has developed riebeckitic oikocrysts (for example the sample with the coin on it in Plate 13). The development of reibeckite oikocrysts in a strikingly similar geological setting, in the Topsails alkaline/peralkaline complex of Newfoundland has been interpretted by Taylor et. al. (1980, 1981) and Strong and Taylor (1983) and Strong and Coyle (1988), to indicate deuteric-metasomatic activity.

Both types of rhyolite dikes commonly have aphyric banded margins. The banding is a series of stretched globules of felsic material (Plate 15) in a mafic groundmass, caused by immiscibility of the felsic magma in mafic magma which lined the fissures along which the dikes were intruded. The dikes have accesory zircon, sphene, allunite, riebeckite and chlorite. Minor pyrite is

disseminated throughout and locally occurs in micro-veinlets.

The most common type of composite intrusive in the Byers Brook Formation is simply a peralkaline or metaluminous rhyolite dike with diabasic margins. The contact between the rhyolitic core and diabasic margins is usually sharp, but some dikes have a transition zone which is 3-10 cm wide. Inclusions of diabase are common in the rhyolitic portion of these dikes. Smaller inclusions are either drop-shaped or angular, but with only a drill core intersection it is difficult to distinguish between xenoliths and magmatic enclaves. The oblate shapes of some inclusions suggests that both are present.

The other types of composite dikes present in the DF-zone are dikes with mafic margins which either grade into or are in sharp contact with an intermediate core (Plate 13). The gradational zone when present, ranges from 5 to 10 cm wide. Depending on the dike, the core may have a diabasic-textured groundmass with quartz and K-feldspar interstitial to the plagioclase laths, or the dike core may be basaltic with abundant K-feldspar phenocrysts and only minor quartz in the groundmass. Others are more siliceous, with up to 67% SiO_2, but most commonly have between 60-65%

SiO_2. The cores of the dikes are commonly altered to a red brown colour, the margins are dark green to black and chloritized. Banding and stretched globule-like structures similar to those observed in the margins of composite dikes with rhyolitic cores are seen in the composite dikes with intermediate cores.

CHAPTER 3

Geochemistry and Alteration

3.1 Introduction

The analyses used in this study are of samples of diamond drill core and outcrops taken over the span of the Cobequid exploration program of Gulf Minerals Canada Ltd. A total of 459 rock samples from the project area were split for thin section and analysis. A discussion of analytical and sampling techniques is included in Appendix 2 and sample locations are tabulated in Appendix 3. Geochemical analysis are compiled in Appendix 4. All analyses were done by X-Ray Assay Laboratories, Ontario.

3.2 Summary

The Byers Brook Formation is a bimodal suite (with respect to SiO_2) divisible into rhyolitic and basaltic compositions. The exceptions to this are a volumetrically small suite of composite dikes in which magma mixing has resulted in dacitic compositions. Bulk rock compositions of some tuffs and ignimbrites are dacitic because of high

proportions of mafic lithic fragments. Some felsic rocks are depleted in SiO2 as a result of hydrothermal alteration. The volcanic rocks of the Byers Brook Formation have been subject to varying degrees of alkali metasomatism. The Hart Lake Granite and late rhyolite and composite dikes were not as strongly affected by this metasomatism, suggesting that it was a late but not the last magmatic event. Possibly the mobilization of alkalis coincided with the emplacement of the late rhyolite dikes. The granophyric margin of the granite shows the same metasomatic effects as the extrusive rhyolites, although fine grained granite just 20 m away is unaffected so it is probable that the alkali metasomatism was caused by late magmatic fluids from the crystallizing granite.

The felsic rocks of the Byers Brook Formation are metaluminous, except for the high-Zr rhyolite and composite dikes which are peralkaline, suggesting that an alkaline phase was developed in the apical regions of the magma chamber represented by the metaluminous Hart Lake Granite.

3.3 Alteration

Geochemical classification of volcanic and igneous rocks can be employed to indicate tectonic environments in which the rocks formed (e.g., Pearce and Cann, 1973; Floyd and Winchester, 1975; Miyashiro, 1975; Winchester and Floyd, 1977; Bailey, 1981). To ensure the effectiveness of geochemical discrimination an assessment of the alteration is necessary.

The most widespread alteration affecting the Byers Brook Formation is alkali metasomatism. The analyses of all rock types have been plotted on the Igneous spectrum diagram (Fig. 11, from Hughes, 1972). Points which plot outside the igneous spectrum field have been metasomatically altered with a resultant gain in either sodium or potassium. Hughes (1972) contends that combinations of metasomatic affects can cause points to plot incorrectly inside the igneous spectrum field and that if a large proportion of analyses plot outside the field then it should be considered that all rocks of the suite have been somewhat affected by metasomatism.

Figures 11a-c show that the felsic rocks of the Byers Brook Formation have undergone strong and pervasive K-metasomatism. Most felsic extrusive rocks plot to the

Figure 11: Igneous spectrum diagrams for the volcanic rocks of the Byers Brook Formation (after Hughes, 1972). Symbols for the J-zone, DL-zone and DF-zone are:

Ash flows and tuffs - O
Rhyolite flows - ●
Diabase dikes - X
Basalt flows - +

Symbols for the granite and High-Zr dikes are:

Granite - X
High-Zr rhyolite dike - ●
High-Zr composite dike - O

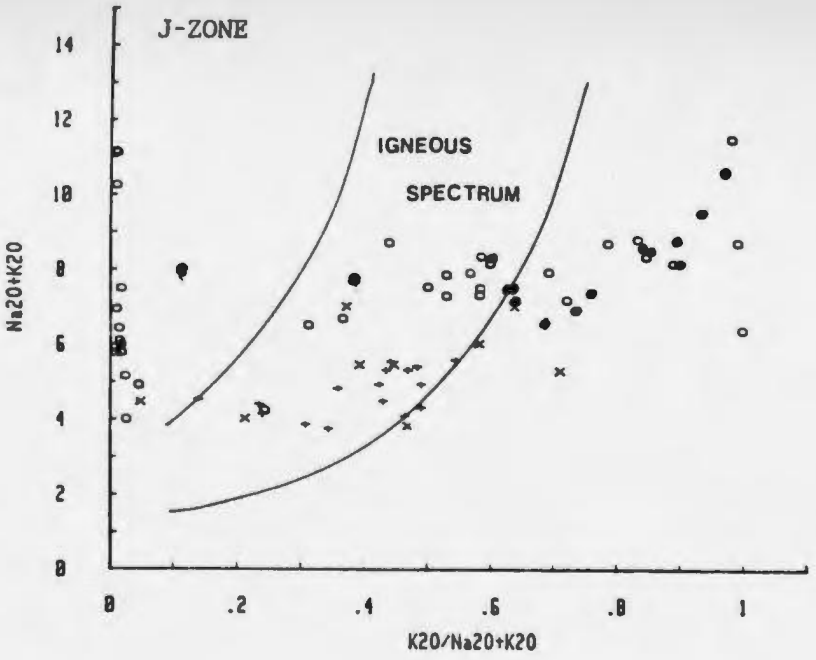
J-ZONE
IGNEOUS
SPECTRUM
Na2O+K2O
K2O/Na2O+K2O

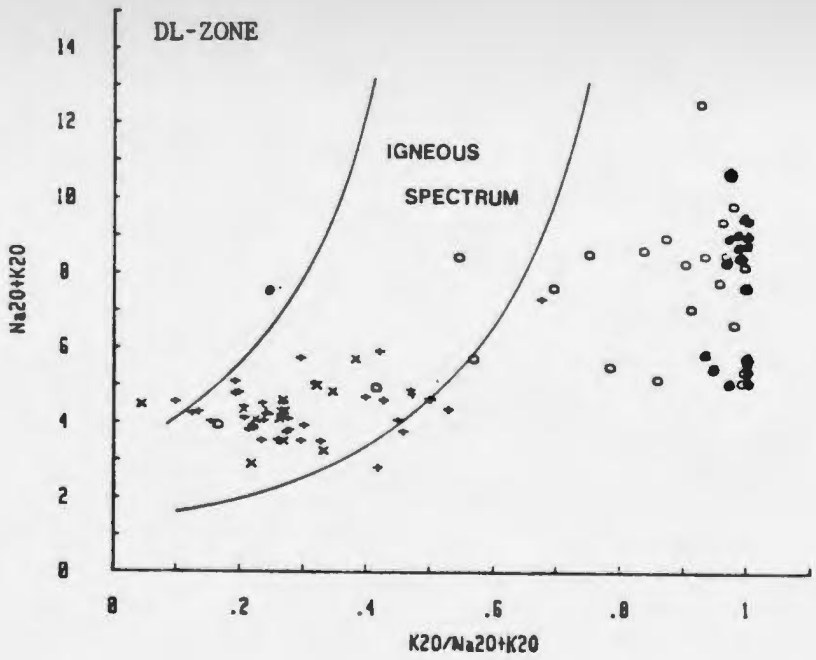
DL-ZONE
IGNEOUS
SPECTRUM
Na2O+K2O
K2O/Na2O+K2O

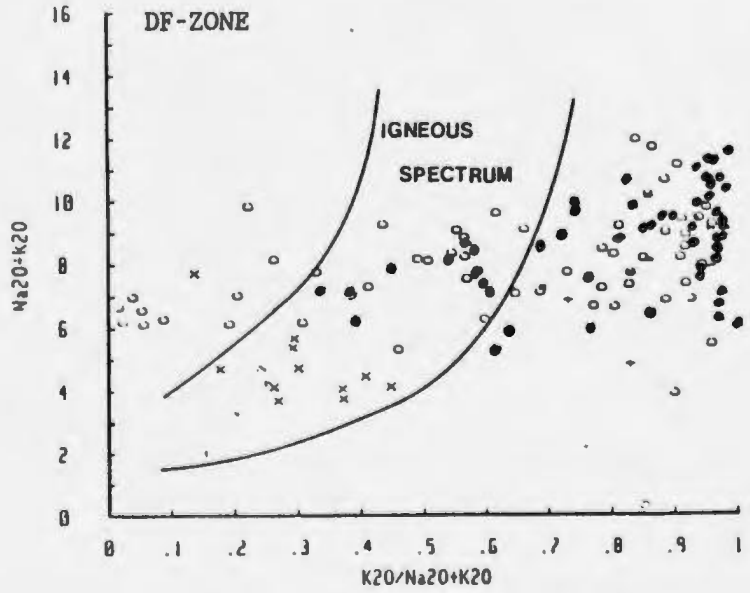
DF-ZONE
IGNEOUS
SPECTRUM
Na2O+K2O
K2O/Na2O+K2O

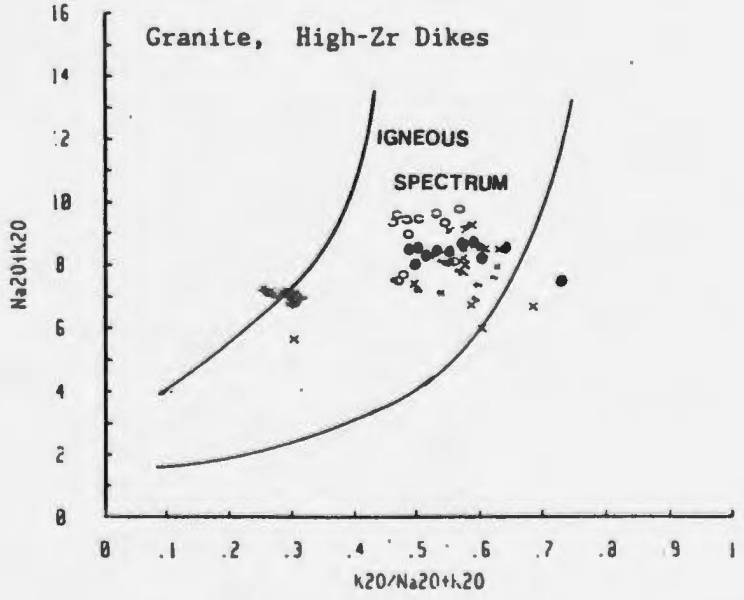
Granite, High-Zr Dikes
IGNEOUS
SPECTRUM
Na2O+K2O
K2O/Na2O+K2O

right of the igneous spectrum except for a zone of strong Na-metasomatism which affected some of the ignimbrites of the J-zone and small zones within the the DF-zone ignimbrites. The Hart Lake granite and the high-Zr composite and rhyolite dikes plot inside the igneous spectrum boundary. The granophyric margin of the granite plots outside the igneous spectrum, suggesting that the alteration was caused by hydrothermal fluids which were in circulation prior to the crystallization of the main granite mass and the emplacement of the high-Zr dikes. Plate 16 shows the variation in degree of K-metasomatism ranging from a relatively unaltered high-Zr rhyolite dike to strongly altered rhyolite flow with a strongly sericitic groundmass to the most highly altered end-member in which the rock is completely converted to potassium feldspar. These rocks which have been completely altered to K-feldspar commonly maintain their primary volcanic textures. Table 4 lists the whole-rock analyses of the samples in Plates 16 and analysis of orthoclase from Deer et al., (1978) and clearly shows the progression of K enrichment from a rock which is typically rhyolitic to one which has a composition corresponding to K-feldspar.

Plate 16 (a-d): Photomicrographs of rhyolites from the Byers Brook Formation which have been affected by alkali metasomatism.
a) Moderate K-metasomatism of a spherulitic rhyolite flow. The spherulitic texture is preserved but the rock has abundant sericite developed throughout the groundmass.
b) Strong K-metasomatism has resulted in the development of a rock comprising almost entirely very fine, irregular K-feldspar crystals, with minor chlorite and epidote and rare zircons the only other minerals preserved in the groundmass of the rock.
c) Relatively unaltered rhyolite dike comprising quartz, K-feldspar and plagioclase, with a well preserved spherulitic texture.
d) Strong Na-metasomatism and moderate silicification characterized by a rock comprising very fine, irregular albite crystals and slightly larger quartz crystals with minor epidote.

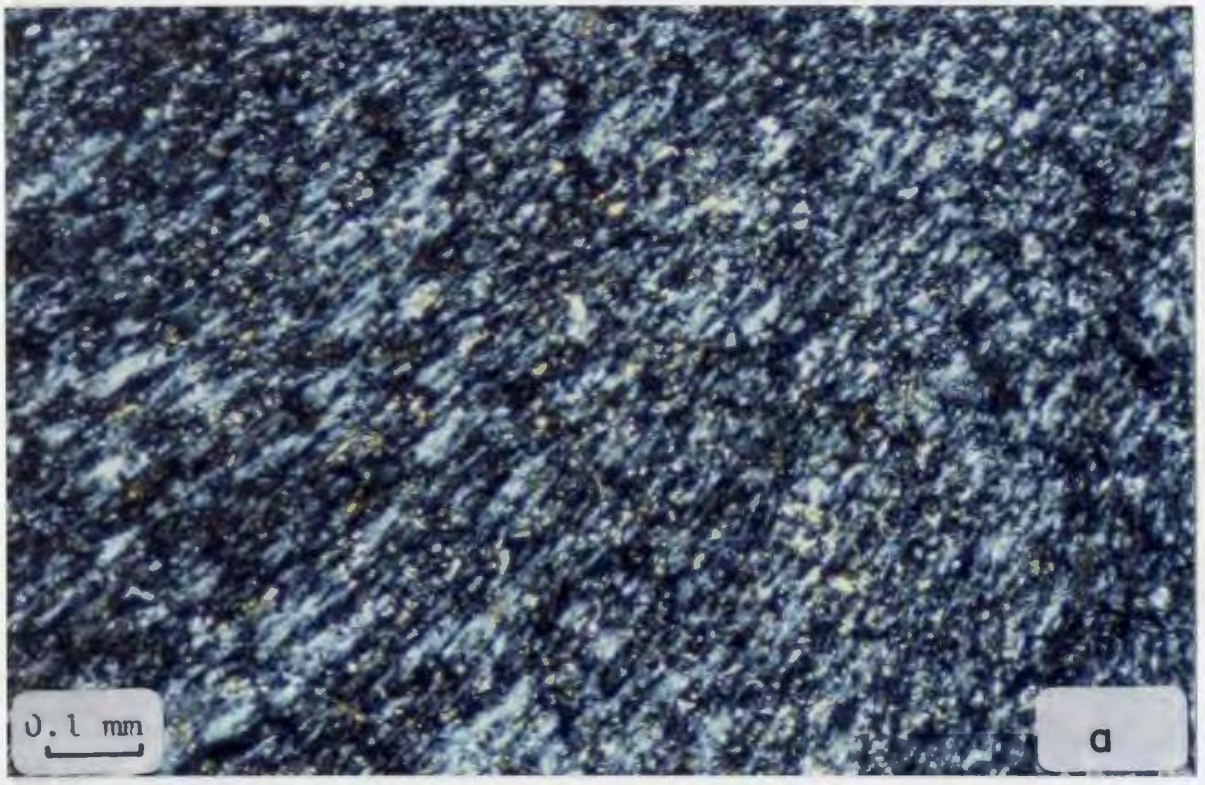
0.1 mm
a

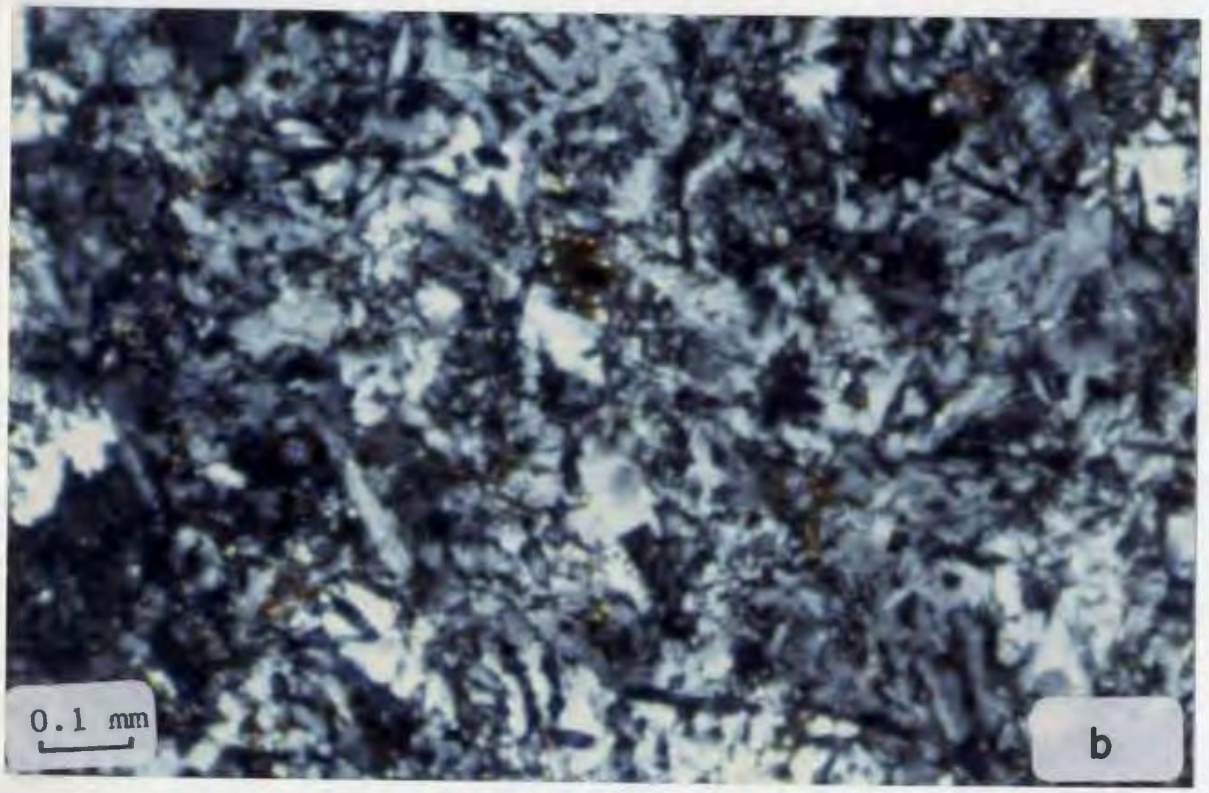
0.1 mm
b

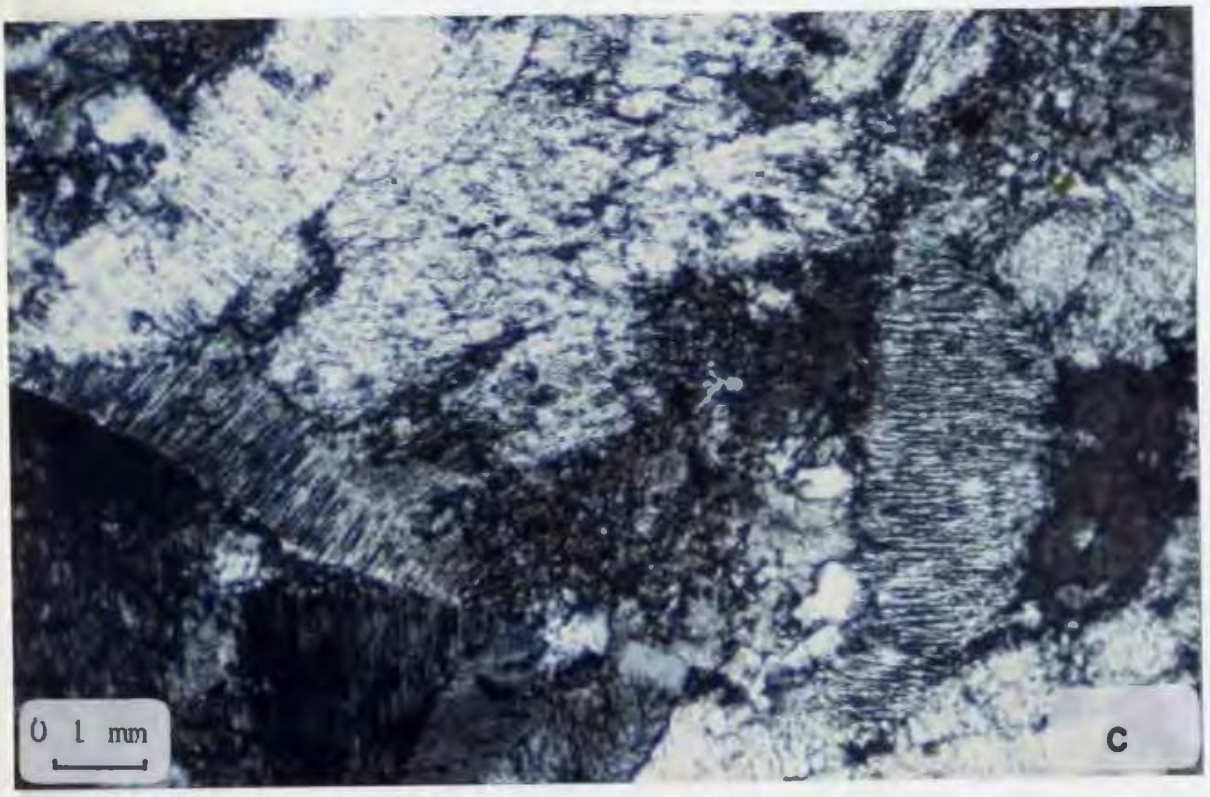
0 1 mm
c

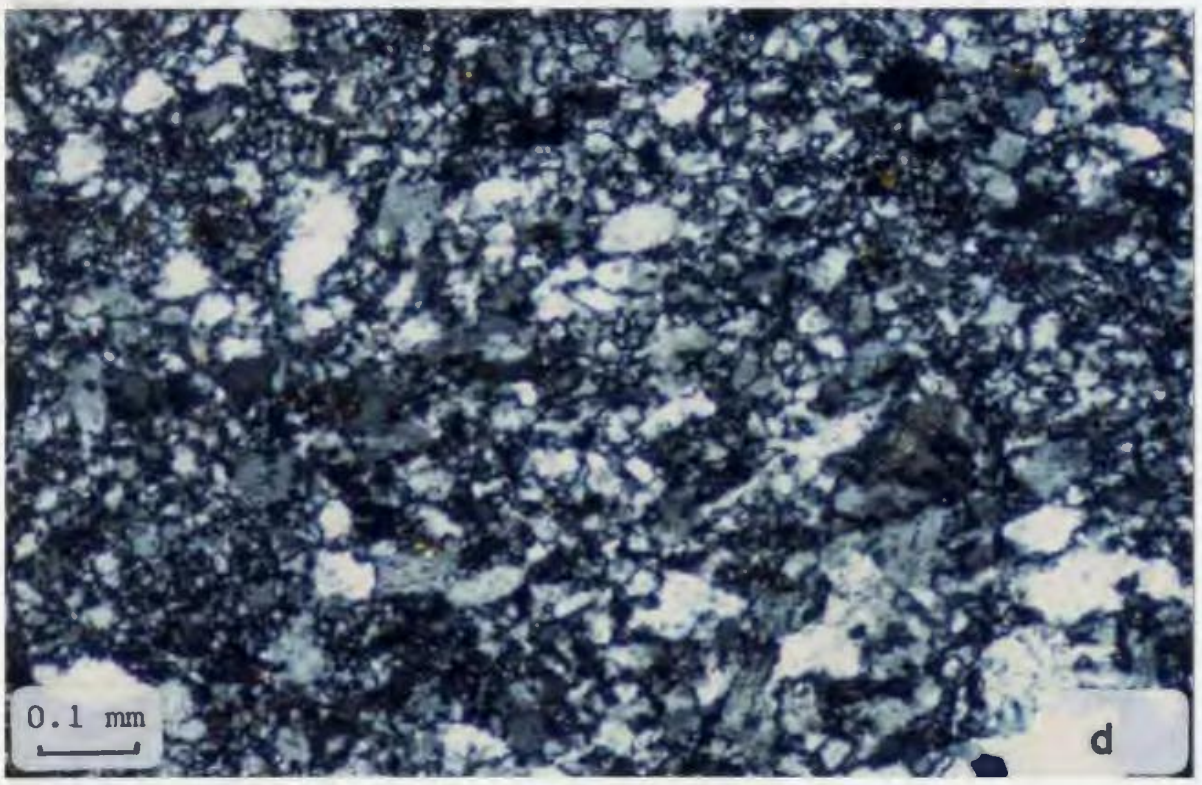
0.1 mm
d

Table 4: Analysis of samples characterizing various stages of alkali metasomatism, from unaltered to strongly altered. Analyses correspond to samples in Plate 16. Analyses of orthoclase and albitite are included for comparison.

Sample	-a-	-b-	-c-	-d-	K-feld*	Alb.**
Sio2	77.5	62.3	78.1	64.56	63.66	61.27
TiO2	.13	.28	.16	.42	--	.09
Al2O3	11.7	18.6	10.4	17.14	19.54	17.79
FeO	1.90	3.39	1.17	3.68	.10	.59
MnO	.07	.02	.02	.07	--	.23
MgO	.41	.53	.29	.39	--	.09
CaO	.21	.30	1.64	5.08	.50	9.58
Na2O	.28	.64	3.20	8.12	.80	10.19
K2O	6.92	13.10	4.45	.14	15.60	.08
P2O5	.02	.03	.01	.38	--	.09
LOI	1.00	1.16	.77	.92	--	.55
Total	100.14	98.35	100.21	97.84	100.2	98.5

* Analysis of orthoclase from Deer et. al. (1971) p. 300.
** Analysis of albitite from Strong, (1982).
a - Sample # R1286
b - Sample # R1251
c - Sample # R1271
d - Sample # B3127

Sodium enrichment is not nearly as widespread as K enrichment. Albitization is best observed in an irregular halo surrounding mineralization in the ignimbrites of the J-zone and in smaller zones in the DF-zone ignimbrites. Strongly albitized rhyolite is compared with potassic altered and unaltered rhyolite in Plate 16. In the relatively unaltered rocks primary features such as spherulites and flattened pumice are abundant and there are numerous quartz veinlets, whereas in the altered rocks only rare sericitized K-feldspar phenocrysts and clots of epidote and iron oxide are preserved. Very narrow calcite veinlets and rare fluorite veinlets fill fractures in these rocks, primary volcanic textures are completely destroyed and the groundmass comprises very fine grained anhedral albite crystals with trace accessory zircons such that the originally rhyolitic rock has been metasomatically altered to albitite.

All rocks in the area, but particularly the felsic ones, are strongly microfractured and alkali enrichment is highest adjacent to the fractures and in strongly brecciated fault zones, suggesting that metasomatism was fracture controlled. Plate 17 shows finely fractured rhyolite from the DF-zone. Fractures are marked by a thin selvage of completely K-metasomatized

Plate 17: Outcrop of porphyritic rhyolite flow. The weathering shows the strongly fractured nature typical of the rocks of the Byers Brook Formation. The bleaching adjacent to the fractures marks an alteration selvage of more intense K-metasomatism, indicating that these fractures acted as channel-ways for the fluids responsible for the pervasive alkali metasomatism.

rhyolite in an otherwise moderately K-metasomatized rock.

There is approximately an inverse relation between K and Na in the moderately altered rocks suggesting that Na-K exchange was the metasomatic replacement process active up to a point (Fig. 12). In the most altered rocks, however, there is an overall increase in Na+K whether the rocks were K-metasomatized or Na-metasomatised. These rocks (with <14% Al_2O_3) are responsible for the strong negative slope seen in the Al_2O_3 versus SiO_2 plot (Fig. 13) suggesting a net increase of Al and loss of Si to accomodate continued production of hydrothermal feldspars.

Secondary minerals occur in variable amounts throughout the rhyolite flows and pyroclastic rocks. These include epidote, quartz, chlorite, calcite and rarely fluorite as very fine clots or micro-veinlets and range from trace amounts to approximately 5% of the rock. Free quartz occurs in most felsic rocks other than those which have been subject to the most extreme alkali metasomatism. Quartz phenocrysts are common but quartz in veinlets and filling cavities suggests that silicification is responsible for the SiO_2 whole-rock values which are commonly over 77%. There is a zone of ignimbrites directly overlying the main dome/flow complex in the DF-zone which is strongly silicified with 80-85% SiO_2. These rocks have

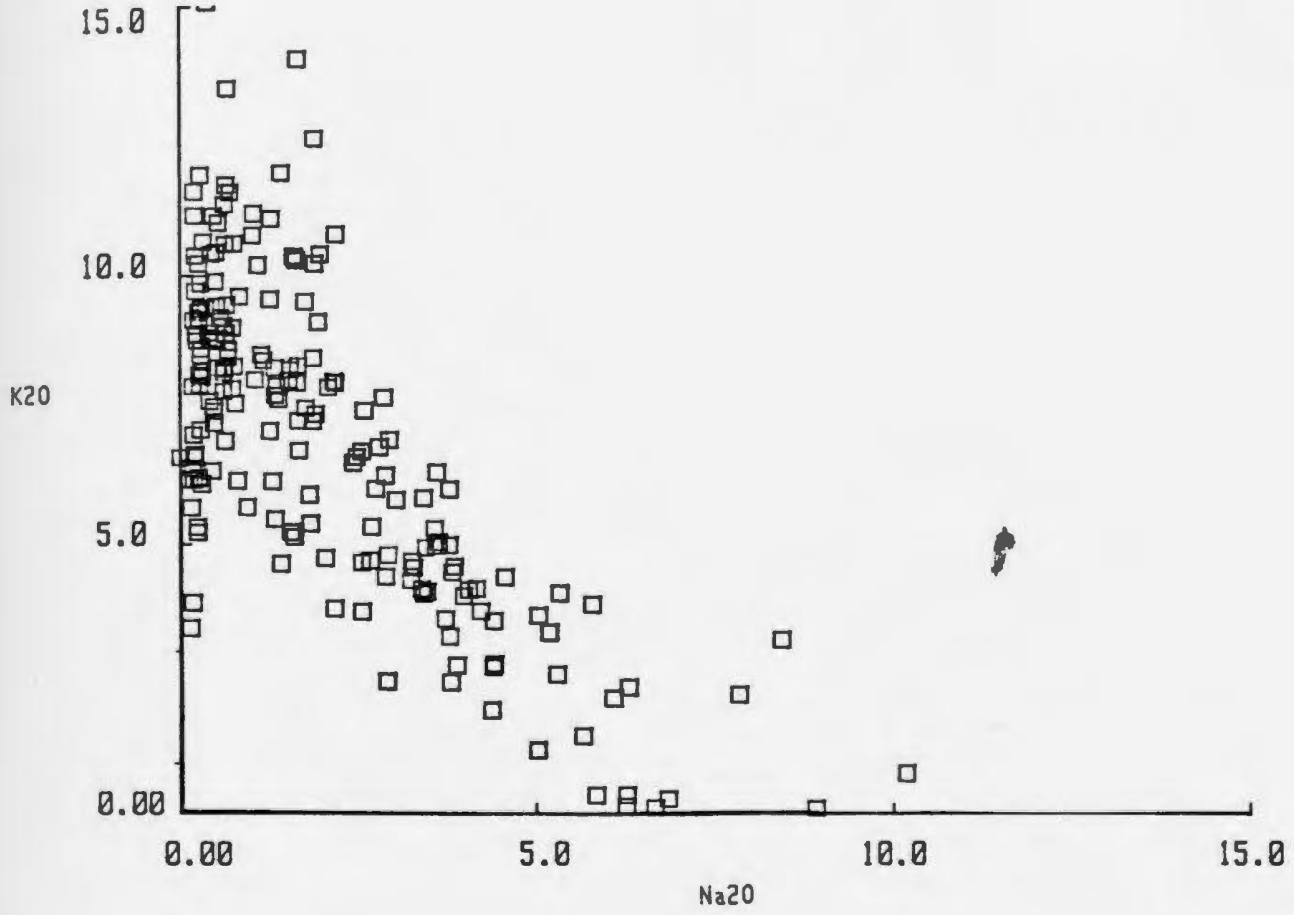

Figure 12: Plot of K2O versus Na2O for rhyolite flows and ash flows of the Byers Brook Formation. The strong negative slope indicates that Na - K exchange was a dominant mechanism in the alkali metasomatism.

abundant quartz microveinlets and a very quartz rich groundmass which locally appears cherty. Epidote, chlorite and calcite are notably more concentrated near (within approximately 0.5m) of diabase dikes and in strongly brecciated zones. In these zones strong chlorite and epidote alteration of the rhyolitic groundmass occurs and the rock may contain up to 20% of these minerals.

The rhyolitic rocks are green or red, depending on the oxidation state of iron, which appears to have been partly controlled by whether the rock was deposited in water, as denoted by the bedding characteristics of the interbedded tuffs. In the zone which is dominated by green flows and ignimbrites there are extensive zones of iron oxidation in the groundmass and hematite altered selvages up to 5 mm wide commonly occur adjacent to fractures and veinlets. The fractures are commonly filled by quartz, epidote, calcite and rarely fluorite.

The high-Zr composite and rhyolite dikes and the granite are relatively unaltered. Microscopic epidote, quartz, calcite and fluorite veinlets fill fractures in these rocks. Locally epidote veins are abundant enough to have a significant influence on the whole-rock geochemistry of the high-Zr dikes. The granophyric margin of the granite has undergone K-metasomatism and comprises very

fine grained, irregularly shaped K-feldspar crystals with minor quartz and chlorite and trace zircon, sphene, allanite and opaques.

The basalt flows and diabase dikes are variably altered, ranging from minor chloritization of pyroxene to complete chloritization of the mafic minerals and strong saussèritization of the plagioclase. Amphibole occurs in many mafic dikes and flows but is usually partially replaced by chlorite. The amphibole most commonly occurs as discrete crystals interstitial to the plagioclase lathes but locally replaces pyroxene. The least altered mafic rocks are dikes which may have been intruded late in the magmatic history of the Byers Brook Formation. Increasing alteration corresponds to an increase in fracturing and density of veinlets.

Chlorite, epidote and calcite veinlets are the most common secondary minerals, and with a few exceptions quartz and fluorite veins are rare in the mafic rocks. Sphene is a common accessory mineral in the basalts, and opaques comprise 3-5% of the mafic rock composition. Microscopic vesicles are common in the basalts and diabase dikes. These may rarely constitute up to 1% of the rock volume but usually much less. The vesicles are most commonly filled with chlorite and/or epidote.

Keppie (1979) indicates that the Fountain Lake Group was metamorphosed to sub-greenschist facies. The presence of pumpellyite and prehnite in the basalt flows and diabase dikes near the Byers Brook/Diamond Brook Formation contact suggest the rocks were metamorphosed to pumpellyite-prehnite facies as defined by Winkler (1979). Prehnite and pumpellyite are not preserved in the Byers Brook Formation in the J-zone, DF-zone or the DL-zone, 2-3 Km stratigraphically lower than the rocks at the Byers Brook/Diamond Brook Formation contact. This deeper burial may be responsible for a slight increase in metamorphic grade. Probably more significant, however, the stratigraphically lower rocks are closer to the Hart Lake/Byers Lake Granite contact where temperatures were elevated and hydrothermal alteration is pervasive.

In summary, the volcanic rocks of the Byers Brook Formation have been subjected to varying degrees of hydrothermal alteration which strongly influences the whole rock analyses of these rocks. This chemical alteration complicates geochemical discrimination of the rocks especially in diagrams which are based on mobile elements such as alkalis.

3.4 Geochemistry

Abundance of the major oxides and trace elements are plotted against SiO2 in Figure 13. The geochemical data are presented for each of the J-Zone, DF-Zone and DL-zone described in Chapter 2. The primary reasons for this division are to illustrate differences between the three zones and that the very large data base tends to become illegible when all analysis are plotted on a single diagram. The diagrams show a distinctly bimodal suite with respect to silica for all three zones. The mafic rocks consistently contain 45-51% SiO2 and the felsic rocks consistently contain 65-80% SiO2. Affects of hydrothermal alteration, especially alkali metasomatism and silicification contribute significantly to the wide range of major elements in rocks of presumed similar primary composition. The widest relative scatter in the Harker Diagrams is in the pyroclastic rocks, especially of the DF-zone in which there has been contamination by mafic material coupled with strong and pervasive alteration. Much of the mafic material responsible for the contamination in the tuffs is very fine grained and cannot be avoided during sampling. All rock types show a wide

Figure 13: Harker variation diagrams for the extrusive rocks and the diabase dikes of the Byers Brook Formation. The symbols represent:
O - ash flows and tuffs
* - rhyolite flows
+ - basalt flows
X - diabase dikes
Graduations on axis with major oxides are in %, and with trace elements are in ppm.

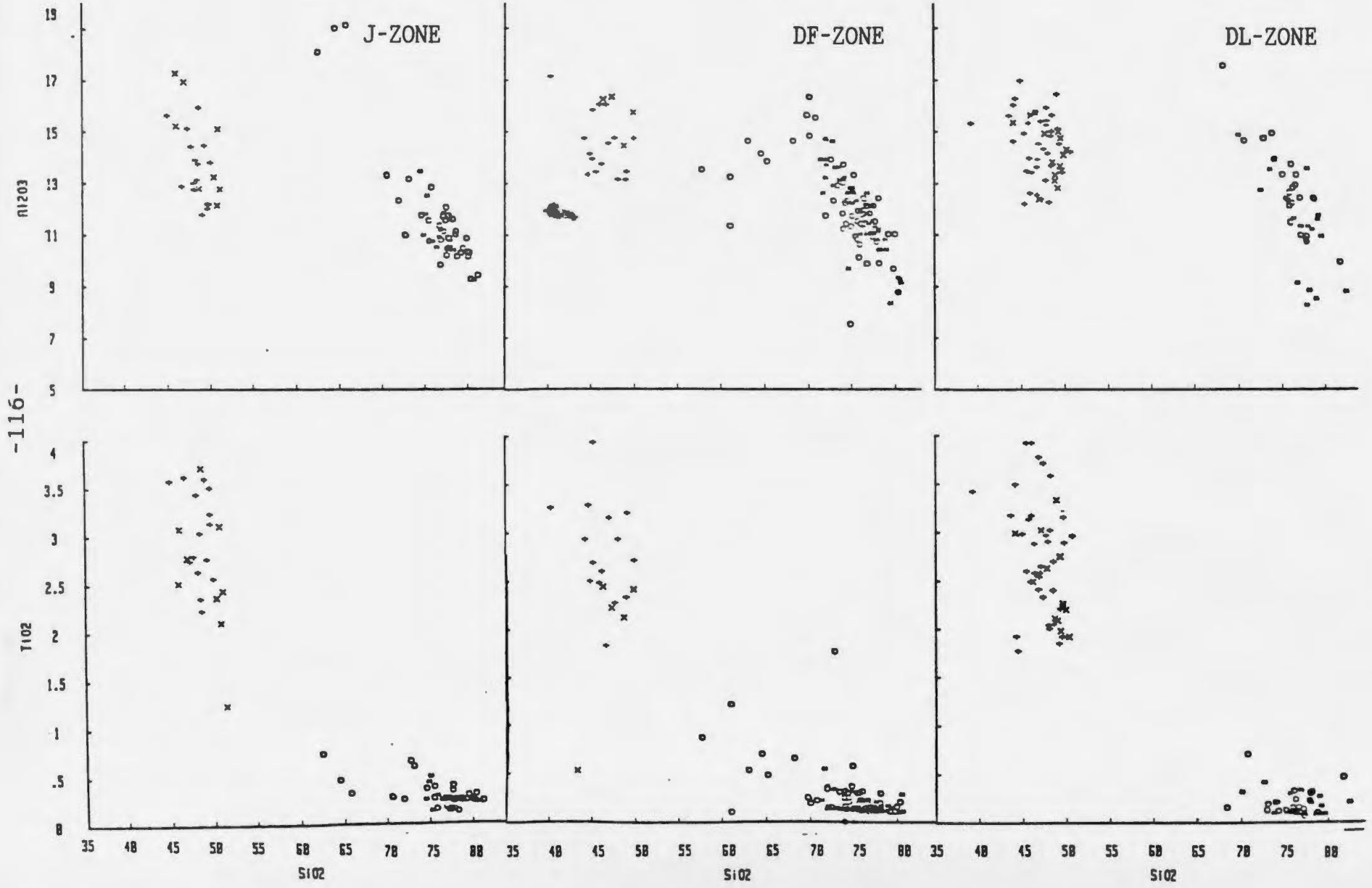
J-ZONE
DF-ZONE
DL-ZONE
Al2O3
TiO2
SiO2
19
17
15
13
11
9
7
5
4
3.5
3
2.5
2
1.5
1
.5
0
35 40 45 50 55 60 65 70 75 80

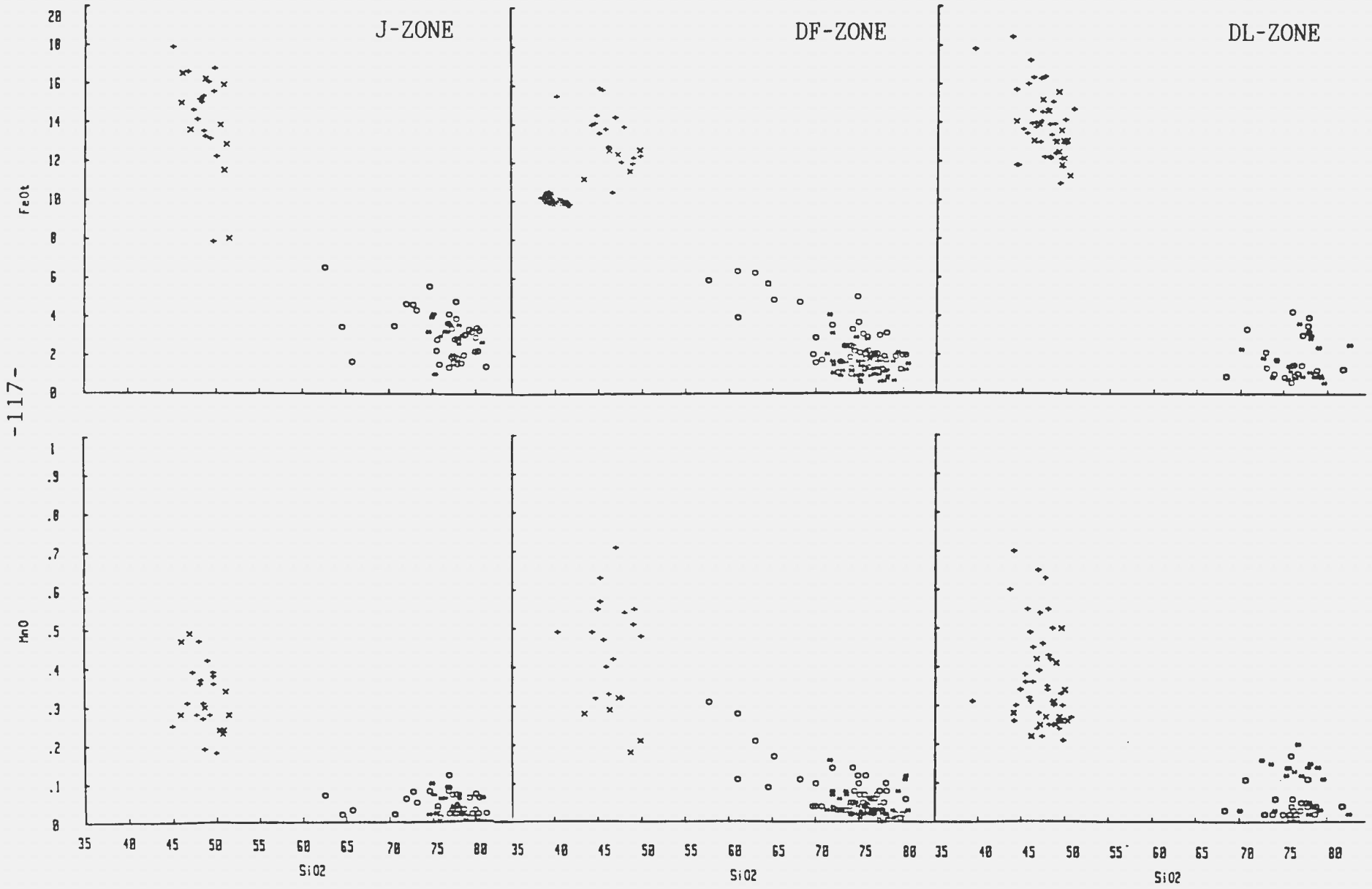
J-ZONE
DF-ZONE
DL-ZONE
FeOt
MnO
SiO2
SiO2
SiO2

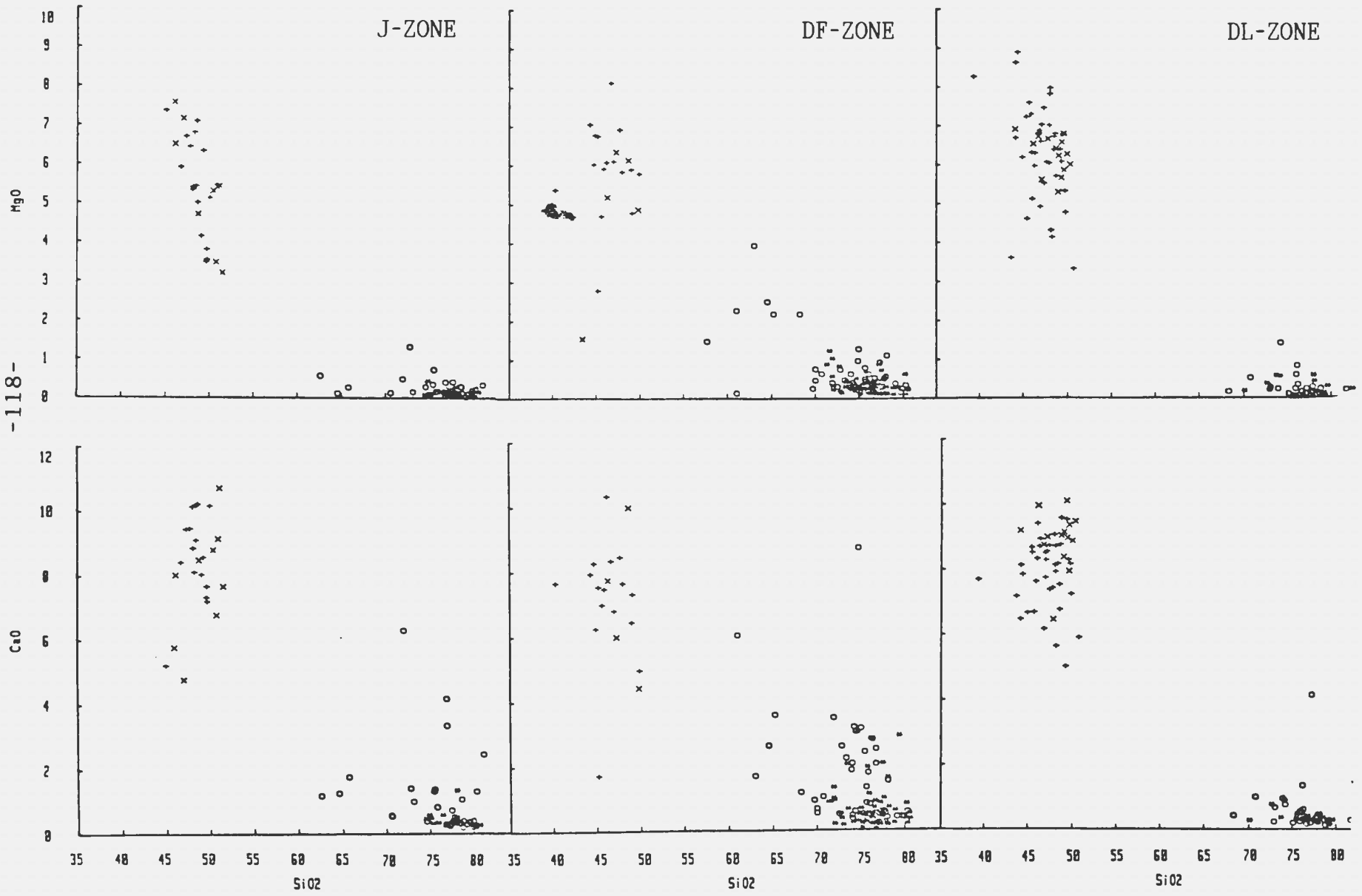
J-ZONE
DF-ZONE
DL-ZONE
MgO
CaO
SiO2
SiO2
SiO2

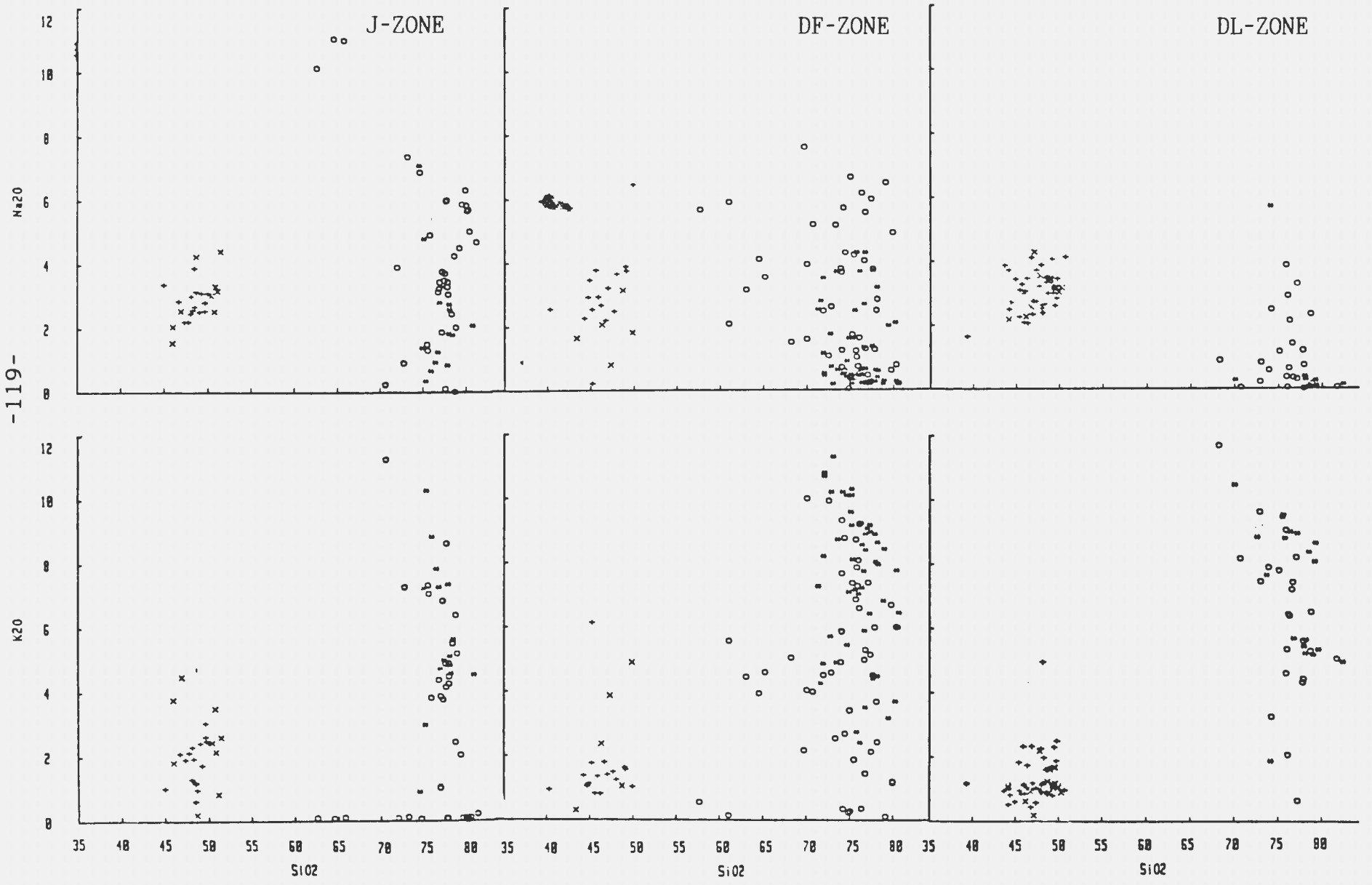
J-ZONE
DF-ZONE
DL-ZONE
Na2O
K2O
SiO2
0
2
4
6
8
10
12
35
40
45
50
55
60
65
70
75
80

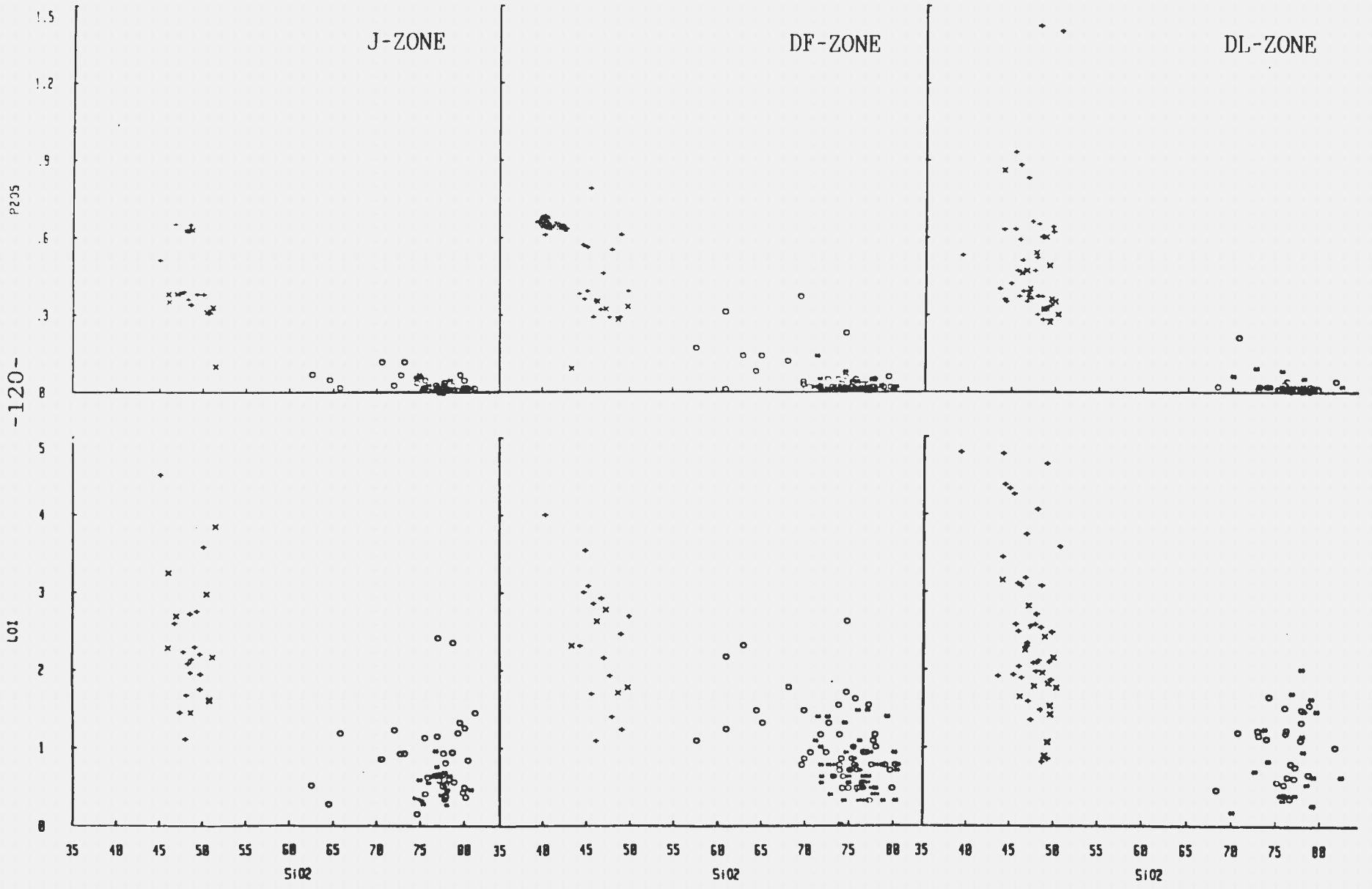
J-ZONE
DF-ZONE
DL-ZONE
P2O5
LOI
SiO2
-120-

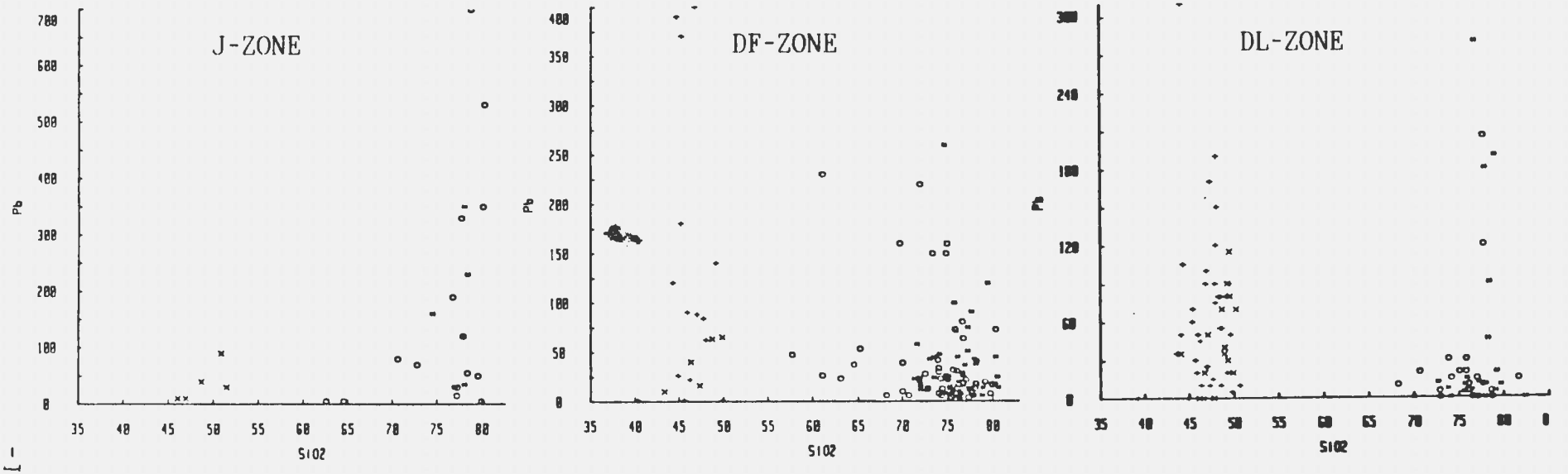
J-ZONE
DF-ZONE
DL-ZONE
Pb
SiO2

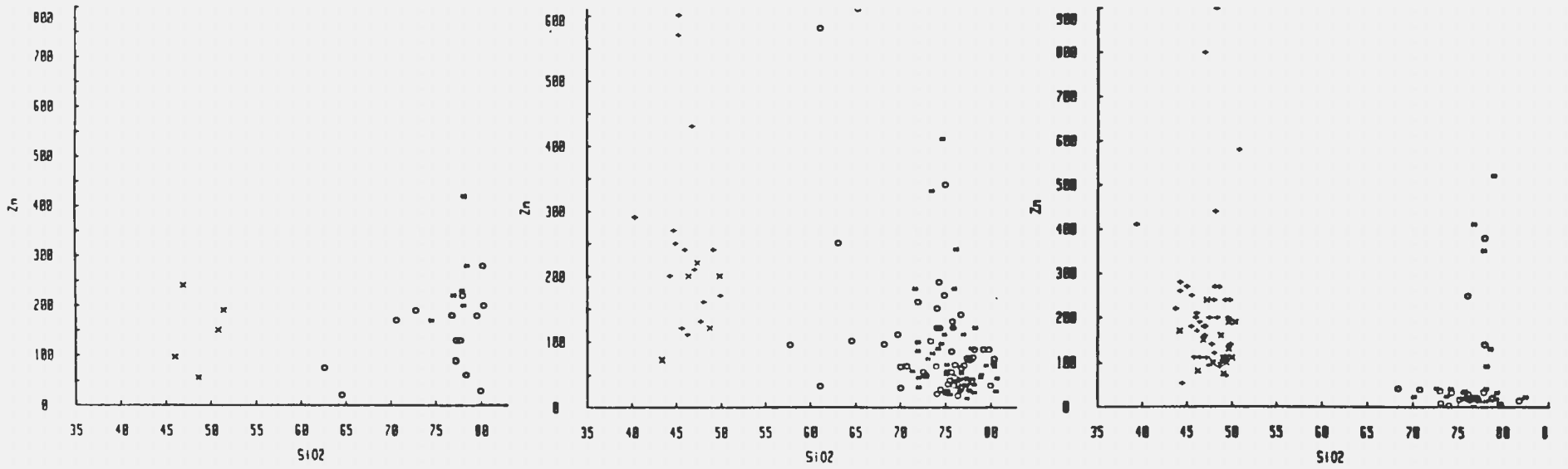
Zn
SiO2

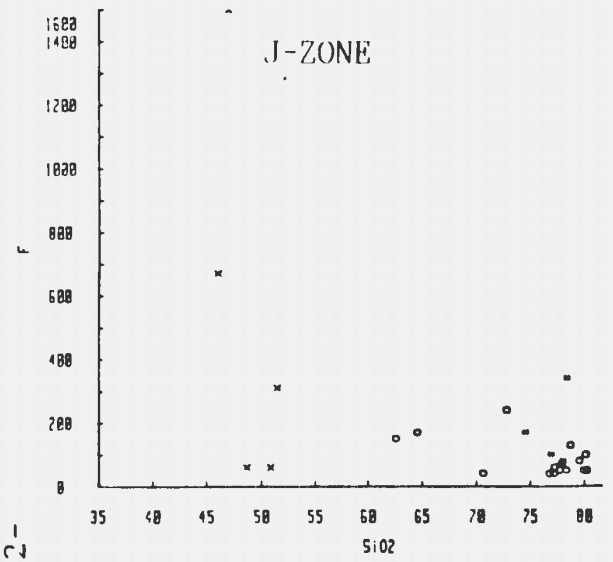
J-ZONE
F
SiO2

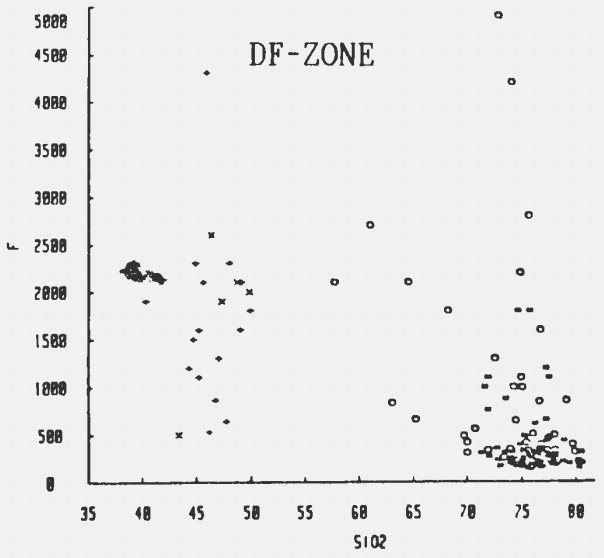
DF-ZONE
F
SiO2

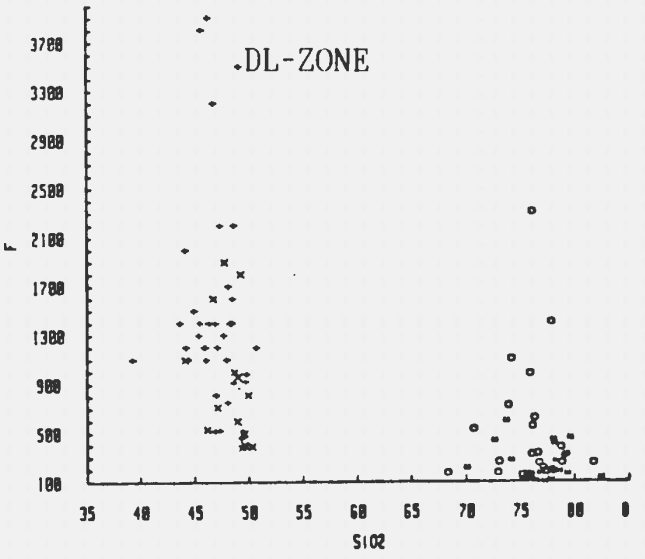
DL-ZONE
F
SiO2

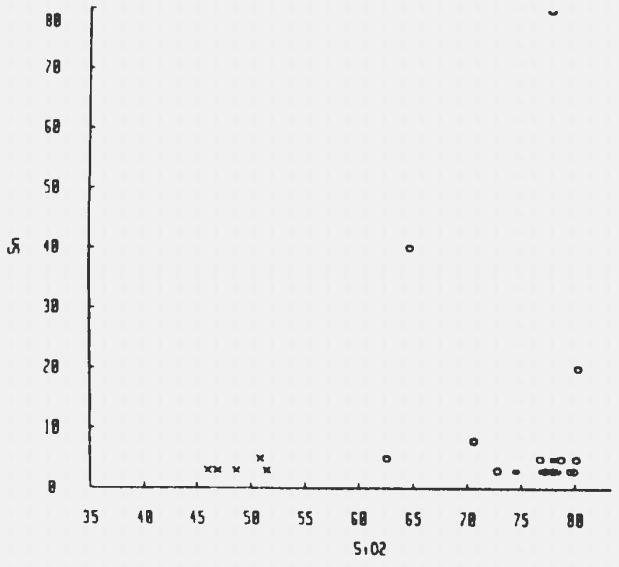
Sn
SiO2

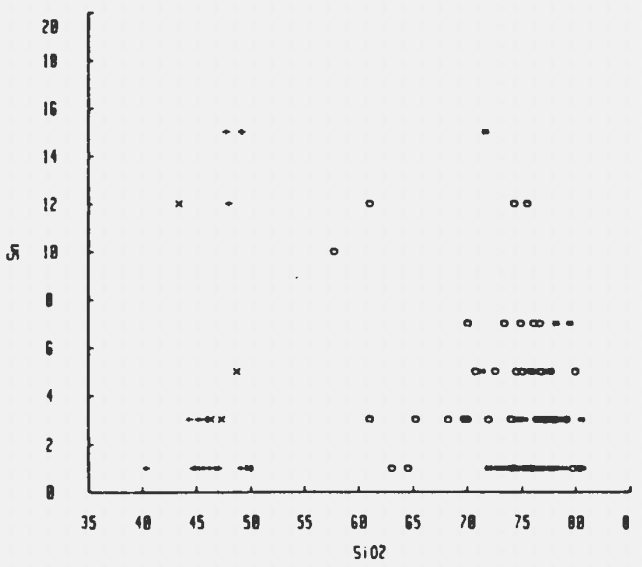
Sn
SiO2

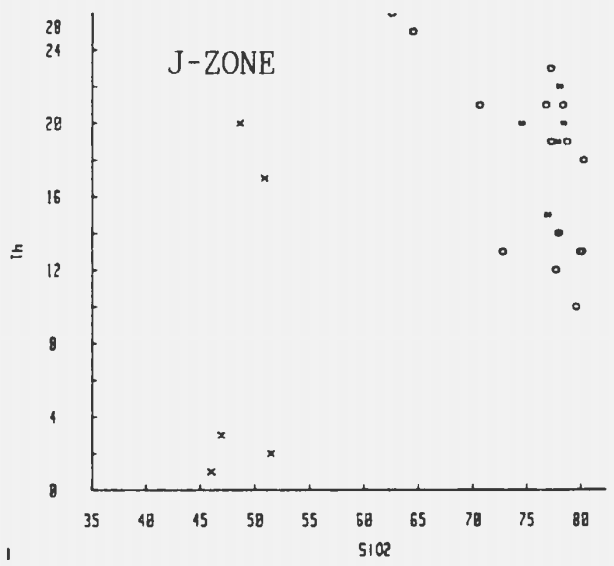
J-ZONE
Th
SiO2

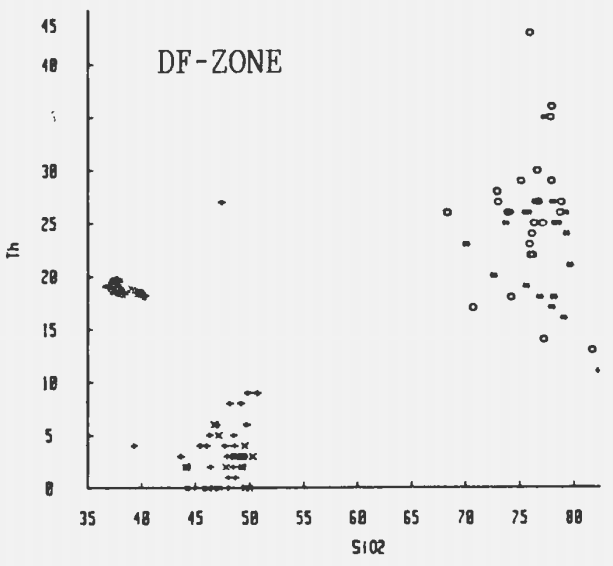
DF-ZONE
Th
SiO2

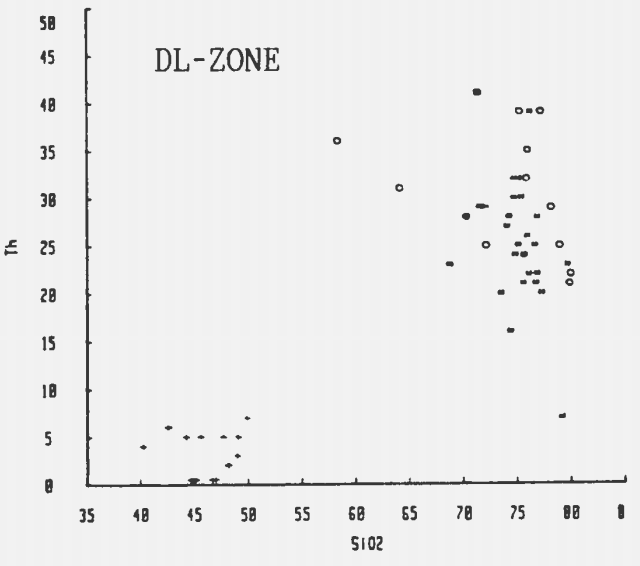
DL-ZONE
Th
SiO2

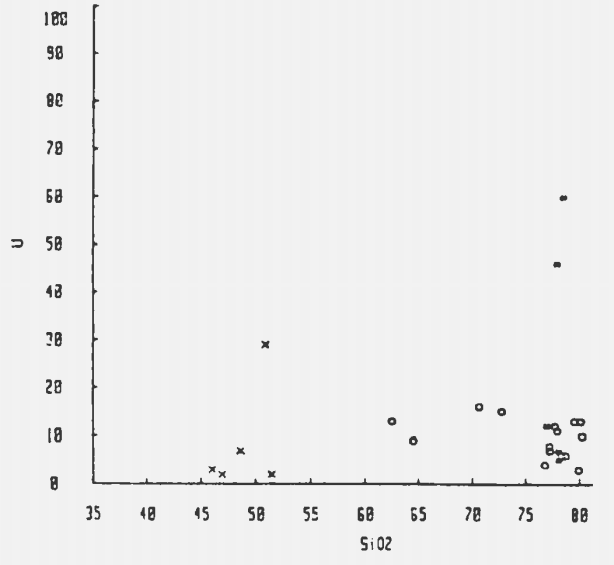
U
SiO2

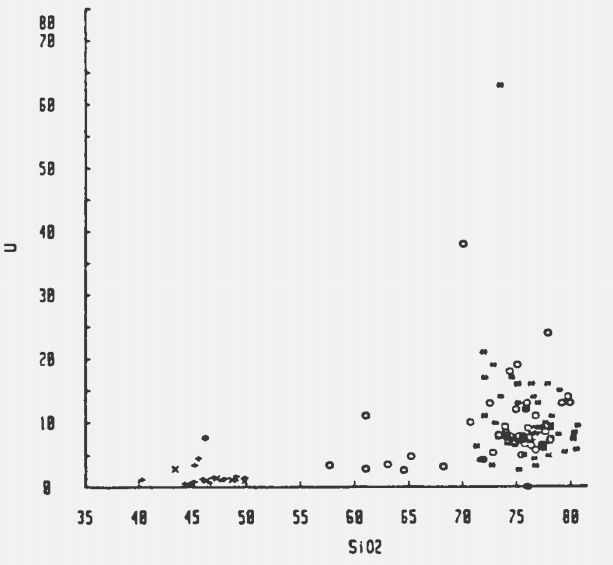
U
SiO2

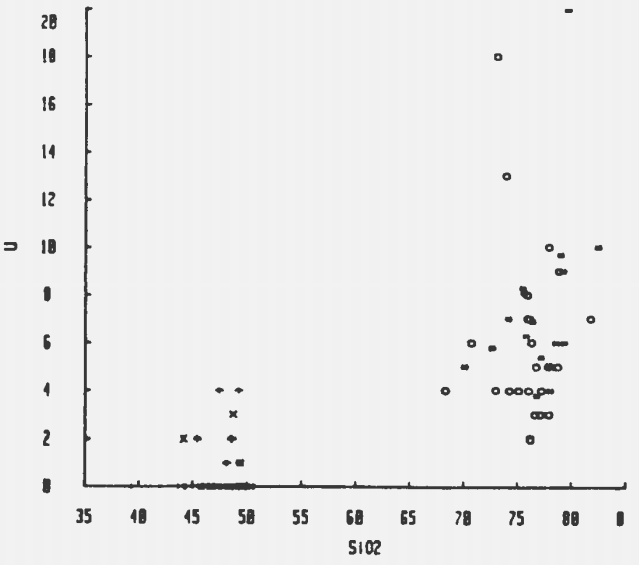
U
SiO2

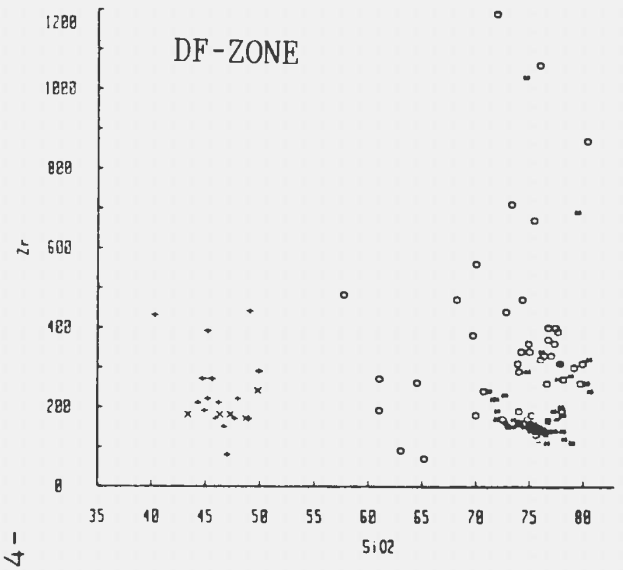
DF-ZONE
Zr
SiO2

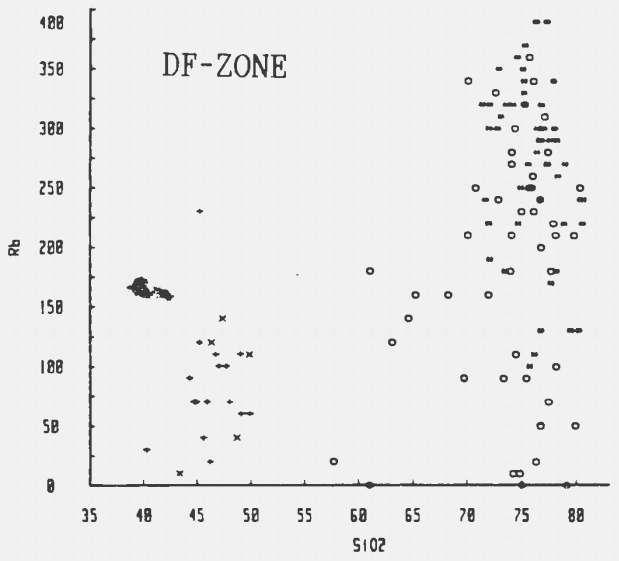
DF-ZONE
Rb
SiO2

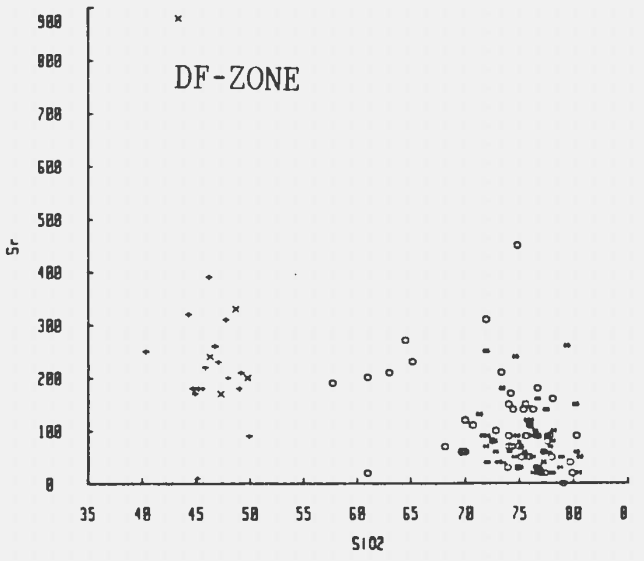
DF-ZONE
Sr
SiO2

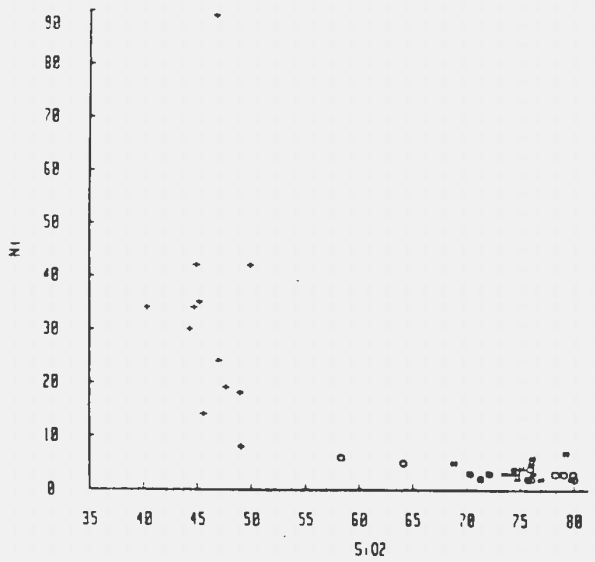
Ni
SiO2

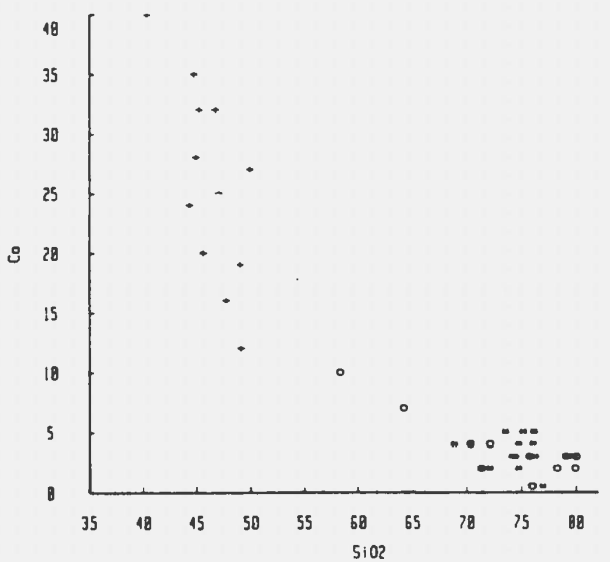
Co
SiO2

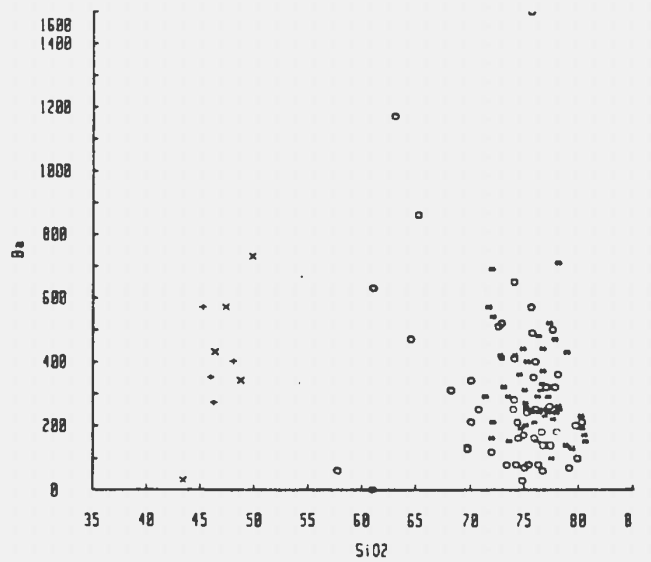
Ba
SiO2

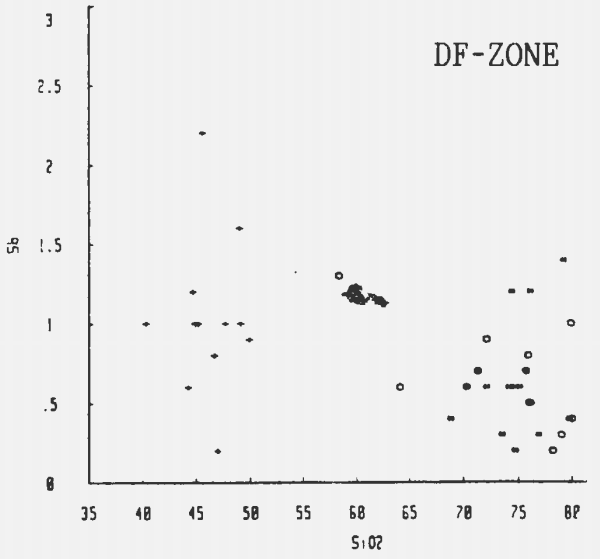
DF-ZONE
Sb
SiO2

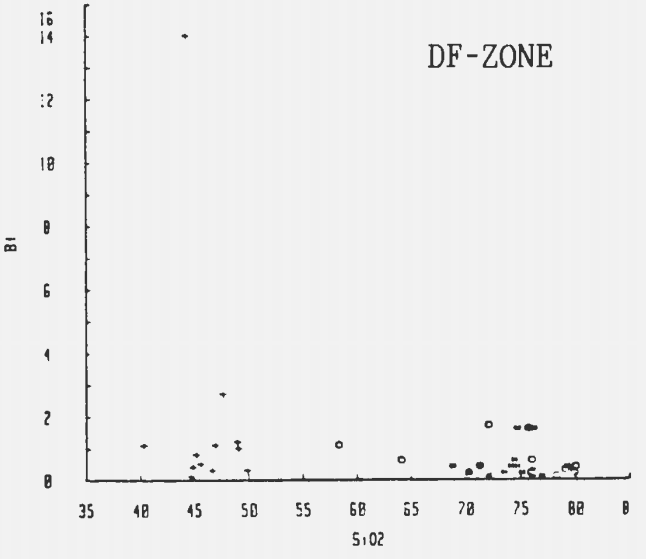
DF-ZONE
Bi
SiO2

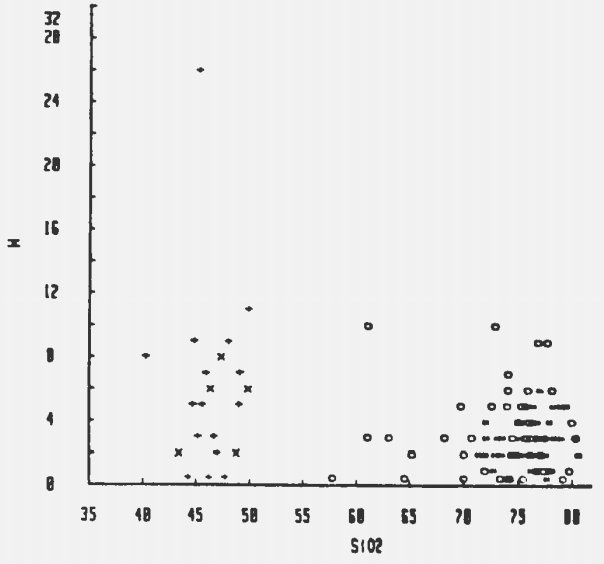
W
SiO2

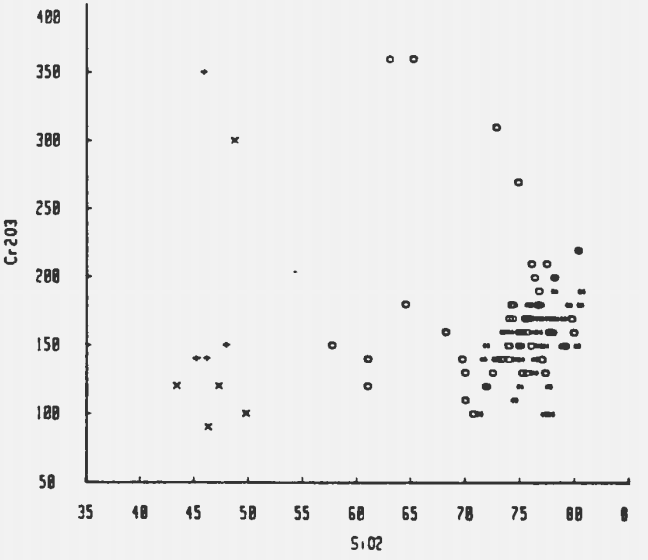
Cr2O3
SiO2

range of Al2O3, ranging from approximately 7.5 to 17% in the felsic rocks and 11.5 to 17% for the mafic dikes and flows.

In general the rocks of the Byers Brook Formation show a general increase in Al2O3, TiO2, FeOt (total Fe as FeO), MnO, MgO, CaO, P2O5, LOI, Sr, Co and Ni with decreasing SiO2 and a general decrease in Cr2O3, U and Th with decreasing SiO2 (Fig. 13). Na2O and K2O show little relation to SiO2, except where values of Na2O or K2O are greater than approximately 7%, in which case samples show a relative decrease in SiO2 with increasing alkalis. This erratic distribution reflects the strong alkali metasomatism which has affected these rocks. Zr is generally more concentrated in the felsic rocks relative to the mafic rocks. There is a strong cluster of points from the rhyolite flows at approximately 200 ppm Zr but there is a wide range of Zr values in the pyroclastic rocks from approximately 100-1175 ppm. F is generally higher in the mafic rocks except where felsic rocks contain veinlets of fluorite. Ba shows a negative correlation with SiO2 in the felsic rocks but is independant of SiO2 in the mafic rocks (based on limited data). There is a general positive correlation between Rb and increasing SiO2 but there is a wide range of Rb values in the felsic rocks. Sb is also

highly variable but there is a weak negative correlation with SiO2. Bi varies independantly of SiO2.

The high-Zr dikes and samples from the granite are plotted on Harker Variation Diagrams (Fig. 14) using the same vertical and horizontal scales as were used to describe the previous data. The data for these rocks are relatively tightly clustered when compared to the extrusive felsic rocks, reflecting a general lack of alteration.

In the high-Zr composite and rhyolite dikes there is a strong negative correlation between SiO2 and Al2O3, TiO2, FeOt, MnO, Na2O, P2O5 and LOI. CaO also shows a negative correlation with SiO2 with some scatter in the rhyolite dikes caused by zones of abundant epidote veinlets. Na2O and K2O show some variability, indicating that there was some mobilization of alkalis in these rocks. K2O shows a very weak positive correlation with SiO2. MgO does not vary significantly with SiO2. The major elements trend toward the compositions of the least altered diabase samples, suggesting this trend may be a mixing line.

Figure 14: Harker variation diagrams for the granite and high-Zr dike samples. The symbols in the diagrams are as follows:
X - granite
* - high-Zr rhyolite dikes
O - high-Zr composite dikes

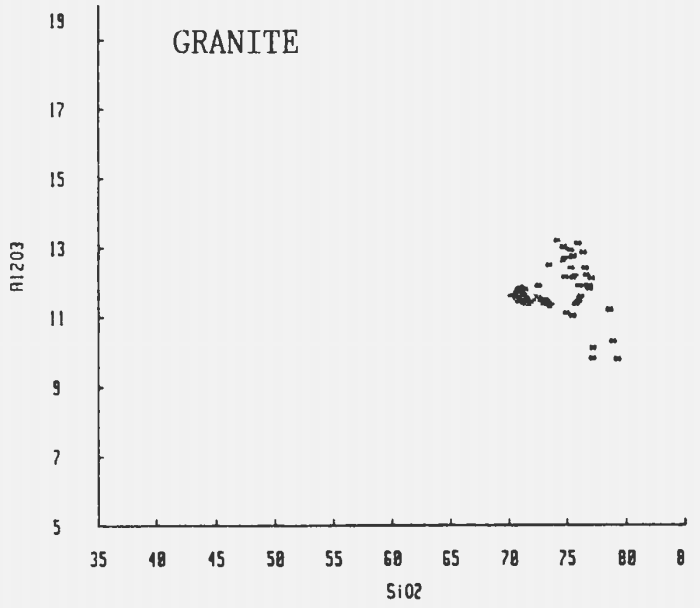
GRANITE
Al2O3
SiO2
19
17
15
13
11
9
7
5
35 40 45 50 55 60 65 70 75 80 8

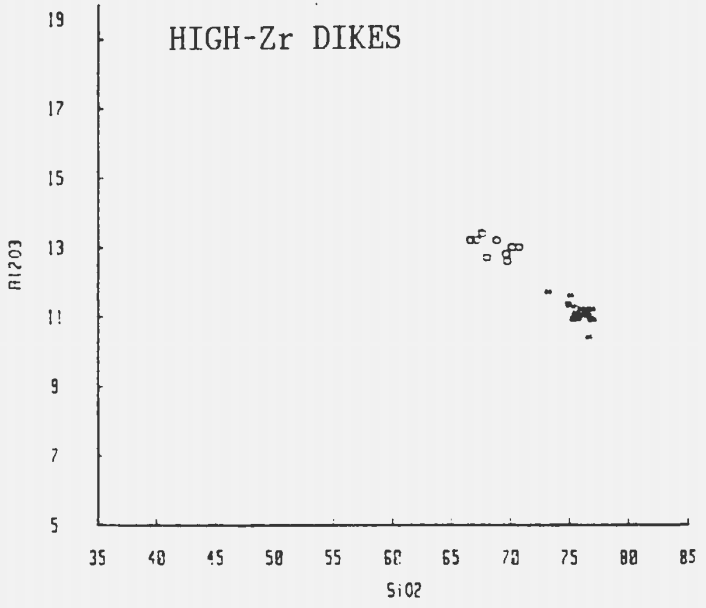
HIGH-Zr DIKES
Al2O3
SiO2
19
17
15
13
11
9
7
5
35 40 45 50 55 60 65 70 75 80 85

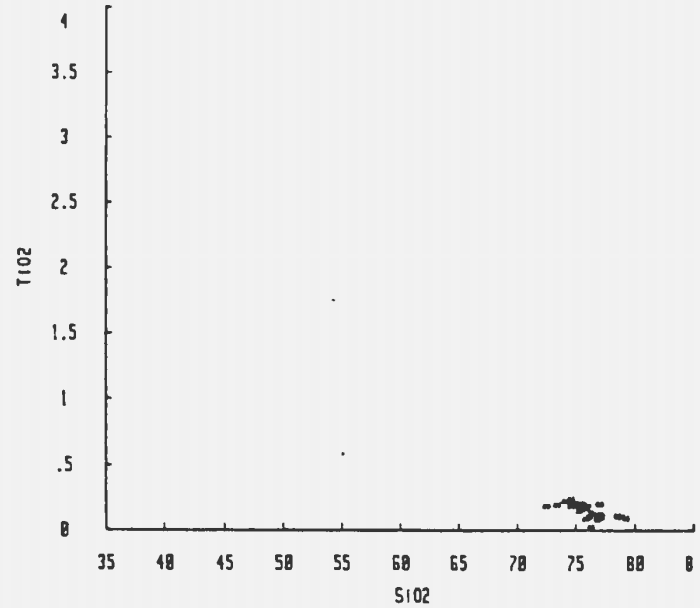
TiO2
SiO2
4
3.5
3
2.5
2
1.5
1
.5
0
35 40 45 50 55 60 65 70 75 80 8

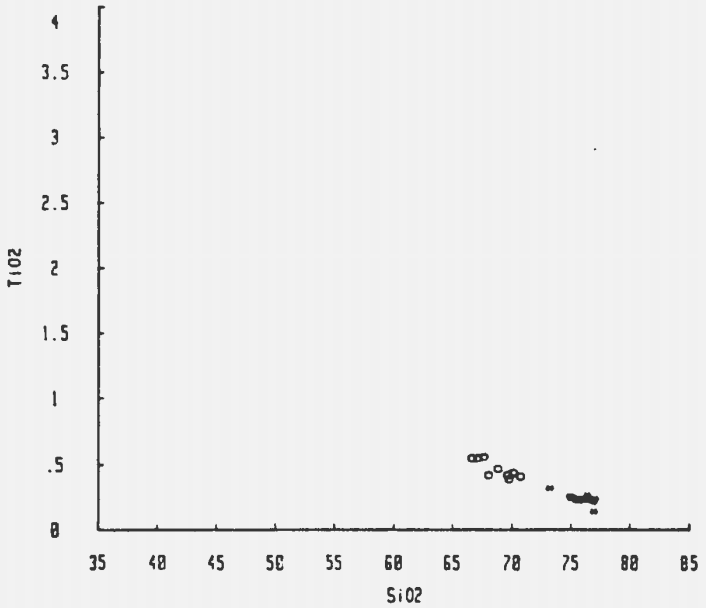
TiO2
SiO2
4
3.5
3
2.5
2
1.5
1
.5
0
35 40 45 50 55 60 65 70 75 80 85

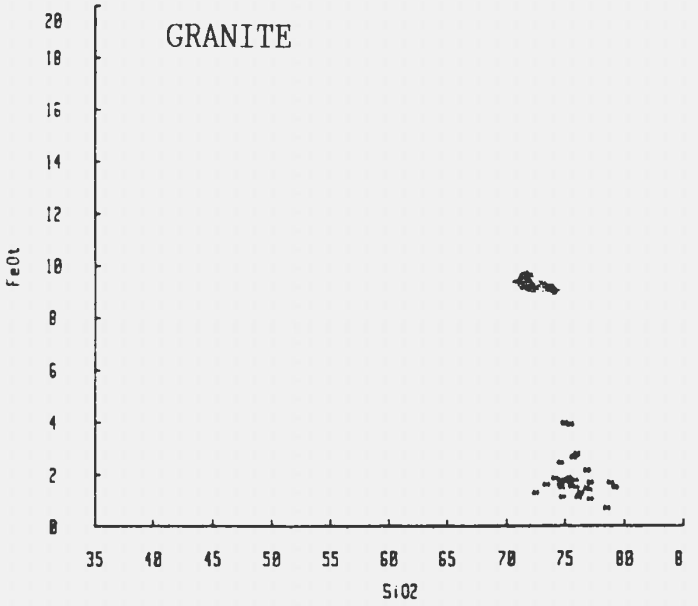
GRANITE
FeOt
SiO2

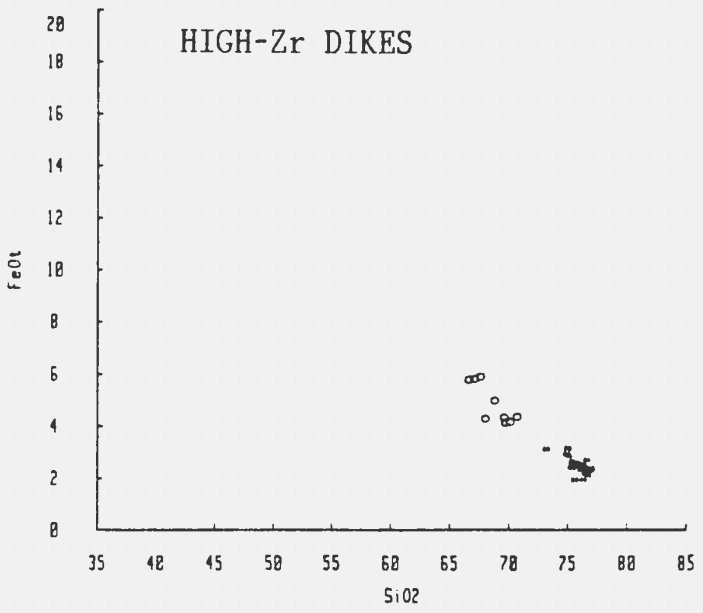
HIGH-Zr DIKES
FeOt
SiO2

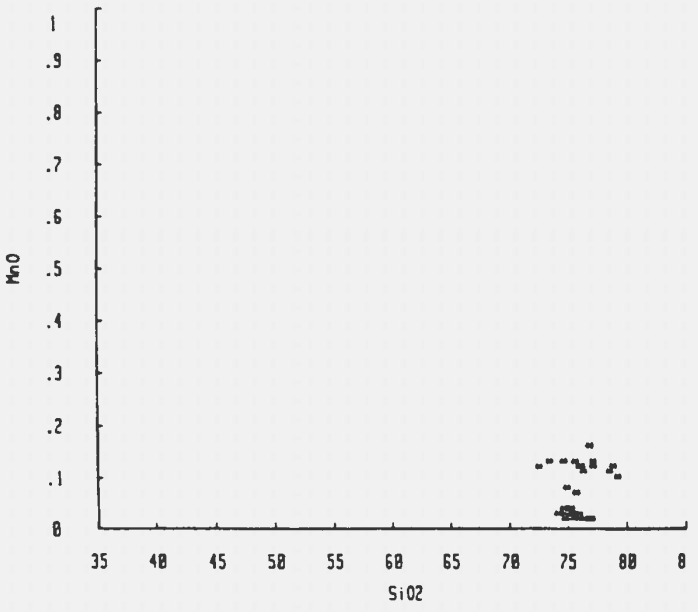
MnO
SiO2

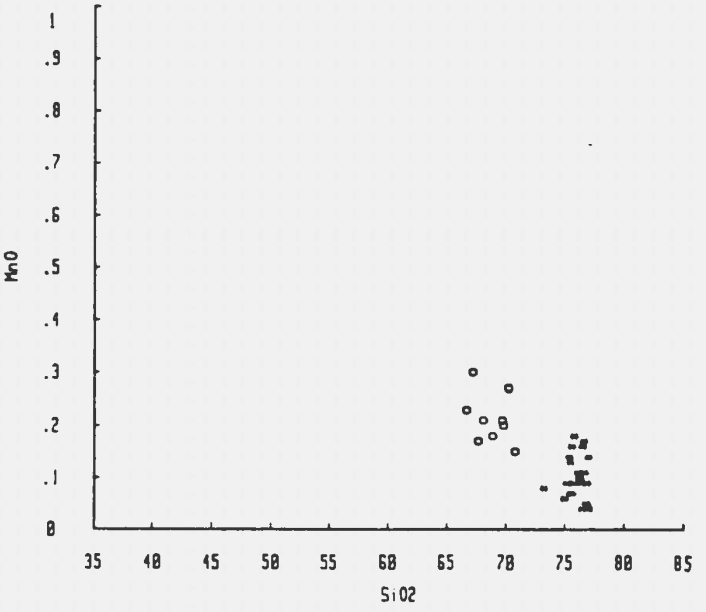
MnO
SiO2

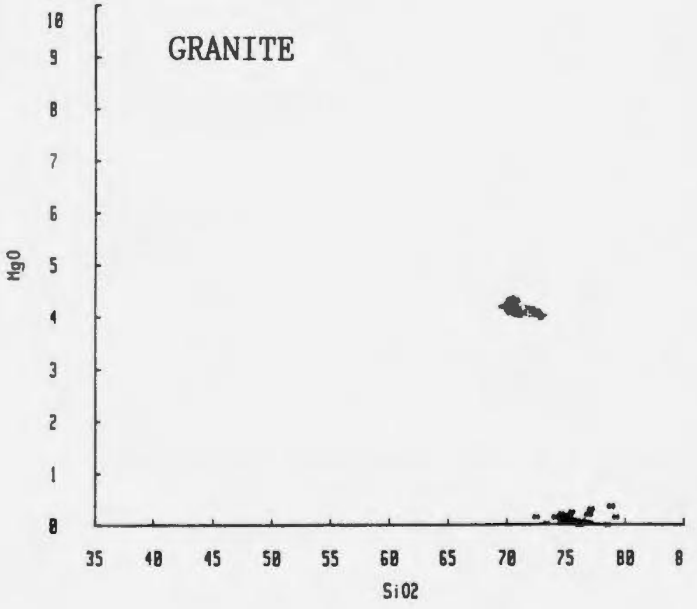
GRANITE
MgO
SiO2

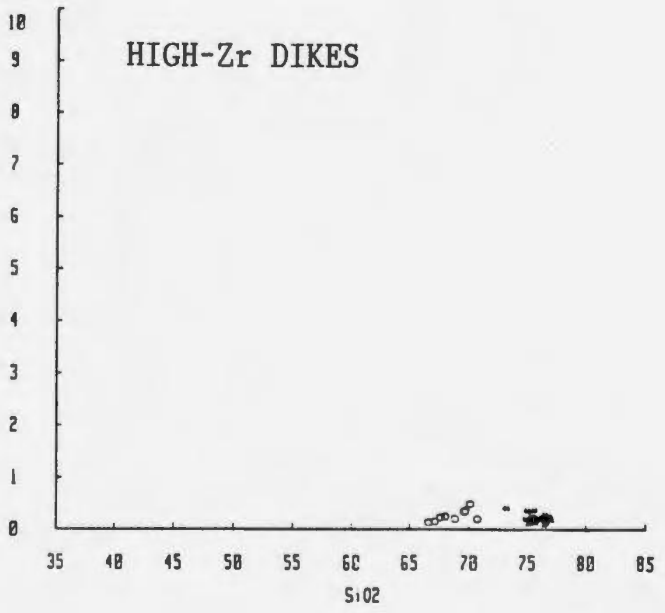
HIGH-Zr DIKES
SiO2

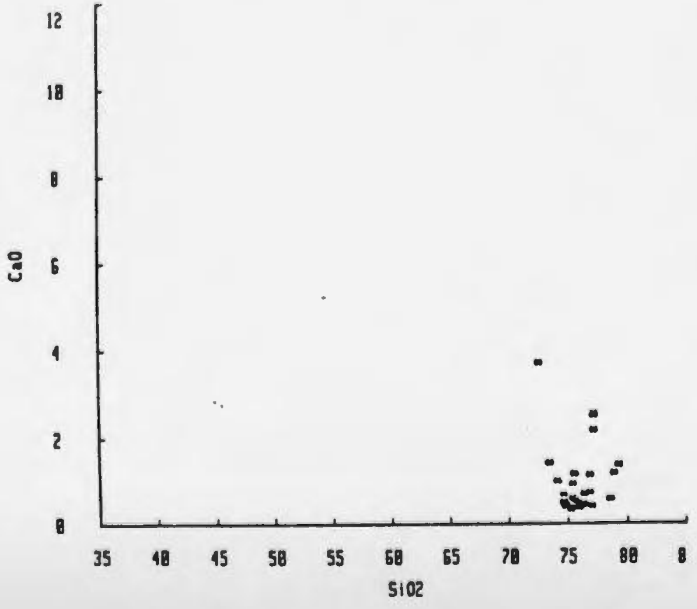
CaO
SiO2

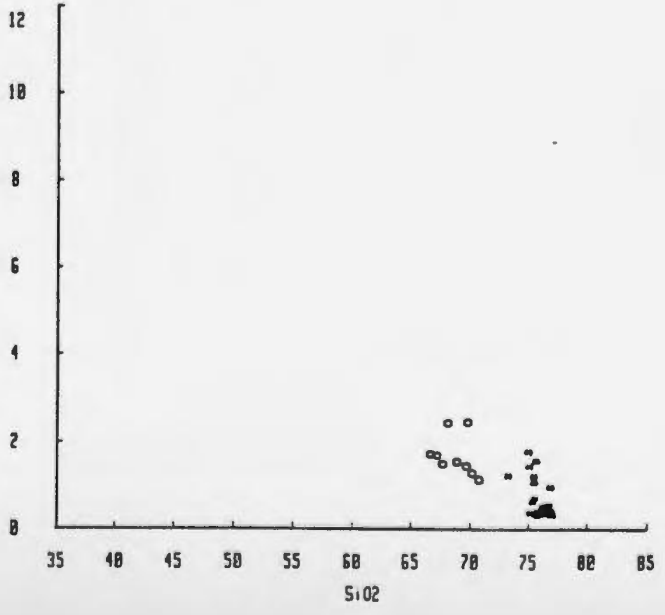
SiO2

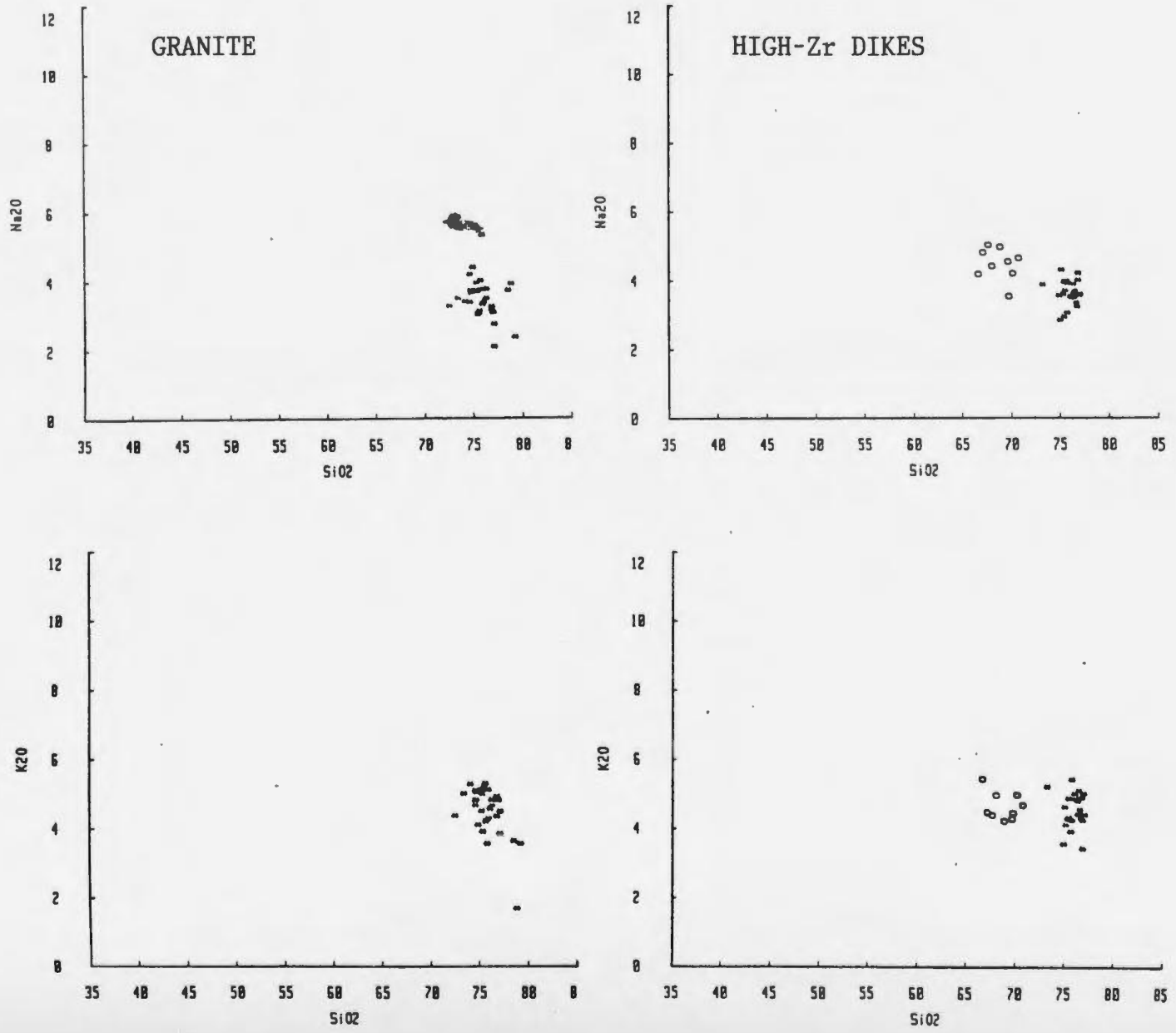
GRANITE
HIGH-Zr DIKES
Na2O
K2O
SiO2
0
2
4
6
8
10
12
35
40
45
50
55
60
65
70
75
80
85

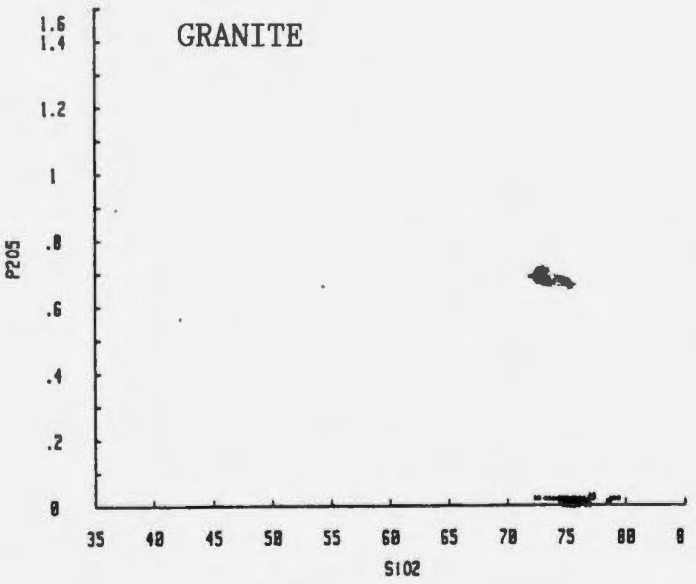
GRANITE
P2O5
SiO2
1.6
1.4
1.2
1
.8
.6
.4
.2
0
35 40 45 50 55 60 65 70 75 80 8

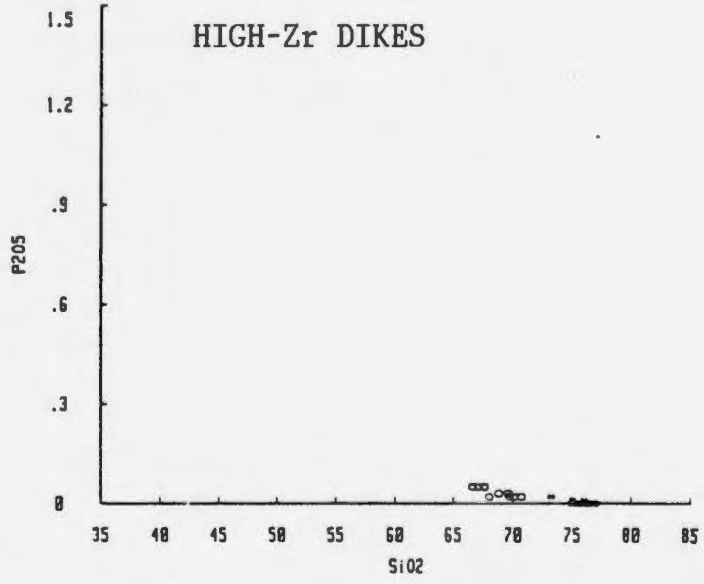
HIGH-Zr DIKES
P2O5
SiO2
1.5
1.2
.9
.6
.3
0
35 40 45 50 55 60 65 70 75 80 85

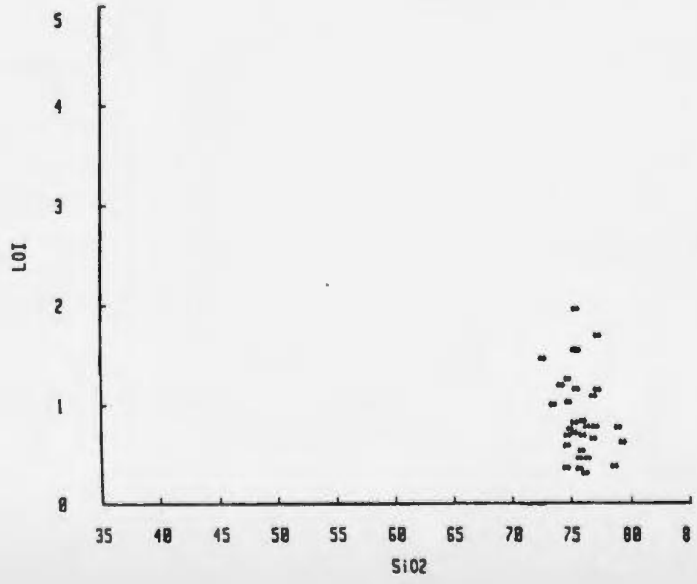
LOI
SiO2
5
4
3
2
1
0
35 40 45 50 55 60 65 70 75 80 8

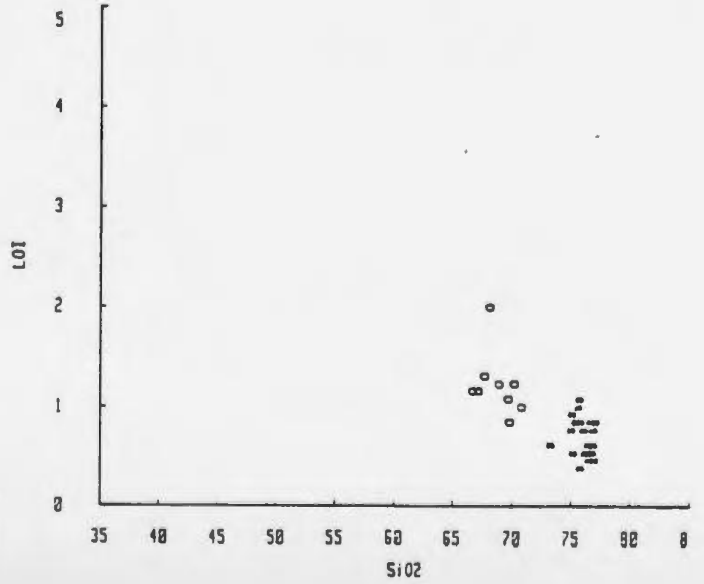
LOI
SiO2
5
4
3
2
1
0
35 40 45 50 55 60 65 70 75 80 8

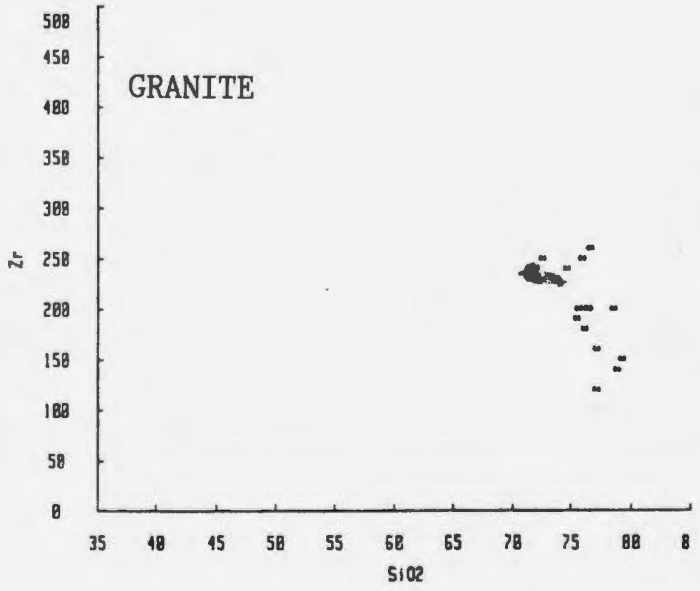
GRANITE
Zr
SiO2

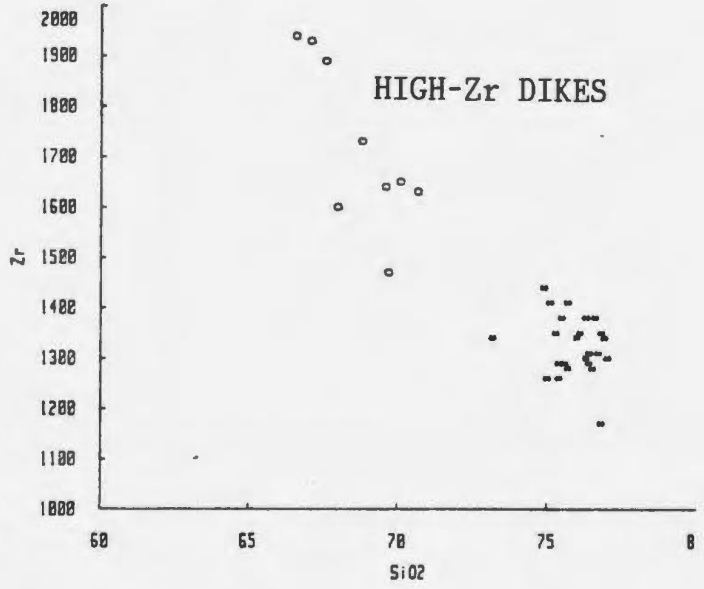
HIGH-Zr DIKES
Zr
SiO2

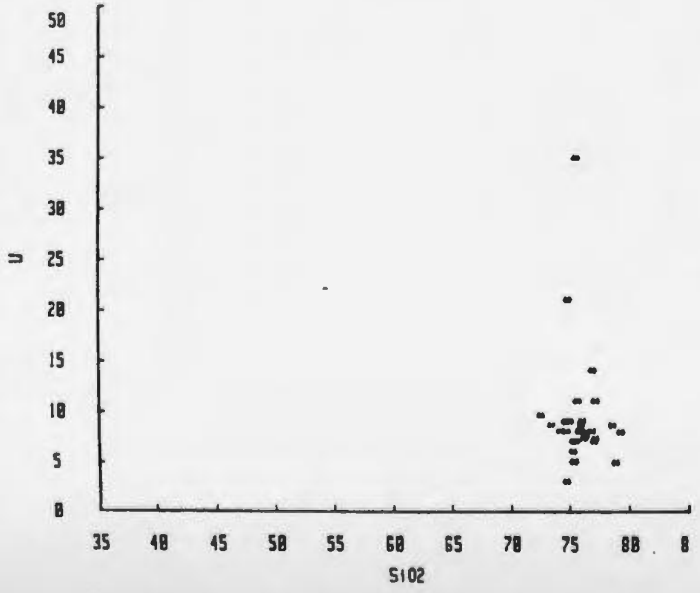
U
SiO2

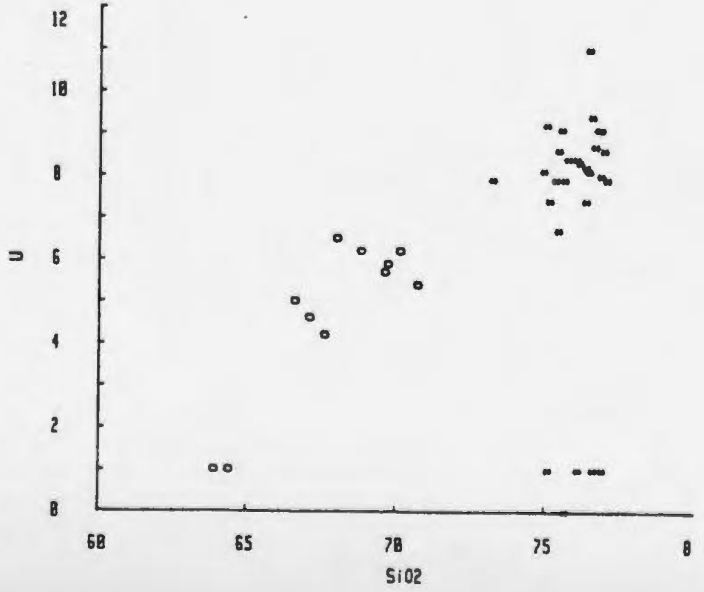
U
SiO2

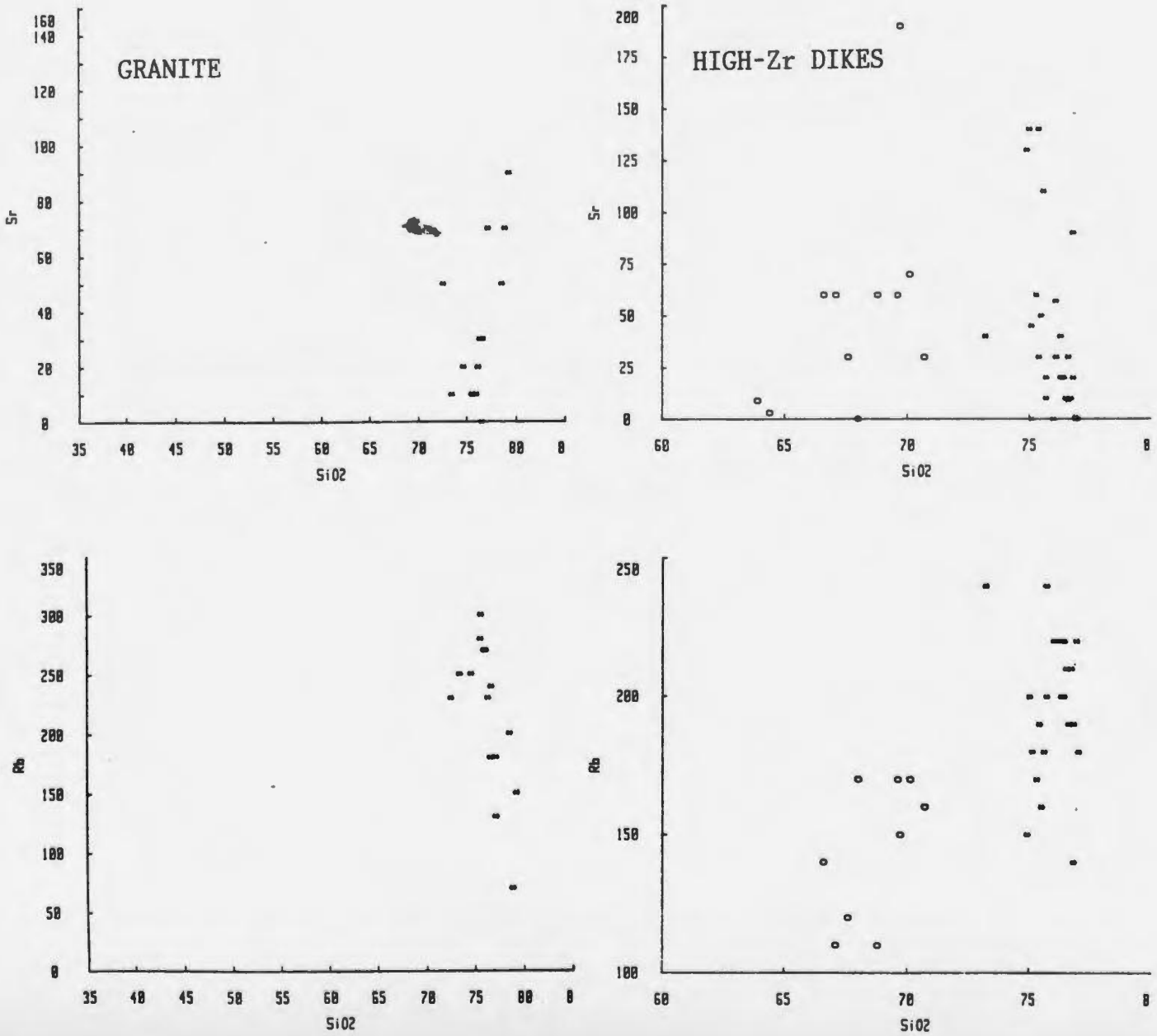
GRANITE
HIGH-Zr DIKES
Sr
Rb
SiO2
160
140
120
100
80
60
40
20
0
200
175
150
125
75
25
350
300
250
50
35
40
45
55
65
70

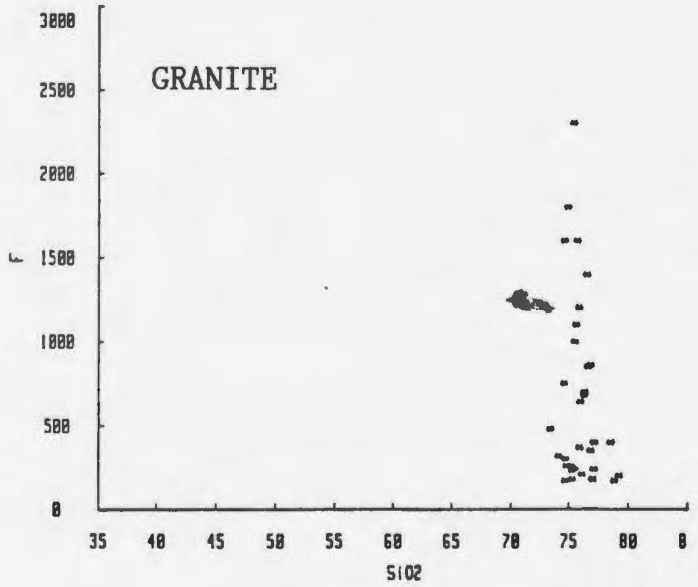
GRANITE
F
SiO2

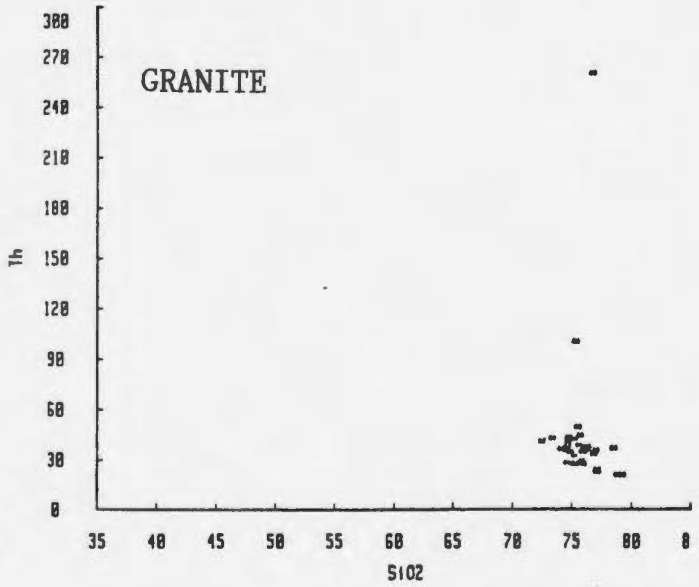
GRANITE
Th
SiO2

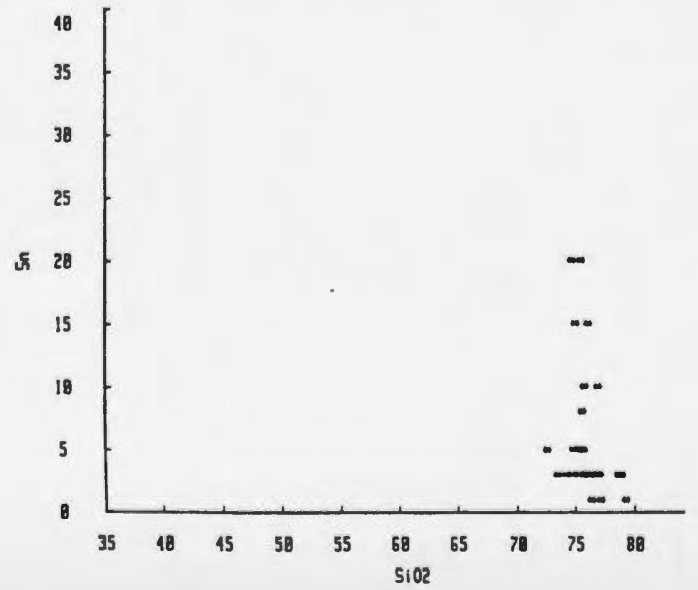
Sn
SiO2

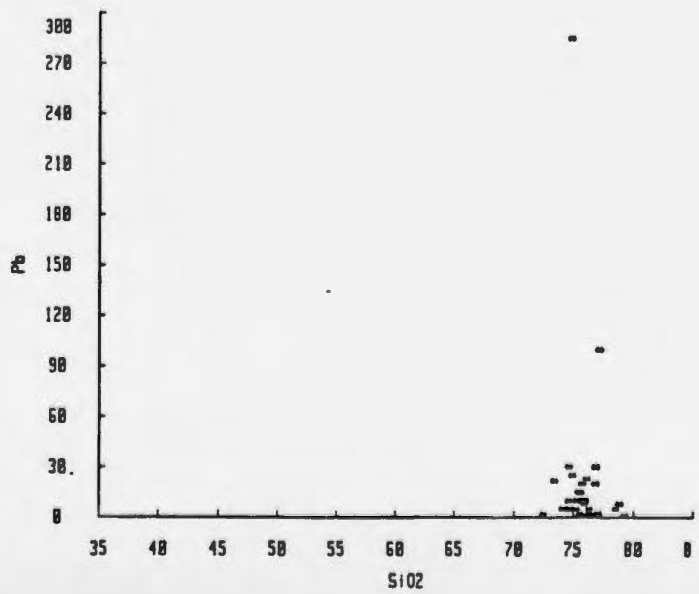
Pb
SiO2

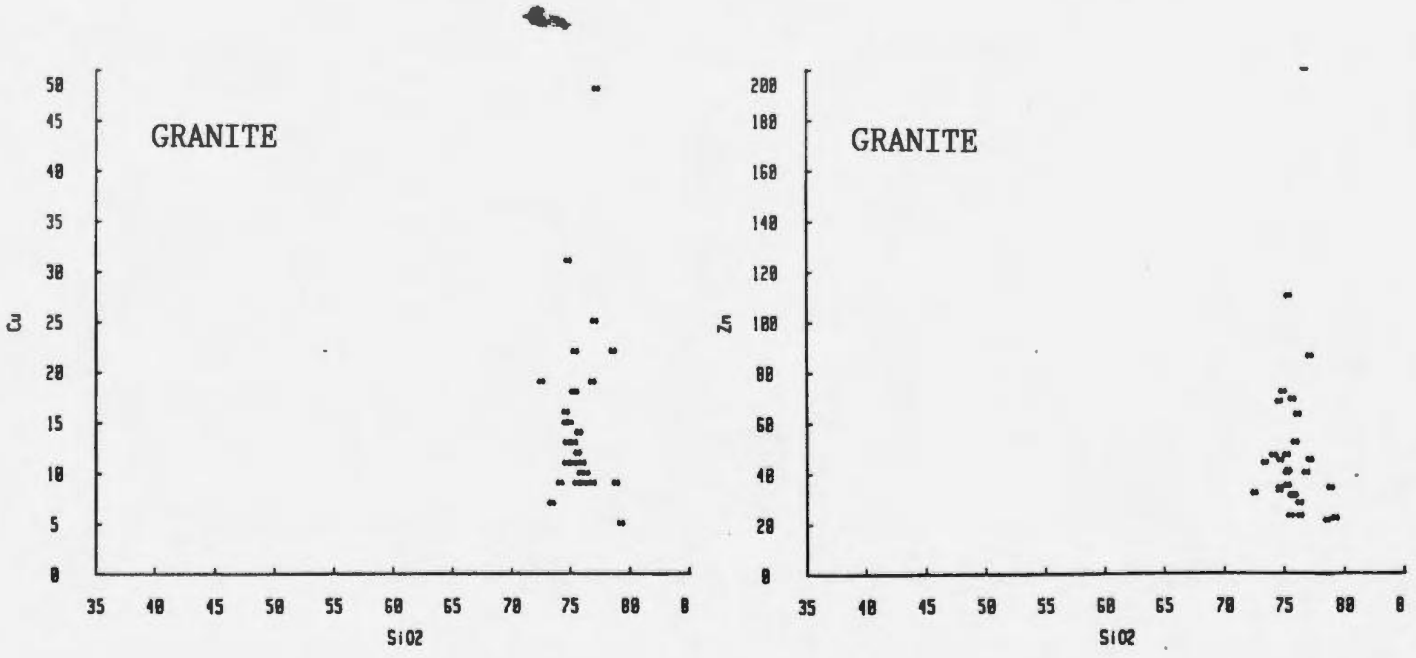
GRANITE
Cu
SiO2
50
45
40
35
30
25
20
15
10
5
0
35 40 45 50 55 60 65 70 75 80 0
GRANITE
Zn
SiO2
200
180
160
140
120
100
80
60
40
20
0
35 40 45 50 55 60 65 70 75 80 0

3.5 Geochemical Classification of the Byers Brook Formation.

3.5.1 Agpaiitic Index

Granites and rhyolites and related rocks are commonly separated into three groups by molar proportions of the major oxides Al2O3, Na2O, K2O and CaO (Shand, 1951):

peraluminous: $Al_2O_3 > Na_2O + K_2O + CaO$

metaluminous: $Na_2O + K_2O < Al_2O_3 < Na_2O + K_2O + CaO$

peralkaline: $Al_2O_3 < Na_2O + K_2O$.

Figure 15 shows plots of the molecular proportions of Al2O3 versus total alkalis. The agpaiitic index suggests that the Byers Brook Formation and the Hart Lake/Byers Lake Granite are metaluminous, with the exception of the high Zr rhyolite dikes which are metaluminous to marginally peralkaline. The validity of using any classification based on alkali content for the Byers Brook Formation is questionable considering the strong alkali metasomatism which has affected the volcanic rocks. However alkali exchange was the major process involved in the alteration except where alteration is

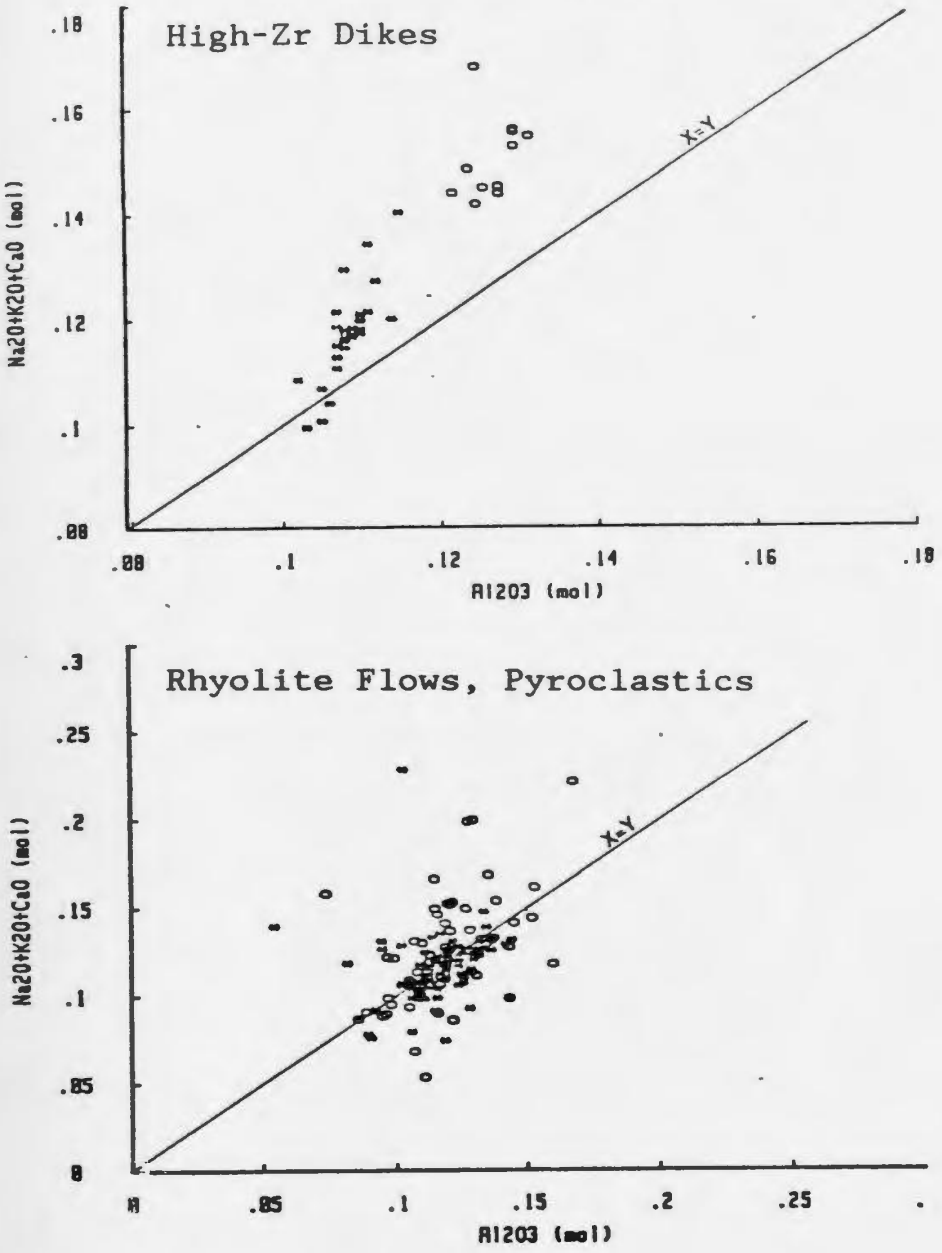

Figure 15: Molecular proportions of Al2O3 plotted against total alkalis. The diagrams indicate that the rocks of the Byers Brook Formation are metaluminous except the high-Zr dikes which are slightly more alkaline. The symbols on the diagram labeled high-Zr dikes represent:
* - high-Zr rhyolite dike
O - high-Zr composite dike
The symbols on the diagram labeled rhyolite flows, pyroclastics represent:
* - rhyolite flows
O - rhyolite pyroclastic rocks

extreme. In the most strongly altered rocks where there is an increase in total alkalis there is a corresponding increase in net Al2O3 and as Figure 15 shows the total alkalis and Al2O3 vary approximately proportionately with a consistent molar ratio which is close to 1. Samples from the granite and the high Zr composite and rhyolite dikes were not strongly affected by alkali metasomatism and agpaiitic indices should be reliable for these rocks. Samples which show a very sharp increase in total alkalis with the addition of CaO generally have secondary Ca in calcite, epidote or fluorite. The agpaiitic index for the rhyolites of the Byers Brook Formation suggests the presence of two distinct suites. The dominant suite, represented by the rhyolite flows and ignimbrites is metaluminous and a minor suite, represented by the high-Zr dikes is peralkaline. The high-Zr dikes are characterized by the appearance of acmite in the CIPW norm. Acmite does not appear in the normative mineralogy of the metaluminous suite.

3.5.2 Alkaline vs Subalkaline

The Byers Brook Formation rocks are plotted on the SiO2 versus Na2O + K2O (Fig. 16) of Irvine and Baragar

Figure 16: The rhyolite flows, pyroclastic rocks and the high-Zr rhyolite and composite dikes all plot in the subalkaline field, although the high-Zr dikes plot substantially closer to the boundary than the rhyolite flows and pyroclastics. The basalt flows and diabase dikes plot on the alkaline - subalkaline boundary. The solid boundary is from Irvine and Baragar, (1972) and the dashed boundary is from MacDonald, (1968). The symbols on the diagram labeled High-Zr dikes represent:
* - High-Zr rhyolite dikes
O - High-Zr composite dikes
The symbols on the diagram labeled rhyolite flows, pyroclastics represent:
* - Rhyolite flows
O - Pyroclastic rocks.

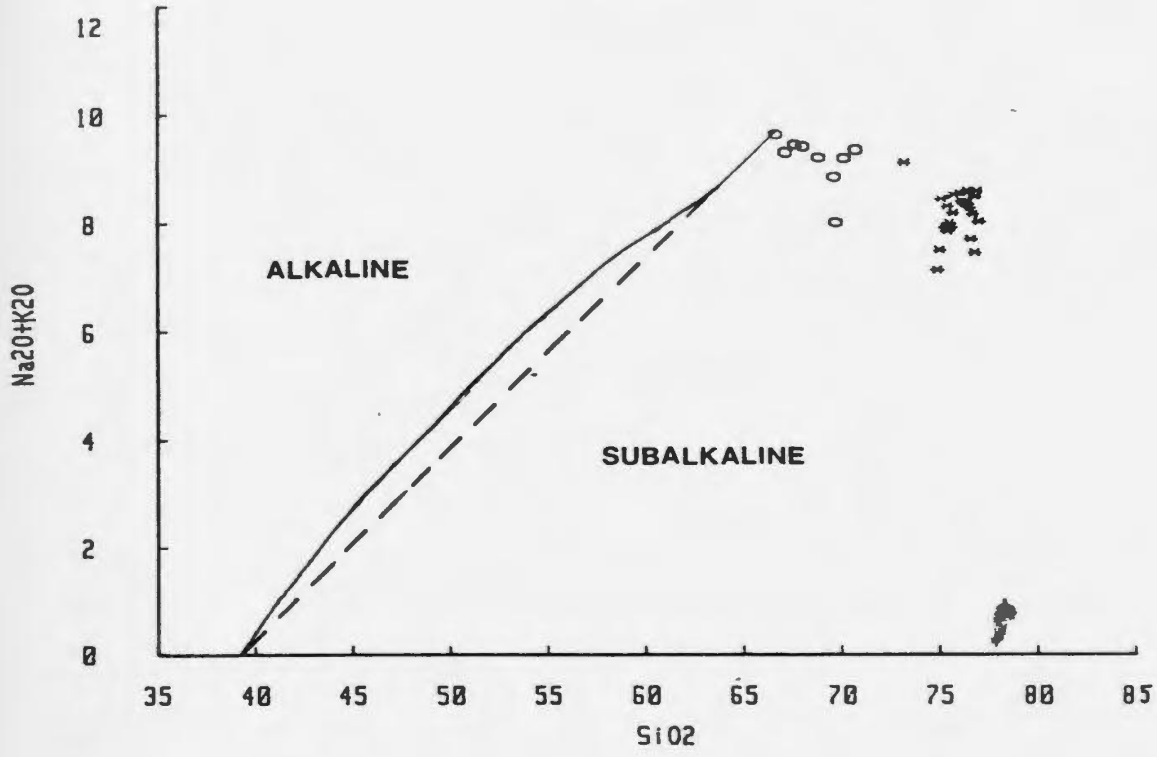
ALKALINE
SUBALKALINE
Na2O+K2O
SiO2
0
2
4
6
8
10
12
35
40
45
50
55
60
65
70
75
80
85

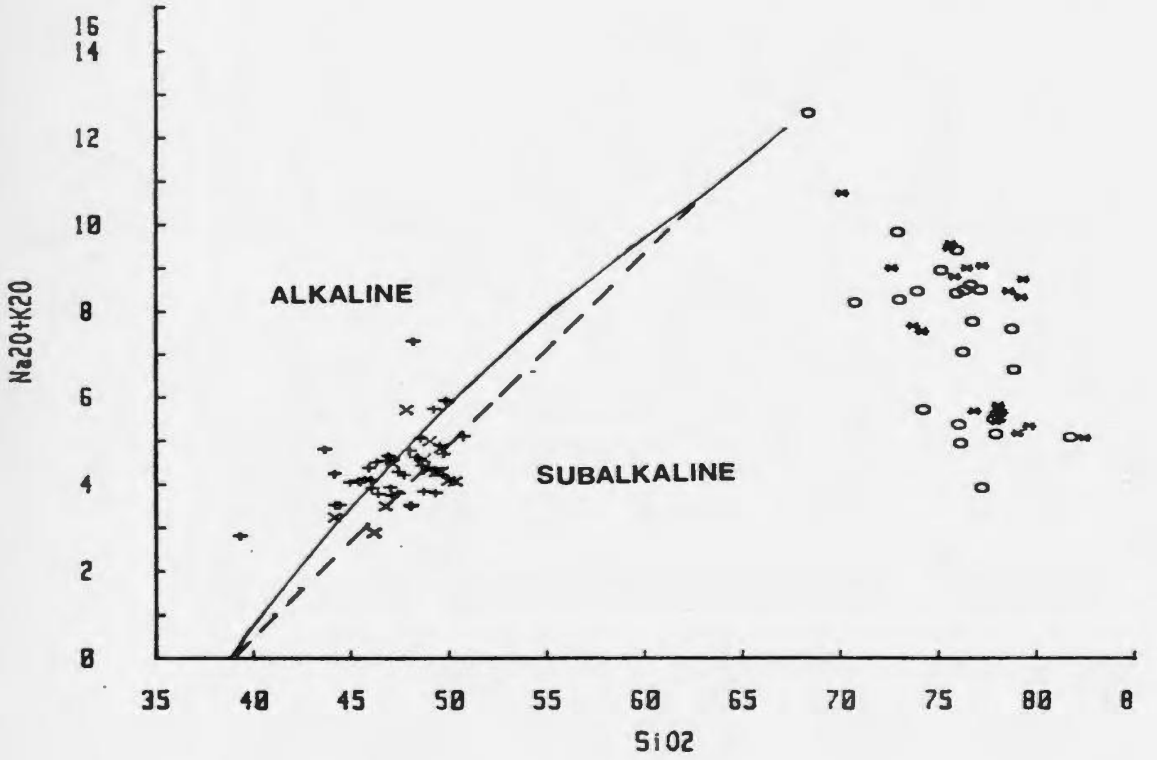
ALKALINE
SUBALKALINE
Na2O+K2O
SiO2
0
2
4
6
8
10
12
14
16
35
40
45
50
55
60
65
70
75
80
8

(1972) and MacDonald (1968). The mafic rocks plot dominantly in the alkali basalt field of MacDonald but straddle the alkaline/subalkaline boundary of Irvine and Baragar. The rhyolite flows and ignimbrites plot in the subalkaline field. The questionable validity of magmatic classification dependant on alkalis in an area affected by alkali metasomatism much reduces the value of these diagrams.

A number of authors (Cann, 1970; Pearce and Cann, 1973; Floyd and Winchester, 1975 and 1978; Winchester and Floyd, 1977; Miyashiro, 1975a and b, 1977; etc.) have devised classifications based on elements which are relatively immobile during alteration and are therefore more reliable for characterizing magmas than the highly mobile alkalis. The data used in this study are from an exploration program and many of the immobile elements required for these classifications were not routinely analyzed. Only plots using TiO_2, P_2O_5, Zr and Sr can be derived from this data set.

The Zr/TiO_2 versus SiO_2 diagram (Fig. 17) from Winchester and Floyd (1977) shows the basaltic rocks of the Byers Brook Formation plotting across the subalkaline-alkaline basalt boundary. In this diagram the

Figure 17: Diagram of SiO_2 plotted against Zr/TiO_2 (from Floyd and Winchester, 1978). The diagram shows the rhyolite flows, pyroclastic rocks and granite all plot in the rhyolite field with scatter, especially in the pyroclastic rocks caused by alteration and locally an abundance of mafic material. The high-Zr dikes clearly plot as pantellerite or commendite. The diabase dikes and basalt flows plot across the alkaline, sub-alkaline basalt boundary.

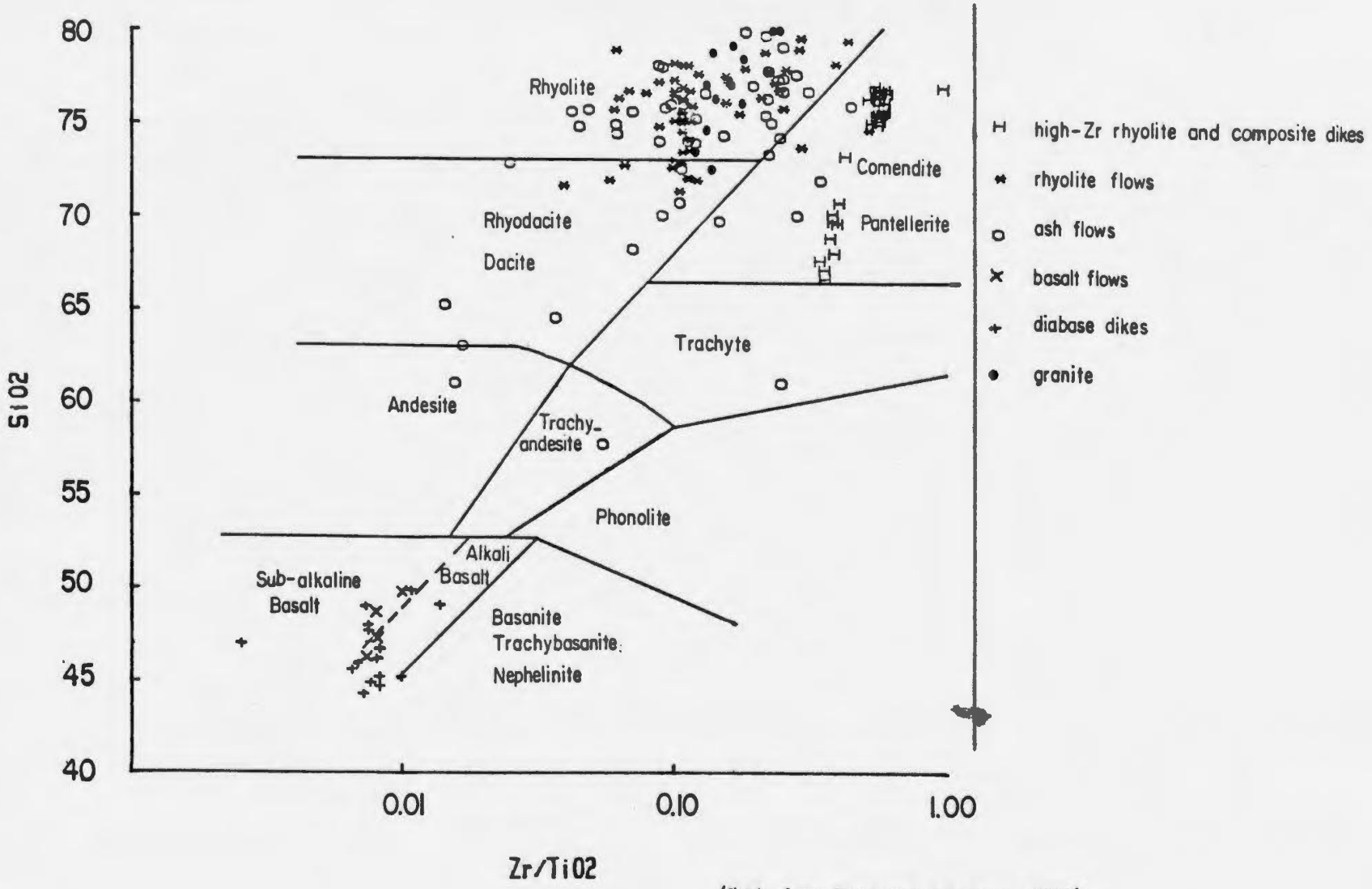

(fields from Floyd and Winchester, 1978)

felsic rocks including the Hart Lake/Byers Lake granite plot dominantly in the rhyolite and rhyodacite field, but near, and with minor overlap into the comendite, pantellerite field. Erratic points are from the pyroclastic rocks which have been altered and/or contain high amounts of mafic material. The high-Zr rhyolite and composite dikes plot well into the comendite, pantellerite field. This plot indicates clearly that the high-Zr dikes are geochemically distinct from the rhyolite flows and pyroclastic rocks.

In considering a petrogenetic model for the Byers Brook Formation in the Wentworth area a number of observations must be considered: (1) a comagmatic suite of basalt, metaluminous granite and rhyolite and peralkaline rhyolite and dacite; (2) emplacement in an anorogenic, extensional tectonic regime; (3) along with higher agpaiitic indices, the peralkaline rocks have markedly higher Zr; (4) secondary riebeckite in the peralkaline rocks, reflecting deuteric-metasomatism by magmatically derived fluids (Taylor et. al. 1980, Strong and Taylor, 1984; Strong and Coyle, 1988; Garson et al., 1984). These observations are applicable to most peralkaline complexes (Taylor et. al. 1980).

It has been suggested that peralkaline rocks are genetically linked to carbonate-rich fluids which have acsended along deeply penetrating fractures (Strong and Coyle, 1988; Garson et. al. 1984). In the Wentworth map area the Rockland Brook Fault is the most likely conduit.

A petrogenetic model with general application, which reconciles all of the above observations has been derived by Taylor et. al. (1980), for the Topsails igneous complex. The model is similar to that proposed by Hildreth (1979) for the Bishop Tuff in California, where a zoned magma chamber was developed by thermogravitational diffusion. This diffusion was promoted by thermal input from basaltic magma rising from the mantle. The density contrast and thickness of the granitic magma would resist penetration by the intruding basaltic magma, resulting in basalt being only a minor phase in the volcanic pile or occurring only peripheral to the main granite body. Taylor et. al. (1980) suggested that basaltic magmas in continental rift environments tend to be alkalic and CO2-rich, and that volatiles escaping from these basalts would also be expected to be alkalic. Taylor et. al. (1981) and Strong and Taylor (1984) indicate that the anomalous concentration of such elements as Zr in peralkaline rocks requires the evolution of an

alkali-enriched fluid. The model invokes fusion processes to cause the development of an alkali phase in the apical region of the magma chamber, as a result of concentration of alkalic volatiles from mantle derived basaltic magma. Incompatible elements such as Zr are partitioned into this alkali phase, especially if it is CO2- and F-rich. The development of peralkaline rocks can either be magmatic or metasomatic, depending on the stage of cooling and the extent to which the fluids have reacted with the granitic melt (Taylor et. al. 1980). The development of this alkali phase may have been an important factor in the pervasive, strong alkali metasomatism, and the subsequent concentration of uranium mineralization in the Byers Brook Formation.

A second possible genesis is that the Byers Brook Formation was derived from two magma sources. The rhyolite flows and ignimbrites from a metaluminous source and the high-Zr rhyolite dikes from a peralkaline source, such as the model suggested by Christiansen et. al. (1980) for the petrogenesis of topaz rhyolites and associated peralkaline rhyolites in the southwestern United States.

Chapter 4

MINERALIZATION

4.1 Introduction

Numerous radioactive occurrences have been discovered in the rocks of the Byers Brook Formation. When exploration ended in 1981 the showings in the DF-zone and the J-zone were the most significant and only for these are there sufficient data to be discussed in detail.

Uranium mineralization in the Byers Brook Formation occurs almost exclusively in the felsic volcanic rocks, except for minor concentrations in fractures or along bedding laminae in the siltstones of the DF-zone and sooty pitchblende along late fractures in the Hart Lake Granite. The rocks of the Byers Brook Formation are host to numerous, small, polymetallic showings, including a concentration of rare earth elements (REE) + Th + Sn + W in the granophyric contact rocks of the Hart Lake/Byers Lake Granite in diamond drill hole DL-16. Thin massive sulfide beds (1-10 cm) occur in the lacustrine siltstones of both the DF-zone and J-zone and copper sulfides + silver are

concentrated in a silicified brecciated zone within the siltstones.

4.2 DF-zone Uranium Mineralization

The DF-zone rhyolite flows host the most significant mineralization discovered on the Wentworth prospect. The zone became the target of extensive drilling after a large concentration of mineralized boulders was discovered by prospectors. Numerous small showings have been revealed by trenching but the most extensive uranium mineralization was intersected by diamond drill holes in the east and west DF-zone. All occurrences are in brecciated and strongly fractured rhyolite flows where uranium mineralization occurs surrounding breccia fragments, as disseminations and veinlets. Fault breccia is the most common host for uranium mineralization but weakly mineralized gas breccias have been observed in massive rhyolite and lithophysae-rich zones. All mineralized zones are strongly hematite altered to a brick-red colour. The principal ore mineral has been identified in polished thin section as pitchblende.

The two largest uranium occurrences were intersected by diamond drill holes DF-27, 32, 34 and DF-13, 15, 4 in the eastern and western DF-zone respectively (Appendix 1).

4.2.1 East DF-zone Showing

In the eastern DF-zone occurrence, diamond drill hole DF-32 intersected a 20 m zone which grades at 4 lb/t U_3O_8. Figure 18 shows a cross-section of the mineralized zone as indicated by diamond drilling. The original 20 m intersection resulted from drilling down the dip of a narrow (approx. 1 m thick) structure. The host rock is massive or lithophysae-rich rhyolite of the main dome flow complex. Lithophysae in the mineralized zone are generally small and best observed with a microscope but are locally up to 1.5 cm in diameter. The mineralization is silvery metallic grey and tarnishes to dull metallic grey (Plate 18). The pitchblende mineralization occurs in veins and as filling in lithophysae. Veins range from microscopic to approximately 2 cm in wide. In the mineralized zone there is a very high density of veinlets (2-5 per mm). Locally slickensides occur on the pitchblende in fractures.

The uranium mineralization is accompanied by strong hematite, sericite and K-feldspar alteration of the rhyolitic groundmass. Veins in which sericite and K-feldspar coexist are common and locally garnet and epidote occur in veinlets (Plate 19). In thin section, hematite alteration is markedly stronger directly adjacent

LEGEND

STRATIFIED ROCKS

8	Basalt flows
7, 7b	(7) Rhyolite flows, flow banded or massive, commonly with spherulites and lithophysae (7b) Porphyritic rhyolite, >25% phenocrysts
6	Rhyolite ash flows and tuffs
5a, 5b	(5a) Laminated siltstone, reworked ash (lacustrine) (5b) Conglomerate

INTRUSIVE ROCKS

4	High- Zr rhyolite dikes
3	High- Zr composite dikes
2	Diabase dikes
1	Granite
	Uranium mineralized structure

ABBREVIATIONS

xl - phenocrysts
ly - lythophysae
fl - flow banding
sp - spherulitic
bx - brecciated
lap - lapilli
f - fiamme
amyg - amygduloidal
lam - laminar bedding
agglom - agglomerate
f.g. - fine grained

F - fluorite
ep - epidote
Ca - calcite veins
Q - quartz veins
Mt - magnetite veins
U - uranium
ga - galena
Sn - cassiterite
REE - rare earth elements
W - tungsten
Th - thorium

Figure 18: East DF-zone uranium occurrence.

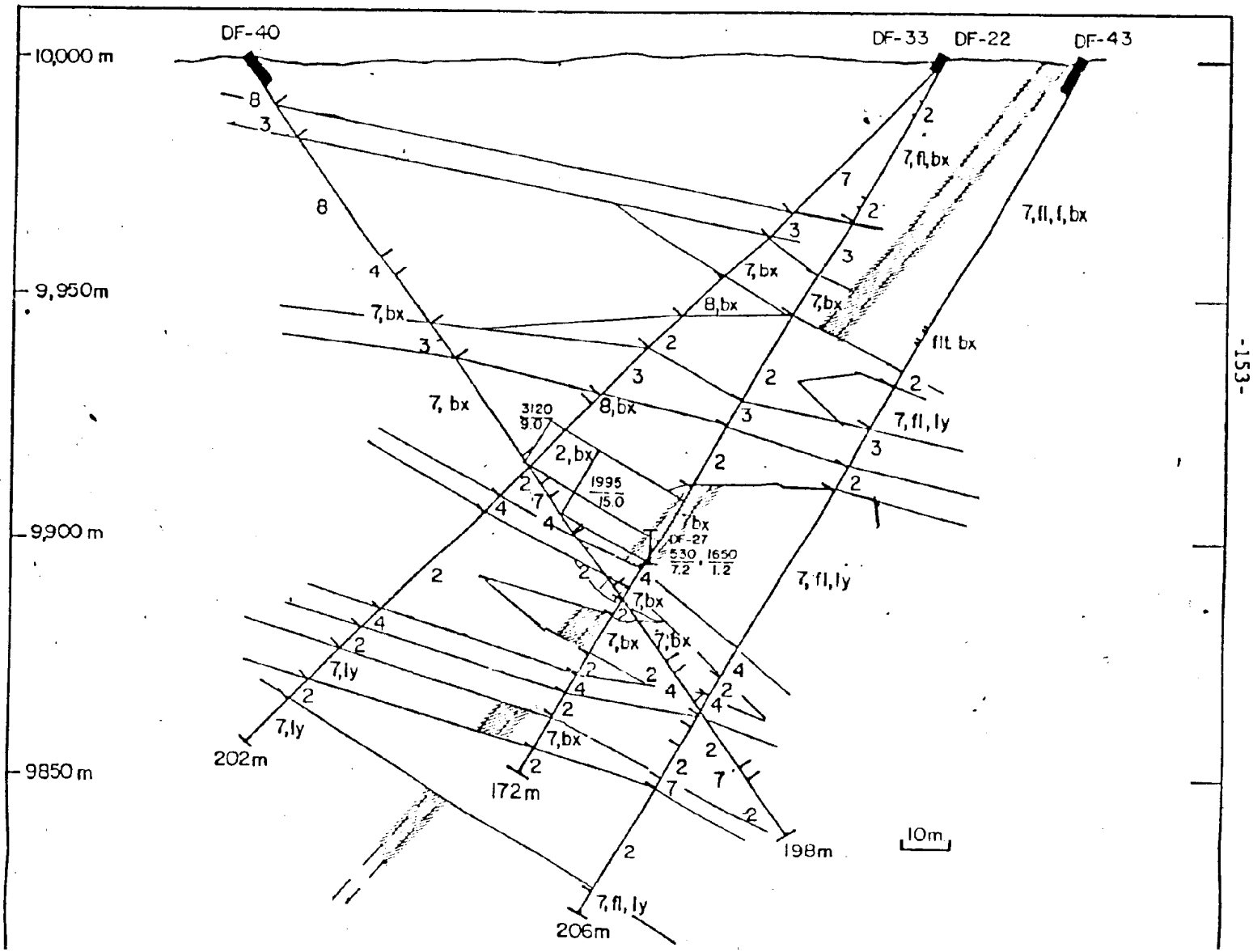
DF-40
DF-33
DF-22
DF-43
10,000 m
9,950m
9,900 m
9850 m
7, bx
8,bx
7,bx
7,fl,bx
7,fl,f,bx
flt bx
7,fl,ly
2,bx
3120/9.0
1995/15.0
DF-27
530/7.2 , 1650/1.2
7,ly
202m
172m
198m
206m
10m

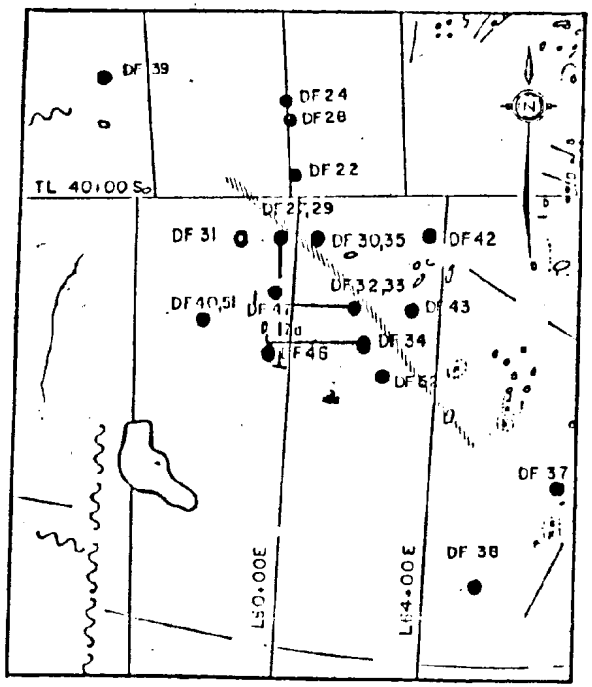

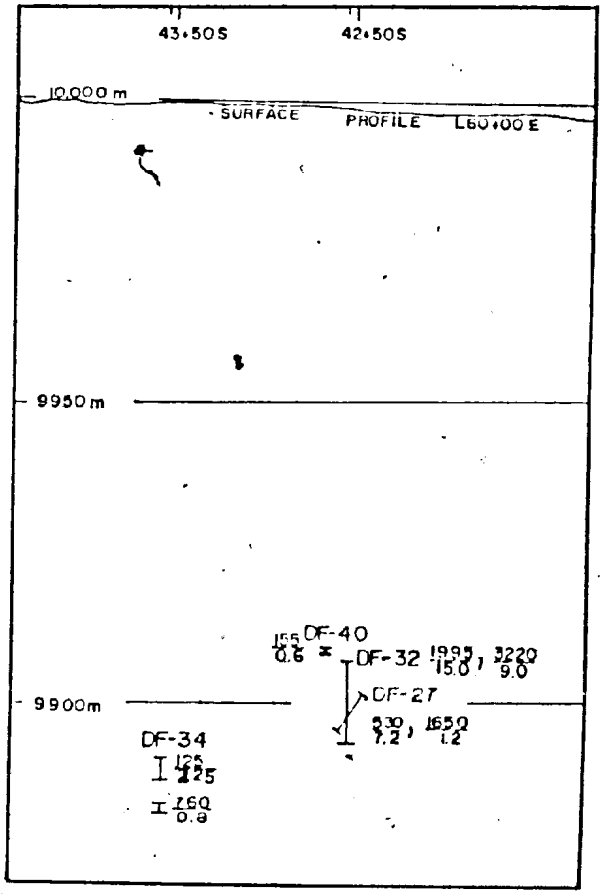

Vertical longitudinal projection of the east DF-zone uranium occurrence (section looking west).

Plate 18: Drill core samples of brecciated rhyolite from DDH DF-32, with dull metallic grey to black pitchblende mineralization.

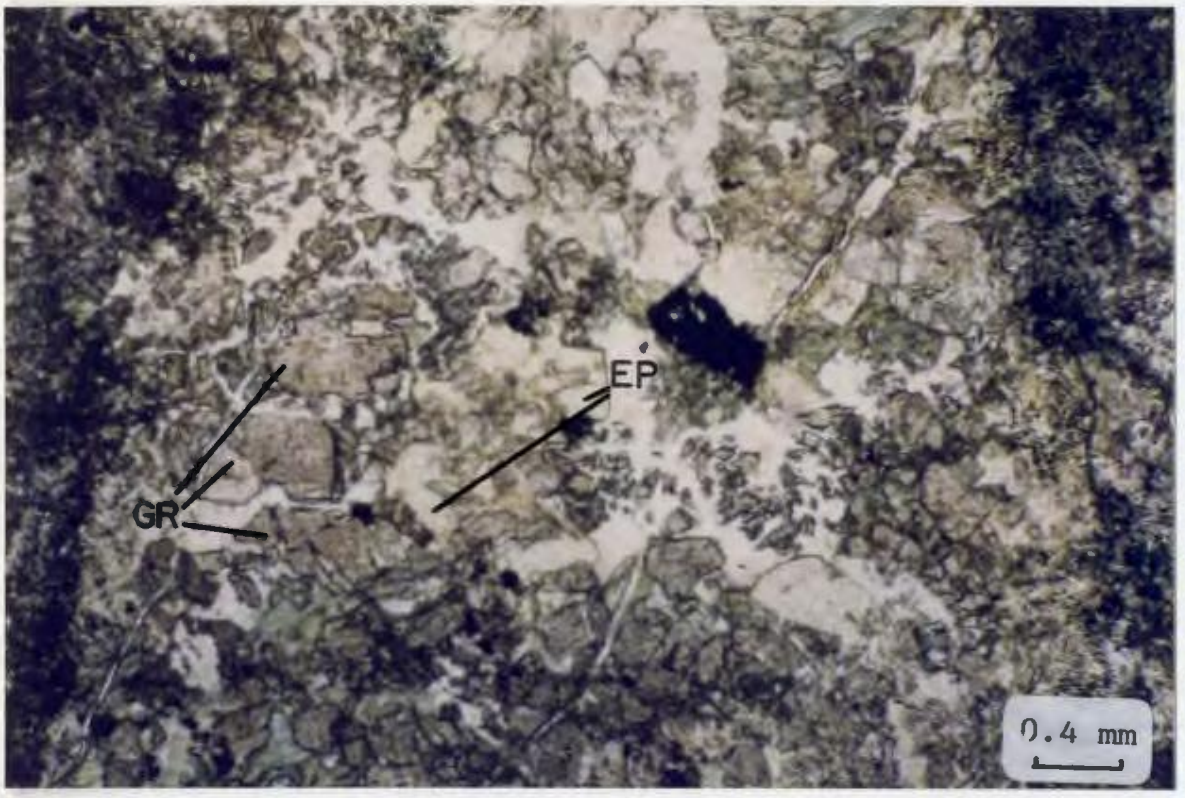

Plate 19: Photomicrograph of a mineralized sample from the east DF-zone uranium occurrence, showing a vein where epidote and garnet are in equilibrium.

to pitchblende veinlets but this is not apparent in hand specimen.

Secondary minerals in veins and lithophysae in the mineralized zone include pitchblende, sericite, K-feldspar, epidote, chlorite, fluorite, garnet, molybdenum and trace zircon, allanite, apatite, chalcopyrite and galena. Pitchblende commonly is the sole component in veinlets in which it occurs but locally pitchblende veins are lined by molybdenum and contain minor fluorite, epidote, chalcopyrite and galena. There is a conspicuous absence of calcite veinlets in this showing. Chlorite veinlets are abundant but are late in the paragenetic sequence, cutting all other vein types. Plates 20-21 characterize the east DF-zone mineralization.

The mineralized zone is cut by a high-Zr rhyolite dike which is neither mineralized nor altered by the mineralizing system. This places an important constraint on the timing of mineralizatron, suggesting that the mineralization was approximately co-magmatic and that the mineralizing system had been shut-down prior to the emplacement of the rhyolite dike.

Plate 20: Photomicrograph of pitchblende in brecciated rhyolite, east DF-zone occurrence.

Plate 21: Autoradiograph showing pitchblende occupying fractures surrounding rhyolite breccia fragments in the east DF-zone occurrence.

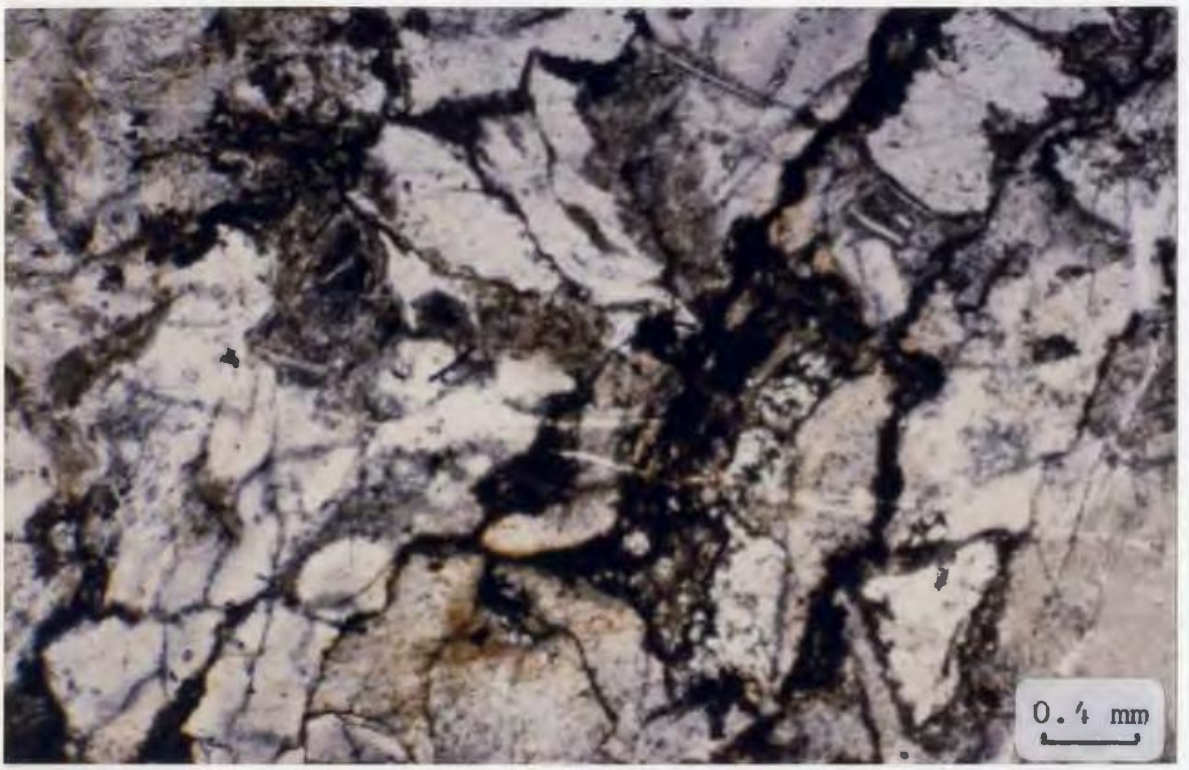
0.4 mm

4.2.2 West DF-zone Showing

In the west DF-zone showing, pitchblende occurs as fine disseminations and micro-veinlets in the groundmass of rhyolitic cataclasite. The zone of fault brecciation is approximately 2-5 m wide and is best observed in diamond drill hole DF-13 (Fig. 19). The host rock grades from cataclasite into a strongly fractured, weakly mineralized zone in which pitchblende occurs as microveinlets in spherulitic rhyolite. Calcite is the dominant secondary mineral in the mineralized zone. Calcite veins and clots are abundant and occur throughout the groundmass of the mineralized zone. Some of the calcite clots appear to be caused by brecciation of pre-existing veinlets, suggesting that calcite is pre- to syn-tectonic as well as post-tectonic. The groundmass of the mineralized zone and the surrounding rocks are hematite altered. Chlorite clots are ubiquitous throughout the groundmass but comprise less than 1% of the rock. Trace very fine subhedral to euhedral pyrite as cubes or with hexagonal outlines are disseminated throughout the mineralized zone and in fractures in the rocks adjacent to the fault breccia. Fractures adjacent to the mineralized cataclasite are filled by quartz-chlorite and rare epidote-fluorite veins. The groundmass is locally spherulitic but most commonly comprises very fine irregular

LEGEND

STRATIFIED ROCKS

- 8 — Basalt flows
- 7, 7b — (7) Rhyolite flows, flow banded or massive, commonly with spherulites and lithophysae
  (7b) Porphyritic rhyolite, >25% phenocrysts
- 6 — Rhyolite ash flows and tuffs
- 5a, 5b — (5a) Laminated siltstone, reworked ash (lacustrine)
  (5b) Conglomerate

INTRUSIVE ROCKS

- 4 — High- Zr rhyolite dikes
- 3 — High- Zr composite dikes
- 2 — Diabase dikes
- 1 — Granite
- Uranium mineralized structure — $\frac{820}{2.1} = \frac{\text{PPM U}}{\text{width m}}$

ABBREVIATIONS

xl – phenocrysts
ly – lythophysae
fl – flow banding
sp – spherulitic
bx – brecciated
lap – lapilli
f – fiamme
amyg – amygduloidal
lam – laminar bedding
agglom – agglomerate
f.g. – fine grained

F – fluorite
ep – epidote
Ca – calcite veins
Q – quartz veins
Mt – magnetite veins
U – uranium
ga – galena
Sn – cassiterite
REE – rare earth elements
W – tungsten
Th – thorium

Figure 19: West DF-zone uranium occurrence.

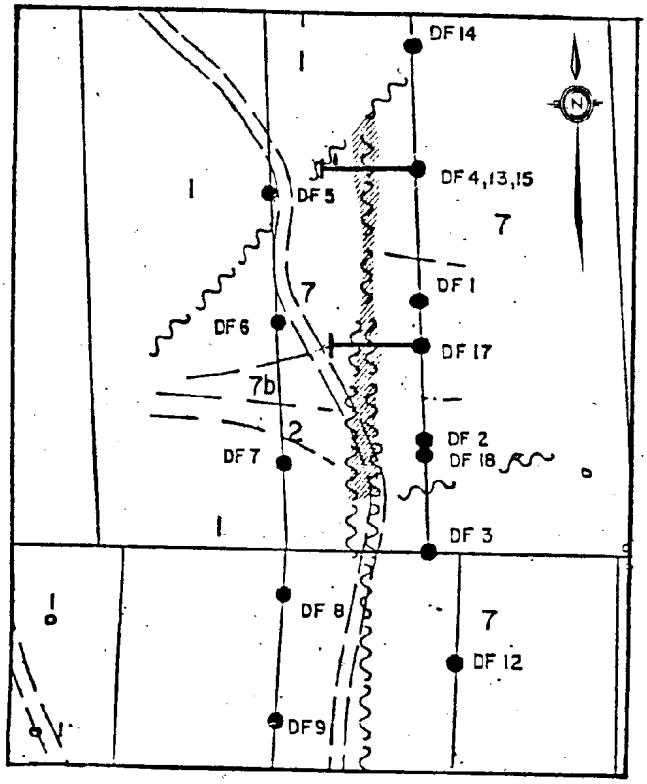
DF14
DF 4,13,15
DF 5
DF 1
DF 6
DF 17
DF 2
DF 18
DF 7
DF 3
DF 8
DF 12
DF 9
1
7
7b
2
N

100 m

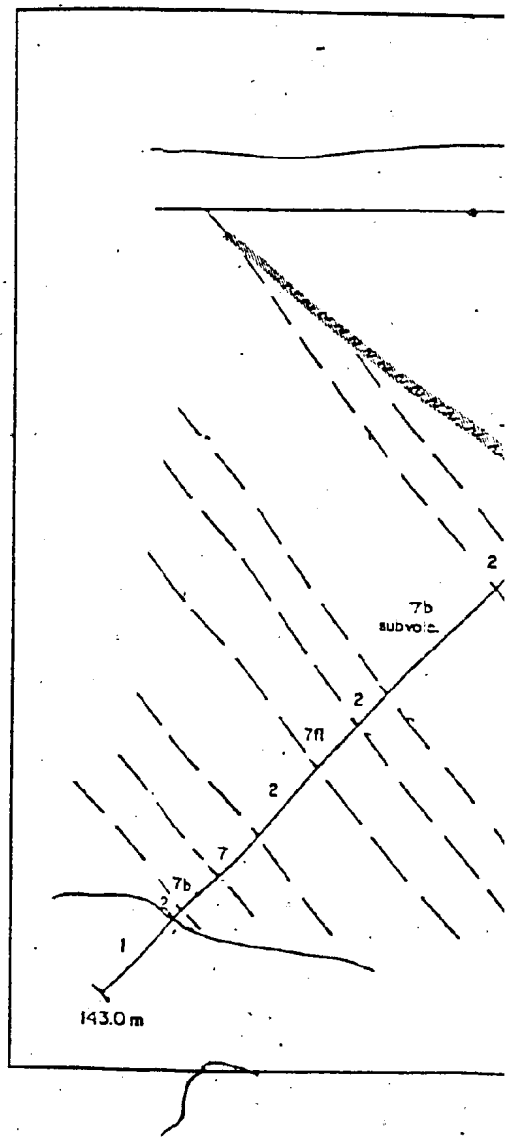
7b
subvolc.
7fl
2
7
1
143.0 m

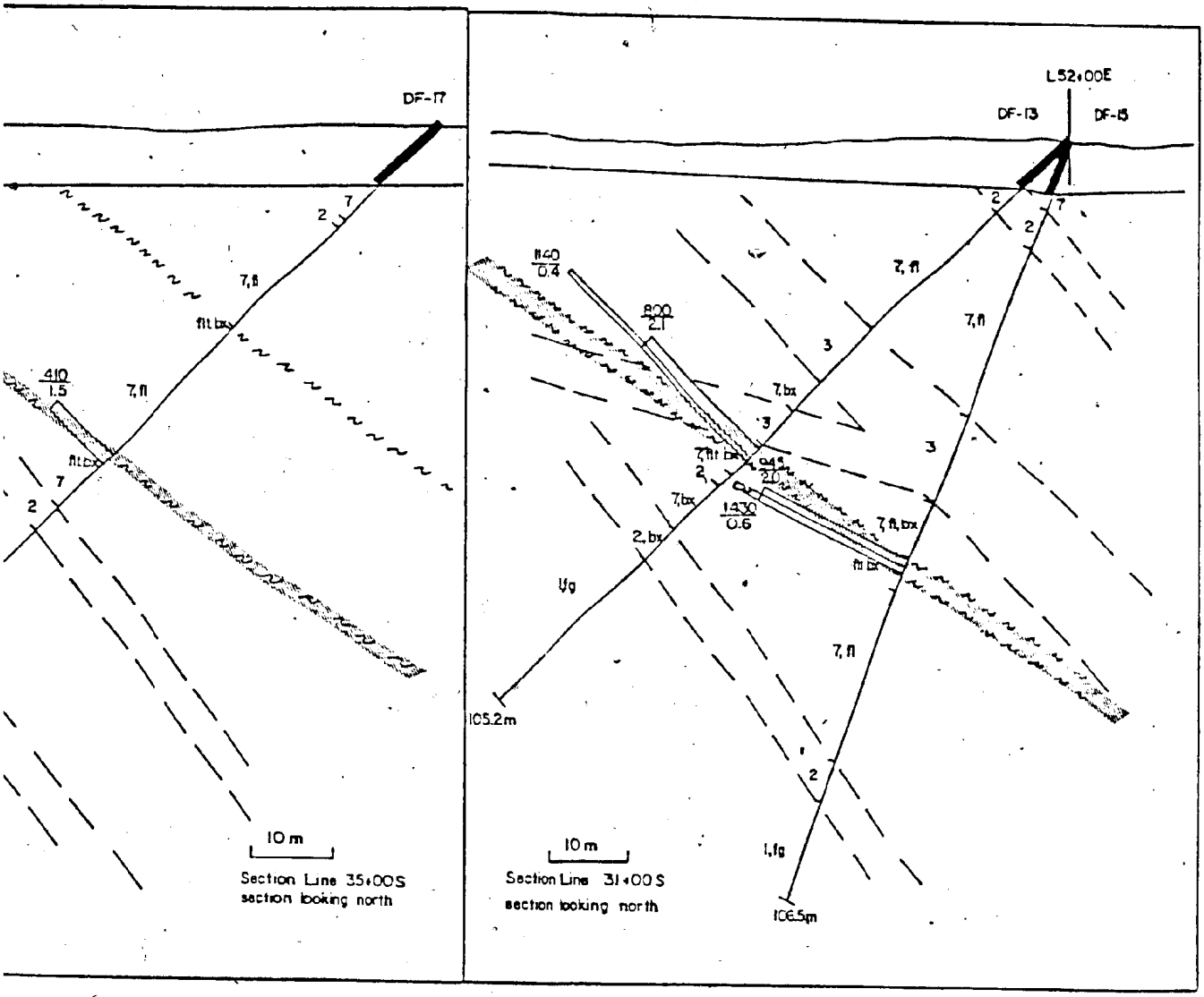
DF-17
2
7
7,fl
flt bx
410
1.5
7,fl
flt bx
7
2
10 m
Section Line 35+00S
section looking north
L52+00E
DF-13
DF-15
2
7
2
1140
0.4
800
2.1
7,fl
7,fl
3
7,bx
3
7,flt bx
2
3
7,bx
1430
0.6
7,fl,bx
2,bx
flt bx
Ufg
7,fl
105.2m
2
1,fg
106.5m
10 m
Section Line 31+00S
section looking north

shaped quartz and feldspar crystals. Poorly preserved flow layering is locally present. Although the whole rock analysis shows the rocks are K-enriched there is a notable absence of sericite in the rocks. Plates 22 and 23 characterize the west DF-Zone uranium occurrence.

The zone has been intruded by a diabase dike which is strongly fractured to brecciated, although not to the same degree as the host rhyolite.

A relatively unaltered rhyolite dike with only minor quartz veining has also intruded the mineralized fault breccia. The dike has a strongly to completely spherulitic groundmass in which spherulites commonly terminate into granophyric zones. The rhyolite dike contains 3-5% combined plagioclase, K-feldspar and embayed quartz phenocrysts which range from 0.5-1 mm in diameter. Trace minerals include rare, very fine grained zircons and allanites. The dike clearly postdates faulting, mineralization and alteration of the host rocks.

The emplacement of the dike places a constraint on the timing of mineralization and alteration. The faulting of the host rhyolite was synchronous with the regional magmatic activity and may have been in response to the intrusion of the granite. The fault zone would be ideal for focusing hydrothermal or magmatic fluids.

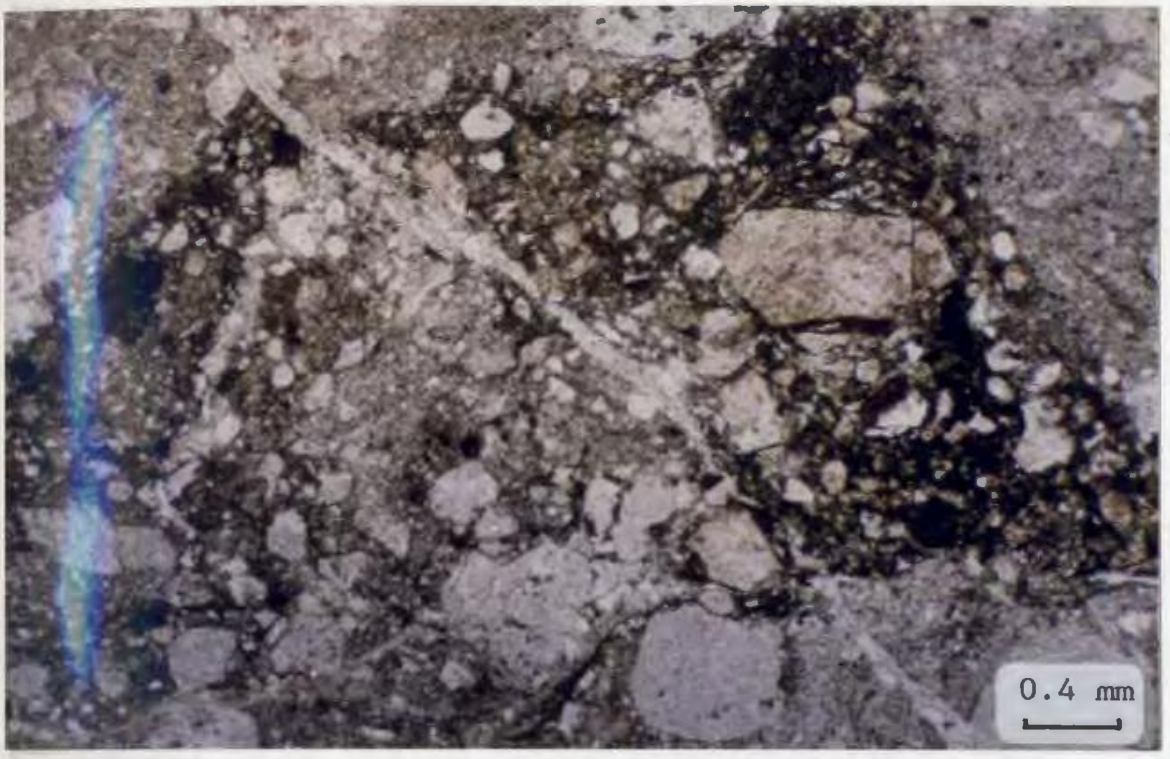

Plate 22: Photomicrograph of uranium in mineralized cataclasite, west DF-zone occurrence.

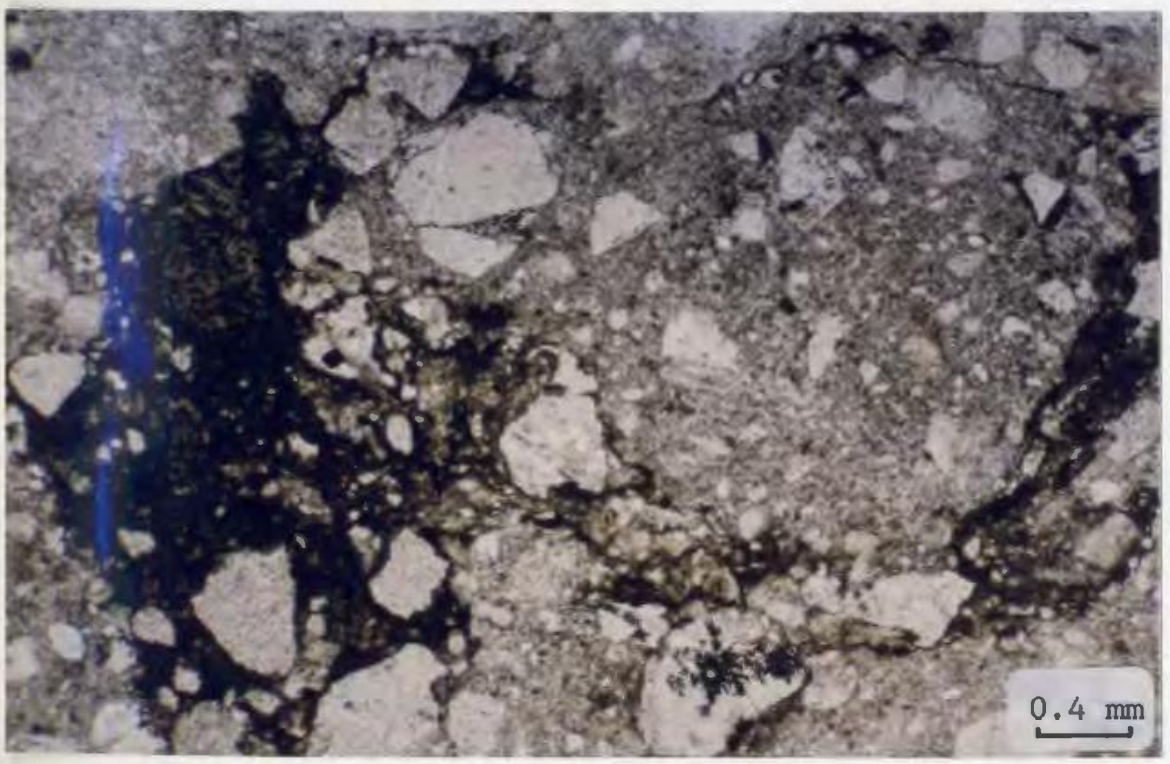

Plate 23: West Df-zone mineralized cataclasite. The black mineral is pitchblende.

4.3 J-zone Mineralization

The J-zone is host to numerous small uranium and base metal-silver occurrences. Figure 6 shows the distribution of uranium mineralization in the J-zone drill core. The largest surface exposure of uranium mineralization in the J-zone is located at 6+00E, 1+50N on the Wentworth grid, where trenching has exposed .025% U_3O_8 over 7 m. A second occurrence is located at 20+00E, 5+00S where approximately 5 m of strongly fractured and mineralized ignimbrite are exposed in a trench. These showings occur near the base of the first ignimbrite deposited above the conglomerate/siltstone marker horizon, referred to in company reports as the J-ignimbrite. This unit is approximately 360 m thick and is overlain by laminated green to black tuff. The J-ignimbrite has higher background uranium than other ignimbrites in the area (21 ppm for J-ignimbrite, 5-7 ppm for average ignimbrite). Significant uranium mineralization was intersected by J-zone drilling at the contact between the base of the J-ignimbrite and an underlying rhyolite flow. The rhyolite flow is intercalated with the marker conglomerate\ siltstone.

Uranium mineralization in the J-zone is hosted by rocks which have undergone two distinct types of alteration. Although K-metasomatized rocks are the most extensive, most mineralized rocks in the J-zone have been subject to strong albitization and locally the host rock is completely altered to albitite. The massive, aphanitic albitites are composed of very fine, irregularly shaped albite crystals. These rocks are commonly, only weakly fractured with small, discontinuous calcite veins. Uranium occurs in fractures or as disseminations in the massive, albitized rhyolites, or less commonly in strongly fractured or brecciated zones. Albitized rhyolite does not always contain uranium mineralization.

Pitchblende is locally hosted by rocks which have undergone similar alteration to the DF-zone occurrences in that they have undergone strong K-metasomatism. Uranium mineralization associated with K-metasomatism in the J-zone occurs in fracture zones, usually adjacent to mineralized albitites.

The areas of Na and K metasomatism are erratically distributed in the J-zone, however K-metasomatized fracture zones commonly cross-cut the albitized rocks implying that K-metasomatism post-dated Na-metasomatism. Variation from albitite to strongly K-metasomatized rhyolite occurs very

sharply, commonly over 10 cm or less with the K alteration restricted to fracture zones and a narrow selvage. In hand speciman the alteration types are very similar in appearance, hence mapping of alteration is very difficult. Both types are characterized by an aphanitic, strongly hematite altered, massive rock which may or may not be porphyritic.

In thin section the K-metasomatism commonly preserves part of the spherulitic texture of the groundmass, except where brecciation is intense. Strong albitization tends to destroy all primary and devitrification textures, except phenocrysts.

4.4 DL-zone REE Occurrence

Anomalous rare earth element concentrations are hosted by brecciated, granophyric granite which was intersected by drill hole DL-16. Up to 2500 ppm Ce and 1350 ppm Dy with correspondingly elevated values for the remaining REEs are hosted by fluorite-calcite-zircon-sphene -allanite-albite veins (Fig. 20 and Plate 24). Anomalous Sn, W and Th are associated with the REE concentration. REE are hosted by allanite and unidentified REE minerals.

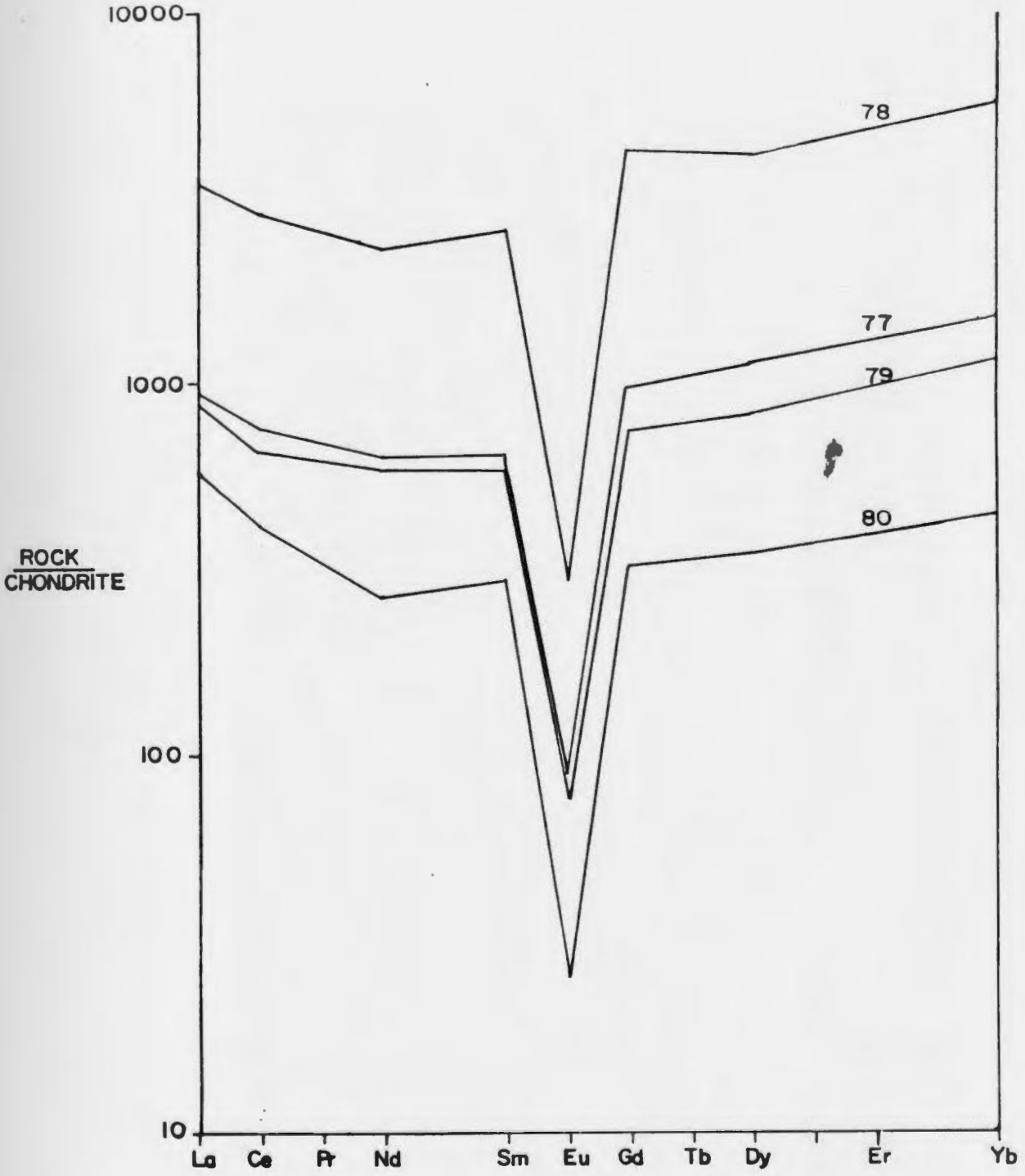

Figure 20: Chondrite normalized rare earth element plot of anomalous samples from DDH DL-16. Normalizing values are those by Evenson et al. (1978).

Plate 24: Photomicrographs showing the complex mineralogy associated with the rare earth element concentration in DDH D1-16. Semi-quantitave micro-probe analyses of minerals have detected measurable quantities of REE's in allanite, zircon, sphene and fluorite along with several unidentified minerals.

a) Nb-Y mineral (REE) intergrown with zircon (Z), albite (A), apatite (P). Top frame is 5X the bottom frame.

b) Zircon (Z), albite (A), calcium-iron silicate (C), Allanite, zoned rim differs from core and contains Yttrium (Y)

c) Zircon (Z), sphene (S), unidentified Nb-Y mineral (Nb-Y).

d) Allanite identified as U-Th silicate (U), albite (A), sphalerite (S), Ce-Ca mineral (CE) possibly yttrofluorite, Fe(Mg)-Al silicate (FE).

e) Nb-Y mineral (N), Nb-U-TH silicate (X), Ca-Fe silicate with minor Ce+Nd (C), albite (A), TH-U silicate (U), bright white speck is galena. Top. frame is 2X the bottom frame.

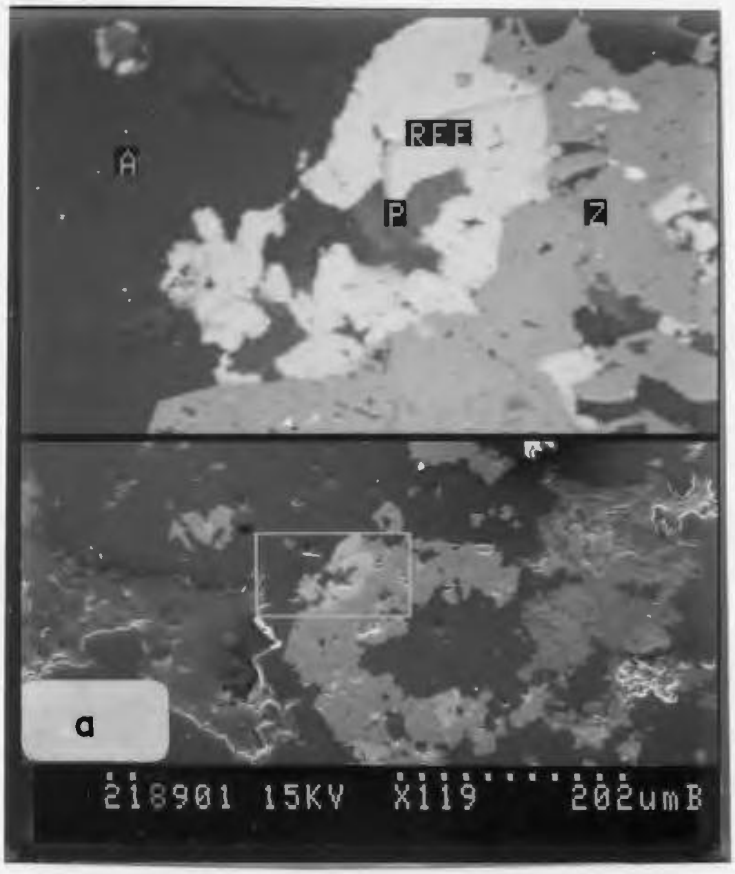
REF
A
P
Z
a
218901 15KV X119 202umB

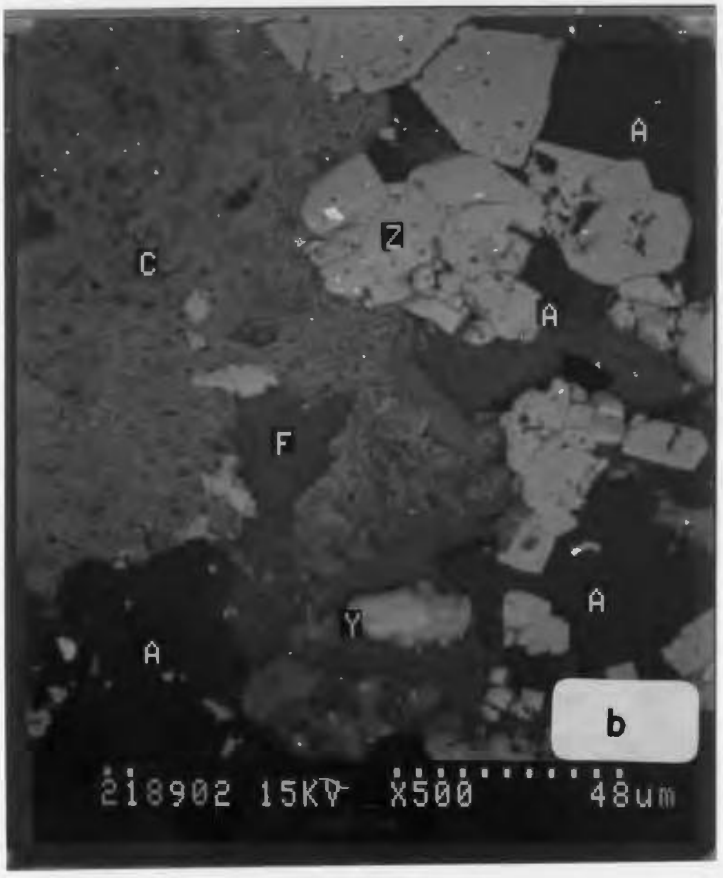
A
Z
C
A
F
A
Y
A
b
218902 15KV X500 48um

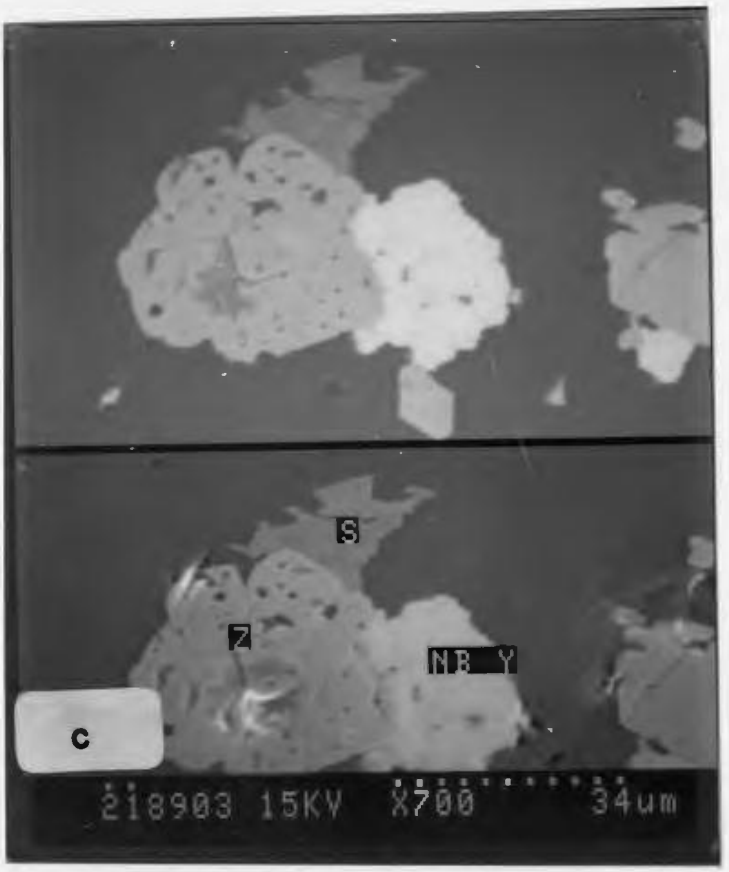
S
Z
NB Y
c
218903 15KV X700 34um

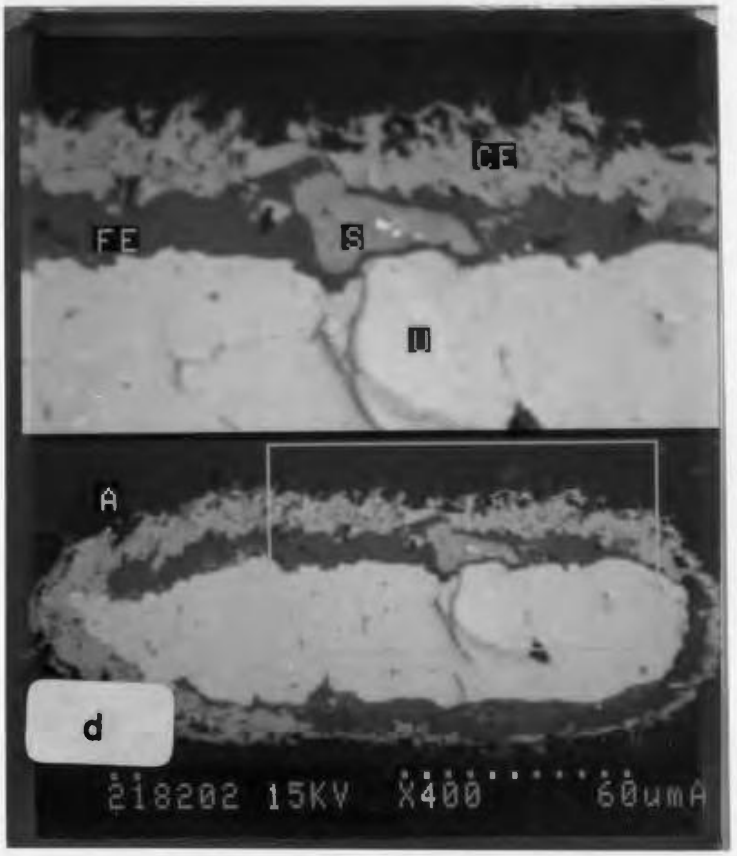
CE
FE
S
M
A
d
218202 15KV X400 60umA

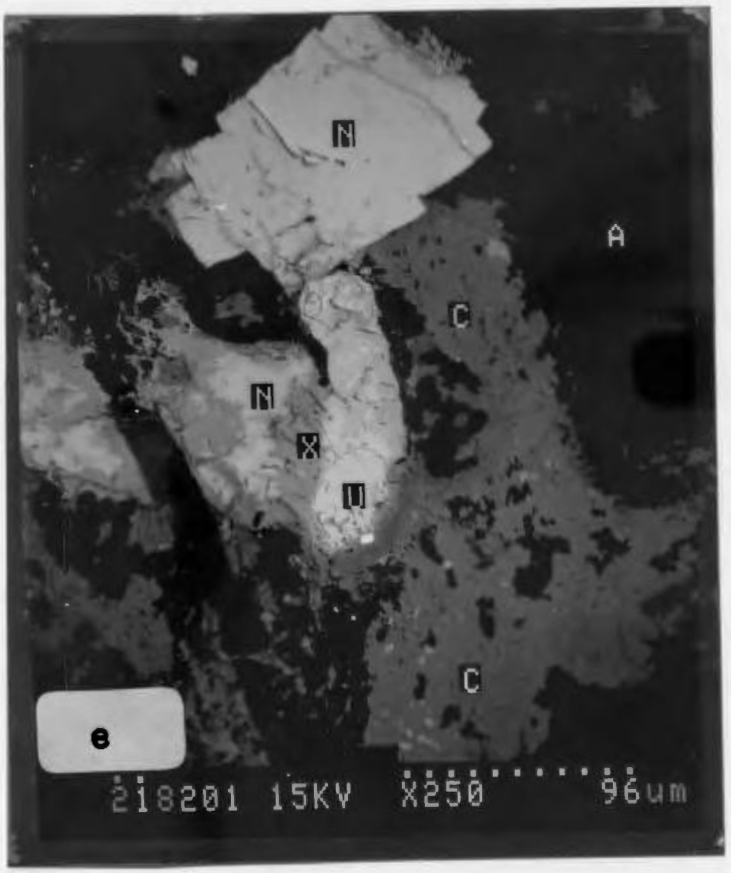
N
A
C
N
X
U
C
e
218201 15KV X250 96um

Table 5: Rare earth element (REE) analysis for samples of granophyric granite, from DL-16 along the east side of Big Snare Lake.

Sample #	Sc ppm	La ppm	Ce ppm	Nd ppm	Sm ppm
C6877	13	310	650	400	130
C6878	2	1150	2500	1460	520
C6879	18	290	570	370	120
C6880	4	190	390	170	60

Sample #	Eu ppm	Tb ppm	Dy ppm	Ho ppm	Yb ppm
C6877	7	51	370	9	340
C6878	23	220	1350	330	1290
C6879	6	39	270	68	260
C6880	2	17	115	29	100

Sample #	Lu ppm	Hf ppm	U ppm	Th ppm
C6877	49	370	28	180
C6878	200	1000	58	600
C6879	38	520	39	250
C6880	14	230	25	160

All elements were analyzed by neutron activation.
Samples are from DDH DL-16: C6877 66.1-66.4m
C6878 66.4-66.6m
C6879 66.6-66.8m
C6880 66.8-67.0m

Analyses of the samples are compiled in Table 5. Although albite is a common component in the REE veins, the host granite has undergone moderate to strong potassic alteration.

4.5 Geochemistry of Uranium Occurrences

Average analyses of the mineralized and adjacent unmineralized rhyolites are listed in Table 5. The East DF-zone occurrence shows a decrease in SiO_2, Na_2O, MnO and CaO and a relative increase in Al_2O_3, TiO_2, K_2O, MgO and an order of magnitude increase in P_2O_5 relative to adjacent unmineralized rocks. There is also an increase in F, Cu, Zn, Mo, Rb, Zr, Ag, Pb and U associated with mineralization. There is only a moderate increase in F in the actual mineralized zone but there is a 24 m section immediately adjacent, down drill core which is strongly enriched in F with values from 1800-6600 ppm. Sr remains approximately the same and there is a slight decrease in Th in the mineralized rocks relative to the unmineralized rocks.

In the west DF-zone showing there is a decrease in SiO_2, K_2O, F, Rb, Sr and Th and an increase in Al_2O_3, Na_2O, Cu, Zn, Zr, Ag, and U in the mineralized rocks relative to the unmineralized rhyolites.

Table 6: Average analysis of mineralized and adjacent unmineralized rhyolites from the Wentworth Prospect, n = number of samples, -- = not analyzed.

		mineralized albitites, J-zone	unmineralized albitites J-zone	west DF-zone mineralized	west DF-zone unmineralized	east DF-zone mineralized	east DF-zone unmineralized	J-zone K-altered mineralized	J-zone K-altered unmineralized
%	SiO2	66.7	72.4	72.4	73.3	68.3	76.8	73.5	76.2
	Al2O3	16.8	13.4	14.2	13.9	14.4	11.5	12.9	11.3
	CaO	1.39	1.08	0.67	0.68	0.44	0.85	0.59	0.67
	MgO	0.20	0.21	0.26	0.29	0.36	0.28	0.15	0.28
	Na2O	9.76	7.59	1.57	1.34	0.34	1.02	0.85	1.35
	K2O	0.15	0.15	7.73	8.53	9.93	7.36	8.10	6.85
	FeO	4.09	3.99	2.61	2.31	1.80	1.33	3.42	2.37
	MnO	0.04	0.05	0.16	0.15	0.06	0.03	0.04	0.04
	TiO2	0.40	0.37	0.13	0.13	0.18	0.17	0.24	0.26
	P2O5	0.42	0.14	0.03	0.02	0.11	0.02	0.09	0.02
ppm	U	580	11	765	19	3971	8	763	9
	Th	25	17	10	29	21	22	26	19
	Cu	35	26	154	35	58	17	55	62
	Zn	91	117	62	48	188	50	128	190
	Ag	9	1	10	1	4	1	1.5	1
	Pb	139	160	69	60	476	30	128	101
	F	340	91	290	463	688	380	179	94
	Sn	19	22	2	2	--	3	5	4
	Mo	--	--	2	2	0-3700	<2	--	--
	Rb	--	--	230	278	450	279	--	--
	Sr	--	--	62	72	79	67	--	--
	Zr	--	--	228	194	263	214	--	--
	W	--	--	2	7	--	3	--	--
	n	23	20	10	10	10	10	10	15

In the J-zone The mineralized albitites show a strong decrease in SiO_2, and an increase in Al_2O_3, CaO, MgO, Na_2O, FeO, TiO_2, P_2O_5 U, Th, Cu, Ag and F- in the mineralized relative to the unmineralized albitized rhyolites. The concentration of K_2O remains constant.

In the K-metasomatized rocks of the J-zone there are increases in Al_2O_3, K_2O, FeO, U, Th, F and slight decreases in SiO_2, CaO, Na_2O, Cu and Zn in the mineralized relative to the unmineralized rocks.

4.6 Discussion

4.6.1 Alteration and Mineralization

There are two distinct types of alteration associated with uranium mineralization in the J-zone, albitization and K-metasomatism. Cross-cutting relations suggest that albitization preceded K-metasomatism.

Na-metasomatized rocks are commonly associated with granite-related ore deposits, such as hydrothermal uranium (Poty et al., 1974, Cuney 1978, Leroy,1978, White and Martin, 1980) and tin (Taylor 1979).

Strong (1982) describes a progression from alaskitic granite to albitite, at the contact of the St. Lawrence alkaline/peralkaline plutonic complex in

Newfoundland, in which the albitized rocks are mineralogically and geochemically comparable to the albitized rocks of the J-zone. At St. Lawrence original quartz and K-feldspar have been partly to completely replaced by albite and calcite resulting in a net loss of K and a net gain of Na, Al, Ca, and Si. Strong (1982) shows that the apparent desilication suggested by the whole rock analysis actually represents a net gain of Si which is masked by the dilution effects of the albite and calcite components. Unfortunately a detailed analysis of the alteration at the Wentworth prospect cannot be done because the original composition of the rocks is unknown. Rocks which are not albitites have been affected by pervasive K-metasomatism. The comparison with the St. Lawrence albitites is not meant to imply a rigorous correlation, however the alteration products are strikingly similar. Strong (1982) suggests that because there is a lack of hydrous and fluorous alteration products within the albitite zone the activities of H_2O and F in the altering fluids in this alteration zone were probably low. REE data for the St. Lawrence rocks suggest high CO_2 activity and Strong suggests that the altering process is better described as carbothermal rather than hydrothermal

metasomatism. Fluorite is abundant in certain alteration zones in the St. Lawrence Granite.

Rare fluorite veinlets and numerous small calcite veinlets and very fine apatite crystals occur in the mineralized J-zone albitites, possibly suggesting a higher activity of F and P associated with mineralization. The barren albitites do not have fluorite veins and are chemically more similar to the St. Lawrence albitites. Strong (1982) notes there is an enrichment of U and Sn in the albitites relative to the unaltered grahites. There is strong enrichment of uranium in the majority of albitites sampled in the J-zone but there are abundant strongly albitized samples which show no uranium enrichment. Sampling was partly controlled by downhole gamma logs, so the total area of barren albitites is not well defined.

Barren albitites appear to envelop mineralized, albitized zones. The envelope is poorly defined because it has been observed only in drill core and has been cross-cut by numerous later zones of K-metasomatism, but in two dimensions at least, barren albitites commonly occur on either side of mineralized albitites. Albitites observed sporadically throughout the DF-zone are barren, but since the zone of alteration is more extensive than the mineralized zone, prospecting for albitite may be an

effective exploration procedure.

K-metasomatism is the most widespread alteration affecting all the volcanic rocks of the J-zone, DF-zone and DL-zone and it is associated with uranium mineralization in most of the occurrences on the prospect. The mineralized rocks tend to have slightly higher K_2O values than the unmineralized rocks, but zones with the most intense K-metasomatism (approx. 10-14% K_2O) are not usually mineralized. Cathelineau (1983) has shown that K-rich fluids are favourable for the transport of uranium.

The alteration assemblages of the K-metasomatized mineralized zones are similar to those described for potassic and phyllic alteration or K-silicate and sericitic alteration zones described by Lowell and Guilbert (1970), Creasey (1959,1966) and Meyer and Hemley (1967). Because the alteration is so extensive the only obvious source for the required large volumes of K-rich fluids is thought to be the granite and a related hydrothermal system.

The Hart Lake Granite was emplaced at a shallow level in the crust, where it intrudes its comagmatic volcanic pile. Plutons associated with porphyry deposits, in spite of numerous differences, are also emplaced at shallow (1-2 km) depths (Titley and Beane, 1981). It is reasonable that a hydrothermal system with similarities to

porphyry systems could have developed in the Wentworth area.

By comparing the alteration assemblages associated with the mineralization in the Wentworth area with those observed in porphyry deposits and less well understood hydrothermal uranium deposits, a qualitative asessment of the mineralizing system at Wentworth should be possible. Diagrams used below are based on thermodynamic data and apply directly only for defined intensive variables. By necessity there is much extrapolation involved in applying such diagrams to natural systems, but they provide valuable insight into the physico-chemical conditions associated with ore deposition. Table 6 is a comparative classification of porphyry copper alteration assemblages.

4.5.2 Mineral Stability and Solubility

The composition of important igneous and hydrothermal silicate minerals in porphyry copper deposits are defined by the chemical components K_2O, Na_2O, CaO, MgO, FeO, Fe_2O_3, Al_2O_3, SiO_2 and H_2O. Quartz and water are in excess in these systems and are considered to have constant activity (Beane, 1982). Al_2O_3 is considered to be immobile (Hemley et al., 1980). Alteration at a given level in the earth's crust may be

Table 7: Comparative classifications of porphyry copper assemblages (from Beane, 1983).

Creasey (1959, 1966)	Lowell and Guilbert (1970)	Rose (1970)	Meyer and Hemley (1967)
K-silicate K-feldspar biotite muscovite	*Potassic* K-feldspar biotite sericite chlorite quartz	*Orthoclase-Sericite-Quartz* *Orthoclase-Biotite-Quartz* *Orthoclase-Sericite-Biotite-Quartz*	*K-silicate* K-feldspar biotite muscovite anhydrite
(Sericite-Quartz-Pyrite)	*Phyllic* quartz sericite pyrite hydromica chlorite	*Sericite-Quartz*	*Sericitic* sericite quartz pyrite ± chlorite
Argillic kaolinite muscovite	*Argillic* kaolinite montmorillonite chlorite	*Sericite-Kaolinite-Quartz*	*Argillic* 1) Advanced kaolinite/dickite pyrophyllite 2) Intermediate kaolinite group montmorillonite ± chlorite
Propylitic muscovite (sericite) epidote chlorite carbonate	*Propylitic* chlorite epidote	*Propylitic* epidote albite calcite chlorite	*Propylitic* epidote albite chlorite septachlorite carbonate

considered to proceed at a constant pressure (Beane, 1982). Therefore the chemical variables involved in the hydrothermal system are K_2O, Na_2O, CaO, MgO, FeO, Fe_2O_3 and temperature.

The following two reactions are very important in the development of alteration which accompanies porphyry copper deposits (Burnham, 1979);

$$3\text{K-feldspar} + 2H^+ = \text{Muscovite} + 6SiO_2 + 2K^+$$

$$3\text{Muscovite} + 2H^+ + 3H_2O = \text{Kaolinite} + 2K^+$$

K (equilibrium constant)$=[K^+]/[H^+]$ for both reactions since the solids and H_2O are saturated.

The ratio of cations/H^+ has been found to be a major control of silicate mineral stability in porphyry deposits (Hemley and Jones, 1964; Montoya and Hemley, 1975; Shade, 1974). Figure 21 shows the stability fields for the relevant silicate minerals based on the ratio of cations to H^+, using $[K^+]/[H^+]$ as a reference since K-metasomatism has been shown to be the dominant alteration (Creasey, 1966; Meyer and Hemley, 1967; Rose, 1970; Lowell and Guilbert, 1970). On these diagrams potassic alteration corresponds to the K-feldspar field, phyllic alteration to

Figure 21: Stability relations among minerals as a function of various pairs of cation activity ratios in a co-existing aqueous phase at 500 bars. All diagrams conserve Al_2O_3 among solids and contain excess SiO_2 and H_2O. Quartz saturation is defined in all cases. In diagram (a), mixed potassium and sodium systems at 350° C the curved portion of the pyrophyllite stability field schematically illustrates limited solid solution in the micas. Diagram (b) shows mixed potassium and calcium systems at 350° C and $aCO_2=20$. In diagram (c) mixed potassium and magnesium systems, the stability of biotite takes account of solid solution to permit stability with K-feldspar at a temperature near 300° C; the chlorite stability field is schematically drawn to depict compatibility with K-feldspar, as suggested for pure phases at 300° C. Diagram (d) is a schematic representation of mixed potassium and magnesium systems at a temperature above the equilibrium value for muscovite-biotite compatibility at a given pressure. From Beane (1982).

In these diagrams the assemblage associated with the east DF-zone and potassic altered J-zone uranium occurrences would generally fall on the muscovite K-spar boundary. The west DF-zone occurrence would fall inside the K-spar stability field.

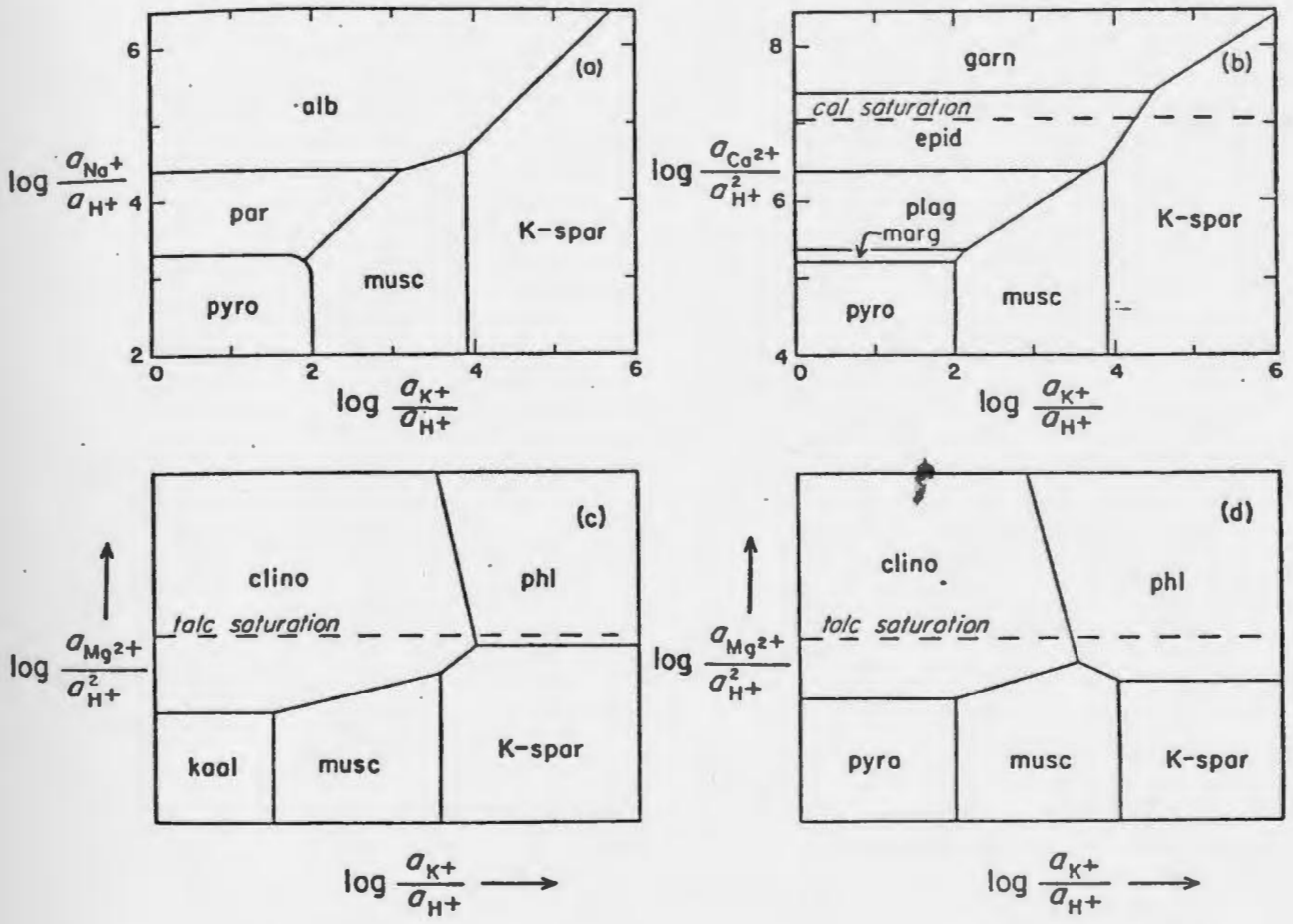

Key to Minerals:

alb = albite
cal = calcite
clino = clinochlore (mg-chlorite)
epid = epidote
garn = garnet (grossular/andradite)
kaol = kaolinite
K-spar = K-feldspar
marg = margarite
musc = muscovite
par = paragonite
phl = phlogopite (Mg-biotite)
plag = plagioclase (albite/anorthite)
pyro = pyrophyllite

the muscovite field, argillic alteration to the kaolinite or pyrophyllite field and propylitic alteration corresponds to the chlorite field.

In the potassic zone strong K-metasomatism alters igneous plagioclase to K-feldspar and igneous amphibole to biotite. Magnesium, Na and Ca are leached from the potassic zone (Beane, 1982).

Figure 22 from Burnham (1979) shows the K/H ratio for an aqueous fluid in equilibrium with a granodiorite magma above the solidus, and the subsolidus mineral assemblages. If an aqueous phase is exsolved from a magma which is in equilibrium with either hornblende or biotite it will have a K/H ratio which is capable of producing K-metasomatism. Most aqueous phases are exsolved from magmas in equilibrium with hornblende or biotite (Burnham, 1979). From point H to point E in Figure 22 the fluid is capable of causing potassic alteration. If the K/H ratio of the fluid decreases during alteration, as for alteration of plagioclase to K-feldspar than the fluid path may be from H to I. When the fluid path hits the boundary between K-feldspar and muscovite it is buffered and will move down temperature along the boundary. Muscovite is commonly included in potassic assemblages and it is likely that

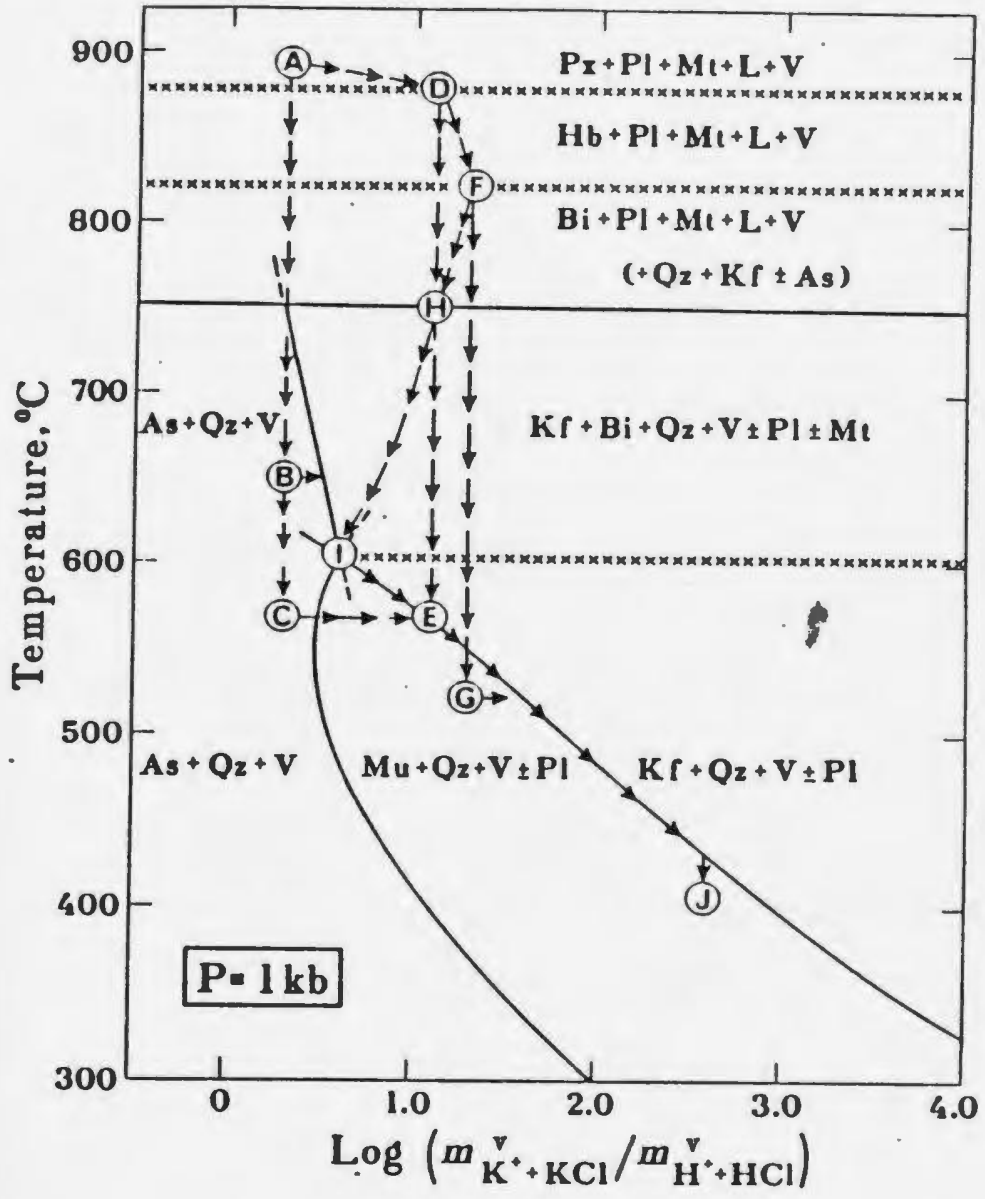

Figure 22: Log ($^{m^v}K^+ + KCl / ^{m^v}H^+ + HCl$) of aqueous chloride solutions in equilibrium or reaction relationship with hypersolidus granodioritic magma (above horizontal solid line through point H) and the indicated subsolidus mineral assemblages at 1.0 kb. From point H to point E a fluid exsolved from the magma would be capable of causing potassic metasomatism (see text for discussion). As - aluminum silicate, Bi - biotite, Hb - hornblende, Kf - K-rich alkali feldspar, L - melt, Mt - magnetite, Mu - muscovite, Pl - plagioclase, Qz - quartz, V - aqueous fluid phase. (from Burnham, 1979)

potassic alteration commonly occurs along the muscovite - K-feldspar univarient line (Burnham, 1979).

Phyllic alteration involves the leaching of Na, Mg, and Ca accompanied by addition of or constant K (Beane, 1982). This results in the destruction of all minerals except quartz, sericite and pyrite which are precipitated in this zone. The mixing of magmatic with meteoric fluids in this zone results in a rapid decrease in temperature and lowering of the K/H ratio so that the fluid moves well into the muscovite field of Figures 21 and 22.

In the Wentworth area the occurrences of uranium mineralization which are associated with K-metasomatism all have typical potassic or phyllic zone assemblages. In the east DF-zone showing and in the J-zone showings K-feldspar and muscovite occur together in veins and are considered to be in equilibrium. The alteration in these zones probably occurred along a univariant line between muscovite and K-feldspar stability as in Figure 22. Burnham (1979) notes that pressure changes of $\pm$0.5 kb. will cause only slight vertical adjustments to the field boundaries in Figure 22. The west DF-zone showing has no sericite associated with it and occurs within 20m of the granite contact. This suggests that alteration at this showing probably occurred at a higher temperature and/or K/H ratio than the east

Figure 23: Calculated stability fields among minerals as a function of temperature and cation activity ratios in a coexisting aqueous phase at 500 bars. All systems conserve Al_2O_3 among solids and contain excess SiO_2 and H_2O. In diagrams of potassium bearing phases (a) and sodium bearing phases (b) solid lines denote quartz saturation while dashed lines show the effects of limiting dissolved silica by amorphous silica saturation. The calcium bearing phases (c) show stoichiometric compositions at quartz saturation. In calcium-bearing phases with provision for solid solution (d), compositions of phases are representative of porphyry copper occurrences. Calcite saturation curve is for $aCO_2 = 40$. Diagrams from Beane (1982).

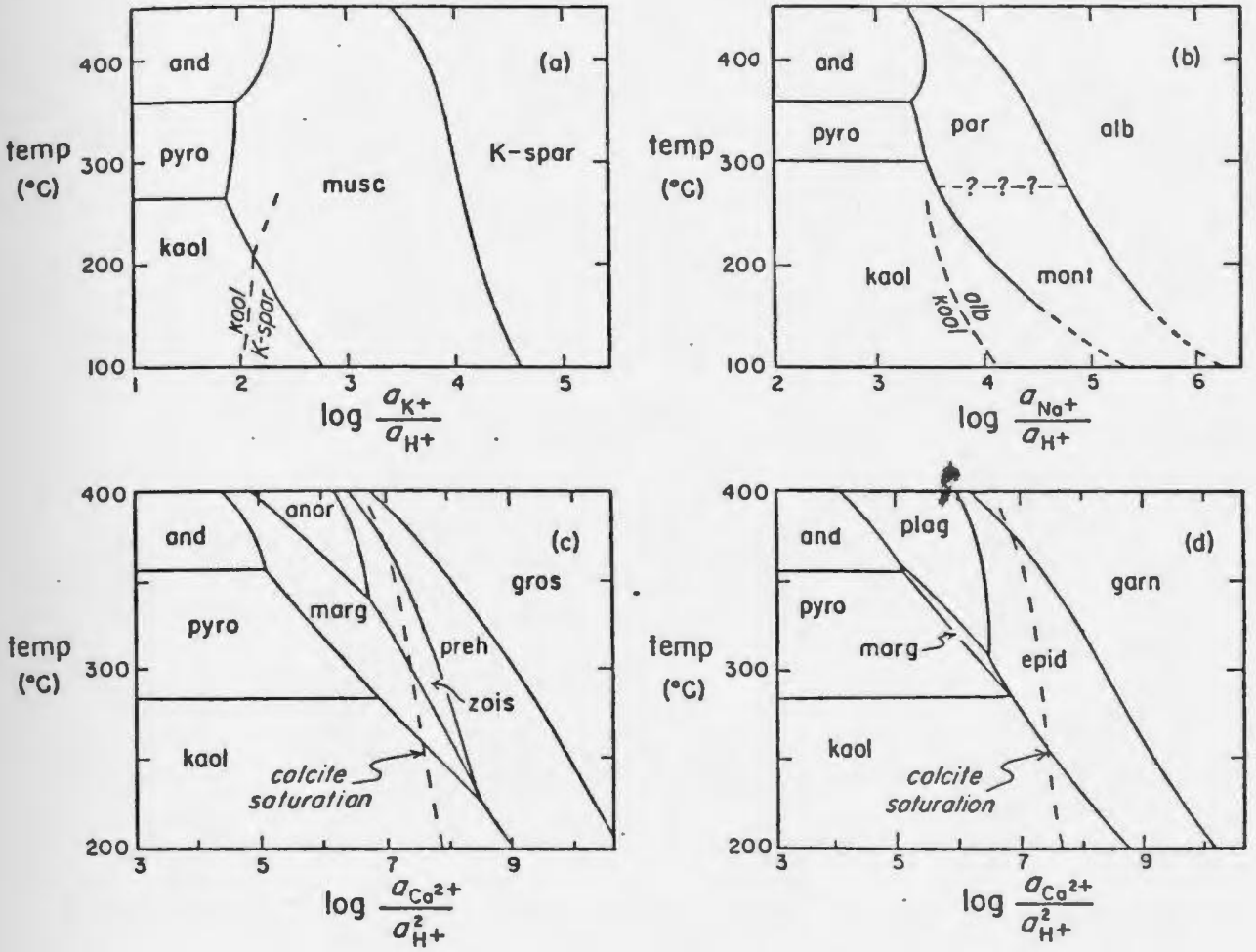

Key to Minerals:

alb = albite
cal = calcite
clino = clinochlore (mg-chlorite)
epid = epidote
garn = garnet (grossular/andradite)
kaol = kaolinite
K-spar = K-feldspar
marg = margarite
musc = muscovite
par = paragonite
phl = phlogopite (Mg-biotite)
plag = plagioclase (albite/anorthite)
pyro = pyrophyllite

DF-zone and J-zone showings, well within the stability field of K-feldspar.

Figure 23 shows the stability relations of minerals as a function of cation activity and temperature in a coexisting aqueous phase at 500 bars pressure. All systems assume excess SiO_2 and H_2O and conserve Al_2O_3. Diagram (a) shows that muscovite and K-feldspar are stable for a wide range of temperatures, and their respective stabilities are far more dependant on K activity in solution than temperature. This diagram suggests that the log a_{K^+}/a_{H^+} ratio at the east DF-zone showing and the J-zone K-metasomatized showings were in the range of 3.5-4.5 depending on temperature and assuming burial of 1-2 Km. However in diagram (d) in which the calcium-bearing phases are plotted with provisions for solid solution, the assemblages at the east DF-showing may suggest that temperatures were in the range of 400 °C, if pressures were near 500 bars. In this occurence there is a notable absence of calcite, which suggests that the activity of Ca^{2+} did not reach the calcite saturation curve. Garnet and epidote occur in veinlets together, suggesting that the fluids were along the garnet-epidote boundary but below the calcite saturation curve. These conditions are only met at log $a_{Ca^{2+}}/a_{H^+}^2$ approximately 7 and temperatures above

approximately 380°C.

Uranium is a lithophile element which is enriched in the upper crust (Nash et al., 1981). In nature it occurs in the tetravalent (U IV), pentavalent (U V) and the hexavalent (U VI). In most subsurface environments uranium occurs as U(IV) because the other two are stable only under oxidizing conditions. The combination of large size and high charge of U(IV) prevents it from entering the lattice of rock-forming minerals except in trace amounts (Rich et al., 1977). Metals dissolved in volcanic glass are released during devitrification and uranium released in this form is precipitated as a secondary oxide which is readily leachable (Romberger, 1984; Zeilinski, 1978 and 1982) and accessible for redistribution and concentration in a hydrothermal system. The geological evidence at the Wentworth prospect indicates that an extensive hydrothermal system was active. A major source for the uranium in all showings is considered to be the volcanic rocks of the Byers Brook Formation, possibly with some input directly from the Hart Lake Granite.

The source of complexing agents may be either the granite or the volcanic rocks. Table 7 lists the uranyl and uranous complexes which are known to form with various anions. Uranous complexes are not considered to be

Table 8: List of uranyl and uranous complexes known to form with various anions (from Romberger, 1984).

H_2O:	U^{4+}, UOH^{3+}, $U(OH)_2^{2+}$, $U(OH)_3^{+}$, $U(OH)_4^{\circ}$, $U(OH)_5^{-}$, UO_2^{2+}, UO_2OH^{+}, $UO_2(OH)_2^{\circ}$, $UO_2(OH)_3^{-}$, $U_2(OH)_5^{3+}$, $(UO_2)_2(OH)_2^{2+}$, $(UO_2)_3(OH)_5^{+}$, U^{3+}, UO_2^{+},
SULFATE:	USO_4^{2+}, $U(SO_4)_2^{\circ}$, $UO_2SO_4^{\circ}$, $UO_2(SO_4)_2^{2-}$,
CARBONATE:	$UO_2CO_3^{\circ}$, $UO_2(CO_3)_2^{2-}$, $UO_2(CO_3)_3^{4-}$,
PHOSPHATE:	$UHPO_4^{2+}$, $U(HPO_4)_2^{\circ}$, $U(HPO_4)_3^{2-}$, $U(HPO_4)_4^{4-}$, $UO_2HPO_4^{\circ}$, $UO_2(HPO_4)_2^{2-}$, $UO_2H_2PO_4^{+}$, $UO_2(H_2PO_4)_2^{\circ}$, $UO_2(H_2PO_4)_3^{+}$,
CHLORIDE:	UCl^{3+}, UO_2Cl^{+}.
FLUORIDE:	UF^{3+}, UF_2^{2+}, UF_3^{+}, UF_4°, UF_5^{-}, UF_6^{2-}, UO_2F^{+}, $UO_2F_2^{\circ}$, $UO_2F_3^{-}$, $UO_2F_4^{2-}$.

important transporters of uranium because of the low solubility of U(IV) (Romberger, 1984; Langmuir, 1978).

Langmuir (1978) has shown that at 25°C fluoride, phosphate and carbonate complexes are important transporters of uranium in acid, neutral and alkaline solutions respectively (Fig. 24), for typical groundwater ligand concentrations. As temperatures increase there is a marked decrease in the stability of uranyl carbonate complexes so that at 100°C and pCO_2 of 10^{-2} carbonate complexes are insignificant at any pH. Experimental data of Rafalski (1958) and Miller (1958) indicate that uranium solubility in carbonate solutions decreases 100 fold between 100 and 200°C. If pCO_2 is increased with temperature, significant solubility can be maintained (Nash et al., 1981).

The uranyl phosphate complex, $UO_2(HPO_4)_2^{2-}$ is so stable that at typical groundwater concentrations of PO_4 =0.1ppm this complex dominates from approximately pH 4 to pH 7.5 (Fig. 24).

Romberger (1984) has used existing thermodynamic data to evaluate the stability of uranium complexes in hydrothermal solutions up to 300°C and the following discussion is summarized from him.

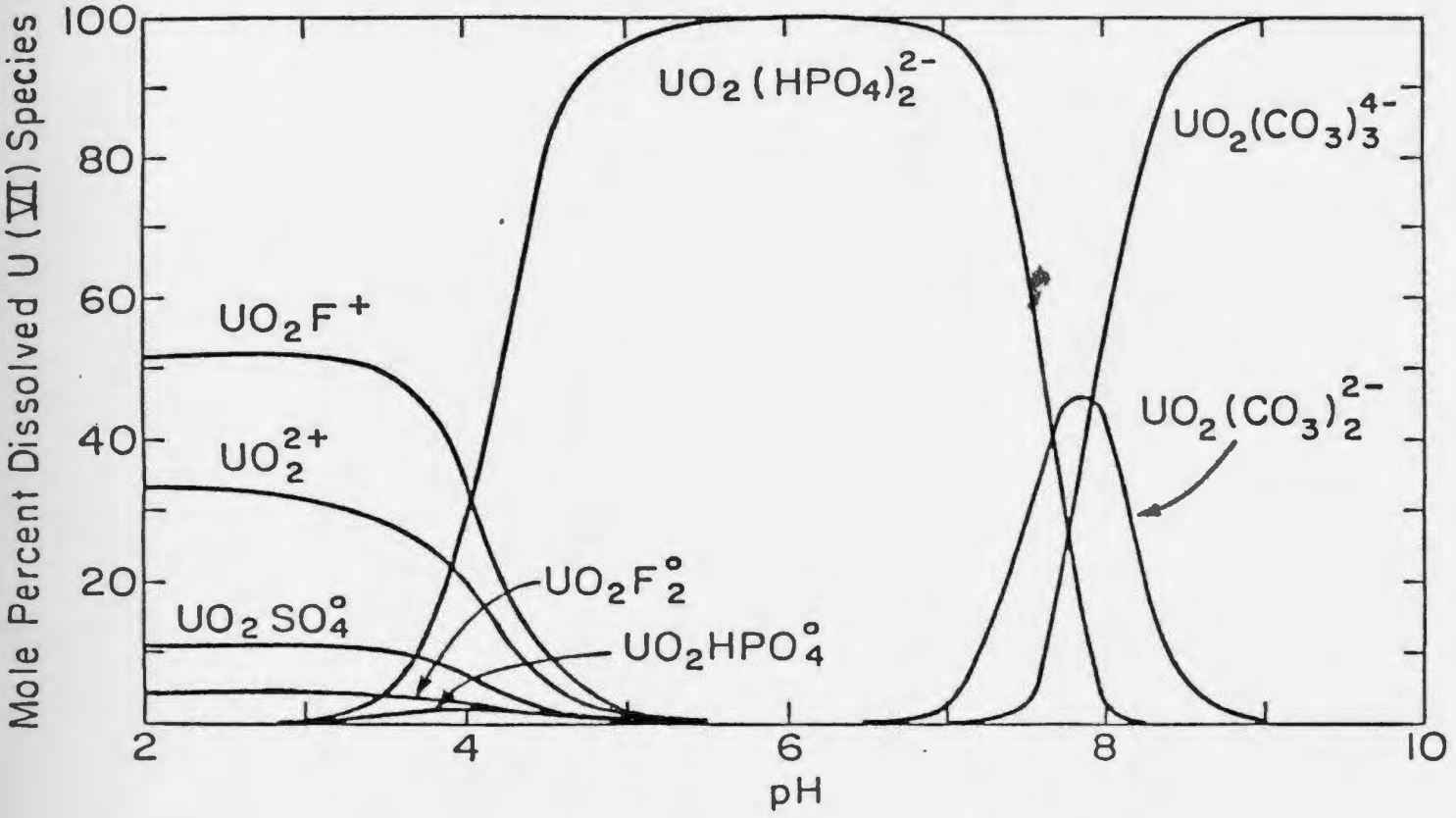

Figure 24: Distribution of uranyl complexes versus pH for some typical ligand concentrations in ground water of the Wind River Formation at 25-C. $P_{CO_2} = 10^{-2.5}$ atm, $\Sigma F = 0.3$ ppm, $\Sigma Cl = 10$ ppm, $\Sigma SO_4 = 100$ ppm, $\Sigma PO_4 = 0.1$ ppm, $\Sigma SiO_2 = 30$ ppm.
(from Langmuir, 1978)

The relative stabilities of various uranyl complexes are evaluated in the Figures 25-27 by plotting the distribution coefficient against pH at a constant temperature and concentration of complexing components and pCO_2.

As temperature increases the pH at which solutions are neutral decreases. The ionization constant of H_2O changes as temperature increases to a maximum of $10^{-11.4}$ at 230 °C. Therefore the concentration of both H^+ and OH^- can be as high as $10^{-5.7}$ M or neutral pH can be as low as 5.7 (Krauskopf, 1967).

Romberger (1984) shows that at 100 °C and pCO_2 of 0.1 atmospheres uranyl fluoride complexes are important under acid and neutral conditions, hydroxyl complexes are important under neutral conditions and uranyl carbonate complexes are important in alkaline fluids (Fig. 25a). With the introduction of 0.1 ppm phosphorus to the solution phosphate complexes are dominant at neutral pH (Fig. 25b).

At 200 °C and pCO_2 of 1 atmosphere the uranyl fluoride complexes are dominant in acid neutral and mildly alkaline solutions. Carbonate complexes are only important in strongly alkaline solutions for the specified ligand concentrations (Fig. 26 a+b). With the addition of 1 ppm

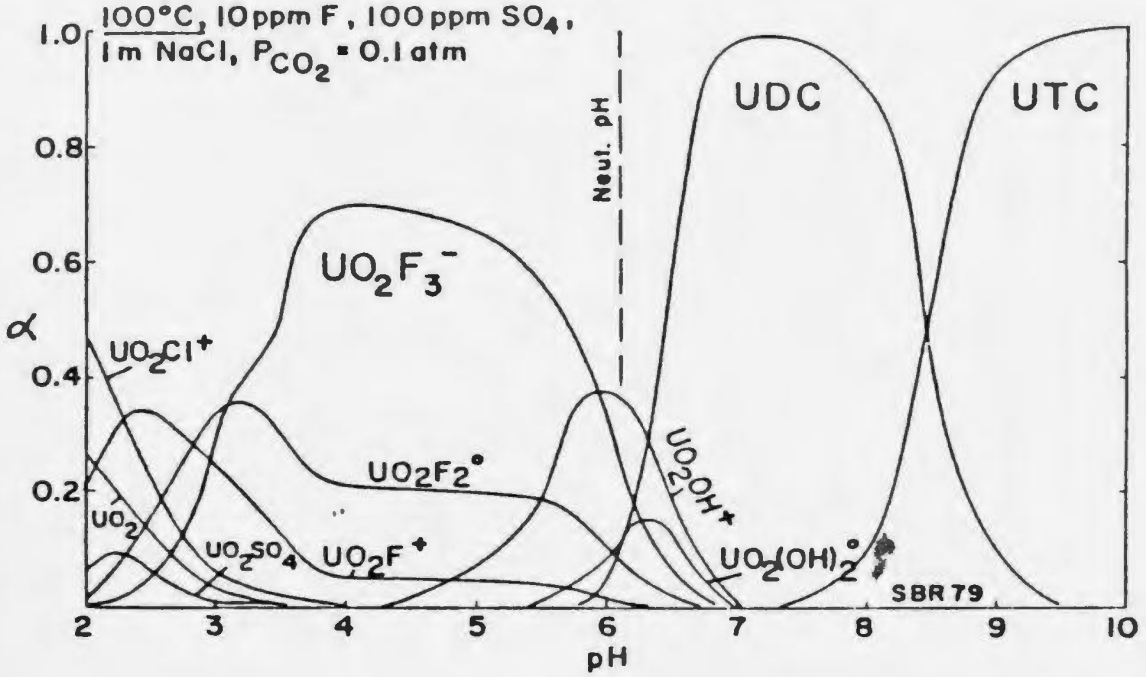

Figure 25a: Distribution diagram showing distribution of uranyl complexes at 100°C in solutions containing 10 ppm F, 100 ppm SO_4 and 1 m NaCl at P_{CO_2} of 0.1 atm

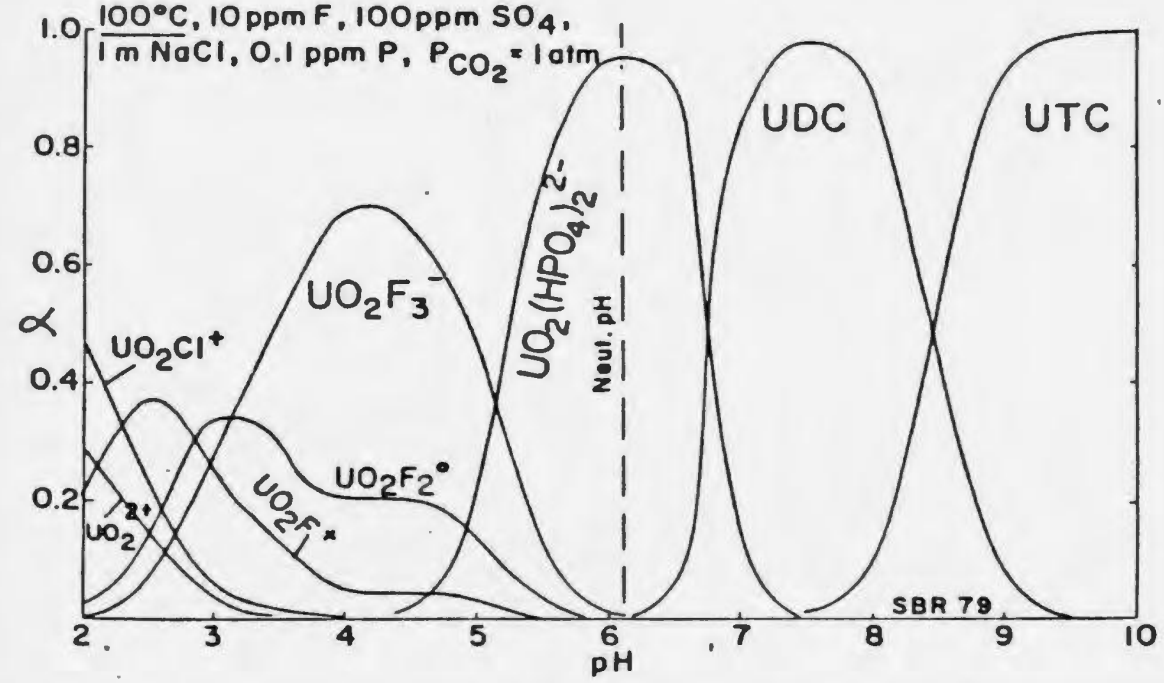

Figure 25b: Distribution diagram showing distribution of uranyl complexes at 100°C in solutions containing 10 ppm F, 100 ppm SO_4, 0.1 ppm P and 1 m NaCl at P_{CO_2} of 1 atm

(from Romberger, 1984)

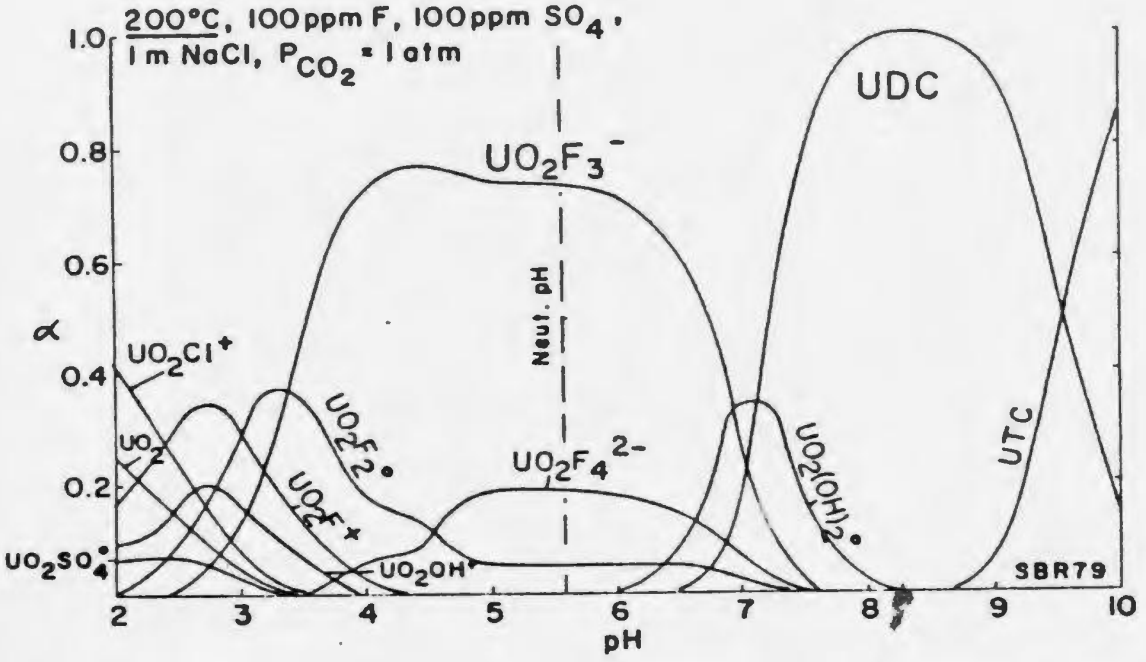

Figure 26a: Distribution diagram showing distribution of uranyl complexes at 200°C in solutions containing 100 ppm F, 100 ppm SO_4 and 1 m NaCl at P_{CO_2} of 1 atm

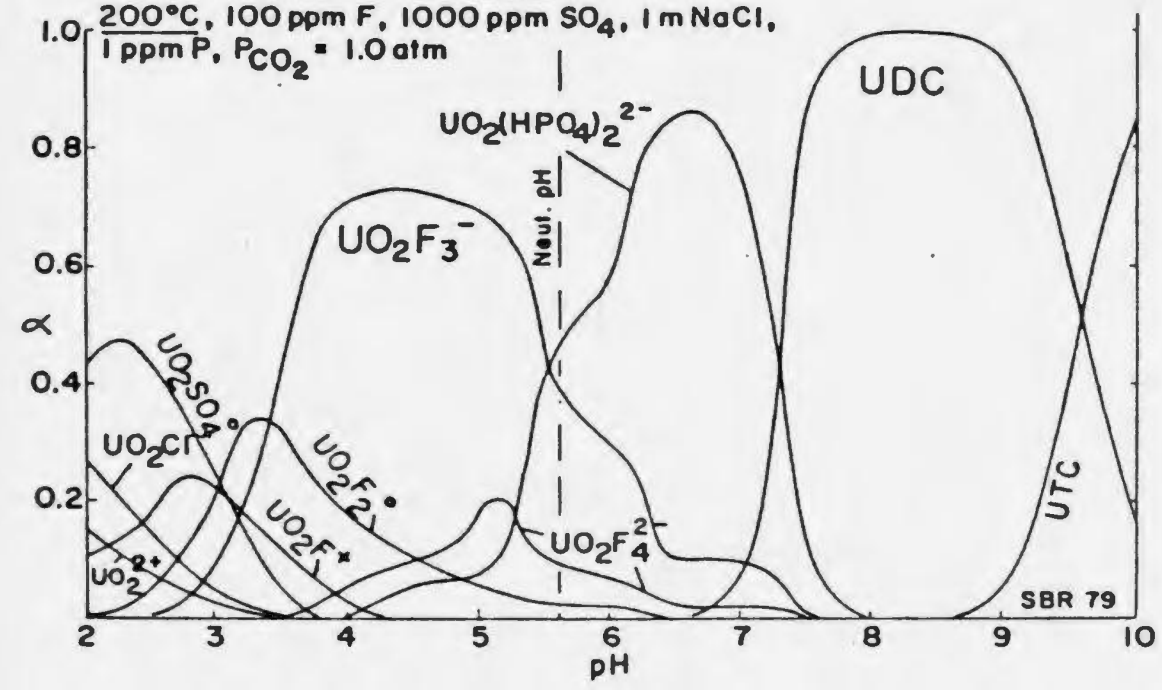

Figure 26b: Distribution diagram showing distribution of uranyl complexes at 200°C in solutions containing 100 ppm F, 1000 ppm SO_4, 1 ppm P and 1 m NaCl at P_{CO_2} of 1 atm

(from Romberger, 1984)

phosphorous to the solution, phosphate complexes are dominant in mildly alkaline solutions.

The thermodynamic data used by Romberger (1984) suggest that carbonate complexes are unstable at any pH at 300°C and pCO_2 of 10 atmospheres. Uranyl fluoride complexes are dominant at neutral pH and hydroxyl complexes are important in both acid and alkaline solutions. The presence of 1 ppm phosphorous results in phosphate complexes being dominant at neutral pH and hydroxide complexes dominant in acidic and basic solutions (Figs. 27 a+b).

In the J-zone albitites there is a slight increase in CaO reflected by increased calcite veining and both the albitites and K-metasomatized, mineralized rhyolites of the J-zone show a marked increase in P_2O_5 and F in the mineralized versus the unmineralized rocks. This may suggest that phosphate and fluoride complexes were important transporters of uranium in the albitized showings. In the east DF-zone showing there is an order of magnitude increase in P_2O_5 and a strong increase in F relative to the adjacent unmineralized rocks, which may indicate that phosphate and fluoride complexes were important transporters of uranium at this showing also. The west DF-zone showing is depleted in F relative to the

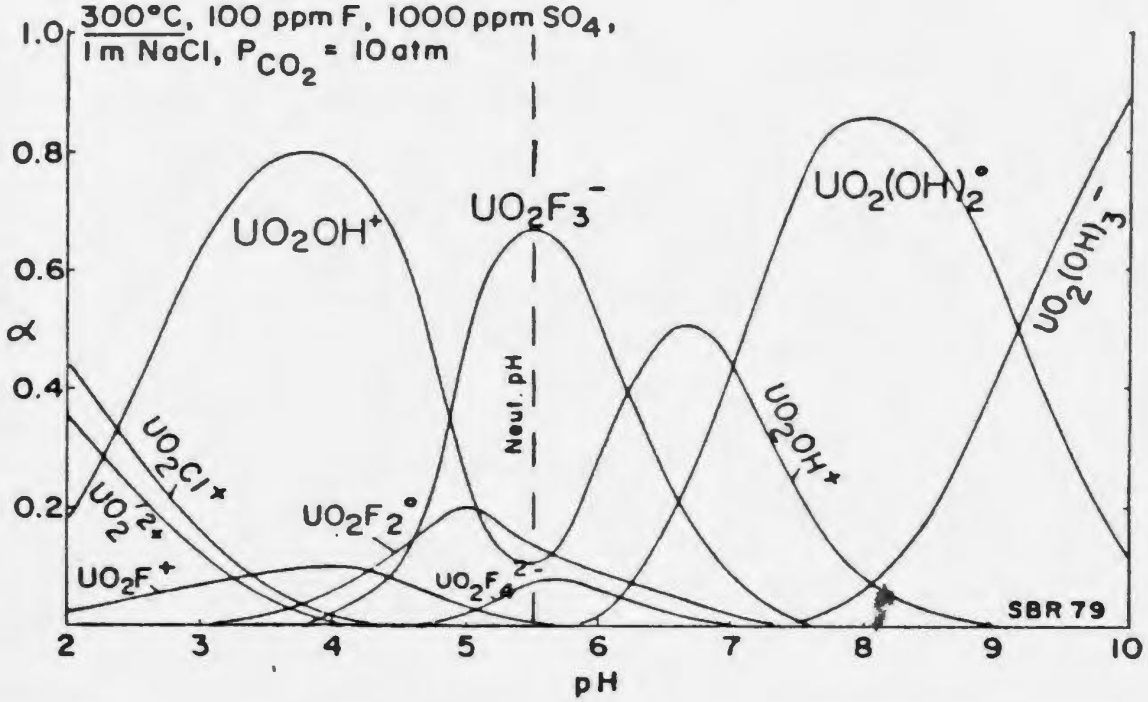

Figure 27a: Distribution diagram showing distribution of uranyl complexes at 300°C in solutions containing 100 ppm F, 1000 ppm SO_4 and 1 m NaCl at P_{CO_2} of 10 atm

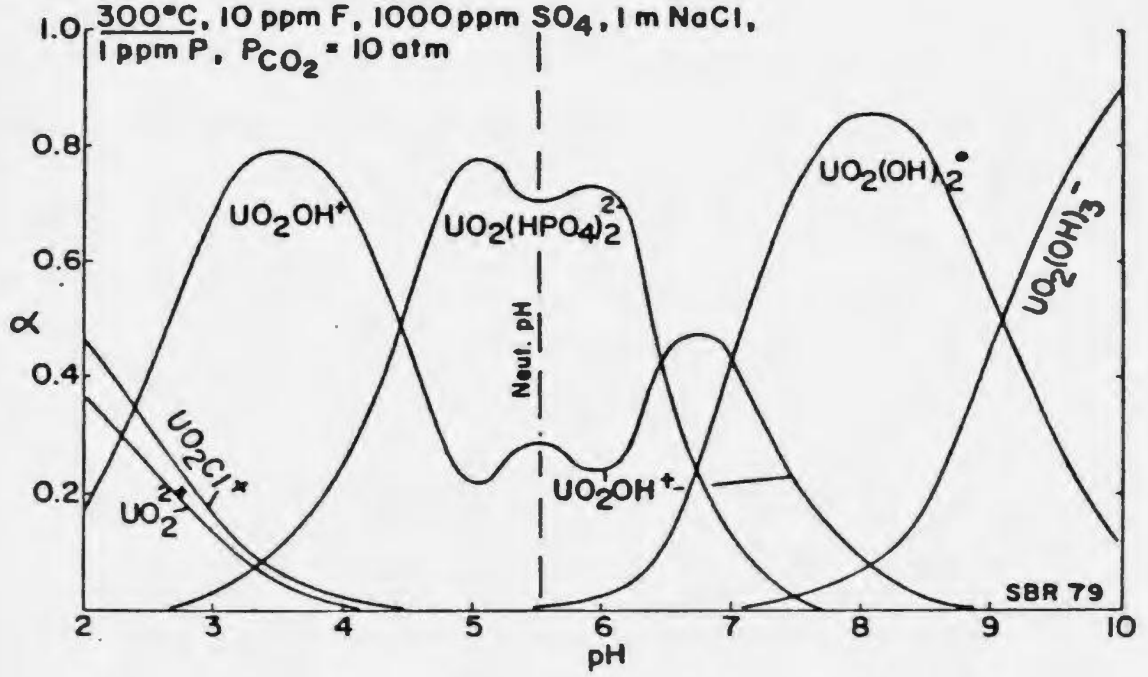

Figure 27b: Distribution diagram showing distribution of uranyl complexes at 300°C in solutions containing 10 ppm F, 1000 ppm SO_4, 1 ppm P and 1 m NaCl at P_{CO_2} of 10 atm

(from Romberger, 1984)

adjacent unmineralized rocks and there is no apparent increase in CaO or P_2O_5 in the mineralized zone. This showing is hosted a by fault zone in which permeability was probably very high and is the closest of all showings to the granite. The alteration minerals and the proximity to the granite suggest that temperatures and activities of K^+ were high at this showing. Heating of solutions carrying complexed uranium aids in precipitation of pitchblende by destabilizing the complexes. Increase in solution temperatures can be caused by lateral movement of uraniferous solutions with respect to an incompletely cooled intrusive, in which case the hotter zones peripheral to the intrusive will be a favourable locus for precipitation of uranium mineralization (Naumov, 1961). Precipitation of uranium in the west DF-zone showing may have been caused by fluids from the hydrothermal system encountering higher temperature magmatic fluids. Destabilization of uranium complexes therefore may have been a function of favourable temperature gradients.

Romberger (1984) notes the increasing importance of hydroxyl complexes with increasing temperature and suggests that above 300 ^{o}C hydroxyl complexes may be the only stable complexes in solution. There do not seem to be

any data to show how very high activities of complexing agents would affect uranium transport above 300 °C.

A summary of fluid inclusion data by Rich et al., (1977) suggests that in most hydrothermal uranium deposits pitchblende was deposited from fluids ranging from 50-200 °C at pressures of less than 1 Kb. The fluids responsible were generally low salinity and CO_2-bearing.

In the Beaverlodge District, Sasano et al. (1972) concluded that initial temperatures of uranium deposition were up to 500 °C with numerous remobilizations of ore at lower temperatures. Poty et al. (1974) reported that ore deposition in the Limousin District, France, occurred at temperatures of 340-350 °C and pressures of 700-800 bars. Both of these studies interpreted large variations in the constituents of inclusions to indicate that boiling had occurred during uranium deposition. Uranium ore grade at Limousin corresponds to the amount of CO_2 in fluid inclusions (Poty et al., 1974). In a study conducted in the Erzbirge Region of central Europe, Tugarinov and Naumov (1974) report that minerals deposited after pitchblende are depleted in CO_2 relative to those deposited with pitchblende, and temperatures of ore deposition ranged from 50 °C to 350 °C.

As pressure decreases the partial pressure of CO_2 in solution decreases, with the result that the activity of carbonate ions available for uranium complexing will be decreased. Pressure decreases which cause loss of volatile components cause pH to increase. An effective mechanism for reducing the partial pressures of volatile components in solutions is boiling (Romberger, 1984). Fluid inclusion data suggest that uranium is transported in CO_2 rich solutions even at temperatures above 300 °C. These data show that CO_2 commonly comprises over 1 mole percent of the fluid associated with hydrothermal uranium deposition (Rich et al., 1977). Uranium cannot be carried as simple ions, either as U(IV) or U(VI) in hydrothermal solutions (Naumov, 1963) suggesting that at very high pCO_2, carbonate complexes may be stable even at high temperatures. The possibility of U(IV) carbonate complexes existing at very high partial pressures of CO_2 seems not to have been investigated (Nash et al., 1981).

Romberger (1984) examines the affect of oxidation state and pH on the solubility of uranium at 200 °C by use of oxygen fugacity/pH diagrams (Fig. 28 and 29). Figure 28 shows that uranyl complexes are dominant at high values of fO_2 and that for the defined conditions, sulphate complexes are dominant in acid solutions, fluoride

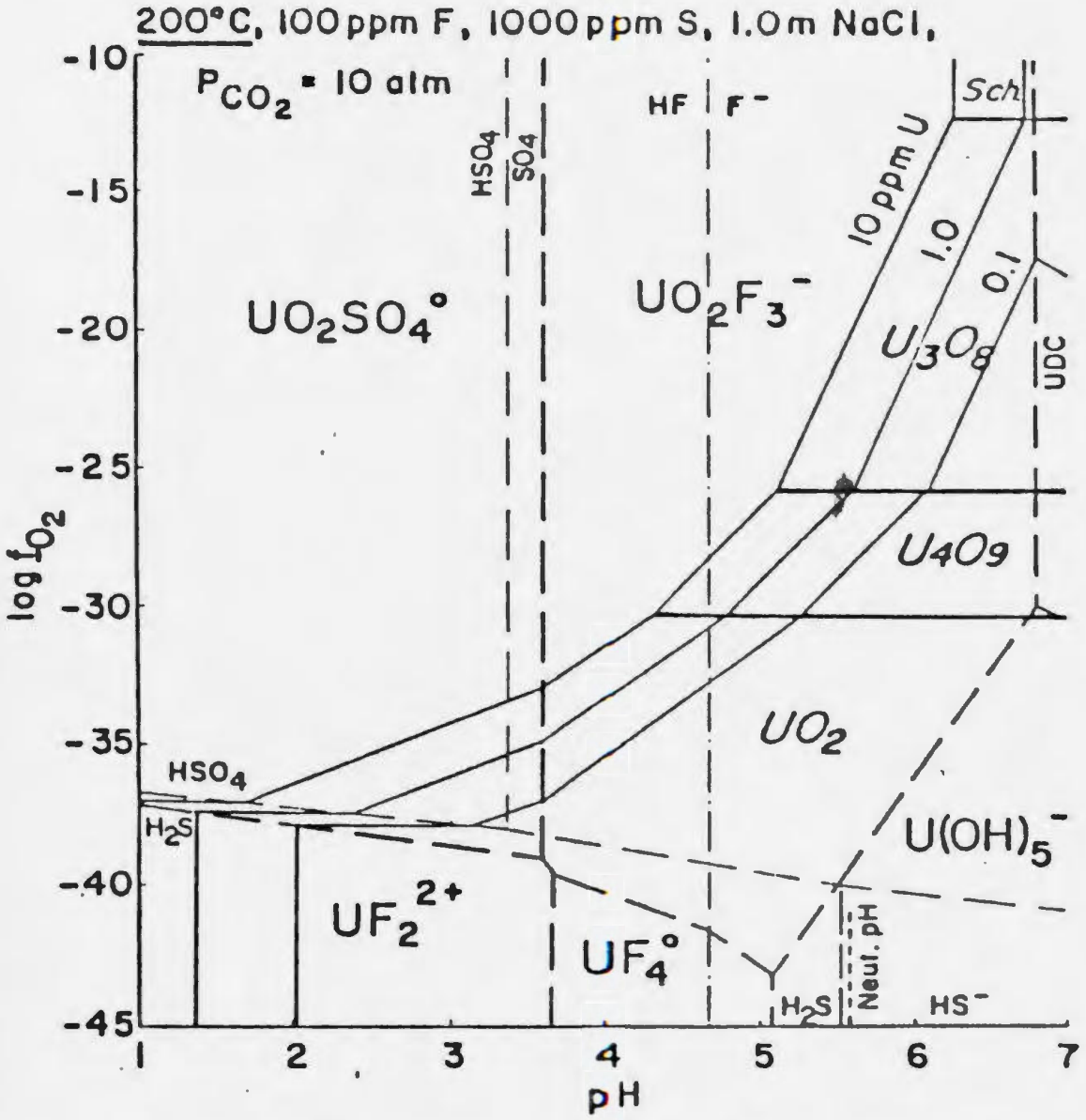

Figure 28: Log f_{O_2}-pH diagram showing distribution of uranyl and uranous complexes and solubility of uranium oxides at 200°C in solutions containing 100 ppm F, 1000 ppm S and 1 m NaCl at P_{CO_2} of 10 atm

(from Romberger, 1984)

complexes dominate in mildly acidic to mildly alkaline solutions and carbonate complexes are dominant at above approximately pH 7. At low fO_2 values uranous complexes are dominant. The stability fields of the solid uranium oxides are marked in heavy black lines. The solid species are actually solid solutions so the sharp boundaries in the diagram actually represent transition zones. The uranium solubility contours of 10, 1 and 0.1 ppm uranium show the trend of the solubility surface.

In Figure 29 the stability fields for various iron solid phases and the stability fields of various potassium and iron silicates which are commonly associated with uranium deposits are included on the diagram. The boundaries have been calculated for 200 ^{o}C in the presence of 1000 ppm K, 100 ppm Mg, 10 ppm Fe, 100 ppm F, 1000 ppm S, 1.0m NaCl and pCO_2 of 10 atm. The boundaries of the Mg-silicates are shown as light, double dot-dashed lines and the K-silicates as light, dot-dashed lines. The positions of all boundaries will change slightly with variations in the cation activities (Romberger, 1984).

Romberger (1984) has outlined four areas of uranium deposition based on observed mineral assemblages (Fig. 29). Areas 3 and 4 are of most interest to this study.

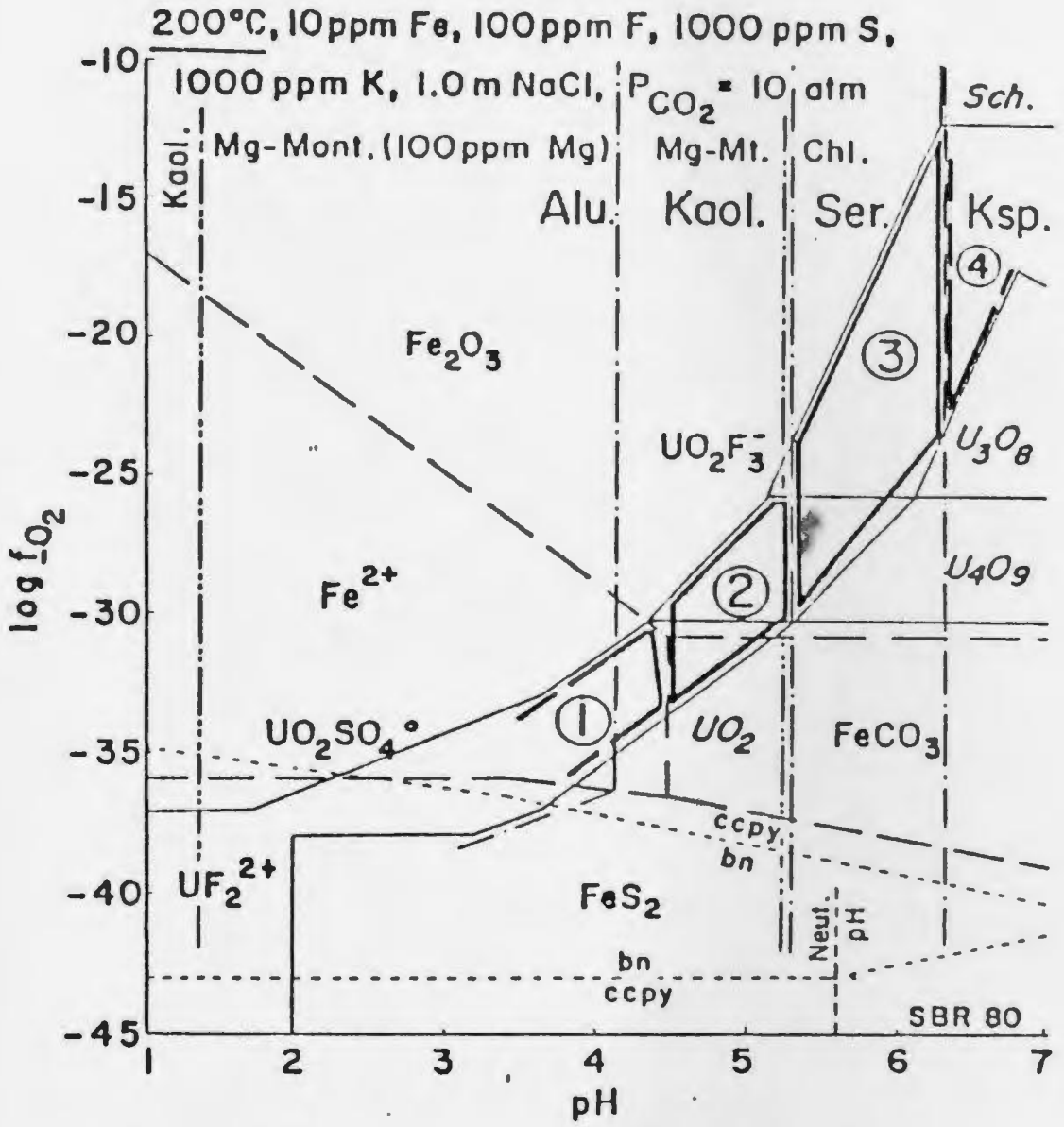

Figure 29: Log fO2-pH diagram showing distribution of uranyl complexes, solubility of uranium oxides, distribution of iron phases, relative stability of chalcopyrite and bornite and relative stability of potassium and magnesium silicates at 200C in aqueous system containing 10 ppm Fe, 100 ppm F, 1000 ppm S, 1000 ppm K, 100 ppm Mg and 1 m NaCl at P-CO2 of 10 atm (from Romberger, 1984). The J-Zone potassic altered uranium mineralization and the east DF-zone occurrence plot on the boundary between fields 3 and 4 on the diagram, the west DF-zone occurrence plots within the boundaries of field 4.

In all mineralized zones in the Wentworth prospect hematite is a stable iron phase suggesting that oxygen fugacity was moderate to high. In the East DF-zone and the J-zone showings sericite and K-feldspar coexist, suggesting mildly alkaline pH. The west DF-zone showing does not contain sericite, suggesting that pH was slightly higher at this showing. Chlorite is ubiquitous with all showings, but it is not clear whether it was deposited during mineralization. There is evidence to show that some of the chlorite in the east DF-zone showing postdates mineralization. The assemblages suggest that the K-metasomatized uranium occurrences were deposited from mildly alkaline fluids with high oxygen fugacity. Under those conditions uranyl fluoride and uranyl phosphate complexes are stable.

4.6.3 Uranium Depositional Model

There are a number of similarities between the geological setting of the Wentworth prospect and topaz rhyolites described by Burt and Sheridan (1980, 1981, 1985), and Christiansen et al. (1980) for example.

The Hart Lake Granite and the Fountain Lake Group are anorogenic and the products of extensional tectonism (Chatterjee, 1983). Topaz rhyolites are emplaced in an

extensional environment and are suggested to be the extrusive equivalents of anorogenic granites (Christianson et al., 1980).

Peralkaline magmas are distinct from topaz rhyolites but peralkaline magmatism is contemporaneous with topaz rhyolites in the Great Basin (Christiansen et al., 1980). This two-fold magmatic character is evident in the Byers Brook Formation. The felsic rocks are dominantly metaluminous but there is a suite of distinctly peralkaline rhyolite dikes cutting the metaluminous rhyolites. As with the Topaz Rhyolites the peralkaline suite are not mineralized.

Burt and Sheridan (1980, 1985) suggest four stages in the devlopment of mineral deposits associated with Topaz Rhyolites: (1) magma intrusion, (2) eruption of pyroclastics and capping lavas, (3) vapour phase and hydrothermal alteration and redistribution of elements, and (4) ground water diagenesis and redistribution of elements.

In stage 1 (Fig. 30) the granitic magma is thought to be water-depleted, enriched in fluorine and lithophile elements and emplaced to shallow levels in the crust. Fluorine reduces the solidus and liquidus temperatures of the melt, greatly aiding in the shallow emplacement of the associated granites (Wylie and Tuttle, 1961). Highly

Figure 30: The proposed genetic model for the uranium mineralization in the Byers Brook Formation is modified from the model for uranium in topaz rhyolites proposed by Burt and Sheridan (1980).

Stage 1: The Hart Lake Granite intrudes its own volcanic pile and highly charged elements are enriched in the apical regions by magmatic processes. The main dome/flow complex of the DF-zone is extruded along with smaller rhyolite flows in the J-zone and DL-zone, intercalated with the conglomerate siltstone marker horizon. A broad hydrothermal system is developed and uranium is concentrated into permeable zones.

Stage 2: Eruption of pyroclastic rocks occurs. The earliest ash flows (J-ignimbrite) are from the apical regions of the granite and are enriched in uranium. Hydrothermal activity continues to leach uranium from the volcanic rocks and concentrate it into favourable structures.

Stage 3: Pyroclastic eruptions wane and extrusions of the rhyolite flows at the Byers Brook - Diamond Brook Formation contact occurs. The broad hydrothermal system continues to leach and concentrate uranium as devitrification of the volcanic pile occurs. The rhyolite flows and domes are the center of the hydrothermal system, aided by heat from late rhyolite and composite dikes, with the result that the flows and domes are the locus for uranium concentration.

Stage 4: Diagenesis and groundwater redistribution results in minor concentration of uranium into fractures.

STAGE 1

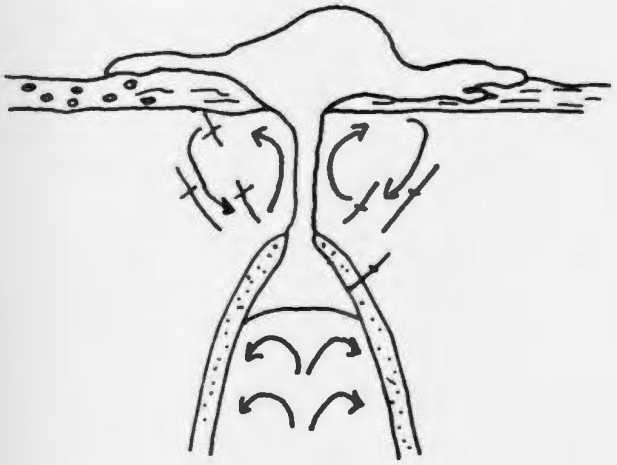

STAGE 2

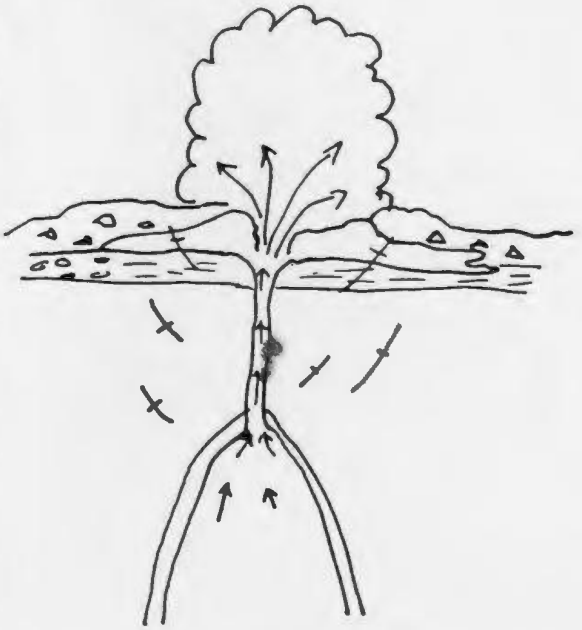

STAGE 3

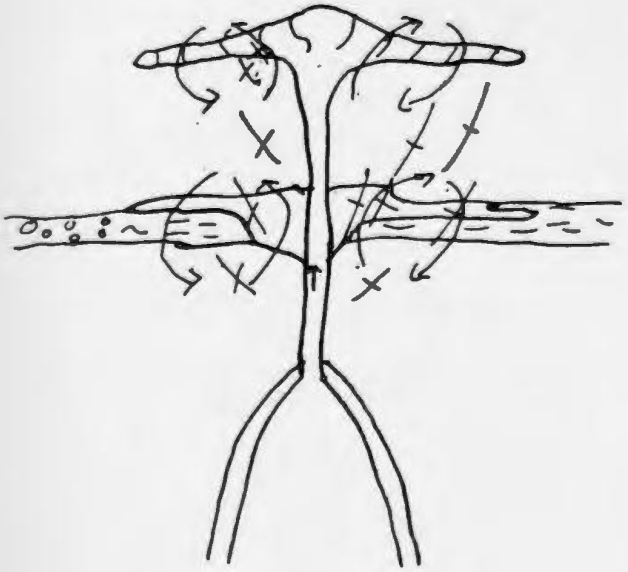

STAGE 4

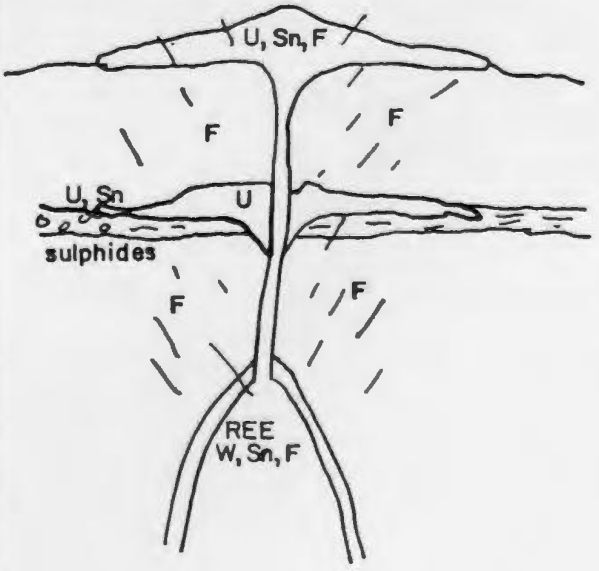

charged trace elements are stabilized by fluorine (Christianson et al., 1980) and these elements may be enriched in the apical parts of the intrusion by diffusion (Kogarko, 1974), thermogravitational diffusion (Hildreth, 1979) or by the evolution of a distinct fluorine-rich phase (Burnham, 1967).

In the Wentworth area, the granite near the margin of the Hart Lake/Byers Lake Granite is strongly fluorine enriched relative to the granophyric contact rocks and in medium grained granites in the south DF-zone (average 1300 ppm F in the unaltered DL-zone granite versus 500 ppm F in the granophyric chill margin and medium grained DF-zone granite). In the DL-zone the granite is interpreted to be a cupola which feeds the main dome/flow complex of the DF-zone, which is host to the east and west DF-zone showings. The occurrence of REE, W, Sn and Th in fluorite-calcite veins adjacent to this cupola along with the fluorine enrichment within the cupola suggests that apical enrichment of these elements occurred in the Hart Lake Granite.

The second stage in the development of Topaz Rhyolite mineralization involves the eruption of pyroclastics and capping lavas. In the Wentworth area two cycles of pyroclastic eruption are followed by extrusion of

rhyolite domes and flows. Uranium mineralization is associated with the domes and flows of the early sequence and the first ignimbrite of the late sequence of the Byers Brook Formation. Uranium mineralization is associated with fluorite in lithophysae-rich zones of the domes and flows which cap the late Byers Brook Formation sequence.

The uranium occurrences in the Byers Brook Formation are hosted by permeable zones and associated with hydrothermal alteration assemblages in the host rhyolites. Stage 3 of the model proposed by Burt and Sheridan (1980)suggests that vapour phase and hydrothermal alteration and redistribution of the elements is an important step in the formation of economic concentrations of lithophile elements. There is evidence that a very large, complex hydrothermal system was responsible for concentration of uranium into permeable structures on the Wentworth prospect. Uranium is readily leachable from devitrifying rhyolite flows and pyroclastic rocks, so the volcanic rocks themselves are suggested as the probable source of the uranium which is reconcentrated by hydrothermal solutions. In the Wentworth area the largest and highest grade uranium occurrances occur in and adjacent to the rhyolite dome/flow complexes. It is suggested that these complexes were areas of high thermal gradient caused

by the injection of late composite and rhyolite dikes, and thus were the locus of the very extensive hydrothermal system which caused the pervasive alkali metasomatism.

Stage 4 of this model which involves diagenesis and groundwater redistribution of uranium is best observed in the Hart Lake/Byers Lake Granite. Locally fractures in unaltered medium grained granite are filled with uranium, near the contact of the Byers Brook Formation. These fracture fillings are always less than 1 cm wide.

Chapter 5

Summary and Conclusions

5.1 Summary

Numerous radioactive occurrences hosted by the felsic volcanic rocks of the Byers Brook Formation in the Wentworth area, were discovered by the exploration efforts of Gulf Minerals Canada Ltd.

The Byers Brook Formation of the Fountain Lake Group is a bimodal, dominantly felsic volcanic and volcaniclastic sequence of Devono-Carboniferous age which has been intruded by the comagmatic Hart Lake Granite and Folly Lake Diorite. The volcanic and intrusive rocks are anorogenic, emplaced in an extensional tectonic regime.

The Byers Brook Formation is represented by two discrete volcanic cycles, separated by a conglomerate/siltstone marker which represents a brief hiatus in volcanic activity. Each cycle is characterized by early deposition of felsic pyroclastics which grade upward into dominantly rhyolite and basalt flows.

The Hart Lake Granite and the Byers Brook Formation rhyolitic rocks are metaluminous, except a

discrete suite of rhyolite and composite dikes which are peralkaline. The bulk of the Byers Brook Formation, and the granophyric margin of the Hart Lake Granite have been affected by pervasive alkali metasomatism. Widespread, moderate to intense K-metasomatism is most common but local areas within the volcanic pile have been strongly albitized. Albitization is not as extensive as K-metasomatism, and predates it where they occur together. There is a distinct suite of rhyolitic and dacitic dikes which are peralkaline. These along with a suite of metaluminous rhyolite dikes are relatively unaltered and postdate alteration and mineralization. The rhyolite dikes are commonly the felsic core of composite dikes which have diabasic margins. These dikes place a constraint on the timing of mineralization and alteration which suggests that the mineralization and alteration were related to the regional magmatic and hydrothermal activity associated with the emplacement of the Byers Brook Formation and the Hart Lake/Byers Lake granite and not caused by a later hydrothermal system.

The highest concentration of uranium, fluorite and associated lithophile elements discovered in the Cobequid Highlands occur within the Byers Brook Formation on the Wentworth Prospect. Although numerous occurrences have

been discovered elsewhere in the Fountain Lake Group, over most of the length of the Cobequid Highlands, no uranium mineralization has been discovered in the older volcanic rocks which are exposed in the area. The most extensive mineralization discovered to date occurs in the DF-zone where uranium is hosted by a large rhyolite dome/flow complex at the top of the first Byers Brook Formation volcanic sequence and in the J-zone where the host of mineralization is the earliest ignimbrite of the second Byers Brook volcanic sequence.

The geological setting and environment of mineralization in the Byers Brook Formation is analogous to the setting of the topaz rhyolites of the mid-western United States and Mexico. The mineralizing system at the Wentworth Prospect was probably similar to the system described by Burt and Sheridan (1980, 1981) in their model for mineralization associated with Topaz Rhyolites.

The sequence of events which was responsible for the widespread uranium mineralization in the Byers Brook Formation was initiated by the emplacement of the Hart Lake/Byers Lake Granite. The abundance of fluorine in the volcanic rocks suggest that the magma was enriched in fluorine. Fluorine reduces the solidus and liquidus temperatures of the magma allowing it to rise to a shallow

level in the crust without completely crystallizing. The apical regions of the granite were enriched in fluorine and lithophile elements by magmatic processes such as thermogravitational diffusion, diffusion or evolution of a discrete fluorine-rich phase.

These processes resulted in the extrusive rocks of the Byers Brook Formation being enriched in uranium, fluorine and other lithophile elements. Uranium does not fit into the lattice of rock forming minerals and was released as a secondary oxide during devitrification of the volcanic rocks. A large hydrothermal system driven by the high thermal gradient associated with the shallow granite and the rhyolite dome complexes remobilized and concentrated the uranium into secondary and primary structures. The highest grade and largest discovery of uranium mineralization is associated with the main dome flow complex of the DF-zone which occurs at the top of the first Byers Brook Formation sequence. This correlation between uranium mineralization and rhyolite domes may suggest that the domes acted as a focus for a very large hydrothermal system. K-metasomatism and albitization are very widespread throughout the Byers Brook Formation, suggesting that the hydrothermal system was large.

The presence of apatite and fluorite, and the fact that the mineralized zone has elevated F and P2O5 relative to the unmineralized rocks suggests that phosphate and fluoride complexes may have been important in the transport and concentration of uranium in the Byers Brook Formation. Alteration assemblages suggest that fluids responsible for the alteration and mineralization were mildly alkaline. Phosphate and fluoride complexes would be stable at elevated temperatures in mildly alkaline fluids. Uranium is hosted by zones in which permeability was increased by brecciation and fracturing or in zones which had primary porosity such as lithophysae-rich zones. The cause of precipitation of uranium in the mineralized zones is not obvious. Increased temperature associated with the dome complexes or the granite may have caused destabilization of uranyl complexes and precipitation of uranium oxide. Precipitation of fluorite and apatite may have resulted in destabilization of fluoride and phosphate complexes, resulting in pitchblende deposition. Mineralization in the J-zone albitites was associated with calcite veining. Precipitation of calcite and/or boiling of CO_2-rich fluids are considered to be important mechanisms for precipitation of uranium oxide in a number of hydrothermal

deposits associated with albitization and may have caused precipitation of uranium in these rocks.

5.2 Considerations For Exploration

The Byers Brook Formation and the Fountain Lake Group in general has potential to host economic deposits of lithophile elements based on this interpretation of the geological evolution of the volcanic sequences. The work done to date has allowed for the development of a model for mineralization. This should be followed up with a systematic exploration program to test and modify the model. The Byers Brook Formation is poorly exposed at surface and drilling has tested only a very small part of the formation. A careful evaluation of dome complexes and permeable structural features which were caused by volcanic activity or granite emplacement should be done. Occurrences which have been discovered but not extensively explored in rhyolite domes near the top of the upper Byers Brook Formation sequence, near the Diamond Brook Formation contact, have excellent potential as host to lithophile element mineralization. Strong reducing horizons such as graphitic sedimentary rocks in the pile should also be considered as potential prospects.

The precious metal potential of the Byers Brook Formation has not been evaluated. Zones of massive silica which occur along strike from the lacustrine siltstones in the DL-zone are interpreted to be sinter deposits and should be sampled for gold.

On a regional scale, it has been shown by Burt and Sheridan, (1980, 1985) and Christiansen et al., (1980) that topaz rhyolites in the southwestern United States have a strong spatial association with Precambrian granites, or radiogenic Precambrian crust along the margin of the Great Basin. In the Appalachian Orogen there are fluorite deposits in the St. Lawrence alkaline/peralkaline complex in Newfoundland, Tungsten and tin mineralization occur in felsic subvolcanic rocks at Mount Pleasant, New Brunswick and widespread occurrences of uranium, thorium, tungsten and tin occur throughout the Fountain Lake Group of northern Nova Scotia. These deposits have a number of common features. They are hosted by anorogenic granites or their extrusive equivalents, emplaced in extensional tectonic regimes (Teng and Strong, 1976; Chatterjee, 1983). The St. Lawrence granite and the Fountain Lake Group are alkaline/peralkaline complexes. All are floored by Avalon Zone basement which in the Cobequid Highlands is

partly composed of Precambrian granites. The host rocks are in each case Devono-Carboniferous to Lower Carboniferous in age.

The concentration of occurrences of fluorite and lithophile element deposits associated with the alkaline/peralkaline complexes of the Avalon Zone relative to similar complexes in other tectonostratigraphic zones within the Appalachian Orogen suggests that area selection should concentrate on rocks within the Avalon Zone. Specifically anorogenic complexes of Devono-Carboniferous to Lower Carboniferous age.

REFERENCES

Alcock, F.J., 1938. GSC Memoir 216, Geology of the Saint John Region.

Ami, H.M., 1900. Synopsis of the Geology of Canada. (Being a Summary of the Principal terms employed in Canadian Geological Nomenclature) Royal Society of Canada Proceedings and Transaction Second Series, Vol. VI, Section IV, p. 187-225.

Bailey, J.C., 1981. Geochemical Criteria for a Refined Tectonic Discrimination of Orogenic Andesites, Chemical Geology, 32, p. 139-154.

Beane, R., 1982. Hydrothermal alteration in silicate rocks. In Titley S. (ed.) Advances in geology of porphyry copper deposits. Tucson Univ. Ariz. Press. Ch. 6.

Benson, D.G., 1974. GSC Memoir 376, Geology of the Antigonish Highlands, N.S.

Blackwood, R.F. and Kennedy, M.J., 1975. The Dover Fault: western boundary of the Avalon Zone in northeastern Newfoundland C.J.E.S., vol. 12, p. 320-325.

Blackwood, R.F. and O'Driscoll, C.F., 1976. The Gander-Avalon zone boundary in southeastern Newfoundland. C.J.E.S., vol. 13, p. 1155-1159.

Blenkinsop, J., Cucman, P.F. and Bell, K., 1976. Age relationships along the Hermitage Bay-Dover Fault system, Newfoundland. Nature 262, p. 377-378.

Buist, D.S., 1959. The Composite Sill of Rudh'an Eireannaich, Skye., Geological Magazine, vol. 96, p. 247-252.

Burnham, C.W., 1979. Magmas and hydrothermal fluids in Barnes, H.L. (ed.). Geochemistry of Hydrothermal Ore Deposits, 2nd edition: New York, Wiley-Interscience, p. 71-136.

Burt, D.M. and Sheridan, M.F., 1980. Model for the formation of uranium/lithophile element deposits in fluorine-rich volcanic rocks. In Goodell, P. and Waters (ed.) Uranium in Volcanic and Volcaniclastic Rocks A.A.P.G. Studies in Geology # 13, p. 99-109.

Burt, D.M. and Sheridan, M.F., 1980. A model for the formation of uranium/lithophile element deposits in fluorine enriched volcanic rocks. In: Burt, D.M. and Sheridan, M.F. (ed.).; Uranium Mineralization in fluorine enriched volcanic rocks. Report prepared for the U.S. Department of Energy, University of Arizona, Ariz., U.S.A.

Cann, J.R., 1971. Major element variations in ocean-floor basalts, Phil. Trans. Roy. Soc. London #268, p. 495.

Cathelineau, M., 1983. Potassic Alteration in French Hydrothermal Uranium Deposits, Mineral. Deposits 18, pp. 89-97.

Christianson, E.H., Bikun, J.V., and Burt, D.M., 1980. Petrology and geochemistry of topaz rhyolites, Western United States. In: Burt, D. and Sheridan, M. (ed.).; Uranium Mineralization in Fluorine Enriched Volcanic Rocks. Report for the U.S. Dept. of Energy, Univ. of Arizona, Ariz., U.S.A.

Clarke, D.B., Barr, S.M., Donohoe, H.V., 1980. Granitoid rocks in Nova Scotia. In: Caledonides in the U.S.A. Proceedings of the International Geological Correlation Project, Blacksburg, Va., p. 107-116.

Cormier, R.F., 1979. Rubidium/Strontium isochron ages of Nova Scotia Granitoid plutons in Mineral Resources Division Report of Activities, NSDM Report 79-1, p. 143-148.

Coyle, M. and Strong, D.F., 1987. Geology of the Springdale Group: a newly recognized Silurian epicontinental-type caldera in Newfoundland. CJES, vol. 24, p. 1135-1148.

Creasey, S.C., 1959. Some phase relations in hydrothermally altered rocks of porphyry copper deposits: Econ. Geol. V. 54, p. 353-373.

Creasey, S.C., 1966. Hydrothermal Alteration. In: Tilley, S.R. and Hicks, C.L. (ed.). Geology of Porphyry Copper Deposits. Tucson Univ. Ariz. Press, p. 51-75.

Cullen, M.P., 1984. Structural geology of the Bass River Complex in the Cobequid Highlands, northern Nova Scotia unpublished M.Sc. thesis, Dalhousie Univ., Halifax, Nova Scotia.

Cullen, M.P., 1983. Observations on Geology and Stream Sediment Geochemistry, Cobequid Highlands. Unpublished Company Report, Selco Inc. - used with permission.

Cung, M., 1978. Geologic Environment, Mineralogy and Fluid Inclusion Studies of Bois-Limouzat Vein, Forey, France. Econ. Geol., vol. 73.

Dallmeyer, R.D., Blackwood, R.F., and Odom, A.L., 1981. Age and origin of the Dover Fault: tectonic boundary between the Gander and Avalon Zones of the northeastern Newfoundland Appalachians. C.J.E.S. vol. 18, p. 1431-1442.

Dawson, Sir J. W., 1878. The Geological Structure of Nova Scotia, New Brunswick, and Prince Edward Island, 3rd edition, MacMillan and Co., London.

Dawson, Sir J.W., 1888. On the Eozoic and Palaeozoic Rocks of the Atlantic Coast of Canada in Comparison with those of Western Europe and of the Interior of North America. Geol. Soc. of London Quarterly Journ., vol. 44, p. 797-817.

Donohoe, H.V. Jr., 1983. Bass River Complex: Part of the Avalonian Basement in Nova Scotia. NSDME Report 83-1, p. 327-348.

Donohoe, H.V., 1976. The Cobequid Mountains Project. In Mineral Resources Division Report of Activities 1975. N.S.D.M. Report 76-2, p. 113-124.

Donohoe, H.V. Jr. and Cullen, M., 1983. Deformation, age, and regional correlation of the Mt. Thom and Bass River Complexes, Cobequid Highlands, Nova Scotia. NSDME Report 83-1, p. 350.

Donohue, H.V. Jr. and Wallace, P.I., 1980. Structure and Stratigraphy of the Cobequid Highlands, N.S., GAC/MAC Field Trip Guidebook, Halifax Conference 1980.

Donohoe, H.V. and Wallace, P.I., 1979. The Portapique River section: a section through the Silurian to Lower Devonian. In: Mineral Resources Division Report of Activities, 1978. NSDM Report 79-1, p. 151-161.

Elias, P. and Strong, D.F., 1982. Palaeozoic granitoid plutonism of southern Nfld.: contrasts in timing, tectonic setting, and level of emplacement. Transactions of the Royal Society of Edinburgh, vol. 73, p. 43-57.

Elias, P. and Strong, D.F., 1982. Timing of arrival of the Avalon zone in the northeastern Appalachians: a new look at the Straddling Granite. CJES, vol. 19, p. 1088-1094.

Evenson, N.M., Hamilton, P.J. and O'Nions, R.K., 1978, Rare earth abundances in chondritic meteorites: Geochim. et Cosmochim. Acta, v. 42, p. 1199-1212.

Finn, Dennis, D., 1979. Prospecting for Magmatic and Hydrothermal Deposits of Uranium and Associated Elements by Computer Evaluation of the Chemistry and Petrogenesis of Igneous Source Rocks. Unpublished M.Sc., East Washington Univ., Cheneg, Washington.

Fletcher, H., 1892. Report on Geological Surveys and Exploration in the Countries of Picton and Colchester, N.S. G.S.C. Annual Report for 1889, 1890, 1891, V. 5, pt. P, p. 5-193.

Floyd, P.A. and Winchester, J.A., 1978. Identification and discrimination of altered and metamorphosed volcanic rocks using immobile elements. Chemical Geology, 21, p. 291-306.

Floyd, P.A. and Winchester, J.A., 1975. Magma Type and Tectonic Setting Discrimination Using Immobile Elements, Earth and Planetary Science Letters, 27, p. 211-218.

Gamble, J.A., 1979. Some relationships between coexisting granitic and basaltic magmas and the genesis of hybrid rocks in the Tertiary Central Complex of Slieve Guillion, Northeast Ireland. Journal of Volcanology and Geothermal Research, vol. 5, p. 297-316.

Garson, M.S., Coats, J.S., Rock, N.M.S., Deans, T., 1984, Fenites, breccia dykes, albitites and carbonatitic veins near the Great Glen Fault, Inverness, Scotland. J. Geol. Soc. London, Vol. 141, p. 711-732

Gaudette, H.E., Olszewski, W.J. Jr., and Donohoe, H.V. Jr., 1983. Age and origin of the basement rocks, Cobequid Highlands, Nova Scotia, NSDME Report 83-1, p. 349.

Gesner, A., 1836. Remarks on geology and mineralogy of Nova Scotia (with maps), Halifax).

Gibson, I.L. and Walker, G.P.L., 1963. Some Composite Rhyolite/Basalt Lavas and Related Composite Dykes in Eastern Iceland. Proceedings of the Geologists Association, vol. 74, part 3, p. 301-318.

Haworth, R.T. and MacIntyre, J.B., 1976. The Gravity and magnetic fields of Atlantic Offshore Canada, G.S.C. Paper 75-9, 22p.

Haworth, R.T. and LaFort, J.P., 1979. Geophysical evidence for the extent of the Avalon Zone in Atlantic Canada, CJES, V. 16, p. 552-562.

Hemley, J.J. and Jones, W.R., 1964. Chemical aspects of hydrothermal alteration with emphasis on hydrogen metasomatism: Econ. Geol., V. 59, p. 538-569.

Hemley, J.J., Montoya, J.W., Marinenko, J.W., and Luce, R.W., 1980. Mineral equilibria in the system Al2O3-SiO2-H2O and some implications of alteration/mineralization processes: Econ. Geol., vol. 75, p. 210-228.

Hildreth, W., 1979. The Bishop Tuff: Evidence for the origin of compositional zonation in silicic magma chambers. G.S.A. Special Paper 180, p. 43-75.

Honeyman, D., 1874. On new localities of fossiliferous Silurian beds in Nova Scotia. Canadian Naturalist, v. p 293.

Honeyman, D., 1881. On the geology of the goldfields of Nova Scotia. Journal of Geol. Soc. XVIII, p. 342.

Hughes, C.J., 1972. Geology of the Avalon Peninsula, Newfoundland; and its possible correspondence with Morocco. Notes et Meon. du Serv. Geol. du Maroc., vol. 236, p. 265-275.

Huspeni, J.R., Kesler, S.E., Ruiz, J., Tuta, Z., Sutter, J.F., Jones, L.M., 1984. Petrology and Geochemistry of Rhyolites Associated with Sn Mineralization in Northern Mexico. Econ. Geol., vol. 70, p. 87-105.

Irvine, T.N. and Baragrar, W.R.A., 1971. A Guide to the Chemical Classification of the Common Volcanic Rocks. CJES, vol. 8, p. 523-542.

Jolly, W.G. and Smith, R.E., 1972. Degredation and Metamorphic Differentiation of the Kewenawan Tholeritic Lavas of Northern Michigan, U.S.A., Journal of Petrology, vol. 13, p. 273-310.

Kelly, D.G., 1965. Cobequid Mountains, G.S.C. Paper 65-1, p. 125-127.

Kelly, D.G., 1966. Cobequid Mountains, G.S.C. Paper 66-1, p. 172-173.

Kelly, D.G., 1967. Cobequid Mountains, G.S.C. Paper 67-1, p. 175.

Kennedy, M.J., 1976. Southeastern margin of the northeastern Appalachians: Late Precambrian orogeny on a continental margin. Geol. Soc. of America. Bull., V. 87, p. 1317-1325.

Keppie, J.D., 1982. The Minas Geofracture, in GAC Special Paper 24, P. St. Julien and J. Beland editors.

Keppie, J.D. (compiler), 1979. Geological map of the Province of Nova Scotia, (1:500,000). NSDME, Halifax.

Keppie and Smith, 1978. Compilation of isotopic age data of Nova Scotia; Nova Scotia Dept. Mines & Energy, Report 78-4.

King, A.F., 1979. The birth of the Caledonides: Late Precambrian rocks of the Avalon Peninsula, Newfoundland and their correlatives in the Appalachian Orogen. In: Wones D. (ed.), Proceedings: The Caledonides in the U.S.A. I.G.C.P. 27, Caledonide Orogen, 1979 meeting. p. 3-8.

King, L.H., Hyndman, R.D. and Keen, C.E., 1975. Geological development of the continental margin of Atlantic Canada: Geoscience Canada, vol. 2, p. 26-35.

Kogarko, L.N., 1974. Role of volatiles, In: H. Sorenson (ed.), The Alkaline Rocks, Wiley, London, p. 474-487.

Langmuir, 1978. Uranium Solution - Mineral equilibria at low temperature with applications to sedimentary ore deposits. Geochemica et Cosmochemica, vol. 42, p. 547-569.

Langmuir, 1978. Uranium solution, mineral equilibria et low temperature with applications to sedimentary ore deposits. MAC short course in Uranium Deposits. p. 17-55.

LeRoy, J., 1978. The Magnac and Favay Uranium deposits of the La Crouzille District (Western Central Massif), France - Geologic and Fluid Inclusion studies. Econ. Geol., vol. 73., p. 1611-1634.

Lindros, H., Smellie, J., 1979. A Stratabound Uranium Occurrence within Middle Precambrian Ignimbrites at Duobblon, Northern Sweden, Economic Geology, vol. 74, p. 1118-1130.

Lowell, J.D. and Guilbert, J.M., 1970. Lateral and vertical alteration - mineralization zoning in porphyry ore deposits. Econ. Geol., V. 65, p. 373-408.

MacDonald, G.A., 1968. Composition and Origin of Hawaiian Lavas. Geol. Soc. Amer. Mem. 116, p. 477-522.

McCutcheon, S.R., 1981. Revised stratigraphy of the Long Reach area, southern New Brunswick, evidence for major northwest thrusting. CJES, vol. 18, p. 646-656.

McSween, H.Y. Jr., Coish, R.A., Norman, M.D.. Coexisting acidic and basic melts: Geochemistry of a composite dike - A discussion, 1979. Journal of Geology, vol. 87, p. 211-216.

Meyer, C. and Hemley, J.J., 1967. Wall rock alteration., in Barnes, H.L. (ed.) Geochemistry of Hydrothermal Ore Deposits: New York, Holt, Reinhart and Winston, p. 166-235.

Miller; L.J., 1958. The chemical environment of pichblende: Econ. Geol. V. 53, p. 521-545.

Miyashiro, A., 1977. Subduction-Zone Ophiolites and Island Arc Ophiolites in Energetics of Geological Processes; editors Saxena S.K. and Bhallacharji S., Springer Verlag, N.Y., p. 62-89.

Miyashiro, A., 1974. Volcanic rock series in island arcs and active continental margins: Am. Jour. Sci., v. 274, p. 321-355.

Miyashiro, A., 1975. Island arc volcanic series: a critical review, Journal of Petrology, #3, 177-187.

Montoya, J.W. and Hemley, J.J., 1975. Activity relations and stabilities in alkali feldspar and mica alteration reactions. Econ. Geol. V. 70, p. 577-582.

Murphy, B., 1977. Preliminary report on part of the Fourchu Group, southeastern Cape Breton Island. In: Mineral Resources Division Report of Activities, 1976. NSDME Report 77-1, p. 139-156.

Murphy, J.B., Keppie, J.D. and Hynes, A., 1979. Geology of the northern Ahtigonish Highlands. In: Mineral Resources Division Report of Activities, 1978, NSDME Report 79-1, p. 105-109.

Nash, L.T., Granger, H.C., Adams, S.S., 1981. Geology and Concepts of Genesis of Important Types of Uranium Deposits. Economic Geology 75th Anniversary Volume p. 63-116, B.J. Skinner editor.

O'Brien, S.J., Wardle, R.J., King, A.F., 1983. The Avalon Zone: A Pan-African Terrane in the Appalachian Orogen of Canada. Geological Journal, vol. 18, p. 195-222.

Pearce, J.A. and Cann. J.R., 1973. Tectonic setting of basic volcanic rocks determined using trace element analysis. Earth and Planetary Science Letters, 19, p.290-300.

Poole, W.H., 1967. Tectonic evolution of the Appalachian region of Canada. In: G.A.C., Special Paper Number 4: p. 9-52.

Poty, B., Leroy, J., Cuney, M., 1974. Les inclusions fluides dans les minerais des gisement d'uranium inbragrazitiques du Limousin et du Forey (Massif Central francais). In: Formation of Uranium Ore Deposits. International Atomic Energy Agency, Vienna, p. 569-582.

Rafalsky, R.P., 1958. The experimental investigation of the conditions of uranium transport and deposition in hydrothermal solutions: Proc. of the second U.N. Inter-Conf. on the Peaceful Uses of Atomic Energy, V. 2, p. 432-444.

Rao, M.S., 1958. Composite and Multiple Intrusions of Lamlash-Whiting Bay Region, Arran., Geological Magazine, vol. 95, #4, p. 265-280.

Rast, N., O'Brien, B.H., Wardle, R.J., 1976. Relationships between Precambrian and Lower Paleozoic rocks of the Avalon Platform in New Brunswick, the northeast Appalachian and the British Isles. Tectonophysics, vol. 30, p. 315-338.

Rich, Holland, Peterson, 1977. Hydrothermal Uranium Deposits, Elsevier Scientific Publishing Co.

Rogers, N.W., Gibson, I.L., 1977. The petrology and geochemistry of the Creag Dubh composite sill, Whiting Bay, Arran, Scotland, Geological Magazine, vol. 114, p. 1-8.

Romberger, S.B., 1984. Transport and deposition of uranium in hydrothermal systems at temperatures up to 300 C: geological implications. In: Uranium geochemistry, mineralogy, geology, exploration and resources. (ed.), DeVivo, Ippolito, Capaldi and Simpson. I.M.M., London, England, p. 1-17.

Rosholt, J.N., Prijana, Noble, D.C., 1971. Mobility of Uranium and Thorium in Glassy and Crystallized Silicic Volcanic Rocks; Economic Geology, vol. 66, p. 1061-1069.

Rose, A.W., Burt, D.M., 1979. Hydrothermal Alteration. In: Geochemistry of Hydrothermal Ore Deposits., 2nd Edition, H.L. Barnes, editor, John Wiley & Sons, p. 173-235.

Rose, A.W., 1970. Zonal relations of wallrock alteration and sulfide distribution at porphyry copper deposits. Econ. Geol., vV. 65, p. 920-936.

Ruitenberg, A.A., Giles, P.S., Venugopal, D.V., Buttimer, S.M., McCutcheon, S.R., and Chandra, J., 1979. Geology and mineral deposits Caledonia Area. New Brunswick Dept. of Natural Resources, Mineral Resources Branch, Memoir 1, 213p.

Sassano, G.P., Fritz, P., and Morton, P.D., 1972. Paragenesis and isotopic composition of some gangue minerals from uranium deposits of Eldorado, Saskatchewan, C.J.E.S., 9, p. 141-157.

Schenk, P.E., 1971. Southeastern Atlantic Canada, Northwestern Africa, and Continental Drift. CJES, vol. 8, p. 1218-1251.

Shade, J.W., 1974. Hydrolysis reactions in the SiO2 excess portion of the system K2O-Al2O3-SiO2-H2O in chloride fluids at magmatic conditions: Econ. Geol., vol. 69, p. 218-229.

Shand, H.S., 1951. Eruptive Rocks 4th edition. John Wiley and Sons, New York 488p.

Stevenson, I.M., 1958. G.S.C. Memoir 297, Truro Map Area, Colchester and Hants Countries, N.S.

Strong, D.F., 1980. Granitoid Rocks and Associated Mineral deposits of Eastern Canada and Western Europe. In: G.A.C. Special Paper 20, Continental Crust and its Mineral Deposits D.W. Strangway editor, p. 742-769.

Strong, D.F., 1982. Carbothermal Metasomatism of Alaskitic Granite, St. Lawrence, Nfld., Canada, Chemical Geology, 35, p. 97-114.

Strong, D.F., O'Brien, S.J., O'Driscoll, C.F., 1980. Stratigraphy and Volcanology of the Western Avalon Zone of Nfld. - from Proterozoic oceanic crust to Carboniferous Ignimbrites, GAC/MAC Field Trip Guidebook, Halifax '80, Joint Meeting.

Strong, D.F., O'Brien, S.J., Taylor, S.W., Strong, P.G., Wilton, D.H., 1978. Aborted Proterozoic Rifting in eastern Nfld. CJES, vol. 15, p. 117-131.

Strong, D.F. and Coyle, M., 1988. Commendites, Fenites, Albitites and Carbonatites Associated with Silurian Magmatic Activity in Western Newfoundland and Scotland. Program with Abstracts, vol. 13, GAC, MAC, CSPG joint annual meeting, p. A120.

Strong, D.F. and Taylor, R.P., 1984. Magmatic-Subsolidus and Oxidation Trends in Composition of Amphiboles from Silica-Saturated Peralkaline Igneous Rocks. Tschermaks. Min. Petr. Mitt., 32, p. 211-222.

Taylor, R.G., 1979. Geology of Tin Deposits American Elsevier, New York, N.Y., 543p.

Taylor, R.P., Strong, D.F., Fryer, B.J., 1981. Volatile Control of Contrasting Trace Element Distributions in Peralkaline Granitic and Volcanic Rocks. Contrib. Mineral. Petrol., vol. 77, p. 267-271.

Taylor, R.P., Strong, D.F., Kean, B.F., 1980: The Topsails igneous complex: Silurian-Devonian peralkaline magmatism in western Newfoundland. CJES, vol. 17, p. 425-439.

Titley, S.R. and Beane, R.E., 1981. Porphyry Copper Deposits: Part I. Geologic setting, petrology and tectonogenesis. Economic Geology Seventy-fifth Anniversary Volume, Skinner, B.J. (ed.), El Paso, Texas, p. 214-234.

Wanless, R.K., Stevens, R.D., Lachance, G.R., and Delabio, R.N., 1973. Age determinations and geological studies, G.S.C. Paper 73-2, 139p.

Weeks, L.J., 1948. Londonderry and Bass River Map Areas, Colchester and Hants Counties, Nova Scotia, G.S.C. Memoir 245.

White, M., 1978. Felsic volcanism within the Aillik Series, Labrador and associated uranium mineralization. Program with abstracts GSA, GAC, MAC - Toronto.

White, Michael and Martin, Robert F., 1980. The Metasomatic Changes that Accompany Uranium Mineralization in the Nonorogenic Rhyolites of the Upper Aillik Group, Labrador, Canadian Mineralogist, vol. 18, p. 459-479.

Williams, H., 1964. The Appalachians of northeastern Newfoundland - a two sided symetrical system. American Journal of Science, . 1137-1158.

Williams, H., 1969. Pre-Carboniferous development of the Newfoundland Appalachians. In: Kay M. (editor) North Atlantic Geology and Continental drift, Memoir of American Assoc. of Petroleum Geol. 12, p. 32-58.

Williams, H., 1978. Tectonic Lithofacies Map of the Appalachians, Memorial University Map No. 1, Dept. of Geology, Memorial University of Newfoundland.

Williams, H., 1979. The Appalachian Orogen in Canada, CJES, vol. 16, p. 792-807.

Williams, H. and Hatcher, R.D. Jr., 1983. Appalachian suspect terranes, in Hatcher, R.D. and others (editors). Contributions to the tectonics and geophysics of mountain chains. G.S.A. Memoir 158, p. 33-53.

Williams, H., Kennedy, M.J. and Neale, E.R.W., 1972. The Appalachian Structural Province. In: Price, R.A. and Edwards, R.J.W. (editors), Variations in Tectonic Style in Canada, GAC Special Paper 11, P. 181-261.

Williams, H. and Stevens, R.K., 1974. The Ancient Continental Margin of Eastern North America. In: Burke, C.A. and Drake, C.L. (editors) The Geology of Continental Margins, p. 781-796, Springer-Verlag pub., New York.

Williams, M.Y., 1914. G.S.C. Memoir 60, Arisaig Antigonish District, Nova scotia.

Winchester, J.A. and Floyd, P.A., 1977. Geochemical descrimination of Different Magma Series and their Differentiation Products using Immobile Elements. Chemical Geology, vol. 20, p. 325-343.

Wyllie, P.J. and Tuttle, O.F., 1961. Experimental investigations of silicate systems containing two volatile components, II. The effects of NH3 and HF, in addition to H2O on the melting temperatures of albite and granite. American Journal of Science, V. 259, p. 128-143.

Yoder, H.S. Jr., 1973. Contemporaneous Basaltic and Rhyolitic Magmas, American Mineralogist, vol. 58, p. 153-171.

Zielinski, R.A., 1978. Uranium abundances and distribution in glassy and crystalline rhyolites of the Western United States. GSA Bulletin, v. 89, p. 409-414.

Zielinski, R.A., 1978. Experimental leaching of volcanic glass: Implications for evaluation of glassy volcanic rocks as sources of uranium. AAPG Studies in Geology, No. 13, Uranium in Volcanic and Volcaniclastic Rocks, p. 1-12.

APPENDIX 1

Diamond Drilling Data:

DDH #	EAST	NORTH	DIP	AZIMUTH	DEPTH
JZ-1	6+75W	1+50S	-50	000	178.3m
JZ-2	7+00	0+15S	-90	---	131.1m
JZ-3	6+75W	1+75N	-50	180	170.7m
JZ-4	6+75W	6+00N	-50	180	199.3m
JZ-5	12+00W	2+00N	-45	180	153.6m
JZ-6	12+00W	5+00N	-45	180	160.3m
JZ-7	7+25W	0+15S	-90	---	70.1m
JZ-8	7+00W	0+10N	-90	---	76.5m
JZ-9	7+25W	0+10N	-90	---	76.2
JZ-10	12+00W	0+00	-45	180	173.7m
JZ-11	7+00W	4+00N	-45	180	143.6m
JZ-12	7+00W	8+80N	-45	180	106.1m
JZ-13	4+00W	12+80N	-45	000	41.5m
JZ-15	7+00W	1+10N	-90	---	101.5m
JZ-16	7+00W	0+75N	-90	---	94.8m
JZ-17	4+00W	1+25N	-45	180	109.1m
JZ-18	7+00W	0+15S	-77	000	138.1m
JZ-19	6+75W	3+50S	-45	180	68.0m
JZ-20	6+75W	5+55S	-45	180	70.6m
JZ-21	12+00W	0+00	-45	090	134.0m
JZ-22	12+00W	11+75N	-60	180	133.5m
JZ-23	12+00W	11+75N	-60	125	129.5m
DF-1	52+00E	34+00S	-50	180	143.9m
DF-2	52+00E	37+00S	-45	180	140.5m
DF-3	52+00E	40+00S	-45	180	140.8m
DF-4	52+00E	31+00S	-45	180	137.8m
DF-5	48+00E	32+15S	-45	180	150.2m
DF-6	48+00E	35+10S	-45	180	129.3m
DF-7	48+00E	38+15S	-45	180	96.2m
DF-8	48+00E	41+15S	-45	180	118.0m
DF-9	48+00E	44+15S	-45	180	129.2m
DF-12	52+00E	42+38S	-45	180	141.3m
DF-13	52+00E	31+00S	-45	270	105.2m
DF-14	52+00E	28+00S	-45	180	162.5m
DF-15	52+00E	31+00S	-70	270	106.5m
DF-16	52+00E	45+50S	-45	180	114.3m
DF-17	52+00E	35+00S	-45	270	126.3m
DF-18	52+00E	37+50S	-45	270	89.0m
DF-19	52+00E	11+75S	-45	180	92.6m
DF-20	48+00E	15+25S	-45	180	69.6m
DF-21	52+00E	48+50S	-45	180	62.0m
DF-22	60+00E	38+80S	-45	180	183.3m

DDH#	EAST	NORTH	DIP	AZIMUTH	DEPTH
DF-23	59+75E	34+20S	-45	180	155.0m
DF-24	59+95E	36+98S	-45	180	228.0m
DF-25	52+00E	8+10S	-45	180	152.0m
DF-26	52+00E	3+92S	-45	180	131.0m
DF-27	59+73E	40+71S	-60	180	184.0m
DF-28	60+00E	37+55S	-60	180	339.0m
DF-29	59+73E	40+71S	-45	180	144.3m
DF-30	60+65E	40+77S	-60	180	178.0m
DF-31	58+70E	40+52S	-60	180	305.0m
DF-32	61+75E	42+44S	-60	270	172.0m
DF-33	61+75E	42+44S	-45	270	202.0m
DF-34	61+95E	43+33S	-60	270	174.0m
DF-35	60+65E	40+77S	-45	180	181.0m
DF-36	68+30E	44+00S	-45	225	158.0m
DF-37	66+31E	47+53S	-45	225	178.0m
DF-38	63+94E	49+77S	-45	225	143.5m
DF-39	55+06E	33+85S	-45	225	178.0m
DF-41	67+14E	41+09S	-45	270	223.0m
DF-42A	63+62E	41+02S	-45	270	43.0m
DF-42B	63+62E	41+02S	-45	270	285.0m
DF-43	62+71E	42+46S	-60	270	206.0m
DF-44	57+52E	34+21S	-45	225	160.0m
DF-45	59+58E	42+05S	-45	225	166.7m
DF-46	59+58E	43+54S	-90	---	135.0m
DF-47	59+60E	42+05S	-90	---	155.0m
DF-48	59+85E	32+42S	-70	225	155.0m
DF-49	60+35E	31+75S	-90	---	143.0m
DF-50	58+00E	30+60S	-90	---	125.0m
DF-51	57+05E	42+56S	-60	270	206.0m
DF-52	62+35E	44+03S	-60	270	185.0m
DL-1	96+00E	24+00S	-45	180	140.8m
DL-2	96+00E	27+00S	-45	180	132.6m
DL-3	96+00E	29+80S	-45	180	137.2m
DL-4	96+00E	33+00S	-45	180	106.7m
DL-5	96+00E	36+00S	-45	180	125.8m
DL-6	96+00E	39+00S	-45	180	135.3m
DL-7	96+00E	42+00S	-45	180	138.3m
DL-8	96+00E	45+00S	-45	180	126.3m
DL-9	102+00E	34+85S	-45	180	118.0m
DL-10	96+00E	48+00S	-45	180	153.3m
DL-11	102+23E	63+88S	-45	180	126.5m
DL-12	96+00E	50+83S	-45	180	138.3m
DL-13	102+23E	66+88S	-45	180	162.5m
DL-14	96+00E	54+83S	-45	180	131.7m
DL-15	96+00E	58+83S	-45	180	132.3m

DDH#	EAST	NORTH	DIP	AZIMUTH	DEPTH
DL-16	96+00E	62+80S	-45	180	144.0m
DL-17	96+00E	67+17S	-45	180	78.3m
DL-18	102+23E	69+82S	-45	180	144.5m
DL-19	96+00E	62+80S	-70	180	138.3m
DL-20	102+20E	72+97S	-45	180	162.3m
DL-21	102+96E	77+30S	-45	180	91.2m
DL-22	96+00E	20+20S	-45	180	173.3m

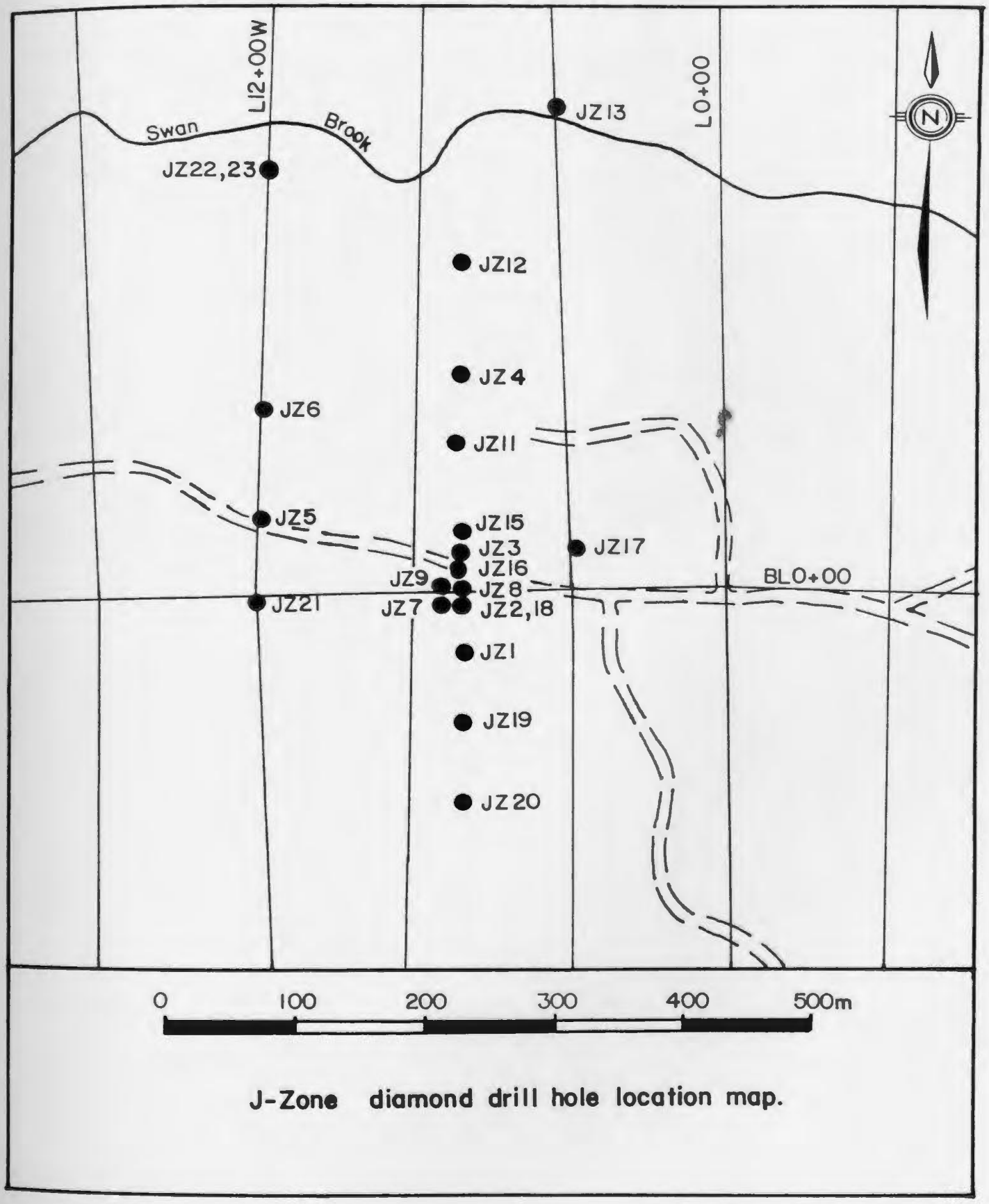

J-Zone diamond drill hole location map.

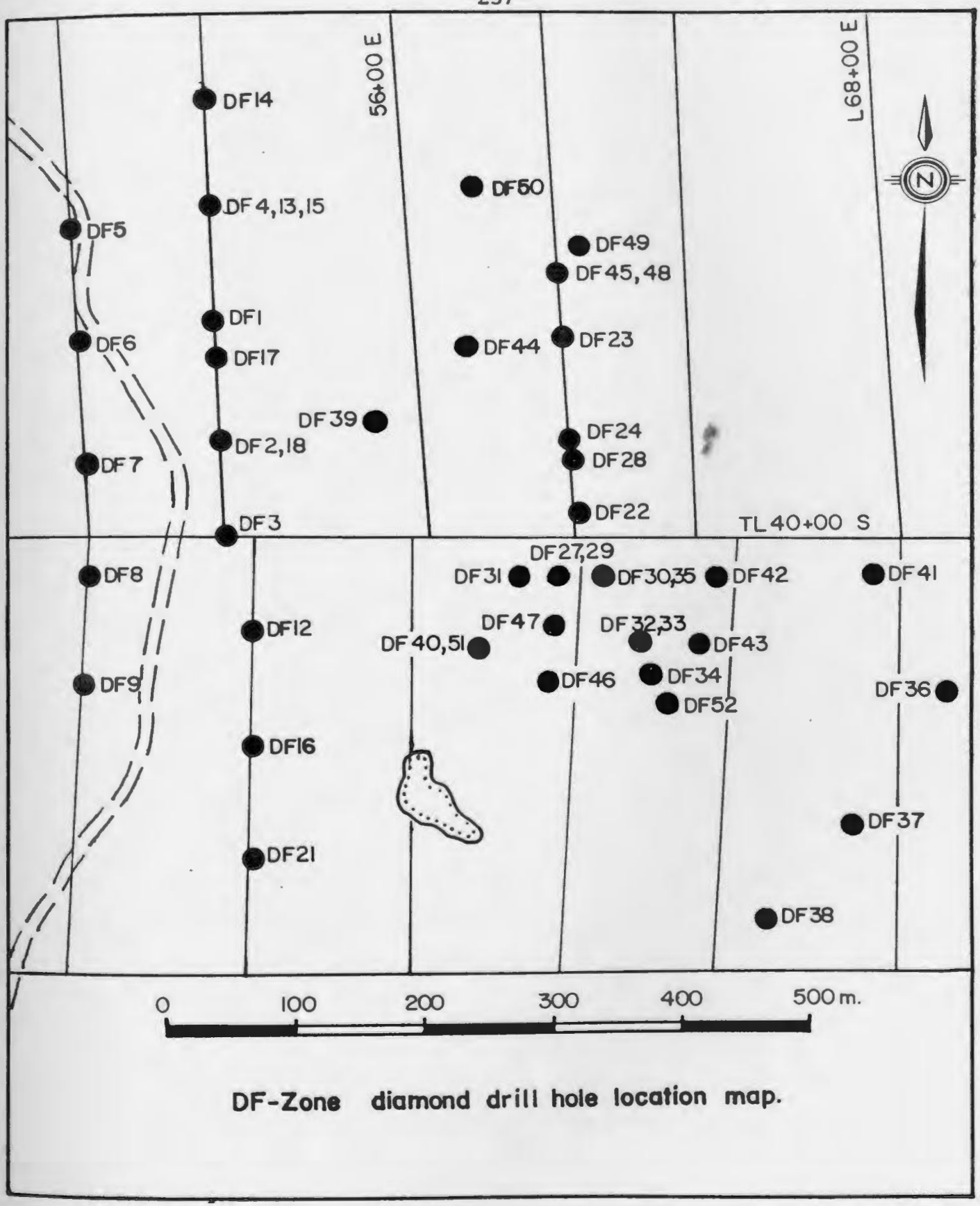

DF-Zone diamond drill hole location map.

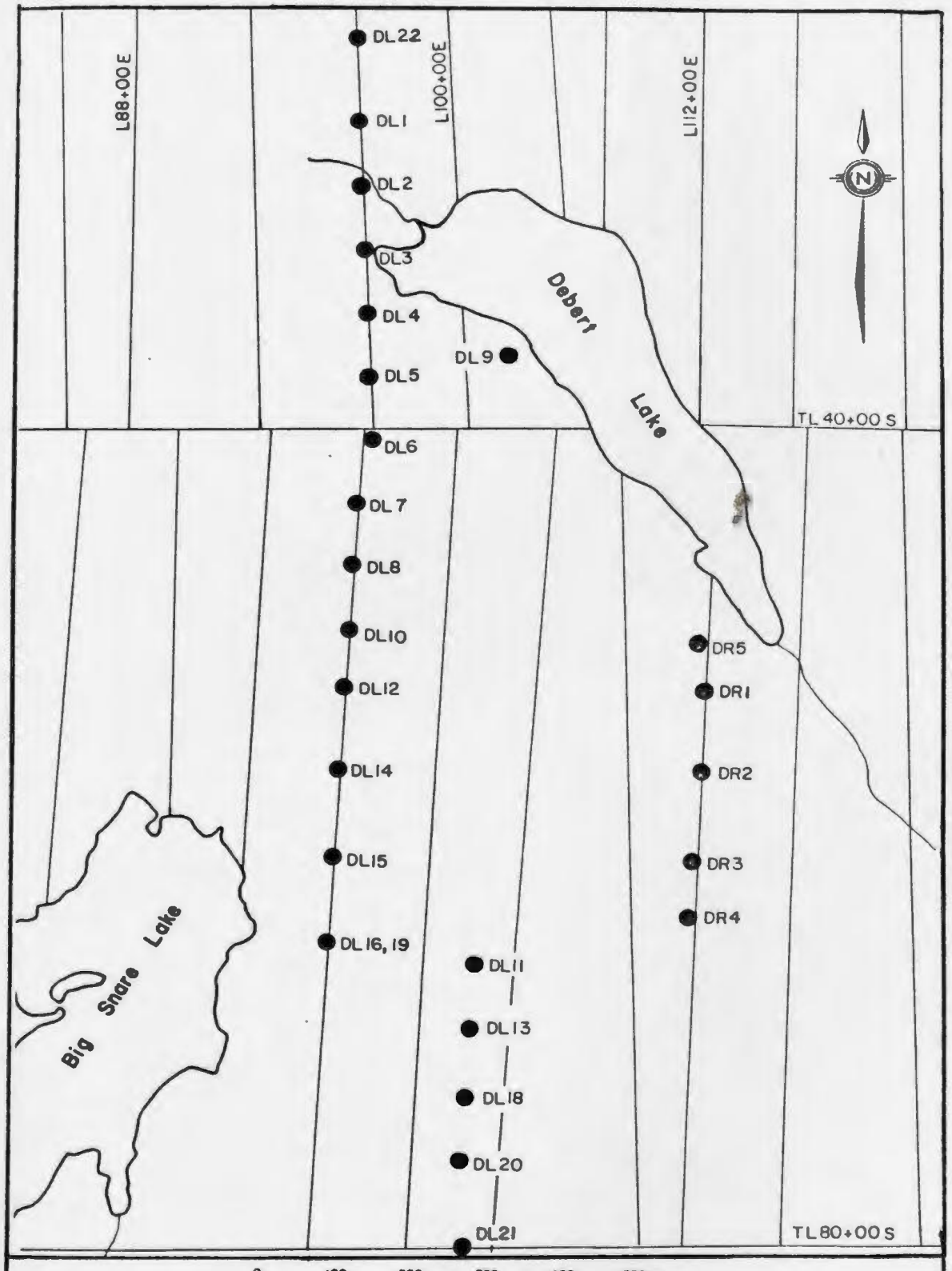

DL-Zone diamond drill hole location map.

Appendix 2

Analytical methods and sampling techniques.

The analyses used in this study are of samples taken over the span of G.M.C.L.'s Cobequid exploration program from 1976-1981. Most of the data are analysis of diamond drill core. 459 samples were run for major and trace elements. Gulf provided approximately 300 thin sections corresponding to geochemistry samples and 60 polished thin sections were prepared at Memorial University.

All analysis were done by X-Ray Assay Labs of Don Mills Ontario. Sample splits and re-analyzed samples generally reproduced data within the detection limits.

The major oxides were analyzed by fully automated sequential x-ray spectrometer, using a power glass disk sample preparation method. The detection limit for the major oxides is 0.01%. Total iron was calculated as Fe2O3 and reported as FeO.

The trace element concentrations are reported in parts per million (ppm). Cu, Zn, Ag and Pb were analyzed by direct current plasma spectrometer at a detection limit of 0.5ppm. Rb, Sr, Zr and Cr2O3 were analyzed by XRF at a detection limit of 10ppm. Bi was assayed by fire assay-AA

at a detection limit of 0.1ppm. U was analyzed by delayed neutron counting at a detection limit of 0.1ppm. Th was analyzed by neutron activation at a detection limit of 1.0ppm. F was analyzed by wet chemistry at a detection limit of 100ppm. Ni, Co and Mo were analyzed by atomic absorption analysis to a detection limit of 1 ppm. Sn, Sb and W were analyzed by XRF to detection limits of 1 ppm for Sn and Sb and 5 ppm for W.

APPENDIX 3

Rock sample locations for lithogeochemistry samples.

Sample #	Depth (m)	Sample #	Depth (m)
		DDH # JZ-1	
B3109	5.2	B3123	97.0
B3110	11.3	B3125	104.3
B3111	18.6	B3128	126.5
B3112	22.6	B3129	128.3
B3113	22.9	B3130	131.7
B3114	24.4	B3132	136.5
B3115	33.5	B3168	146.0
B3116	42.7	B3138	151.2
B3117	44.5	B3140	160.9
B3118	50.3	B3141	164.0
B3119	55.8	B3134	167.6
B3120	58.0	B3133	173.4
		DDH # JZ-5	
B3287	19.5	B3182	82.0
B3179	28.0	B3857	87.3
B3180	30.3	B3292	113.4
B3181	32.2	B3864	120.1
B3290	55.2	B3293	144.8
B3291	73.2		
		DDH # JZ-6	
B3294	6.1	B3301	100.0
B3295	18.3	B3302	114.6
B3296	39.6	B3183	139.6
B3297	51.8	B3303	140.2
B3299	70.1	B3184	149.5
B3300	85.3	B3304	159.4

Sample #	Depth (m)	Sample #	Depth (m)
	DDH # JZ-7		
B3305	7.3	B3310	34.4
B3306	11.3	B3311	51.8
B3308	16.2		
B3309	22.9		
	DDH # JZ-8		
B3314	13.1	B3188	39.3
B3187	14.3	B3317	58.8
B3315	25.9	B3318	76.2
B3316	39.0		
	DDH # JZ-11		
E0101	42.0	B3194	88.7
B3190	53.2	B3197	114.3
B3191	63.8	B3199	142.0
B3192	70.7	B3198	144.8
	DDH # JZ-12		
B3200	33.5	E0102	88.1
	DDH # JZ-18		
E0116	94.8	E0119	135.8
E0117	100.0		

Sample #	Depth (m)	Sample #	Depth (m)
	DDH # DF-1		
C5365	22.3	C5372	71.9
C5366	32.3	B3891	72.4
C5367	49.1	C5373	81.7
B3890	55.5	C5374	97.5
C5368	57.6	C5375	107.9
C5369	65.2	B3893	109.7
C5370	65.8	C5376	139.6
C5371	69.5	C5377	141.7
	DDH # DF-2		
B3894	14.0	B3897	120.7
B3895	96.5		
	DDH # DF-4		
B3159	46.5	B3321	83.5
B3160	53.3	B3164	122.8
B3161	76.0		
	DDH # DF-5		
C5010	53.3	C5013	116.1
C5011	68.6	C5014	116.6
C5012	112.8	C5015	137.2
	DDH # DF-6		
C5341	15.8	C5346	59.1
C5342	26.5	C5348	78.6
C5343	28.3	C5018	82.3
C5344	44.2	C5349	85.6
C5016	44.5	C5350	96.0
C5345	54.9	C5019	106.7

Sample #	Depth (m)	Sample #	Depth (m)
	DDH # DF-7		
C5023	61.0	C5024	83.8
	DDH # DF-8		
C5005	17.1	C5007	91.4
C5006	44.5		
	DDH # DF-9		
C5001	27.4	C5003	76.2
C5002	62.8	C5004	100.6
	DDH # DF-12		
C5038	53.3	C5040	130.8
C5039	99.1		
	DDH # DF-13		
C5321	18.3	C5333	77.7
C5324	25.3	C5334	85.3
C5325	25.9	C5335	86.6
C5327	44.5	C5337	90.5
C5328	50.9	C5055	91.4
C5330	59.1	C5338	93.0
C5331	59.7	C5339	105.8
	DDH # DF-14		
C5351	34.4	C5359	79.9
C5025	36.6	C5027	83.8
C5352	46.0	C5028	90.5
C5353	48.5	C5361	97.5
C5354	50.3	C5029	114.3
C5355	51.8	C5030	134.1
C5356	57.0	C5362	135.3
C5026	60.7	C5363	150.9
C5357	62.8	C5031	158.5
C5358	75.6	C5364	160.6

Sample #	Depth (m)	Sample #	Depth (m)
	DDH # DF-15		
C5315	62.2	C5319	81.1
C5317	64.6	C5320	95.4
C5318	71.9		
	DDH # DF-16		
C5042	45.7	C5044	91.4
	DDH # DF-19		
C5033	30.5	C5037	85.3
	DDH # DF-20		
C5050	61.6		
	DDH # DF-27		
C5738	110.1	C5746	116.1
C5739	110.8	C5747	116.7
C5740	111.6	C5748	117.3
C5741	112.3	C5749	118.0
C5742	113.1	C5750	118.8
C5743	113.8	C5551	119.5
C5744	114.6	C5552	120.3
C5745	115.3		
	DDH# DF-28		
C5529	19.1	C5544	149.5
C5530	19.9	C5545	150.3
C5531	20.6	C5546	153.95
C5532	21.4	C5751	212.4
C5533	22.1	C5752	215.4
C5534	22.9	C5753	229.0
C5535	23.6	C5754	229.6
C5536	29.3	C5755	230.8
C5537	30.0	C5756	232.0
C5538	86.2	C5547	236.8
C5539	89.4	C5548	237.6
C5540	112.0	C5549	238.3
C5541	145.2	C5550	239.1
C5542	145.9	C5757	293.1
C5543	146.7		

Sample #	Depth (m)	Sample #	Depth (m)
	DDH# DF-29		
C5587	120.0	C5592	123.7
C5588	120.7	C5593	124.5
C5589	121.5	C5594	125.2
C5590	122.2	C5595	126.0
C5591	123.0	C5596	119.2
	DDH# DF-31		
C5484	135.5	C5499	191.9
C5486	148.3	C5500	192.7
C5487	149.2	C5501	200.0
C5485	156.1	C5502	200.1
C5488	161.0	C5503	201.5
C5489	161.8	C5504	202.3
C5490	162.5	C5505	203.0
C5491	163.3	C5506	203.8
C5492	166.1	C5507	204.5
C5493	187.0	C5508	205.3
C5494	187.9	C5509	206.0
C5495	188.9	C5510	206.8
C5496	189.7	C5511	207.6
C5497	190.4	C5512	223.1
C5498	191.2	C5513	223.7
	DDH # DF-32		
C5597	104.7	C5467	120.2
C5598	105.5	C5468	121.0
C5599	106.7	C5469	121.7
C5600	107.5	C5470	122.5
C5451	108.2	C5471	123.2
C5452	109.0	C5472	124.0
C5453	109.7	C5473	129.3
C5454	110.5	C5474	130.0
C5455	111.2	C5475	130.8
C5456	112.0	C5476	131.5
C5457	112.7	C5477	153.4
C5458	113.5	C5478	154.0
C5459	114.2	C5479	161.7
C5460	115.0	C5480	162.5
C5461	115.7	C5481	163.2
C5462	116.5	C5482	164.0
C5463	117.2	C5483	164.7
C5464	118.0	C5466	119.5
		C5465	118.7

Sample #	Depth (m)	Sample #	Depth (m)
	DDH # DF-34		
C5516	114.2	C5523	125.8
C5517	115.0	C5524	126.5
C5518	115.7	C5525	127.3
C5519	116.5	C5526	134.7
C5520	123.5	C5527	135.4
C5521	124.3	C5528	136.2
C5522	125.0		
	DDH # DF-36		
R1496	3.7	R1302	76.0
R1497	15.4	R1303	90.7
R1498	38.3	R1304	106.0
R1499	58.0	R1305	124.0
R1500	61.0	R1306	148.0
R1301	70.0	R1307	157.7
	DDH # DF-37		
R1273	4.0	R1278	119.3
R1274	14.5	R1279	133.0
R1275	39.7	R1280	141.7
R1276	63.6	R1281	150.7
R1277	90.6		
	DDH # DF-38		
R1487	19.0	R1492	91.0
R1488	28.0	R1493	109.0
R1489	40.0	R1494	127.0
R1490	58.0	R1495	128.6
R1491	76.0		
	DDH # DF-39		
R1353	16.2	R1358	101.1
R1354	34.0	R1359	121.0
R1355	46.7	R1360	134.7
R1356	54.7	R1361	148.0
R1357	71.5	R1362	165.7

Sample #	Depth (m)	Sample #	Depth (m)
	DDH # DF-40		
R1253	15.0	R1263	110.1
R1254	33.0	R1264	109.9
R1255	42.0	R1265	109.8
R1256	46.3	R1266	109.3
R1257	57.0	R1267	135.4
R1258	58.5	R1268	150.0
R1259	72.0	R1269	159.1
R1260	88.2	R1270	163.0
R1261	92.6	R1271	165.5
R1262	103.7	R1272	182.5
	DDH # DF-41		
R1251	218.3	R1252	220.0
	DDH # DF-42		
R1316	5.5	R1326	124.0
R1317	20.9	R1327	135.7
R1318	22.7	R1328	160.0
R1319	23.7	R1329	164.5
R1320	31.0	R1330	177.5
R1321	44.3	R1331	186.5
R1322	60.8	R1332	190.5
R1323	75.6	R1333	202.0
R1324	95.2	R1334	237.8
R1325	105.7	R1335	280.0
	DDH# DF-43		
R1363	19.7	R1368	142.7
R1364	54.9	R1369	154.8
R1365	81.5	R1370	162.5
R1366	104.0	R1371	204.2
R1367	139.6		
	DDH # DF-44		
R1404	30.7	R1412	83.5
R1405	34.0	R1413	91.6
R1406	37.0	R1414	107.6
R1407	58.1	R1415	125.5
R1408	44.3	R1416	129.6
R1409	74.6	R1417	159.8
R1410	81.0	R1418	86.1
R1411	85.4		

Sample #	Depth (m)	Sample #	Depth (m)
	DDH # DF-45		
R1472	22.0	R1480	131.0
R1473	40.0	R1481	133.0
R1474	55.0	R1482	133.9
R1475	64.0	R1483	134.0
R1476	67.0	R1484	138.7
R1477	87.2	R1485	143.5
R1478	119.5	R1486	149.8
R1479	124.0		
	DDH # DF-46		
R1282	14.0	R1289	115.3
R1283	18.5	R1290	116.7
R1284	43.8	R1291	118.9
R1285	76.4	R1292	119.9
R1286	80.0	R1293	122.1
R1287	112.5	R1294	126.3
R1288	114.0	R1295	131.0
	DDH # DF-47		
R1463	23.0	R1468	112.4
R1464	30.7	R1469	121.7
R1465	53.5	R1470	148.8
R1466	68.0	R1471	149.9
R1467	93.5		
	DDH # DF-48		
R1296	18.0	R1455	81.4
R1297	25.1	R1456	78.5
R1298	38.7	R1457	99.0
R1299	44.0	R1458	101.5
R1300	56.4	R1459	103.2
R1451	61.0	R1460	109.5
R1452	66.5	R1461	114.0
R1453	80.4	R1462	147.0
R1454	81.0		
	DDH # DF-49		
R1419	22.7	R1425	71.0
R1420	36.7	R1426	79.7
R1421	42.5	R1427	83.5
R1422	52.2	R1428	89.3
R1423	55.0	R1429	115.8
R1424	66.3	R1430	142.7

Sample #	Depth (m)	Sample #	Depth (m)
	DDH # DF-50		
R1308	8.0	R1312	43.5
R1309	17.0	R1313	50.2
R1310	32.0	R1314	59.5
R1311	37.2	R1315	124.7
	DDH # DF-51		
R1336	40.7	R1345	99.5
R1337	47.0	R1346	103.6
R1338	49.8	R1347	123.3
R1339	68.7	R1348	133.7
R1340	72.5	R1349	135.5
R1341	75.5	R1350	149.4
R1342	80.0	R1401	169.7
R1343	82.7	R1402	185.3
R1344	86.0	R1403	198.0
	DDH # DF-52		
R1431	7.7	R1442	132.0
R1432	34.5	R1443	132.55
R1433	23.5	R1444	136.7
R1434	68.0	R1445	142.5
R1435	89.2	R1446	144.5
R1436	104.0	R1447	146.0
R1437	112.7	R1448	147.5
R1438	118.7	R1449	149
R1439	127.7	R1450	150.5
R1440	128.0	R1351	164.0
R1441	129.5	R1352	185.0
	DDH # DL-6		
C5389	45.4	C5397	72.0
C5390	50.9	C5398	79.3
C5391	54.0	C5399	85.6
C5392	59.2	C5400	96.1
C5395	68.6	C5401	100.7
C5396	69.5	C5403	114.1
	DDH # DL-8		
C5131	15.3	C5136	73.0
C5134	56.7	C5137	96.2
C5135	63.0		

Sample #	Depth (m)	Sample #	Dep h (m)
	DDH # DL-9		
C5140	15.3	C5144	79.6
C5143	61.5	C5145	96.5
	DDH # DL-10		
C5151	41.2	C5156	139.7
C5153	86.8		
	DDH # DL-11		
C5158	11.7	C5162	40.6
C5160	23.8	C5167	114.8
	DDH # DL-12		
C5168	6.3	C5175	95.7
C5170	21.7	C5176	114.7
C5171	25.0	C5178	132.5
C5172	56.7	C5179	138.2
C5173	69.5		
	DDH # DL-13		
C5180	5.5	C5185	83.9
C5181	12.2	C5186	94.7
C5182	28.4	C5187	106.7
C5183	61.1	C5188	122.0
C5184	78.2	C5190	154.6
	DDH # DL-14		
C5191	11.4	C5195	89.1
C5193	44.2	C5196	104.2
C5194	76.4	C5198	127.9
	DDH # DL-15		
C5199	30.6	C5204	92.2
C5200	52.5	C5205	95.2
C5202	85.1	C5206	131.2
C5203	89.4		

Sample #	Depth (m)	Sample #	Depth (m)
	DDH # DL-16		
C5207	3.7	C5214	99.2
C5208	9.9	C5215	108.2
C5209	28.2	C5216	120.9
C5210	36.4	C5217	123.8
C5212	61.0	C5218	128.4
C5213	82.7	C5219	141.1
	DDH # DL-17		
C5220	1.8	C5222	63.6
C5221	40.9	C5223	77.6
	DDH # DL-18		
C5242	24.8	C5248	93.8
C5243	47.6	C5249	110.7
C5244	59.1	C5250	127.9
C5246	75.8	C5252	144.2
C5247	86.0		
	DDH # DL-19		
C5224	2.1	C5233	86.6
C5225	3.3	C5234	91.6
C5226	20.9	C5235	102.6
C5227	31.7	C5236	109.9
C5228	38.3	C5237	118.6
C5229	59.0	C5238	120.5
C5230	63.7	C5239	121.8
C5231	67.9	C5241	135.5
C5232	72.4		
	DDH # DL-20		
C5253	3.4	C5257	139.4
C5254	30.5	C5259	159.5
C5255	94.8		
	DDH # DL-21		
C5261	19.8	C5265	57.0
C5262	34.2	C5266	62.9
C5263	46.6	C5267	86.3
C5264	48.5		

DDH DL-22

Sample #	Depth (m)	Sample #	Depth (m)
C5269	24.2	C5275	141.1
C5271	36.3	C5276	149.1
C5273	93.5	C5277	168.5

APPENDIX 4

GEOCHEMICAL ANALYSES

RHYOLITE FLOWS

	6C5396	6C5397	6C5398	6C5399	6C5400
SiO2	79.60	72.60	75.80	77.20	76.40
TiO2	.09	.42	.10	.09	.13
Al2O3	10.90	12.70	12.30	11.30	11.60
FeOt	.60	1.88	1.21	.92	.85
MnO	.11	.16	.14	.12	.13
MgO	.29	.36	.06	0.00	0.00
CaO	.30	.78	.32	.31	.34
Na2O	0.00	.17	0.00	.11	0.00
K2O	5.33	8.84	8.81	8.96	9.01
P2O5	.02	.09	.01	.02	.02
LOI	1.46	.69	.31	.38	.38
TOTAL	98.70	98.69	99.06	99.41	98.86
Cu	8	9	7	10	6
Zn	8	41	35	18	16
Ag	0	0	0	0	0
Sn	3	1	1	1	1
Zr	260	410	250	210	270
F	460	440	140	100	110
Sr	30	30	20	30	20
Rb	320	400	400	420	410
W	0	2	2	18	2
Pb	10	12	15	12	6
U	20	6	6	5	7
Th	21	20	26	35	27
Bi	0	0	0	0	0
Mo	0	0	0	0	0
Sb	2	1	2	0	2
Co	0	2	0	0	0
Ni	2	4	2	1	65

RHYOLITE FLOWS

	6C5401	6C5403
SiO2	75.60	75.50
TiO2	.30	.11
Al2O3	12.40	12.40
FeOt	1.45	.76
MnO	.14	.12
MgO	0.00	0.00
CaO	.48	.34
Na2O	.03	0.00
K2O	9.54	9.47
P2O5	.08	.02
LOI	.38	.38
TOTAL	100.40	99.10
Cu	28	10
Zn	32	19
Ag	0	0
Sn	1	1
Zr	320	190
F	170	130
Sr	20	40
Rb	420	450
W	2	0
Pb	10	4
U	8	8
Th	19	26
Bi	0	0
Mo	0	0
Sb	1	2
Co	0	0
Ni	3	2

RHYOLITE FLOWS

	1C5366	1C5367	1C5370	1C5371	1C5372
SiO2	76.10	74.40	79.20	73.50	75.10
TiO2	.14	.11	.07	.14	.12
Al2O3	11.70	9.62	5.55	12.20	11.80
FeOt	1.64	2.12	.87	1.02	1.40
MnO	.13	.14	.13	.11	.13
MgO	.37	.43	.12	.11	.11
CaO	.96	3.79	5.14	.90	.45
Na2O	4.73	0.00	2.52	.56	.18
K2O	2.40	5.92	.63	9.28	8.69
P2O5	.04	.03	.01	.02	.02
LOI	.69	1.62	3.77	.46	.33
TOTAL	98.90	98.18	98.01	98.30	98.33
Cu	20	13	44	17	27
Zn	47	61	28	28	26
Ag	1	0	0	0	0
Sn	1	1	3	1	1
Zr	430	220	80	150	170
F	800	7100	200	1400	330
Sr	60	190	80	40	50
Rb	100	240	200	350	350
W	0	4	0	0	2
Pb	12	12	33	10	7
U	11	5	4	5	6
Th	22	16	7	20	32
Bi	0	1	0	0	0
Mo	1	1	1	1	1
Sb	1	1	1	0	1
Co	5	3	3	5	5
Ni	6	4	7	3	4

RHYOLITE FLOWS

	6C5389	6C5390	6C5391	6C5392	6C5395
SiO2	79.00	77.90	76.80	78.20	73.70
TiO2	.27	.29	.34	.31	.10
Al2O3	8.49	8.25	9.10	8.82	13.50
FeOt	2.42	3.20	3.67	3.04	.88
MnO	.14	.14	.20	.15	.15
MgO	.05	.02	.04	.13	.56
CaO	.31	.46	.42	.46	.37
Na2O	0.00	0.00	0.00	0.00	0.00
K2O	5.17	5.44	5.68	5.64	7.67
P2O5	.02	.02	.02	.01	.02
LOI	1.62	2.00	1.69	1.46	1.23
TOTAL	97.49	97.72	97.96	98.24	98.18
Cu	8	12	26	23	10
Zn	520	350	410	91	23
Ag	0	0	0	0	0
Sn	1	1	3	3	3
Zr	770	740	820	1200	290
F	310	190	170	270	600
Sr	20	30	20	20	60
Rb	250	250	280	280	440
W	3	2	1	2	0
Pb	190	180	280	46	7
U	10	5	4	5	125
Th	16	17	18	25	25
Bi	0	0	0	0	0
Mo	0	0	0	0	0
Sb	3	3	4	9	2
Co	2	3	3	3	0
Ni	5	3	5	3	3

RHYOLITE FLOWS

	1C5373	1C5374	13C5322	13C5324	13C5330
SiO2	79.70	76.00	74.10	74.70	72.10
TiO2	.09	.18	.12	.12	.14
Al2O3	9.39	10.80	12.60	12.20	12.40
FeOt	.56	1.72	1.31	1.15	1.59
MnO	.11	.15	.13	.13	.14
MgO	0.00	.16	.05	.14	.31
CaO	.37	.47	1.07	.52	1.53
Na2O	.35	.27	2.49	.98	1.23
K2O	7.50	8.06	6.38	8.46	7.86
P2O5	.01	.03	.02	.02	.02
LOI	.31	.46	.38	.46	1.15
TOTAL	98.39	98.30	98.65	98.88	98.47
Cu	31	13	23	1[illegible]	8
Zn	30	30	32	79	34
Ag	0	0	0	0	0
Sn	1	1	1	1	1
Zr	140	150	150	190	220
F	180	410	160	130	130
Sr	30	40	100	50	70
Rb	290	280	220	300	240
W	4	6	0	0	0
Pb	23	4	19	30	3
U	4	5	18	16	7
Th	23	26	27	30	29
Bi	0	0	0	2	0
Mo	1	1	1	1	1
Sb	0	1	1	1	1
Co	3	4	3	4	2
Ni	2	5	3	2	3

RHYOLITE FLOWS

	13C5333	14C5357	14C5358	14C5359	15C5315
SiO2	76.90	75.70	70.30	71.30	74.70
TiO2	.21	.12	.17	.15	.12
Al2O3	10.80	11.10	14.00	13.40	11.90
FeOt	2.13	1.89	1.48	1.59	1.49
MnO	.11	.13	.14	.13	.15
MgO	0.00	.21	.23	.14	.18
CaO	.56	.72	.49	.40	1.15
Na2O	2.95	1.31	1.88	1.46	1.13
K2O	4.36	6.31	8.77	8.66	6.86
P2O5	.01	.03	.03	.02	.02
LOI	.38	.85	.38	.46	1.23
TOTAL	98.41	98.37	97.87	97.71	98.93
Cu	5	13	13	14	8
Zn	18	150	44	120	82
Ag	0	1	1	1	0
Sn	5	1	1	1	1
Zr	400	170	230	210	160
F	130	420	340	260	440
Sr	30	50	40	40	60
Rb	180	250	350	340	250
W	4	3	2	3	4
Pb	1	110	10	180	52
U	8	16	10	9	7
Th	28	24	28	41	32
Bi	0	2	0	0	0
Mo	1	230	1	100	1
Sb	0	1	1	1	0
Co	1	3	4	2	2
Ni	2	2	3	2	3

RHYOLITE FLOWS

	15C5318
SiO2	68.80
TiO2	.11
Al2O3	10.50
FeOt	.78
MnO	.13
MgO	0.00
CaO	7.93
Na2O	2.17
K2O	4.83
P2O5	.02
LOI	3.23
TOTAL	98.50

Cu	16
Zn	180
Ag	1
Sn	1
Zr	140
F	33000
Sr	50
Rb	220
W	1
Pb	3
U	12
Th	23
Bi	0
Mo	1
Sb	0
Co	4
Ni	5

RHYOLITE FLOWS

	15C5318	15C5319
SiO2	68.80	76.20
TiO2	.11	.17
Al2O3	10.50	12.10
FeOt	.78	1.50
MnO	.13	.12
MgO	0.00	.13
CaO	7.93	.54
Na2O	2.17	3.18
K2O	4.83	5.15
P2O5	.02	.02
LOI	3.23	.62
TOTAL	98.50	99.73
Cu	16	10
Zn	180	73
Ag	1	0
Sn	1	5
Zr	140	250
F	33000	310
Sr	50	30
Rb	220	240
W	0	0
Pb	3	22
U	12	9
Th	23	39
Bi	0	2
Mo	1	1
Sb	0	1
Co	4	3
Ni	5	3

RHYOLITE FLOWS

	12C5171	12C5172	18C5243	18C5246	18C5248
SiO2	78.54	79.29	78.10	74.13	78.00
TiO2	.08	.09	.33	.21	.21
Al2O3	11.17	11.71	11.29	13.88	13.53
FeOt	.91	.86	2.88	1.80	1.14
MnO	.04	.03	.05	.03	.02
MgO	.13	.06	.42	.54	.57
CaO	.37	.19	.49	.91	.20
Na2O	.10	.09	.28	5.68	.38
K2O	8.38	8.66	5.21	1.86	5.43
P2O5	.01	.01	.05	.02	.02
LOI	.52	.62	.94	.82	1.14
TOTAL	100.25	101.61	100.04	99.88	100.64
Cu	26	29	15	7	9
Zn	130	34	42	42	14
Ag	0	0	0	0	0
Sn	0	0	3	0	3
F	180	160	410	270	440
W	20	0	0	0	0
Pb	90	20	10	0	0
U	6	6	5	7	4
Th	25	24	18	26	27

RHYOLITE FLOWS

	18C5249	18C5250	20C5254
SiO2	70.06	82.40	79.19
TiO2	.32	.21	.17
Al2O3	14.82	8.76	11.56
FeOt	2.33	2.55	.98
MnO	.03	.02	.03
MgO	.17	.21	.11
CaO	.28	.20	.16
Na2O	.26	.13	.25
K2O	10.47	4.94	8.09
P2O5	.06	.02	.01
LOI	.17	.62	.25
TOTAL	98.97	100.06	100.80
Cu	13	32	12
Zn	24	23	19
Ag	0	0	0
Sn	0	3	0
F	210	130	320
W	0	20	0
Pb	0	0	5
U	5	10	9
Th	23	11	26

RHYOLITE FLOWS

	1B3891	1B3893	2B3894	2B3895	2B3897
SiO2	74.82	77.28	75.59	71.50	75.41
TiO2	.14	.25	.15	.17	.17
Al2O3	13.14	11.30	12.58	14.49	13.07
FeOt	1.43	2.80	1.99	1.76	2.32
MnO	.04	.13	.05	.02	.03
MgO	.33	.22	.46	.48	.66
CaO	.29	.39	1.14	.33	.24
Na2O	.57	3.48	3.99	.63	.41
K2O	9.23	4.13	4.04	10.59	7.67
P2O5	.01	.01	.01	.02	.02
LOI	1.56	.52	.96	.62	1.20
TOTAL	101.56	100.51	100.96	100.61	101.20
Cu	23	17	30	24	15
Zn	35	63	240	69	42
Ag	1	1	1	1	1
Sn	3	8	3	3	8
F	100	150	80	170	260
W	20	20	20	20	20
Pb	5	40	55	5	5
U	7	8	10	9	14
Th	24	20	21	29	30

RHYOLITE FLOWS

	4B3159	4B3160	4B3161	4B3721	4B3164
SiO2	76.76	74.26	76.90	75.12	76.66
TiO2	.13	.14	.13	.16	.13
Al2O3	12.17	13.43	12.14	12.79	12.15
FeOt	1.24	1.39	1.31	1.42	1.44
MnO	.04	.04	.02	.03	.02
MgO	.12	.20	.13	.12	.18
CaO	.34	.32	.23	.30	.31
Na2O	1.87	2.19	1.34	2.09	1.39
K2O	7.29	8.01	7.78	7.93	7.70
P2O5	.03	.01	.02	.01	.02
LOI	.75	1.32	1.67	.58	.77
TOTAL	100.74	101.31	101.67	100.55	100.77
Cu	22	30	26	25	19
Zn	26	37	38	20	74
Ag	1	1	1	1	1
Sn	3	3	3	3	3
F	240	250	170	80	90
W	20	20	20	20	20
Pb	10	5	20	10	40
U	4	9	8	7	4
Th	21	28	22	25	25

RHYOLITE FLOWS

	5B3179	5B3180	5B3181	5B3182	6B3301
SiO2	77.81	78.38	74.51	76.92	78.01
TiO2	.21	.25	.25	.26	.25
Al2O3	10.37	10.38	13.41	11.15	10.50
FeOt	2.88	2.99	3.20	3.60	2.59
MnO	.05	.02	.02	.09	.06
MgO	.14	.10	.08	.11	.28
CaO	.32	.38	.46	.33	1.35
Na2O	.85	1.79	7.09	2.81	1.83
K2O	7.34	5.62	.90	4.70	5.09
P2O5	.03	.05	.06	.02	.01
LOI	.68	.63	.35	.75	.42
TOTAL	100.68	100.59	100.33	100.74	100.39
Cu	80	43	34	29	50
Zn	230	280	170	220	420
Ag	1	2	1	1	1
Sn	3	3	3	3	3
F	70	340	170	100	80
W	20	20	20	20	20
Pb	120	230	160	30	350
U	46	60	210	12	5
Th	19	20	20	15	22

RHYOLITE FLOWS

	6B3302
SiO2	78.01
TiO2	.24
Al2O3	10.74
FeOt	2.84
MnO	.04
MgO	.04
CaO	.51
Na2O	2.75
K2O	4.81
P2O5	.01
LOI	.26
TOTAL	100.25

Cu	31
Zn	200
Ag	1
Sn	5
F	80
W	20
Pb	35
U	7
Th	14

RHYOLITE FLOWS

	36R1305	36R1306	36R1307	38R1491	38R1492
SiO2	76.60	76.20	75.20	76.70	72.70
TiO2	.14	.13	.14	.25	.35
Al2O3	11.80	12.00	12.60	12.60	14.60
FeOt	1.01	.86	.93	.94	1.61
MnO	.02	.02	.02	.03	.06
MgO	.28	.10	.23	.45	.82
CaO	.91	.53	.46	.60	.53
Na2O	2.68	.64	1.62	4.29	1.75
K2O	5.87	9.24	8.10	3.48	5.69
P2O5	.01	.01	.01	.01	.01
LOI	.47	.31	.70	.62	1.39
TOTAL	99.79	100.04	100.01	99.97	99.51
Cu	17	15	10	13	6
Zn	43	40	25	34	48
Ag	0	0	0	0	0
Ba	330	290	400	440	420
Au	1	1	4	1	1
Sn	1	3	3	1	1
Zr	110	140	150	170	230
Cr	170	180	160	150	140
F	360	620	490	220	360
Sr	90	90	70	160	80
Rb	240	390	370	130	300
W	1	4	4	3	1
Pb	29	20	15	16	11
U	5	7	3	3	3

RHYOLITE FLOWS

	38R1493	38R1494	40R1271	42R1316	42R1317
SiO2	71.90	71.60	78.10	76.30	80.60
TiO2	.38	.56	.16	.24	.12
Al2O3	14.70	12.60	10.40	11.70	9.12
FeOt	1.64	4.04	1.17	1.91	1.51
MnO	.08	.16	.02	.03	.03
MgO	1.02	1.22	.29	.31	.21
CaO	1.33	.89	1.64	.40	.36
Na2O	3.50	2.78	3.20	.46	.20
K2O	4.84	4.23	4.45	7.22	6.44
P2O5	.05	.14	.01	.04	.02
LOI	1.00	1.39	.77	1.08	.77
TOTAL	100.44	99.61	100.21	99.69	99.38
Cu	9	12	22	22	17
Zn	85	180	22	40	44
Ag	0	1	0	0	0
Ba	690	570	710	240	150
Au	1	2	1	3	3
Sn	1	15	7	1	1
Zr	220	220	180	150	240
Cr	120	140	190	130	190
F	1100	1000	270	320	200
Sr	250	90	80	50	50
Rb	220	240	180	280	240
W	2	2	5	5	2
Pb	20	58	38	10	14
U	5	4	9	8	10

RHYOLITE FLOWS

	42R1318	42R1319	42R1320	42R1321	42R1323
SiO2	77.80	80.30	80.20	78.80	78.20
TiO2	.14	.12	.11	.13	.12
Al2O3	10.80	9.33	8.76	10.80	10.40
FeOt	.58	1.19	2.02	1.61	.87
MnO	0.00	.12	.11	.03	.01
MgO	.10	.10	.61	.25	.10
CaO	.33	.22	.83	.23	.72
Na2O	.26	.27	2.10	.18	.59
K2O	8.89	7.76	3.67	6.81	7.95
P2O5	.05	.02	.01	.02	.01
LOI	.39	.31	.93	.77	.39
TOTAL	99.34	99.74	99.35	99.63	99.36
Cu	4	22	9	9	11
Zn	89	62	67	45	120
Ag	0	0	0	0	2
Ba	470	190	230	140	250
Au	3	2	1	1	1
Sn	1	1	1	3	1
Zr	310	260	260	280	120
Cr	100	220	150	150	170
F	190	150	230	220	180
Sr	60	60	150	30	100
Rb	340	240	130	220	260
W	4	3	3	5	3
Pb	6	45	18	6	41
U	16	8	8	8	11

RHYOLITE FLOWS

	42R1324	42R1325	42R1326	42R1327	42R1334
SiO2	75.10	73.00	76.90	76.70	76.30
TiO2	.14	.15	.13	.14	.13
Al2O3	12.70	13.60	11.40	11.80	11.30
FeOt	.91	1.14	1.25	.95	1.22
MnO	.02	.03	.03	.02	.02
MgO	.12	.13	.11	.16	.26
CaO	.09	.17	.22	.08	.19
Na2O	.20	.19	.25	.18	.22
K2O	10.10	11.30	9.07	8.89	8.56
P2O5	.01	.01	.01	.01	.01
LOI	.54	.39	.31	.62	.70
TOTAL	99.93	100.11	99.68	99.55	98.91
Cu	12	16	17	10	13
Zn	65	73	110	27	30
Ag	1	0	0	0	0
Ba	260	320	230	250	480
Au	1	1	4	1	1
Sn	1	1	1	1	1
Zr	140	150	140	140	140
Cr	150	140	180	160	140
F	160	170	160	160	180
Sr	30	40	30	20	20
Rb	320	310	300	320	300
W	2	3	6	4	2
Pb	26	43	37	26	4
U	16	10	13	9	16

RHYOLITE FLOWS

	42R1335	43R1365	43R1366	43R1369	43R1371
SiO2	75.50	76.50	75.00	74.50	72.80
TiO2	.15	.13	.14	.14	.15
Al2O3	12.30	11.50	12.20	12.60	12.90
FeOt	1.11	1.22	.68	.89	.88
MnO	.02	.02	.01	.02	.03
MgO	.24	.25	.08	.17	.18
CaO	.53	.71	.68	.29	.37
Na2O	2.48	1.33	.47	.42	.73
K2O	7.15	7.74	9.58	10.10	10.20
P2O5	.01	.02	.02	.01	.01
LOI	1.00	.54	.54	.31	.77
TOTAL	100.49	99.96	99.40	99.45	99.02
Cu	12	16	6	9	14
Zn	19	23	50	96	46
Ag	0	0	2	0	0
Ba	250	310	310	360	410
Au	1	1	7	1	1
Sn	1	1	1	1	1
Zr	160	130	150	150	160
Cr	170	180	120	110	140
F	150	190	200	170	240
Sr	60	100	80	50	60
Rb	270	290	350	360	350
W	2	2	2	2	2
Pb	10	8	22	8	13
U	8	14	16	17	19

RHYOLITE FLOWS

	44R1404	44R1413	44R1415	44R1417	45R1478
SiO2	75.10	78.90	77.20	74.10	77.30
TiO2	.13	.18	.16	.14	.14
Al2O3	12.20	10.40	11.10	13.20	11.50
FeOt	.53	.62	.93	1.15	.57
MnO	.01	.01	.01	.02	0.00
MgO	.11	.09	.12	.21	.10
CaO	.23	.62	.85	.24	.44
Na2O	.31	.29	.29	.49	.26
K2O	10.30	8.43	9.17	10.20	8.96
P2O5	.01	.03	.01	.01	.01
LOI	.62	.31	.54	.02	.62
TOTAL	99.55	99.88	100.38	99.78	99.90
Cu	10	11	24	24	17
Zn	24	50	32	38	13
Ag	0	0	0	0	0
Ba	270	430	240	420	520
Au	2	1	1	1	1
Sn	1	1	1	1	1
Zr	150	110	140	160	140
Cr	140	170	170	160	150
F	240	440	1200	320	440
Sr	30	50	60	60	40
Rb	340	270	270	320	270
W	3	3	2	1	3
Pb	8	14	51	48	13
U	7	15	9	7	9

RHYOLITE FLOWS

	45R1480	45R1486	46R1285	46R1293	46R1295
SiO2	80.50	74.60	76.10	77.60	76.70
TiO2	.30	.20	.22	.22	.14
Al2O3	9.23	9.66	11.90	11.30	11.00
FeOt	1.48	2.87	1.72	1.07	2.03
MnO	.03	.05	.06	.02	.02
MgO	.23	.50	.40	.25	.37
CaO	.53	3.03	2.82	1.00	.22
Na2O	.18	.90	3.70	3.73	.66
K2O	5.98	5.42	2.38	4.37	8.40
P2O5	.02	0.00	.04	.02	.01
LOI	.70	1.31	1.47	.47	.47
TOTAL	99.18	98.54	100.81	100.05	100.02
Cu	13	17	14	31	50
Zn	24	410	240	24	52
Ag	1	1	1	0	0
Ba	170	190	150	220	370
Au	1	1	1	1	1
Sn	3	3	5	5	1
Zr	320	1030	340	270	160
Cr	180	140	160	120	170
F	320	1800	7400	480	350
Sr	20	240	120	90	30
Rb	220	220	110	170	290
W	2	2	1	1	4
Pb	25	260	45	91	26
U	6	8	0	10	8

RHYOLITE FLOWS

	47R1465	47R1467	48R1460	49R1419	49R1420
SiO2	75.70	75.10	79.40	77.90	71.30
TiO2	.25	.15	.16	.11	.23
Al2O3	11.60	12.80	8.33	11.10	13.90
FeOt	2.18	1.38	2.10	1.08	2.00
MnO	.04	.03	.08	.02	.03
MgO	.69	.21	.27	.16	.87
CaO	1.95	.23	2.92	.21	.88
Na2O	4.30	.35	2.01	.61	2.52
K2O	2.71	9.16	3.15	8.03	7.26
P2O5	.04	.02	0.00	0.00	.02
LOI	.85	.70	1.39	.47	1.08
TOTAL	100.31	100.13	99.81	99.69	100.09
Cu	27	13	4	23	3
Zn	120	55	64	43	55
Ag	0	0	0	0	0
Ba	240	200	130	240	290
Au	1	1	4	1	1
Sn	1	1	7	1	5
Zr	150	160	690	200	240
Cr	180	150	180	170	100
F	1800	340	200	220	310
Sr	120	30	260	70	130
Rb	100	330	130	300	320
W	5	2	5	1	2
Pb	100	23	120	43	23
U	5	13	6	5	6

RHYOLITE FLOWS

	49R1421	49R1424	52R1431	52R1434	52R1435
SiO2	77.50	77.20	74.80	73.40	72.00
TiO2	.11	.12	.33	.14	.17
Al2O3	11.00	12.10	12.80	13.60	13.70
FeOt	1.32	1.61	1.62	1.56	1.02
MnO	.03	.03	.04	.08	.03
MgO	.71	.87	.25	.29	.31
CaO	2.07	.18	.49	2.04	.94
Na2O	1.37	.19	1.62	3.70	.52
K2O	4.48	6.41	7.08	4.87	10.70
P2O5	0.00	0.00	.08	.01	.01
LOI	.93	1.47	.93	.62	.62
TOTAL	99.52	100.18	100.04	100.31	100.02
Cu	6	3	14	8	8
Zn	26	45	110	350	30
Ag	0	0	0	0	0
Ba	100	290	440	290	540
Au	1	1	1	1	1
Sn	3	5	3	1	1
Zr	170	190	290	150	190
Cr	170	100	160	160	120
F	1100	660	400	320	270
Sr	140	40	90	180	90
Rb	290	390	250	180	190
W	2	3	2	2	3
Pb	13	75	27	45	16
U	6	7	7	63	11

RHYOLITE FLOWS

	52R1436	52R1437	52R1438	52R1440	52R1441
SiO2	78.10	72.00	75.90	73.50	71.90
TiO2	.13	.15	.12	.15	.14
Al2O3	11.20	13.90	11.00	13.10	13.20
FeOt	.72	1.43	2.78	2.40	3.09
MnO	.02	.04	.05	.07	.07
MgO	.11	.21	.42	.43	.56
CaO	.17	.20	1.13	.66	1.00
Na2O	.40	.45	.46	.63	1.15
K2O	8.63	10.80	7.02	8.72	8.20
P2O5	.05	.03	.02	.02	.02
LOI	.47	.54	.77	.77	.77
TOTAL	100.00	99.75	99.67	100.45	100.10
Cu	13	17	44	10	10
Zn	34	45	180	81	98
Ag	0	0	0	0	0
Ba	260	210	210	150	160
Au	1	2	3	1	1
Sn	1	1	5	1	1
Zr	140	170	140	170	170
Cr	200	120	180	160	150
F	290	270	260	880	760
Sr	20	40	110	40	70
Rb	290	320	250	320	300
W	1	4	2	3	2
Pb	16	12	71	24	24
U	10	17	12	14	21

RHYOLITE FLOWS

	5B3291	5B3293	6B3294	6B3295	6B3297
SiO2	75.91	75.29	80.76	77.29	75.11
TiO2	.29	.13	.22	.13	.49
Al2O3	10.74	12.50	9.24	11.85	11.79
FeOt	3.00	1.01	2.67	2.03	4.13
MnO	.06	.02	.06	.04	.07
MgO	.19	.10	.15	.07	.10
CaO	.33	.31	.25	.31	.47
Na2O	.65	.34	2.07	3.29	4.78
K2O	8.84	10.28	4.53	4.97	2.97
P2O5	.03	.02	.02	0.00	.06
LOI	.54	.27	.45	.38	.32
TOTAL	100.58	100.27	100.42	100.56	100.29

RHYOLITE FLOWS

	6B3299	6B3303	6B3183	6B3184
SiO2	74.89	76.42	76.70	78.06
TiO2	.43	.24	.24	.24
Al2O3	10.98	10.52	10.92	10.44
FeOt	3.95	3.23	3.21	3.58
MnO	.10	.06	.09	.07
MgO	.43	.16	.07	.08
CaO	.57	.57	.24	.37
Na2O	1.37	.92	1.24	2.57
K2O	7.23	7.84	7.26	4.56
P2O5	.07	.01	.01	.02
LOI	.58	.62	.95	.45
TOTAL	100.60	100.59	100.93	100.44

ASH FLOWS

	6C5348	14C5356	14C5357	14C5358	14C5359
SiO2	78.20	72.10	75.70	70.30	71.30
TiO2	.14	.12	.12	.17	.15
Al2O3	10.70	13.50	11.10	14.00	13.40
FeOt	1.17	1.78	1.89	1.48	1.59
MnO	.12	.13	.13	.14	.13
MgO	.02	.22	.21	.23	.14
CaO	.63	1.07	.72	.49	.40
Na2O	3.23	3.06	1.31	1.88	1.46
K2O	4.23	5.93	6.31	8.77	8.66
P2O5	.02	.03	.03	.03	.02
LOI	.69	.92	.85	.31	.46
TOTAL	99.15	98.86	98.37	97.80	97.71
Cu	10	9	13	15	11
Zn	30	63	150	44	120
Ag	1	2	1	1	1
Sn	1	1	1	1	1
Zr	150	210	170	230	210
F	360	270	420	340	260
Sr	20	60	50	40	40
Rb	170	230	250	350	340
W	2	1	3	2	3
Pb	8	18	110	10	180
U	4	9	16	10	9
Th	29	25	24	28	41
Bi	0	2	2	0	0
Mo	1	80	230	1	100
Sb	0	1	1	1	1
Co	2	4	3	4	2
Ni	3	3	2	3	2

ASH FLOWS

	1C5376	1C5377	6C5341	6C5342	6C5344
SiO2	58.30	64.10	80.00	79.00	76.00
TiO2	.30	.18	.08	.16	.10
Al2O3	17.10	13.00	9.05	10.00	11.40
FeOt	3.85	3.19	1.21	1.24	2.24
MnO	.26	.26	.11	.11	.11
MgO	.16	.29	.01	.08	.02
CaO	4.74	5.35	.84	.40	.51
Na2O	1.93	.83	.52	2.23	4.26
K2O	9.91	8.40	6.30	4.85	2.97
P2O5	.05	.03	.01	.03	.01
LOI	.77	1.31	.46	.15	.54
TOTAL	97.37	96.94	98.59	98.25	98.16
Cu	8	7	36	28	18
Zn	61	41	37	30	67
Ag	1	1	1	1	1
Sn	3	3	1	1	5
Zr	270	190	150	160	560
F	620	1200	170	190	280
Sr	100	80	60	30	30
Rb	370	320	210	140	140
W	1	1	1	1	1
Pb	36	8	11	16	21
U	11	7	4	5	11
Th	36	31	22	25	35
Bi	1	1	0	0	1
Mo	1	1	1	12	1
Sb	1	1	0	0	1
Co	10	7	3	3	1
Ni	6	5	2	3	2

ASH FLOWS

	14C5361	14C5362
SiO2	75.90	79.90
TiO2	.11	.10
Al2O3	11.30	9.80
FeOt	.90	1.05
MnO	.11	.12
MgO	0.00	.08
CaO	.47	.23
Na2O	1.82	1.56
K2O	6.60	5.64
P2O5	.02	.02
LOI	.23	.23
TOTAL	97.46	98.73
Cu	12	12
Zn	22	72
Ag	1	1
Sn	1	1
Zr	170	140
F	250	150
Sr	40	20
Rb	240	220
W	2	4
Pb	12	30
U	14	280
Th	32	21
Bi	0	0
Mo	1	1
Sb	1	1
Co	1	2
Ni	4	3

ASH FLOWS

	8C5135	8C5136	9C5143	9C5144	13C5180
SiO2	77.20	78.70	76.01	77.90	78.80
TiO2	.07	.10	.33	.31	.11
Al2O3	10.95	12.40	11.45	10.90	12.35
FeOt	3.06	1.06	4.27	3.97	1.24
MnO	.05	.02	.17	.11	.04
MgO	.22	.09	.58	.27	.22
CaO	4.13	.29	.56	.25	.13
Na2O	3.27	2.32	.03	0.00	.14
K2O	.65	5.29	5.34	5.60	6.51
P2O5	.01	0.00	.01	.01	.02
LOI	.75	.65	1.51	1.48	1.54
TOTAL	100.36	100.92	100.26	100.80	101.10
Cu	36	10	11	22	18
Zn	17	20	250	380	22
Ag	0	0	0	2	0
Sn	0	0	8	8	0
F	180	380	320	1400	250
W	0	0	0	0	0
Pb	0	5	5	120	0
U	4	5	4	3	9
Th	14	26	22	29	27

ASH FLOWS

	13C5182	13C5183	13C5185	13C5187	14C5194
SiO2	72.90	81.70	75.90	75.90	68.30
TiO2	.13	.47	.16	.15	.16
Al2O3	14.70	9.90	12.10	12.61	17.50
FeOt	2.18	1.28	.61	1.45	.90
MnO	.02	.04	.01	.02	.03
MgO	.20	.19	.03	.22	.15
CaO	.23	.29	.25	.55	.43
Na2O	.21	.04	.36	3.84	.88
K2O	9.63	5.04	9.06	4.59	11.70
P2O5	.01	.04	.03	.01	.02
LOI	1.21	1.00	.52	.38	.45
TOTAL	101.42	99.99	99.03	99.72	100.52
Cu	10	10	13	9	110
Zn	37	15	21	22	42
Ag	0	0	0	0	0
Sn	3	8	0	8	0
F	170	250	150	980	170
W	0	0	0	0	0
Pb	5	15	20	30	10
U	4	7	7	8	4
Th	28	13	23	43	26

ASH FLOWS

	14C5196	15C5199	15C5203	15C5205	15C5206
SiO2	70.70	76.20	74.20	76.10	77.10
TiO2	.71	.24	.12	.12	.14
Al2O3	14.60	12.20	13.90	13.70	12.40
FeOt	3.35	1.52	1.77	1.52	1.50
MnO	.11	.06	.06	.04	.03
MgO	.50	.33	1.41	.82	.09
CaO	1.00	1.36	.77	.52	.20
Na2O	.03	.63	2.47	2.89	.29
K2O	8.18	6.43	3.24	2.05	8.22
P2O5	.21	.04	.02	.01	.01
LOI	1.19	1.22	1.65	1.18	.60
TOTAL	100.58	100.23	99.61	98.95	100.58
Cu	28	10	6	7	32
Zn	40	18	33	30	22
Ag	0	0	0	0	0
Sn	3	3	3	3	0
F	530	2300	1100	550	210
W	0	0	0	0	20
Pb	20	10	15	10	15
U	6	2	4	7	3
Th	17	22	18	24	25

ASH FLOWS

	16C5207	16C5209	16C5210	19C5224	19C5226
SiO2	73.90	76.60	75.10	73.00	76.30
TiO2	.21	.16	.13	.19	.11
Al2O3	14.90	12.90	13.30	14.70	12.80
FeOt	1.06	1.11	.89	1.38	.96
MnO	.02	.02	.02	.02	.03
MgO	.22	.15	.09	.26	.04
CaO	.96	.34	.20	.68	.62
Na2O	.57	1.41	1.15	.81	2.12
K2O	7.91	7.21	7.81	7.47	6.39
P2O5	.02	0.00	.01	.02	.01
LOI	1.11	.34	.55	1.15	.62
TOTAL	100.88	100.24	99.25	99.68	100.00
Cu	7	11	11	5	6
Zn	5	22	18	19	17
Ag	0	0	0	0	0
Sn	3	0	0	0	0
F	720	330	150	260	620
W	0	0	0	40	20
Pb	30	0	20	0	5
U	13	3	4	18	6
Th	26	30	29	27	25

ASH FLOWS

	19C5228	22C5275	22C5277
SiO2	76.70	77.90	77.80
TiO2	.11	.22	.23
Al2O3	13.30	10.70	10.80
FeOt	1.08	3.23	3.55
MnO	.01	.04	.05
MgO	.14	.15	.12
CaO	.17	.38	.35
Na2O	.34	.73	1.19
K2O	7.44	4.42	4.31
P2O5	.01	0.00	.01
LOI	.79	1.32	1.09
TOTAL	100.09	99.09	99.50
Cu	8	8	8
Zn	10	140	34
Ag	0	0	0
Sn	0	15	10
F	250	190	140
W	0	20	20
Pb	0	205	10
U	5	10	5
Th	27	36	35

ASH FLOWS

	6C5016	6C5018
SiO2	77.20	75.20
TiO2	.11	.16
Al2O3	12.20	13.10
FeOt	1.81	1.98
MnO	.02	.03
MgO	0.00	.07
CaO	.33	1.10
Na2O	4.09	5.09
K2O	4.30	3.30
P2O5	0.00	.01
LOI	1.05	.98
TOTAL	101.11	101.02
Cu	23	35
Zn	36	53
Ag	1	1
Sn	5	3
F	200	320
W	5	5
Pb	15	20
U	14	7
Th	39	39

ASH FLOWS

	8B3314	11B3190	11B3191	11B3192	11B3194
SiO2	70.59	76.76	78.31	77.18	64.53
TiO2	.28	.26	.13	.14	.47
Al2O3	13.29	11.31	11.56	11.67	18.95
FeOt	3.51	3.63	1.58	1.88	3.44
MnO	.02	.08	.02	.03	.02
MgO	.13	.14	.11	.12	.11
CaO	.55	.29	.34	.25	1.25
Na2O	.24	3.14	2.45	1.88	11.06
K2O	11.25	4.36	5.49	6.83	.09
P2O5	.12	.03	.01	0.00	.05
LOI	.85	.64	.59	.58	.27
TOTAL	100.83	100.64	100.59	100.56	100.24
Cu	96	34	26	14	12
Zn	170	180	62	90	21
Ag	1	1	1	1	1
Sn	8	5	3	3	40
F	40	40	50	40	170
W	20	20	20	20	20
Pb	80	190	55	15	5
U	16	4	6	8	9
Th	21	21	21	23	25

ASH FLOWS

	11B3197	1183198	11B3199	11E0101	1283200
SiO2	62.55	77.22	78.70	77.90	80.23
TiO2	.74	.26	.24	.25	.23
Al2O3	18.03	11.09	11.09	10.82	10.27
FeOt	6.51	3.36	3.04	2.75	2.22
MnO	.07	.07	.01	.03	.02
MgO	.56	.15	.29	.05	.09
CaO	1.18	.31	.20	.37	.25
Na2O	10.15	3.77	.02	3.07	5.71
K2O	.10	3.76	6.39	4.25	.05
P2O5	.07	.01	.01	.02	.02
LOI	.52	.65	2.35	.80	.36
TOTAL	100.48	100.65	102.34	100.31	99.45
Cu	15	16	180	54	24
Zn	76	130	3100	220	200
Ag	1	1	1	1	1
Sn	5	3	5	3	20
F	150	60	130	70	50
W	20	20	20	20	20
Pb	5	30	700	120	530
U	13	7	6	11	10
Th	26	19	19	14	18

ASH FLOWS

	12E0102	12E0108	18E0116	18E0117	18E0119
SiO2	79.91	72.74	77.68	80.10	79.51
TiO2	.26	.66	.34	.24	.29
Al2O3	10.82	10.95	10.44	10.11	10.44
FeOt	2.19	4.59	4.77	3.41	3.20
MnO	.03	.08	.02	.01	.02
MgO	.12	1.31	.12	.03	.10
CaO	.22	1.41	.50	.27	.37
Na2O	6.33	.92	5.98	5.67	5.88
K2O	.09	7.26	.09	.10	.10
P2O5	.02	.07	.03	.02	.07
LOI	.42	.92	5.98	1.25	1.32
TOTAL	100.41	100.91	105.95	101.21	101.30
Cu	35	35	60	24	29
Zn	30	190	130	280	180
Ag	1	1	1	1	1
Sn	3	3	80	5	3
F	50	240	50	100	80
W	20	20	20	20	20
Pb	5	70	330	350	50
U	3	15	12	13	13
Th	13	13	12	13	10

ASH FLOWS

	40R1258	40R1260	40R1261	40R1262	40R1266
SiO2	76.00	77.40	77.00	70.00	74.00
TiO2	.33	.16	.17	.20	.33
Al2O3	11.40	12.10	11.80	16.30	11.20
FeOt	2.19	1.76	2.04	1.85	2.44
MnO	.03	.04	.07	.10	.05
MgO	.62	.28	.42	.74	.62
CaO	.81	.48	.24	.67	2.06
Na2O	1.63	5.98	.46	3.93	.71
K2O	6.58	2.11	7.38	4.02	7.67
P2O5	.05	.03	.03	.03	.05
LOI	.70	.31	.93	1.47	1.16
TOTAL	100.34	100.65	100.54	100.31	100.29
Cu	23	17	44	19	15
Zn	65	38	64	62	150
Ag	0	0	0	0	1
Ba	400	140	320	210	650
Au	5	1	1	1	1
Sn	7	3	3	7	1
Zr	320	400	330	560	290
Cr	210	210	140	130	170
F	230	460	300	310	4200
Sr	110	20	20	60	150
Rb	230	70	310	210	210
W	2	3	2	2	6
Pb	31	12	22	10	30
U	0	7	9	38	130

ASH FLOWS

	37R1273	37R1273	37R1276	37R1277	46R1287
SiO2	79.90	79.10	74.00	75.20	70.00
TiO2	.17	.12	.01	.15	.20
Al2O3	11.00	11.00	13.00	13.30	14.80
FeOt	1.94	1.88	1.27	1.51	1.57
MnO	.02	.02	.02	.02	.04
MgO	.24	.37	.27	.29	.45
CaO	.41	.42	.36	.28	.53
Na2O	4.91	6.49	1.24	1.73	1.59
K2O	1.16	.11	9.32	7.37	10.00
P2O5	.02	.02	.01	.01	.04
LOI	.47	.77	.77	.70	.85
TOTAL	100.24	100.30	100.27	100.56	100.07
Cu	17	17	32	9	9
Zn	33	87	120	35	29
Ag	0	0	0	0	4
Ba	100	70	280	240	340
Au	7	8	3	1	4
Sn	5	3	1	1	3
Zr	310	300	160	180	180
Cr	160	150	150	130	110
F	320	860	210	300	420
Sr	20	0	90	50	120
Rb	50	0	280	320	340
W	4	1	7	5	1
Pb	17	20	34	10	39
U	13	13	8	8	130

ASH FLOWS

	36R1302	36R1303	36R1301	42R1330	51R1338
SiO2	75.40	70.70	74.00	75.80	72.80
TiO2	.31	.23	.17	.13	1.77
Al2O3	10.90	15.50	13.70	10.10	12.30
FeOt	3.05	1.71	.95	1.42	1.61
MnO	.05	.04	.02	.04	.03
MgO	.33	.62	.28	.31	.73
CaO	2.41	1.04	.45	1.78	2.59
Na2O	4.22	5.18	3.68	.74	2.60
K2O	1.86	3.97	5.85	7.28	4.56
P2O5	.02	.02	.01	.01	.05
LOI	.85	.93	.70	1.62	1.31
TOTAL	99.40	99.94	99.81	99.23	100.35
Cu	14	4	14	25	10
Zn	41	63	20	120	49
Ag	0	0	0	3	1
Ba	80	250	410	350	520
Au	1	1	1	1	1
Sn	12	5	3	5	140
Zr	670	240	190	120	440
Cr	170	100	140	170	310
F	420	560	240	150	4900
Sr	140	110	70	50	100
Rb	90	250	270	250	240
W	1	3	1	6	10
Pb	4	6	8	73	13
U	5	10	8	12	5

ASH FLOWS

	51R1340	51R1342	51R1344	51R1345	51R1346
SiO2	77.60	73.90	75.70	75.60	78.00
TiO2	.14	.26	.31	.20	.21
Al2O3	11.50	11.80	11.90	11.50	12.40
FeOt	1.21	1.84	1.75	1.24	1.69
MnO	.03	.04	.12	.04	.10
MgO	.41	.34	.43	.48	.55
CaO	.59	1.86	.34	1.34	.39
Na2O	3.77	3.79	1.03	.39	2.49
K2O	4.48	4.88	7.86	8.72	3.66
P2O5	.01	.02	.04	.02	.02
LOI	.77	1.54	.77	1.00	1.16
TOTAL	100.51	100.27	100.25	100.53	100.67
Cu	7	14	20	17	12
Zn	72	63	130	84	75
Ag	0	0	0	0	0
Ba	500	250	490	1500	180
Au	1	1	1	1	1
Sn	5	3	1	1	3
Zr	390	310	150	140	190
Cr	160	150	160	130	160
F	240	350	300	2800	500
Sr	80	30	90	90	50
Rb	180	180	250	360	210
W	9	5	3	3	6
Pb	10	42	15	6	13
U	9	9	7	8	7

ASH FLOWS

	51R1347	51R1348	51R1349	51R1350	52R1351
SiO2	74.20	76.30	77.30	78.10	72.50
TiO2	.14	.15	.15	.31	.16
Al2O3	12.20	12.40	10.90	9.87	13.90
FeOt	3.29	1.90	2.97	3.09	1.04
MnO	.14	.06	.08	.08	.03
MgO	.39	.18	.92	1.10	.29
CaO	3.18	2.81	.57	1.54	.50
Na2O	5.70	6.16	.23	2.83	1.07
K2O	.34	.35	5.12	2.40	9.93
P2O5	.01	.01	.01	.05	.01
LOI	.85	.47	1.54	1.00	.93
TOTAL	100.44	100.79	99.79	100.37	100.36
Cu	19	16	14	12	30
Zn	190	17	74	87	54
Ag	0	0	0	0	0
Ba	80	80	260	360	510
Au	8	1	1	4	1
Sn	12	3	3	3	5
Zr	340	330	360	270	170
Cr	180	200	130	200	130
F	1000	260	340	340	1300
Sr	170	140	60	160	80
Rb	10	20	280	100	330
W	1	4	1	6	5
Pb	23	4	4	18	28
U	7	7	7	7	13

ASH FLOWS

	52R1352	39R1353	39R1354	39R1355	39R1358
SiO2	76.00	80.30	75.90	74.30	76.70
TiO2	.13	.22	.24	.31	.12
Al2O3	11.90	8.75	10.60	11.40	12.10
FeOt	1.30	1.96	2.90	2.37	1.73
MnO	.04	.06	.03	.05	.06
MgO	.16	.33	.20	.29	.25
CaO	.28	.58	.49	.58	2.05
Na2O	.50	.78	.74	.59	5.55
K2O	9.20	5.99	8.08	8.77	1.42
P2O5	.01	.01	.01	.02	.03
LOI	.47	.77	.39	.47	.54
TOTAL	99.99	99.75	99.58	99.15	100.55
Cu	12	130	25	6	11
Zn	45	73	33	120	29
Ag	0	1	0	0	0
Ba	250	210	160	210	60
Au	3	1	5	1	1
Sn	1	1	1	1	5
Zr	140	870	1060	470	370
Cr	150	220	170	170	190
F	510	210	170	230	400
Sr	50	90	50	70	90
Rb	340	250	260	300	50
W	3	3	4	2	9
Pb	13	73	8	6	19
U	9	750	13	18	11

ASH FLOWS

	39R1359	39R1360	39R1361	43R1363	43R1364
SiO2	75.60	74.40	77.80	79.70	69.70
TiO2	.31	.26	.14	.12	.26
Al2O3	10.80	12.30	10.70	9.66	15.60
FeOt	2.02	2.17	1.89	1.21	1.99
MnO	.07	.08	.05	.01	.04
MgO	.78	.34	.50	.15	.24
CaO	.84	3.04	.54	.42	.94
Na2O	1.22	4.29	1.26	.61	7.59
K2O	6.85	2.66	5.98	6.68	2.15
P2O5	.04	.03	.02	.06	.37
LOI	1.00	.62	1.08	.70	.77
TOTAL	99.53	100.19	99.96	99.32	99.65
Cu	25	9	9	20	60
Zn	54	27	39	87	110
Ag	0	0	0	0	1
Ba	570	160	320	200	130
Au	1	1	3	1	10
Sn	1	5	3	1	3
Zr	130	160	310	260	380
Cr	170	180	160	170	140
F	330	650	270	400	490
Sr	150	140	90	40	60
Rb	250	110	220	210	90
W	5	3	1	1	5
Pb	32	13	6	8	160
U	7	8	24	14	160

ASH FLOWS

	51R1401	51R1402	51B1403	49R1451	49R1461
SiO2	75.00	61.00	76.70	74.90	74.80
TiO2	.15	.11	.16	.59	.38
Al2O3	11.70	11.30	9.85	11.30	7.52
FeOt	2.09	3.91	2.02	3.65	4.97
MnO	.07	.11	.03	.10	.12
MgO	.27	.13	.52	1.26	.96
CaO	3.15	13.40	2.51	.63	8.69
Na2O	6.66	5.88	1.29	.38	.04
K2O	.27	.14	5.27	3.39	.23
P2O5	.01	.01	.01	.23	.06
LOI	.47	2.16	.93	2.62	1.70
TOTAL	99.84	98.15	99.29	99.05	99.47
Cu	5	2	389	19	5
Zn	22	32	60	340	170
Ag	0	1	0	0	1
Ba	70	0	140	170	30
Au	1	1	4	2	1
Sn	5	12	3	5	7
Zr	340	270	400	360	170
Cr	160	120	180	150	270
F	1000	41000	1600	1100	2200
Sr	70	20	180	30	450
Rb	0	0	200	230	10
W	4	10	1	4	2
Pb	22	26	64	160	150
U	19	11	6	12	7

ASH FLOWS

	48R1462	38R1488	38R1489	38R1490	38R1495
SiO2	73.30	61.00	63.00	65.20	76.60
TiO2	.32	1.22	.54	.49	.20
Al2O3	12.90	13.20	14.60	13.80	12.20
FeOt	2.43	6.30	6.21	4.82	1.37
MnO	.03	.28	.21	.17	.02
MgO	.46	2.25	3.91	2.15	.16
CaO	2.22	6.01	1.68	3.55	.42
Na2O	5.16	2.07	3.14	3.53	4.04
K2O	2.52	5.55	4.42	4.56	4.96
P2O5	.02	.31	.14	.14	.01
LOI	.62	1.23	2.31	1.31	.47
TOTAL	99.98	99.42	100.16	99.72	100.45
Cu	17	14	13	37	35
Zn	100	580	250	610	140
Ag	0	0	1	1	1
Ba	80	630	1170	860	180
Au	1	1	1	1	1
Sn	7	3	1	3	7
Zr	710	190	90	70	260
Cr	140	140	360	360	180
F	260	2700	830	660	850
Sr	210	200	210	230	30
Rb	90	180	120	160	240
W	1	3	3	2	3
Pb	150	230	23	53	81
U	8	3	4	5	8

ASH FLOWS

	36R1496	36R1497	36R1498	36R1499
SiO2	64.50	71.90	57.70	68.20
TiO2	.71	.35	.88	.67
Al2O3	14.10	11.70	13.50	14.60
FeOt	5.65	3.50	5.84	4.70
MnO	.09	.14	.31	.11
MgO	2.47	.39	1.46	2.15
CaO	2.61	3.47	12.10	1.18
Na2O	4.09	2.47	5.64	1.50
K2O	3.91	4.49	.54	5.03
P2O5	.08	.02	.17	.12
LOI	1.47	1.16	1.08	1.77
TOTAL	99.68	99.59	99.22	100.03
Cu	33	16	4	4
Zn	100	160	94	95
Ag	1	1	1	1
Ba	470	120	60	310
Au	1	1	1	1
Sn	1	3	10	3
Zr	260	1190	480	470
Cr	180	120	150	160
F	2100	340	2100	1800
Sr	270	310	190	70
Rb	140	160	20	160
W	1	1	1	3
Pb	37	220	47	6
U	3	4	3	3

ASH FLOWS

	14C5026	14C5027	14C5028	14C5029	14C5030
SiO2	74.25	72.59	76.72	76.80	76.23
TiO2	.13	.13	.12	.14	.14
Al2O3	13.47	13.26	12.04	12.10	12.74
FeOt	1.28	1.16	1.02	1.19	1.29
MnO	.03	.03	.03	.04	.04
MgO	.25	.15	.20	.18	.14
CaO	.38	1.43	.40	.51	.28
Na2O	2.12	2.84	2.43	2.83	2.76
K2O	7.85	6.68	6.45	6.15	6.69
P2O5	.02	.01	.01	.01	.02
LOI	1.01	1.53	1.59	.77	.67
TOTAL	100.79	99.81	101.01	101.72	101.00

ASH FLOWS

	14C5031	19C5033
SiO2	75.49	76.90
TiO2	.26	.11
Al2O3	11.71	11.90
FeOt	2.78	2.48
MnO	.02	.03
MgO	.04	0.00
CaO	.43	.32
Na2O	2.61	3.38
K2O	5.14	4.83
P2O5	0.00	0.00
LOI	.76	.62
TOTAL	99.24	100.57

ASH FLOWS

	1B3119	1B3120	1B3128	1B3129	1B3130
SiO2	65.75	78.62	80.40	77.73	74.61
TiO2	.33	.25	.30	.39	.36
Al2O3	19.11	11.01	9.27	10.87	11.75
FeOt	1.65	2.01	3.29	3.89	5.56
MnO	.03	.03	.06	.07	.08
MgO	.26	.29	.22	.41	.28
CaO	1.74	1.05	1.29	.50	.37
Na2O	11.00	4.24	5.01	6.00	6.87
K2O	.12	2.44	.12	.09	.07
P2O5	.02	.03	.02	.04	.04
LOI	1.18	.93	.83	.33	.15
TOTAL	101.19	100.90	100.81	100.32	100.14

ASH FLOWS

	1B3132	1B3133	1B3141	1B3168	7B3306
SiO2	79.23	73.16	76.87	80.00	77.57
TiO2	.24	.60	.25	.24	.24
Al2O3	10.29	13.15	9.83	10.34	10.20
FeOt	3.34	4.31	4.12	2.92	2.83
MnO	.06	.05	.12	.07	.03
MgO	.02	.15	.40	.19	.18
CaO	.28	.98	4.14	.38	.37
Na2O	4.49	7.35	3.22	5.83	.09
K2O	2.03	.13	1.03	.05	8.63
P2O5	.01	.12	.02	.05	.02
LOI	1.18	.92	1.14	.48	.92
TOTAL	101.17	100.92	101.14	100.55	101.08

ASH FLOWS

	1B3110	1B3112	1B3114	1B3116	1B3118
SiO2	75.80	81.21	75.53	76.92	77.83
TiO2	.15	.23	.38	.17	.15
Al2O3	12.83	9.43	10.75	10.79	11.74
FeOt	1.52	1.43	2.80	1.36	1.54
MnO	.01	.02	.04	.02	.03
MgO	.16	.33	.72	.21	.11
CaO	.81	2.43	1.36	3.31	.42
Na2O	4.90	4.68	1.29	3.43	3.28
K2O	3.81	.22	7.06	3.86	4.87
P2O5	.01	.02	.05	.01	.01
LOI	.61	1.44	.40	2.41	.52
TOTAL	100.61	101.44	100.39	102.49	100.50

ASH FLOWS

	7B3308	7B3310	8B3314	8B3316	8B3318
SiO2	75.46	77.46	70.59	77.85	71.96
TiO2	.26	.15	.28	.15	.25
Al2O3	11.55	11.55	13.29	11.65	12.32
FeOt	2.23	1.61	3.51	1.86	4.64
MnO	.03	.02	.02	.04	.06
MgO	.34	.06	.13	.15	.48
CaO	1.30	.71	.55	.40	6.24
Na2O	1.48	3.48	.24	3.43	3.89
K2O	7.32	4.86	11.25	4.47	.10
P2O5	.02	0.00	.12	0.00	.03
LOI	1.12	.64	.85	.36	1.22
TOTAL	101.11	100.54	100.83	100.36	101.19

ASH FLOWS

	8B3187	8B3188
SiO2	78.80	77.53
TiO2	.24	.14
Al2O3	10.16	12.05
FeOt	3.08	1.93
MnO	.01	.03
MgO	.12	.09
CaO	.38	.37
Na2O	2.01	3.70
K2O	5.18	4.15
P2O5	.01	0.00
LOI	.55	.50
TOTAL	100.54	100.49

BASALT

	8C5137	10C5151	10C5153	12C5170	12C5173
SiO2	49.35	44.13	50.29	46.74	46.15
TiO2	1.98	2.99	1.92	2.57	2.49
Al2O3	14.97	15.32	14.28	15.71	15.60
FeOt	11.82	14.06	11.25	13.93	13.07
MnO	.27	.28	.26	.42	.22
MgO	6.57	6.90	5.99	6.72	6.53
CaO	8.97	9.19	9.47	8.75	9.95
Na2O	3.23	2.16	3.15	2.55	2.25
K2O	1.05	1.07	.91	.94	.63
P2O5	.27	.86	.30	.47	.46
LOI	1.81	3.15	1.76	2.25	1.65
TOTAL	100.29	100.11	99.58	101.05	99.00
Cu	43	51	67	34	80
Zn	100	170	190	150	82
Ag	0	0	0	0	0
Sn	0	0	0	0	0
F	380	1100	390	1600	530
W	0	0	0	0	0
Pb	30	35	70	20	0
U	1	2	0	0	0
Th	3	2	3	6	0

BASALT

	12C5175	12C5176	14C5191	14C5193	14C5198
SiO2	47.13	48.95	49.55	49.60	49.95
TiO2	3.02	3.33	2.23	2.26	2.20
Al2O3	12.36	13.08	13.65	14.72	14.07
FeOt	15.19	15.58	13.06	12.15	13.08
MnO	.25	.41	.50	.26	.34
MgO	5.60	5.28	6.79	5.84	6.26
CaO	8.99	8.38	7.94	9.36	8.88
Na2O	4.27	3.44	3.16	3.13	3.01
K2O	.20	.89	1.67	1.16	1.07
P2O5	.40	.60	.36	.34	.35
LOI	2.82	.89	1.53	1.42	2.15
TOTAL	100.23	100.83	100.44	100.24	101.36
Cu	110	23	110	95	30
Zn	240	110	190	130	110
Ag	1	0	0	0	0
Sn	0	0	0	0	0
F	710	600	500	400	810
W	0	20	0	0	0
Pb	50	35	115	80	20
U	0	0	0	0	0
Th	5	3	4	0	0

BASALT

	18C5242	18C5244	20C5255	20C5257
SiO2	48.70	49.30	49.00	47.80
TiO2	2.11	2.75	2.09	2.63
Al2O3	13.80	12.80	13.30	14.90
FeOt	13.00	13.60	12.50	14.60
MnO	.31	.26	.25	.27
MgO	6.41	5.65	6.22	6.66
CaO	9.04	10.10	9.14	6.45
Na2O	3.36	3.14	3.39	3.53
K2O	1.23	1.13	1.60	2.18
P2O5	.32	.49	.32	.54
LOI	1.95	1.06	2.42	1.78
TOTAL	100.23	100.28	100.23	101.34
Cu	88	94	86	90
Zn	160	110	76	100
Ag	0	0	0	0
Sn	0	0	0	0
F	1000	1800	960	1900
W	40	0	0	20
Pb	70	90	40	0
U	3	0	0	0
Th	3	2	3	2

BASALT

	1B3138	5B3857	5B3858	5B3864	8B3315
SiO2	50.84	46.00	51.43	46.92	48.64
TiO2	2.10	3.07	1.24	2.77	3.70
Al2O3	15.08	15.18	21.06	16.87	12.77
FeOt	11.54	16.54	8.01	13.62	16.27
MnO	.24	.47	.28	.49	.30
MgO	5.39	6.50	3.19	7.15	4.70
CaO	9.13	8.00	7.66	4.76	8.47
Na2O	3.32	2.05	4.41	2.55	4.25
K2O	2.14	1.80	2.60	4.47	.21
P2O5	.31	.35	.10	.38	.63
LOI	1.60	2.28	3.84	2.69	1.45
TOTAL	101.69	102.24	103.82	102.67	101.39
Cu	28	12	11	17	15
Zn	150	96	190	240	56
Ag	1	1	1	1	1
Sn	5	3	3	3	3
F	60	670	310	1500	60
W	20	20	20	20	20
Pb	90	10	30	10	40
U	29	3	2	2	7
Th	17	1	2	3	20

BASALT

	40R1254	40R1255	46R1283	48R1299	47R1463
SiO2	47.30	48.70	49.80	43.40	46.30
TiO2	2.22	2.12	2.41	.54	2.44
Al2O3	16.30	14.40	15.70	20.30	16.20
FeOt	12.40	11.50	12.60	11.10	12.60
MnO	.32	.18	.21	.29	.29
MgO	6.33	6.11	4.84	1.53	5.16
CaO	5.98	9.96	4.40	17.20	7.72
Na2O	.80	3.13	1.81	1.64	2.06
K2O	3.85	1.03	4.88	.30	2.33
P2O5	.32	.28	.33	.09	.35
LOI	2.77	1.70	1.77	2.31	2.62
TOTAL	98.59	99.11	98.75	98.69	98.09
Cu	11	24	47	5	5
Zn	220	120	200	72	200
Ag	1	0	1	1	0
Ba	570	340	730	30	430
Au	1	2	1	1	1
Sn	3	5	1	12	3
Zr	180	170	240	180	180
Cr	120	300	100	120	90
F	1900	2100	2000	500	2600
Sr	170	330	200	880	240
Rb	140	40	110	10	120
W	8	2	6	2	6
Pb	16	63	65	10	40
U	1	1	1	3	1

BASALT

	19C5037	20C5048	20C5050
SiO2	50.10	55.20	50.90
TiO2	2.18	2.14	3.44
Al2O3	14.70	15.40	12.00
FeOt	12.90	11.90	15.10
MnO	.27	.23	.34
MgO	6.53	4.92	4.78
CaO	8.02	4.52	8.03
Na2O	3.27	4.69	3.70
K2O	1.77	.56	1.10
P2O5	.34	.46	.61
LOI	2.52	3.87	1.08
TOTAL	102.60	103.89	101.08

BASALT

	1B3117	5B3292	6B3300	8B3317
SiO2	50.36	45.91	51.08	50.73
TiO2	2.36	2.51	2.43	3.10
Al2O3	13.23	17.23	12.77	12.14
FeOt	13.89	15.02	12.89	15.96
MnO	.24	.28	.34	.23
MgO	5.30	7.57	5.42	3.46
CaO	8.78	5.75	10.70	6.77
Na2O	3.03	1.54	3.17	2.53
K2O	2.44	3.77	.85	3.50
P2O5	.31	.38	.33	1.52
LOI	2.97	3.25	2.16	1.61
TOTAL	102.91	103.21	102.14	101.55

DIABASE DIKES

	1C5365	1C5368	1C5369	6C5343	13C5321
SiO2	49.00	44.70	44.90	49.10	45.20
TiO2	2.33	3.28	2.50	3.20	2.69
Al2O3	13.10	13.30	14.10	13.40	13.90
FeOt	11.90	14.00	14.40	12.20	13.50
MnO	.51	.32	.55	.55	.57
MgO	5.88	6.02	6.77	4.76	6.74
CaO	6.44	8.25	6.23	7.30	7.52
Na2O	3.87	2.92	3.45	3.74	2.54
K2O	1.60	1.03	1.09	1.53	1.74
P2O5	.29	.57	.36	.61	.39
LOI	2.46	3.00	3.54	1.23	3.08
TOTAL	97.38	97.39	97.89	97.62	97.87
Cu	88	90	13	230	63
Zn	710	270	250	240	570
Ag	1	1	1	1	1
Sn	1	1	1	15	1
Zr	170	270	190	440	220
F	1600	1500	2300	2100	1100
Sr	180	180	170	210	180
Rb	110	70	70	60	120
W	5	5	9	7	3
Pb	450	390	26	140	180
U	1	0	0	2	1
Th	3	1	1	5	1
Bi	1	0	0	1	1
Mo	1	1	1	16	1
Sb	2	1	1	1	1
Co	19	35	28	12	32
Ni	18	34	42	8	35

DIABASE DIKES

	13C5325	13C5326	13C5327	13C5328	13C5331
SiO2	47.00	44.30	47.70	45.60	49.90
TiO2	3.15	2.93	2.27	4.15	2.71
Al2O3	14.50	14.70	14.70	13.40	14.70
FeOt	14.30	13.90	12.00	15.70	12.30
MnO	.71	.49	.32	.47	.48
MgO	6.09	7.04	6.90	4.68	5.77
CaO	6.78	7.92	8.44	6.96	4.95
Na2O	3.21	2.27	2.49	3.77	6.45
K2O	1.37	1.34	1.46	.81	1.02
P2O5	.46	.38	.29	.79	.39
LOI	2.15	2.31	1.92	1.69	2.69
TOTAL	99.72	97.58	98.42	98.02	101.36
Cu	19	72	29	5	4
Zn	210	200	130	120	170
Ag	1	1	1	1	1
Sn	1	3	15	1	1
Zr	80	210	170	270	290
F	1300	1200	640	2100	1800
Sr	230	320	310	180	90
Rb	100	90	100	40	60
W	2	1	1	5	11
Pb	88	120	84	1	1
U	2	1	1	5	1
Th	1	5	5	5	7
Bi	1	14	3	1	0
Mo	1	1	1	1	1
Sb	0	1	1	2	1
Co	25	24	16	20	27
Ni	24	30	19	14	42

DIABASE DIKES

	14C5355	15C5317
SiO2	40.30	46.70
TiO2	3.26	1.83
Al2O3	17.10	16.00
FeOt	15.40	10.40
MnO	.49	.42
MgO	5.36	8.10
CaO	7.64	8.32
Na2O	2.55	2.20
K2O	.93	1.77
P2O5	.61	.32
LOI	4.00	2.92
TOTAL	97.64	98.98
Cu	15	110
Zn	290	430
Ag	1	1
Sn	1	1
Zr	430	150
F	1900	860
Sr	250	260
Rb	30	110
W	8	3
Pb	1	400
U	1	1
Th	4	1
Bi	1	0
Mo	1	1
Sb	1	1
Co	40	32
Ni	34	89

DIABASE DIKES

	8C5131	8C5134	9C5140	9C5145	10C5156
SiO2	48.60	44.94	46.80	48.30	45.90
TiO2	2.05	2.98	2.41	3.58	2.49
Al2O3	14.99	16.93	15.73	12.24	15.30
FeOt	12.43	13.67	13.98	15.08	13.96
MnO	.25	.34	.24	.42	.32
MgO	6.79	6.18	6.81	4.12	7.29
CaO	8.77	6.66	6.17	8.18	7.62
Na2O	3.50	3.41	4.09	2.64	2.06
K2O	.91	.62	.45	1.97	2.31
P2O5	.28	.42	.35	1.42	.37
LOI	3.08	4.33	3.18	2.11	3.11
TOTAL	101.65	100.48	100.21	100.06	100.73
Cu	92	6	17	26	12
Zn	92	270	180	200	200
Ag	0	0	0	0	0
Sn	0	0	160	0	0
F	910	1500	3200	1400	1200
W	0	0	40	0	0
Pb	10	0	0	80	20
U	2	0	0	0	0
Th	4	0	0	3	0

DIABASE DIKES

	11C5158	11C5160	11C5162	11C5165	12C5168
SiO2	49.70	48.16	47.98	47.40	47.36
TiO2	3.15	3.02	2.04	3.71	2.33
Al2O3	13.54	14.14	15.89	12.37	15.36
FeOt	14.14	13.37	12.24	16.39	12.23
MnO	.30	.25	.34	.46	.22
MgO	5.31	4.30	7.00	5.51	7.45
CaO	8.17	5.63	8.14	7.38	8.73
Na2O	2.82	2.37	2.51	3.69	2.73
K2O	1.87	4.94	2.25	.58	1.05
P2O5	.64	.65	.30	.66	.36
LOI	1.86	4.06	1.97	1.35	2.56
TOTAL	101.50	100.89	100.66	99.50	100.38
Cu	32	23	8	40	85
Zn	240	900	120	200	94
Ag	0	0	0	0	0
Sn	0	0	0	3	0
F	920	1700	1100	2200	520
W	20	20	0	0	0
Pb	50	150	75	170	10
U	0	1	0	4	0
Th	6	8	0	27	0

DIABASE DIKES

	12C5178	12C5179	13C5181	13C5184	13C5186
SiO2	46.06	49.30	48.53	44.39	46.94
TiO2	3.92	2.21	2.70	1.77	3.77
Al2O3	12.60	15.09	13.65	16.25	12.52
FeOt	16.34	12.13	13.95	11.79	16.27
MnO	.31	.24	.50	.30	.28
MgO	5.11	6.07	6.71	8.88	4.91
CaO	9.41	9.53	6.76	7.84	8.50
Na2O	3.04	2.98	3.45	2.69	2.31
K2O	.86	.81	1.60	.82	2.32
P2O5	.88	.33	.37	.35	.83
LOI	2.03	.85	2.54	4.38	2.30
TOTAL	100.56	99.54	100.76	99.46	100.95
Cu	48	90	110	84	64
Zn	170	71	270	54	160
Ag	0	0	0	0	0
Sn	0	0	0	0	0
F	1100	460	1600	1100	1400
W	20	20	0	0	20
Pb	50	20	80	105	25
U	0	1	0	0	0
Th	4	2	5	0	6

DIABASE DIKES

	13C5188	14C5195	15C5200	15C5202	15C5204
SiO2	45.70	45.45	47.92	45.99	46.36
TiO2	3.13	3.92	2.90	3.17	2.58
Al2O3	13.46	12.18	13.10	13.96	15.62
FeOt	17.22	16.01	13.90	14.64	13.75
MnO	.55	.36	.35	.49	.45
MgO	7.58	4.60	6.03	6.30	6.29
CaO	6.68	8.52	9.07	8.33	8.94
Na2O	3.26	3.08	3.85	2.96	2.04
K2O	.85	.96	.92	1.13	1.73
P2O5	.47	.93	.52	.59	.39
LOI	2.58	4.26	2.58	2.49	1.89
TOTAL	101.48	100.27	101.14	100.05	100.04
Cu	34	56	20	50	8
Zn	110	250	240	210	110
Ag	0	0	0	0	0
Sn	0	0	3	3	10
F	3800	1400	11000	1200	1400
W	20	20	0	40	0
Pb	30	70	90	50	10
U	0	0	0	0	0
Th	0	4	3	4	2

DIABASE DIKES

	16C5208	16C5215	16C5217	17C5222	19C5225
SiO2	48.07	47.00	43.66	45.40	48.04
TiO2	2.01	2.58	3.17	2.60	2.00
Al2O3	15.40	13.90	15.59	14.90	15.23
FeOt	12.14	14.10	18.42	13.45	12.20
MnO	.43	.39	.60	.38	.55
MgO	7.96	6.58	3.60	7.22	7.81
CaO	8.71	8.28	7.17	8.67	7.93
Na2O	2.60	2.74	3.85	2.24	2.35
K2O	.91	1.18	.95	1.83	1.14
P2O5	.37	.38	.40	.63	.37
LOI	2.08	2.34	1.91	1.93	2.71
TOTAL	100.68	99.47	99.32	99.25	100.33
Cu	94	41	47	32	150
Zn	440	180	220	80	270
Ag	0	0	0	0	0
Sn	0	3	35	0	3
F	750	810	1400	1300	1100
W	0	0	0	0	20
Pb	190	100	35	60	120
U	0	0	0	2	1
Th	0	0	3	4	1

DIABASE DIKES

	19C5227	19C5229	19C5231	19C5234	19C5236
SiO2	49.20	47.70	47.10	44.15	46.30
TiO2	1.85	2.97	2.65	3.49	2.88
Al2O3	16.40	14.30	14.50	14.60	13.40
FeOt	10.85	14.70	14.55	15.70	14.00
MnO	.26	.63	.54	.70	.36
MgO	6.38	6.06	7.02	6.68	5.95
CaO	5.00	7.43	8.56	6.47	8.71
Na2O	4.04	3.19	2.71	3.70	3.44
K2O	1.69	1.01	1.02	.53	1.06
P2O5	.33	.47	.39	.63	.51
LOI	4.65	2.08	1.59	3.45	3.08
TOTAL	100.65	100.54	100.63	100.10	99.69
Cu	20	13	72	18	28
Zn	240	140	110	260	190
Ag	0	0	0	0	0
Sn	0	5	3	3	15
F	3500	1300	1200	2000	3900
W	0	0	0	20	0
Pb	80	15	25	50	45
U	4	0	0	0	0
Th	8	4	0	0	5

DIABASE DIKES

	19C5238	18C5247	20C5253	21C5266	22C5269
SiO2	44.20	48.70	48.50	49.80	39.30
TiO2	1.92	2.09	2.40	2.89	3.42
Al2O3	16.00	15.60	14.80	13.40	15.30
FeOt	11.80	12.40	13.10	12.90	17.80
MnO	.26	.30	.31	.21	.31
MgO	8.61	5.69	6.38	4.76	8.26
CaO	8.13	9.58	7.53	7.24	7.69
Na2O	2.47	2.98	3.32	3.43	1.63
K2O	1.04	.85	1.22	2.49	1.17
P2O5	.36	.32	.60	.62	.53
LOI	4.78	.81	1.48	2.48	4.80
TOTAL	99.57	99.32	99.64	100.22	100.21
Cu	64	99	12	35	36
Zn	280	100	91	140	410
Ag	0	0	0	0	0
Sn	0	0	3	0	0
F	1200	2200	1400	980	1100
W	0	0	0	0	0
Pb	310	55	55	5	0
U	0	0	2	0	0
Th	2	1	2	9	4

DIABASE DIKES

	22C5271	22C5273	22C5276
SiO2	49.50	46.90	50.70
TiO2	1.92	2.54	2.96
Al2O3	14.50	13.60	14.20
FeOt	11.70	13.00	14.70
MnO	.33	.65	.27
MgO	6.77	6.87	3.32
CaO	8.30	7.74	5.90
Na2O	2.59	2.33	4.11
K2O	2.30	2.32	.98
P2O5	.28	.37	1.40
LOI	2.09	3.74	3.58
TOTAL	100.28	100.06	102.12
Cu	80	74	34
Zn	200	800	580
Ag	0	0	0
Sn	0	0	0
F	510	520	1200
W	0	0	20
Pb	90	90	10
U	0	0	0
Th	3	0	9

	1B3890	5C5012
SiO2	48.15	42.60
TiO2	3.35	3.88
Al2O3	13.58	16.20
FeOt	14.81	20.00
MnO	.32	.36
MgO	6.18	7.53
CaO	7.46	4.94
Na2O	3.51	3.52
K2O	1.17	.24
P2O5	.53	.69
LOI	3.35	5.54
TOTAL	102.41	105.50
Cu	56	7
Zn	260	580
Ag	1	2
Sn	3	5
F	830	2300
W	20	5
Pb	130	45
U	2	1
Th	2	6

DIABASE DIKES

	40R1264	37R1279	50R1313	48R1452
SiO2	45.90	48.00	46.20	45.20
TiO2	2.48	2.93	2.60	3.93
Al2O3	16.00	13.10	13.70	15.80
FeOt	13.70	13.80	12.80	15.80
MnO	.40	.54	.33	.63
MgO	5.89	5.81	6.06	2.76
CaO	7.45	7.63	10.30	1.70
Na2O	2.93	3.64	2.66	.21
K2O	1.32	1.21	.80	6.12
P2O5	.29	.55	.35	.56
LOI	2.85	1.39	1.08	5.93
TOTAL	99.21	98.60	96.88	98.64
Cu	3	10	56	43
Zn	240	160	110	600
Ag	1	0	0	0
Ba	350	400	270	570
Au	1	1	1	8
Sn	3	12	1	3
Zr	170	220	210	390
Cr	350	150	140	140
F	4300	2300	530	1600
Sr	220	200	390	10
Rb	70	70	20	230
W	7	9	1	26
Pb	90	62	22	370
U	1	1	8	3

DIABASE DIKES

	12C5038	12C5039	12C5040	16C5042
SiO2	47.70	48.60	42.70	51.40
TiO2	2.24	2.45	4.02	3.68
Al2O3	14.60	16.00	14.00	12.60
FeOt	14.40	14.80	17.60	14.70
MnO	.41	.33	.32	.28
MgO	7.08	5.30	6.68	4.09
CaO	8.28	6.72	10.40	8.48
Na2O	2.93	3.78	2.82	2.34
K2O	2.06	1.66	.69	1.21
P2O5	.31	.37	.84	1.14
LOI	2.93	1.88	7.95	3.34
TOTAL	102.94	101.89	108.02	103.26

DIABASE DIKES

	1B3109	1B3111	1B3113	1B3115	1B3123
SiO2	47.72	48.02	44.97	49.24	49.62
TiO2	2.79	3.43	3.57	2.76	3.13
Al2O3	14.42	13.00	15.60	14.46	12.20
FeOt	14.17	15.23	17.91	13.18	7.85
MnO	.28	.47	.25	.28	.39
MgO	6.44	5.33	7.36	6.33	3.47
CaO	9.44	10.11	5.19	8.56	7.32
Na2O	2.21	2.46	3.37	3.10	2.80
K2O	2.12	1.29	1.03	1.73	2.62
P2O5	.39	.63	.51	.38	1.54
LOI	2.23	1.11	4.51	2.75	2.20
TOTAL	102.21	101.08	104.27	102.77	93.14

DIABASE DIKES

	1B3125	1B3134	1B3140	5B3287	5B3290
SiO2	49.69	48.08	46.67	47.29	49.63
TiO2	3.23	3.43	3.61	2.74	3.50
Al2O3	12.19	12.76	12.88	15.11	12.01
FeOt	16.82	15.20	16.65	14.66	15.62
MnO	.36	.36	.31	.39	.38
MgO	3.53	5.40	5.91	6.70	3.79
CaO	7.19	8.84	8.39	9.41	7.66
Na2O	2.83	3.01	2.85	2.20	2.55
K2O	2.49	2.30	2.09	1.90	3.04
P2O5	1.61	.62	.65	.38	1.78
LOI	1.94	1.67	2.60	1.45	1.75
TOTAL	101.88	101.67	102.61	102.[illegible]	101.71

DIABASE DIKES

	6B3296	6B3304	7B3305	7B3307	7B3309
SiO2	48.23	49.02	48.48	49.99	48.44
TiO2	2.63	3.59	2.35	2.56	3.03
Al2O3	13.90	11.78	13.75	13.81	13.13
FeOt	15.06	16.12	13.58	12.25	15.40
MnO	.37	.42	.31	.18	.27
MgO	6.80	4.14	7.09	5.12	5.43
CaO	8.10	8.03	10.17	10.15	9.08
Na2O	2.57	2.52	2.68	3.10	3.89
K2O	1.93	2.42	1.19	2.45	.63
P2O5	.36	1.91	.34	.38	.65
LOI	2.08	2.29	1.96	3.58	2.72
TOTAL	102.03	102.24	101.90	103.57	102.67

DIABASE DIKES

	7B3311
SiO2	48.63
TiO2	2.22
Al2O3	15.93
FeOt	13.30
MnO	.19
MgO	5.00
CaO	10.20
Na2O	3.15
K2O	.99
P2O5	.34
LOI	2.13
TOTAL	102.08

HIGH-ZR DIKES

	1C5375	13C5333	14C5363	14C5364
SiO2	75.10	76.90	76.10	76.60
TiO2	.20	.21	.21	.21
Al2O3	10.50	10.80	10.70	10.70
FeOt	2.21	2.13	2.10	2.42
MnO	.18	.11	.13	.11
MgO	.02	0.00	0.00	.07
CaO	.65	.56	.77	.59
Na2O	2.78	2.95	3.26	2.00
K2O	4.03	4.36	3.80	5.43
P2O5	0.00	.01	.01	0.00
LOI	1.23	.38	.38	.38
TOTAL	96.90	98.41	97.46	98.51
Cu	19	5	26	7
Zn	180	18	77	33
Ag	0	1	1	1
Sn	3	5	3	3
Zr	1400	1400	1400	1600
F	770	130	240	170
Sr	30	30	10	30
Rb	180	180	160	230
W	2	4	2	2
Pb	45	1	57	9
U	5	8	7	7
Th	19	28	23	28
Bi	0	0	0	0
Mo	1	1	1	1
Sb	0	0	0	0
Co	5	1	0	0
Ni	3	2	2	3

HIGH-ZR DIKES

	6C5345	6C5346
SiO2	64.40	63.90
TiO2	1.09	1.14
Al2O3	12.40	12.70
FeOt	6.02	6.19
MnO	.34	.29
MgO	.90	.90
CaO	2.52	2.26
Na2O	3.87	3.92
K2O	3.43	3.59
P2O5	.32	.33
LOI	2.08	1.77
TOTAL	97.37	96.99
Cu	5	11
Zn	300	470
Ag	1	1
Sn	3	3
Zr	1300	1300
F	650	730
Sr	80	80
Rb	140	150
W	2	1
Pb	3	9
U	4	9
Th	23	18
Bi	0	0
Mo	1	1
Sb	0	0
Co	6	3
Ni	3	3

HIGH-ZR DIKES

	40R1257	40R1263	40R1269	40R1270	46R1294
SiO2	76.30	75.00	76.90	75.60	76.50
TiO2	.27	.24	.14	.22	.23
Al2O3	11.20	11.30	11.20	11.30	11.00
FeOt	2.54	3.14	2.36	1.93	2.22
MnO	.09	.06	.14	.07	.17
MgO	.22	.38	.23	.38	.30
CaO	.55	1.45	.40	1.57	.45
Na2O	3.88	2.84	3.55	3.97	3.70
K2O	4.45	4.66	5.04	3.95	4.58
P2O5	0.00	.01	0.00	0.00	0.00
LOI	.54	.93	.47	1.08	.62
TOTAL	100.04	100.01	100.43	100.07	99.77
Cu	14	6	58	300	58
Zn	82	410	150	140	94
Ag	0	1	1	1	0
Ba	120	170	110	170	70
Au	1	1	1	1	1
Sn	10	5	7	10	10
Zr	1380	1260	1340	1290	1280
Cr	190	170	150	150	140
F	250	350	240	250	240
Sr	20	140	0	110	10
Rb	200	200	220	180	210
W	2	8	3	1	1
Pb	24	96	100	200	34
U	7	9	9	8	9

HIGH-ZR DIKES

	48R1296	42R1329	42R1332	51R1337	51R1339
SiO2	75.40	76.60	76.30	76.00	77.00
TiO2	.23	.23	.23	.24	.24
Al2O3	10.90	10.40	11.10	11.20	10.90
FeOt	2.65	2.70	1.95	2.49	2.35
MnO	.13	.11	.10	.11	.04
MgO	.25	.12	.23	.23	.18
CaO	1.22	.45	.47	.39	.31
Na2O	2.93	3.35	3.56	3.51	3.59
K2O	4.91	4.35	4.82	5.04	4.43
P2O5	0.00	0.00	0.00	.01	0.00
LOI	.85	.85	.62	.77	.85
TOTAL	99.47	99.16	99.38	99.99	99.89
Cu	12	10	10	13	67
Zn	240	190	210	440	230
Ag	0	0	0	0	0
Ba	70	90	100	90	80
Au	1	1	1	1	1
Sn	10	2	1	7	10
Zr	1260	1380	1300	1340	1300
Cr	130	170	170	150	180
F	220	130	180	200	240
Sr	140	30	40	0	0
Rb	190	190	220	220	180
W	1	0	3	0	2
Pb	62	18	220	120	200
U	7	9	8	8	8

HIGH-ZR DIKES

	51R1341	51R1343	39R1356	43R1368	43R1370
SiO2	76.40	76.80	76.40	74.90	75.70
TiO2	.24	.23	.23	.26	.22
Al2O3	11.10	11.20	11.10	11.40	10.90
FeOt	2.38	2.32	2.20	2.93	2.54
MnO	.16	.05	.04	.06	.09
MgO	.23	.24	.09	.21	.17
CaO	.41	.42	.34	1.78	.30
Na2O	3.65	4.21	3.47	3.55	3.06
K2O	4.90	4.27	5.13	3.58	5.45
P2O5	0.00	0.00	0.00	0.00	0.00
LOI	.54	.62	.47	.77	.39
TOTAL	100.01	100.36	99.47	99.44	98.82
Cu	21	8	8	5	22
Zn	710	180	140	56	60
Ag	0	0	0	0	0
Ba	90	60	50	100	70
Au	1	1	3	1	2
Sn	10	7	5	10	7
Zr	1310	1350	1290	1440	1280
Cr	170	160	160	140	140
F	190	200	340	180	210
Sr	20	20	20	130	20
Rb	200	190	220	150	240
W	4	3	6	1	2
Pb	300	19	68	20	18
U	8	8	11	8	8

HIGH-ZR DIKES

	44R1408	44R1416	52R1444	47R1469	47R1470
SiO2	76.70	76.10	75.10	75.70	75.40
TiO2	.23	.23	.25	.24	.23
Al2O3	11.00	11.00	11.60	11.00	11.00
FeOt	2.12	2.31	2.85	2.57	2.41
MnO	.05	.10	.09	.18	.07
MgO	.22	.19	.12	.13	.17
CaO	.56	.51	.37	.41	1.08
Na2O	3.23	3.52	4.30	3.91	3.95
K2O	4.93	4.88	4.14	4.27	4.35
P2O5	0.00	0.00	0.00	0.00	0.00
LOI	.54	.54	.54	.85	.85
TOTAL	99.58	99.38	99.36	99.26	99.51
Cu	51	26	13	120	37
Zn	250	390	28	310	120
Ag	0	0	0	1	0
Ba	90	30	50	40	50
Au	1	1	1	1	3
Sn	7	5	5	5	3
Zr	1310	1350	1410	1410	1290
Cr	170	160	140	160	170
F	270	550	240	210	580
Sr	10	30	0	10	30
Rb	210	220	180	200	190
W	2	4	0	2	3
Pb	180	94	14	210	50
U	9	8	7	0	9

HIGH-ZR DIKES

	47R1471	45R1472	45R1476	45R1485
SiO2	73.20	75.50	75.30	76.80
TiO2	.32	.24	.24	.21
Al2O3	11.70	11.10	10.90	10.90
FeOt	3.11	2.51	2.43	2.31
MnO	.08	.16	.14	.09
MgO	.42	.26	.35	.26
CaO	1.23	.71	.62	.97
Na2O	3.87	3.70	3.59	4.00
K2O	5.24	4.30	4.32	3.45
P2O5	.02	0.00	0.00	0.00
LOI	.62	1.00	.85	.77
TOTAL	99.81	99.48	98.74	99.76
Cu	21	50	6	25
Zn	140	220	560	99
Ag	0	0	0	0
Ba	110	60	50	40
Au	1	1	1	1
Sn	3	5	7	5
Zr	1340	1380	1350	1170
Cr	160	130	150	150
F	520	240	190	250
Sr	40	50	60	90
Rb	240	160	170	140
W	2	4	1	1
Pb	28	23	330	67
U	8	9	8	9

HIGH-ZR DIKES

	40R1253	40R1259	37R1275	16P1[illegible]	43R1204
SiO2	68.80	70.10	70.70	67.10	67.60
TiO2	.47	.44	.41	.55	.56
Al2O3	13.20	13.00	13.00	13.20	13.40
FeOt	4.98	4.15	4.35	5.81	5.90
MnO	.18	.27	.15	.30	.17
MgO	.21	.50	.21	.16	.24
CaO	1.55	1.29	1.14	1.70	1.50
Na2O	4.96	4.19	4.64	4.80	5.02
K2O	4.24	5.00	4.70	4.49	4
P2O5	.03	.02	.02	.05	.05
LOI	1.23	1.23	1.00	1.16	1.31
TOTAL	99.85	100.19	100.37	99.32	100.16
Cu	11	15	9	9	10
Zn	290	180	190	210	190
Ag	0	0	0	0	0
Ba	240	130	110	140	150
Au	1	1	1	4	1
Sn	3	3	5	1	1
Zr	1730	1650	1630	1930	1870
Cr	130	120	130	100	110
F	430	310	240	390	520
Sr	60	70	30	60	30
Rb	110	170	160	110	120
W	4	1	6	1	1
Pb	76	24	24	160	28
U	6	6	5	5	4

HIGH-ZR DIKES

	44R1405	47R1463	38R1487	38R1540
SiO2	69.70	66.60	68.00	69.30
TiO2	.39	.55	.42	.42
Al2O3	12.60	13.20	12.70	12.30
FeOt	4.11	5.77	4.28	4.32
MnO	.20	.23	.21	.21
MgO	.37	.14	.26	.39
CaO	2.46	1.72	2.44	1.45
Na2O	3.53	4.17	4.41	4.54
K2O	4.47	5.45	4.99	4.30
P2O5	.02	.05	.02	.03
LOI	.85	1.16	2.00	1.08
TOTAL	98.70	99.04	99.73	99.10
Cu	34	4	9	8
Zn	70	240	540	97
Ag	0	0	1	1
Ba	120	120	80	120
Au	1	1	1	1
Sn	3	1	1	1
Zr	1470	1940	1600	1640
Cr	110	110	110	100
F	270	450	320	1300
Sr	190	60	0	60
Rb	150	140	170	170
W	2	3	20	9
Pb	34	66	84	11
U	6	5	7	6

GRANOPHYRE

	14C5197	19C5230	19C5232	19C5233	19C5237
SiO2	74.70	76.60	75.45	78.12	77.86
TiO2	.10	.10	.13	.09	.10
Al2O3	13.24	12.55	12.43	11.59	11.82
FeOt	.92	.75	1.51	1.09	1.30
MnO	.03	.02	.03	.03	.04
MgO	.16	.15	.29	.13	.12
CaO	.36	.24	.90	.35	.22
Na2O	.14	.96	.55	.85	.33
K2O	8.36	8.31	8.14	7.63	8.35
P2O5	.02	0.00	.02	.01	.01
LOI	.95	.31	.46	.44	.38
TOTAL	98.98	99.99	99.91	100.33	100.53
Cu	8	10	11	11	15
Zn	14	30	2	19	48
Ag	0	0	0	0	0
Sn	0	0	0	0	0
F	170	420	200	560	130
W	0	0	0	0	0
Pb	0	5	0	0	10
U	3	3	5	9	4
Th	29	28	36	27	25

GRANOPHYRE

	19C5239	19C5241	16C5212	16C5213	16C5214
SiO2	77.14	79.52	76.10	77.75	79.35
TiO2	.09	.09	.10	.10	.10
Al2O3	12.59	11.45	12.85	12.43	12.42
FeOt	.96	.91	1.09	.93	1.37
MnO	.03	.03	.03	.03	.02
MgO	.08	.10	.16	.09	.20
CaO	.33	.17	.22	.36	.17
Na2O	.88	.31	.34	2.46	.26
K2O	8.61	7.99	8.75	5.29	7.32
P2O5	.01	.02	0.00	0.00	.01
LOI	.25	.22	.35	.12	.44
TOTAL	100.97	100.81	99.99	99.52	100.66
Cu	15	22	10	20	10
Zn	28	18	54	34	47
Ag	0	0	0	0	0
Sn	0	0	3	0	0
F	140	130	200	440	220
W	0	0	0	0	0
Pb	10	5	10	30	10
U	5	5	6	5	4
Th	25	23	31	24	25

GRANOPHYRE

	16C5216	16C5218	16C5219	17C5220	11C5167
SiO2	77.90	78.20	76.11	74.03	76.45
TiO2	.10	.09	.16	.11	.10
Al2O3	12.10	12.21	11.21	12.38	12.74
FeOt	.50	.72	2.53	1.47	.74
MnO	.02	.03	.11	.05	.03
MgO	.14	.15	.23	.14	.15
CaO	.21	.24	.45	.26	.38
Na2O	.69	.61	.85	1.19	.49
K2O	8.39	8.66	6.72	8.41	9.20
P2O5	.01	.01	0.00	.01	.01
LOI	.50	.49	.60	.77	.36
TOTAL	100.56	101.41	98.97	99.82	100.63
Cu	10	15	21	11	17
Zn	20	30	120	94	28
Ag	0	0	0	0	0
Sn	0	0	15	0	0
F	220	490	1100	710	1100
W	20	0	0	60	20
Pb	5	10	30	10	10
U	6	5	30	6	8
Th	29	27	99	54	48

GRANOPHYRE

	18C5252	21C5261	21C5262	21C5264	21C5267
SiO2	76.98	73.73	77.00	77.00	75.05
TiO2	.20	.62	.29	.29	.16
Al2O3	13.54	15.22	11.30	10.76	10.65
FeOt	1.45	3.61	2.12	2.54	4.00
MnO	.02	.14	.08	.09	.05
MgO	.49	.52	.06	.15	.07
CaO	.39	.53	.28	.34	1.47
Na2O	.43	.90	.66	1.02	4.28
K2O	5.34	4.10	7.69	6.98	2.91
P2O5	.03	.11	.02	.02	0.00
LOI	1.31	1.81	.42	.69	1.35
TOTAL	100.18	101.29	100.42	100.68	99.99
Cu	5	6	10	44	8
Zn	15	30	36	300	130
Ag	0	0	0	0	0
Sn	3	3	0	0	20
F	660	620	130	190	1700
W	40	20	0	0	0
Pb	0	0	10	55	15
U	5	7	4	1	13
Th	28	23	19	17	50

GRANITE

	13C5335	13C5337	13C5338	13C5339	14C5351
SiO2	77.10	78.80	72.50	73.40	76.10
TiO2	.09	.10	.18	.19	.10
Al2O3	9.81	10.30	11.90	12.50	11.60
FeOt	1.66	1.66	1.26	1.58	1.09
MnO	.13	.12	.12	.13	.12
MgO	.30	.36	.15	.03	0.00
CaO	2.51	1.18	3.69	1.41	.42
Na2O	2.73	3.90	3.26	3.49	3.37
K2O	3.85	1.69	4.37	5.00	4.57
P2O5	.02	.02	.02	.02	.01
LOI	1.69	.77	1.46	1.00	.31
TOTAL	99.89	98.90	98.91	98.75	97.69
Cu	48	9	19	7	9
Zn	45	34	32	44	63
Ag	1	1	1	1	1
Sn	1	3	5	3	3
Zr	120	140	250	230	180
F	240	170	19500	480	210
Sr	70	70	50	10	20
Rb	130	70	230	250	270
W	0	0	1	1	1
Pb	100	8	2	22	23
U	7	5	10	9	7
Th	24	21	41	43	36
Bi	2	0	0	0	7
Mo	1	1	1	1	1
Sb	0	1	0	0	0
Co	5	3	3	2	1
Ni	3	5	3	2	1

GRANITE

	14C5352	14C5353	14C5354	13C5[illegible]4	6C5349
SiO2	78.50	76.30	77.10	79.20	75.90
TiO2	.11	.14	.12	.09	.16
Al2O3	11.20	11.90	10.10	9.78	11.90
FeOt	.67	1.27	1.04	1.49	1.50
MnO	.11	.11	.12	.10	.12
MgO	0.00	0.00	.03	.15	.04
CaO	.58	.69	2.16	1.37	.41
Na2O	3.71	3.48	2.08	2.36	3.31
K2O	3.64	4.66	4.49	3.56	5.11
P2O5	.01	.02	.03	.02	.02
LOI	.38	.46	1.15	.62	.69
TOTAL	98.91	99.03	98.42	98.74	99.16
Cu	22	55	48	5	10
Zn	21	23	86	22	52
Ag	1	1	1	1	1
Sn	3	1	1	1	3
Zr	200	200	160	150	250
F	400	700	400	200	370
Sr	50	30	70	90	10
Rb	200	230	180	150	270
W	1	1	2	2	3
Pb	5	2	2	1	8
U	9	8	11	8	9
Th	37	38	23	21	35
Bi	9	1	11	0	0
Mo	1	1	1	1	1
Sb	0	0	0	1	1
Co	2	2	2	5	1
Ni	2	2	5	3	2

GRANITE

	6C5350	15C5320
SiO2	75.60	74.60
TiO2	.17	.18
Al2O3	12.20	12.60
FeOt	1.50	1.61
MnO	.13	.13
MgO	.07	.03
CaO	.53	.68
Na2O	3.12	3.37
K2O	5.29	5.09
P2O5	.02	.02
LOI	.46	.69
TOTAL	99.09	99.00
Cu	12	16
Zn	31	33
Ag	1	1
Sn	5	3
Zr	200	240
F	1100	1600
Sr	10	20
Rb	300	250
W	3	2
Pb	15	10
U	11	9
Th	39	36
Bi	0	0
Mo	1	1
Sb	0	1
Co	3	3
Ni	3	3

GRANITE

	19C5235	17C5221	17C5223	13C51[illegible]0	20C5259
SiO2	75.85	74.90	74.60	76.80	75.69
TiO2	.08	.21	.24	.12	.19
Al2O3	13.12	11.11	13.00	11.80	11.36
FeOt	1.74	3.94	2.41	2.12	2.62
MnO	.02	.08	.04	.16	.07
MgO	.04	.09	.13	.19	.10
CaO	.50	.42	.51	.74	.55
Na2O	5.31	4.38	4.17	3.14	4.00
K2O	3.56	4.10	4.81	4.72	4.20
P2O5	0.00	0.00	.02	0.00	.01
LOI	.53	.75	.36	.65	.35
TOTAL	100.75	99.98	100.2[illegible]	100.64	99.14
Cu	10	15	13	9	14
Zn	31	72	66	200	69
Ag	0	0	0	0	0
Sn	3	15	20	10	10
F	1200	1800	750	860	1600
W	0	0	0	0	0
Pb	10	25	30	20	20
U	8	9	9	8	8
Th	29	34	28	33	44

GRANITE

	21C5263	21C5265
SiO2	75.96	75.39
TiO2	.18	.17
Al2O3	11.47	11.02
FeOt	2.75	3.88
MnO	.03	.03
MgO	.08	.04
CaO	.37	.94
Na2O	3.74	3.02
K2O	4.28	3.91
P2O5	0.00	0.00
LOI	.83	1.15
TOTAL	99.69	99.55
Cu	11	18
Zn	240	110
Ag	0	0
Sn	15	20
F	640	2300
W	0	0
Pb	10	15
U	9	35
Th	27	100

GRANITE

	8C5005	8C5006	8C5007	?C5001	?C5002
SiO2	76.98	75.22	75.50	75.27	75.35
TiO2	.20	.20	.20	.14	.20
Al2O3	12.10	12.94	12.75	12.41	12.72
FeOt	1.36	1.77	1.50	1.87	1.68
MnO	.02	.04	.02	.04	.03
MgO	.20	.12	.25	.04	.17
CaO	.42	.38	1.17	.33	.61
Na2O	3.07	3.71	3.03	3.92	3.66
K2O	4.82	5.07	5.18	4.50	4.99
P2O5	.02	.02	.01	0.00	.02
LOI	.77	.71	1.54	1.54	1.95
TOTAL	99.96	100.18	101.15	100.06	101.38
Cu	25	18	9	13	22
Zn	230	47	23	35	41
Ag	1	1	1	1	1
Sn	3	3	8	3	5
F	180	260	240	180	250
W	5	5	5	5	5
Pb	2	5	2	10	10
U	7	6	7	5	5
Th	35	42	49	27	100

GRANITE

	9C5003	9C5004	5C5010	5C5011	5C5013
SiO2	74.70	74.75	76.81	74.11	74.65
TiO2	.20	.20	.08	.22	.19
Al2O3	12.69	12.14	11.89	13.19	13.01
FeOt	1.44	1.09	1.45	1.82	1.74
MnO	.02	.02	.02	.03	.03
MgO	.15	.08	.09	.15	.22
CaO	.47	.41	1.14	1.01	.51
Na2O	3.70	3.63	3.24	3.40	3.71
K2O	5.05	4.83	4.36	5.28	4.67
P2O5	.01	.02	.01	.02	.01
LOI	1.25	1.02	1.08	1.19	.58
TOTAL	99.68	98.19	100.17	100.42	99.32
Cu	13	31	19	9	11
Zn	45	12600	40	47	34
Ag	1	3	1	1	1
Sn	3	5	3	3	3
F	300	260	350	320	170
W	5	5	5	5	5
Pb	5	285	30	5	5
U	3	21	14	8	8
Th	40	43	260	56	37

GRANITE

	5C5014	6C5019
SiO2	75.25	76.29
TiO2	.18	.03
Al2O3	12.92	12.85
FeOt	1.72	1.24
MnO	.03	.02
MgO	.15	.08
CaO	.32	.47
Na2O	3.71	3.75
K2O	5.11	4.83
P2O5	.01	.01
LOI	.81	.77
TOTAL	100.21	100.34
Cu	11	10
Zn	40	28
Ag	1	4
Sn	3	3
F	230	680
W	5	5
Pb	10	5
U	7	8
Th	32	37

GRANITE

	50R1315	49R1430	38R1495
SiO2	75.50	76.50	76.60
TiO2	.19	.17	.20
Al2O3	12.10	12.40	12.20
FeOt	1.46	1.27	1.37
MnO	.02	.02	.02
MgO	.15	.11	.16
CaO	.55	.50	.42
Na2O	3.80	3.83	4.04
K2O	5.38	5.21	4.96
P2O5	.01	.01	.01
LOI	.54	.47	.47
TOTAL	99.70	100.49	100.45
Cu	7	7	20
Zn	42	27	140
Ag	1	0	1
Ba	90	80	180
Au	1	1	1
Sn	1	3	7
Zr	190	200	260
Cr	180	160	180
F	1000	1400	850
Sr	10	0	30
Rb	280	180	240
W	6	4	3
Pb	16	13	81
U	11	11	8

GRANITE

	13C5055	14C5025	7C5024	5C5015	7C5023
SiO2	75.83	76.80	74.21	74.38	73.67
TiO2	.12	.13	.21	.20	.21
Al2O3	11.84	12.24	13.04	13.11	12.82
FeOt	1.12	1.01	1.67	1.61	1.80
MnO	.02	.02	.03	.02	.05
MgO	.09	.04	.18	.18	.17
CaO	.17	.41	.43	.30	.46
Na2O	3.31	3.51	3.87	3.62	3.53
K2O	4.78	4.60	5.23	5.10	5.19
P2O5	.01	0.00	.02	.01	.02
LOI	.58	.38	1.31	1.42	.85
TOTAL	97.87	99.14	100.20	100.75	98.77

GRANITE

	16C5044
SiO2	75.42
TiO2	.20
Al2O3	12.34
FeOt	1.63
MnO	.03
MgO	.18
CaO	.79
Na2O	3.20
K2O	4.92
P2O5	.02
LOI	.68
TOTAL	99.41

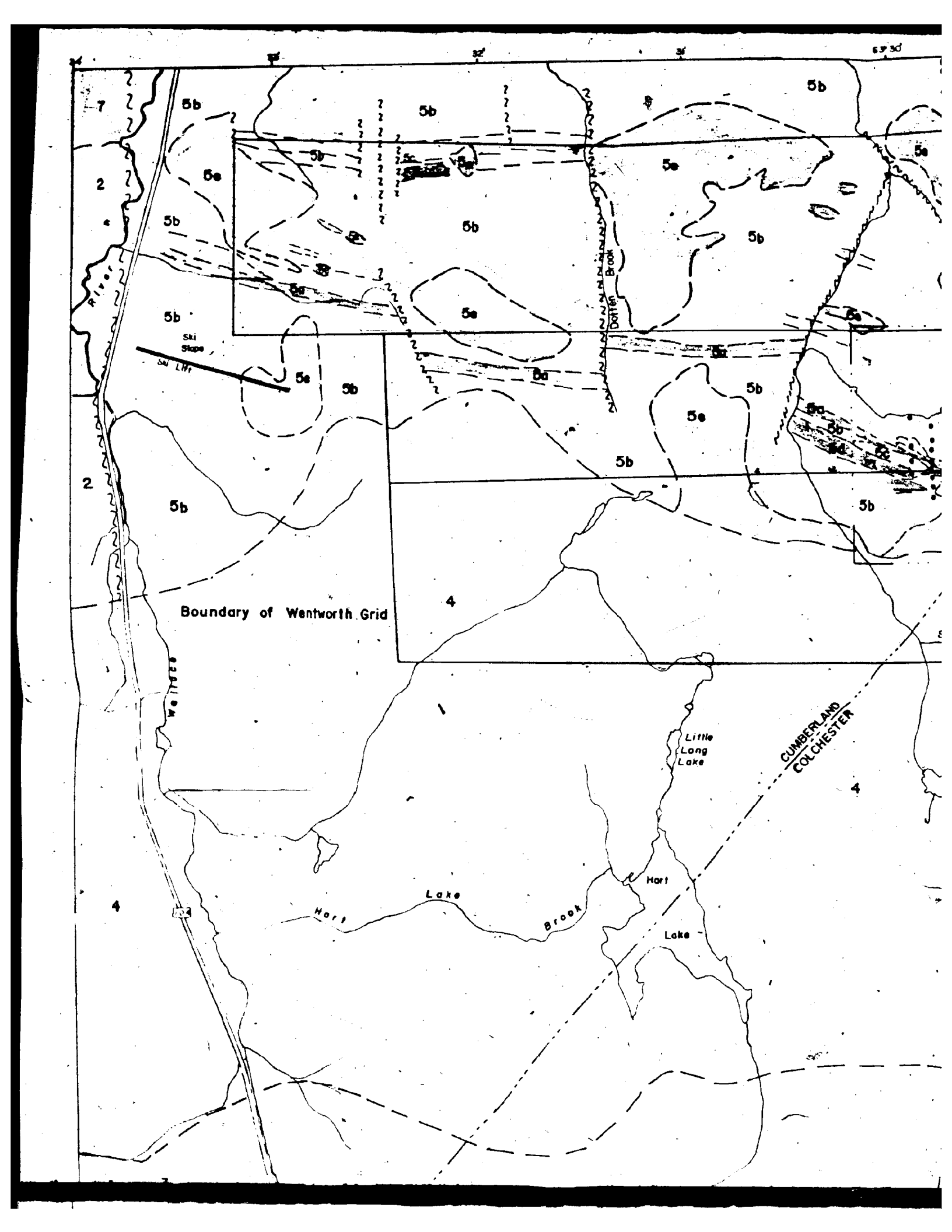
5b
5e
5a
2
4
Ski Slope
Ski Lift
Dorten Brook
Boundary of Wentworth Grid
Little Long Lake
CUMBERLAND
COLCHESTER
Hart Lake Brook
Hart Lake

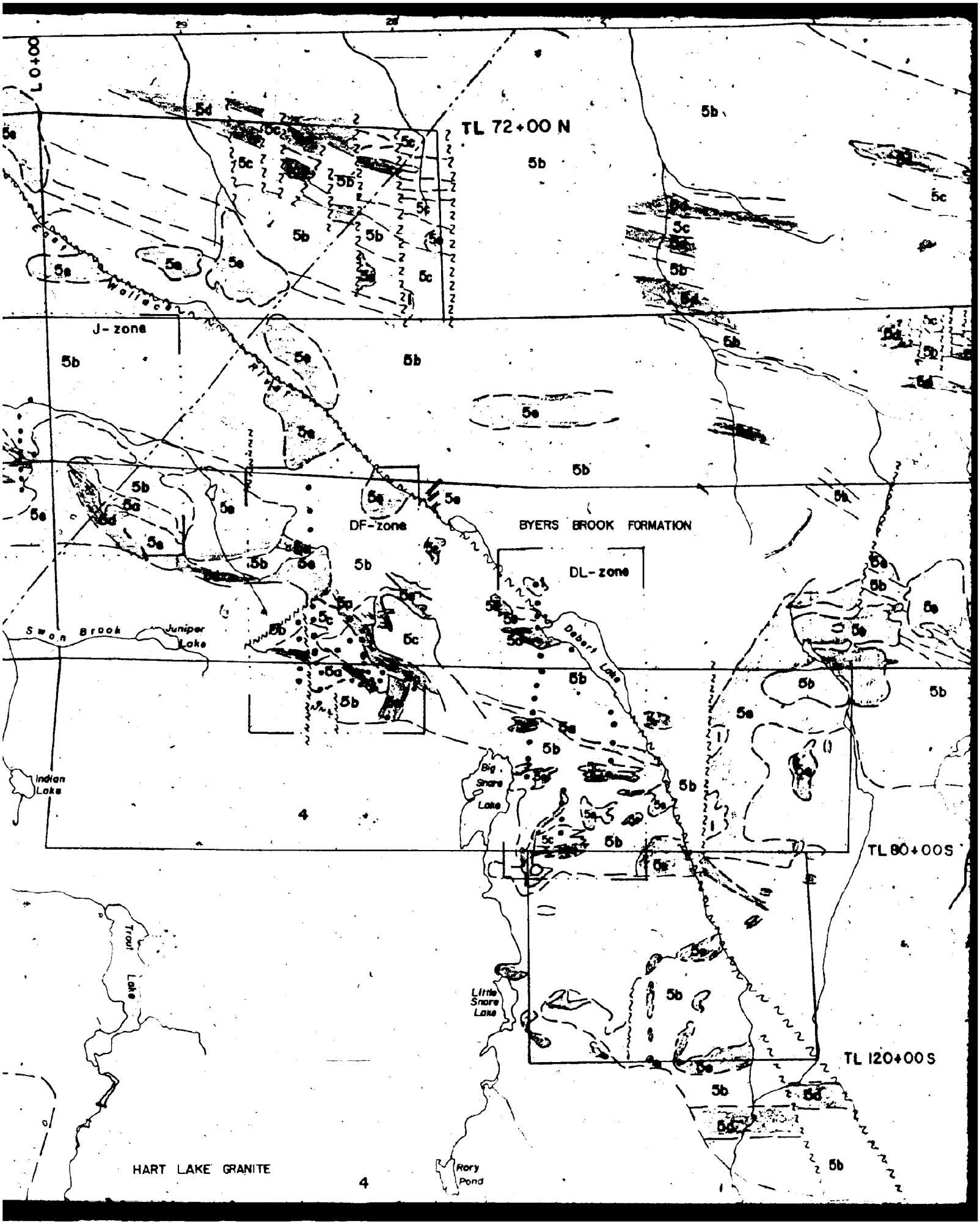
TL 72+00 N
TL 80+00S
TL 120+00S
J-zone
DF-zone
DL-zone
BYERS BROOK FORMATION
HART LAKE GRANITE
Swan Brook
Juniper Lake
Indian Lake
Big Snare Lake
Little Snare Lake
Trout Lake
Rory Pond
Dabert Lake
5b
5c
5d
5e
4

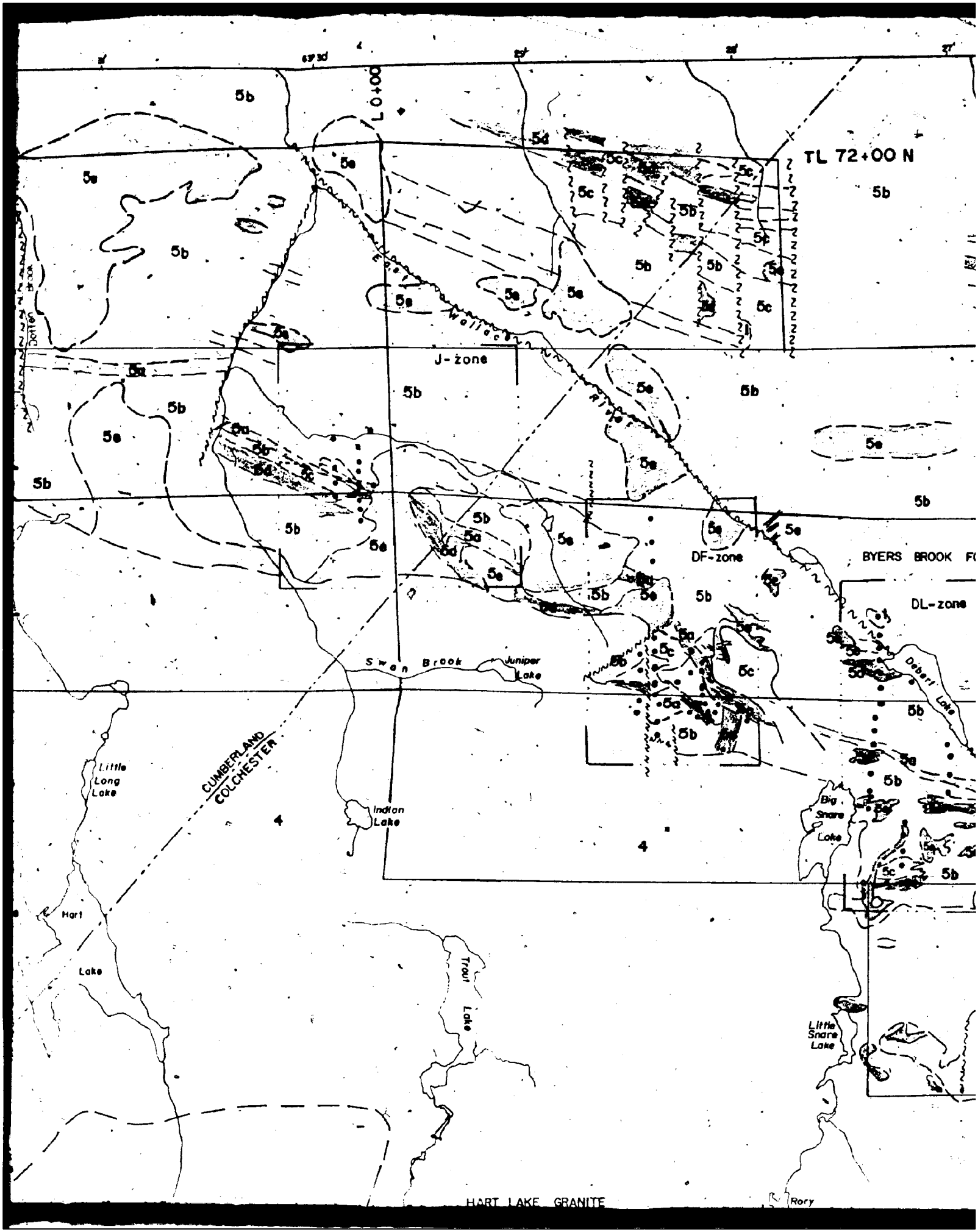
TL 72+00 N
L 0+00
J-zone
DF-zone
DL-zone
BYERS BROOK FO
Wallace
Swan Brook
Juniper Lake
CUMBERLAND
COLCHESTER
Little Long Lake
Indian Lake
Hart Lake
Trout Lake
Big Snare Lake
Little Snare Lake
Debert Lake
HART LAKE GRANITE
Rory
5a
5b
5c
5d
5e
4

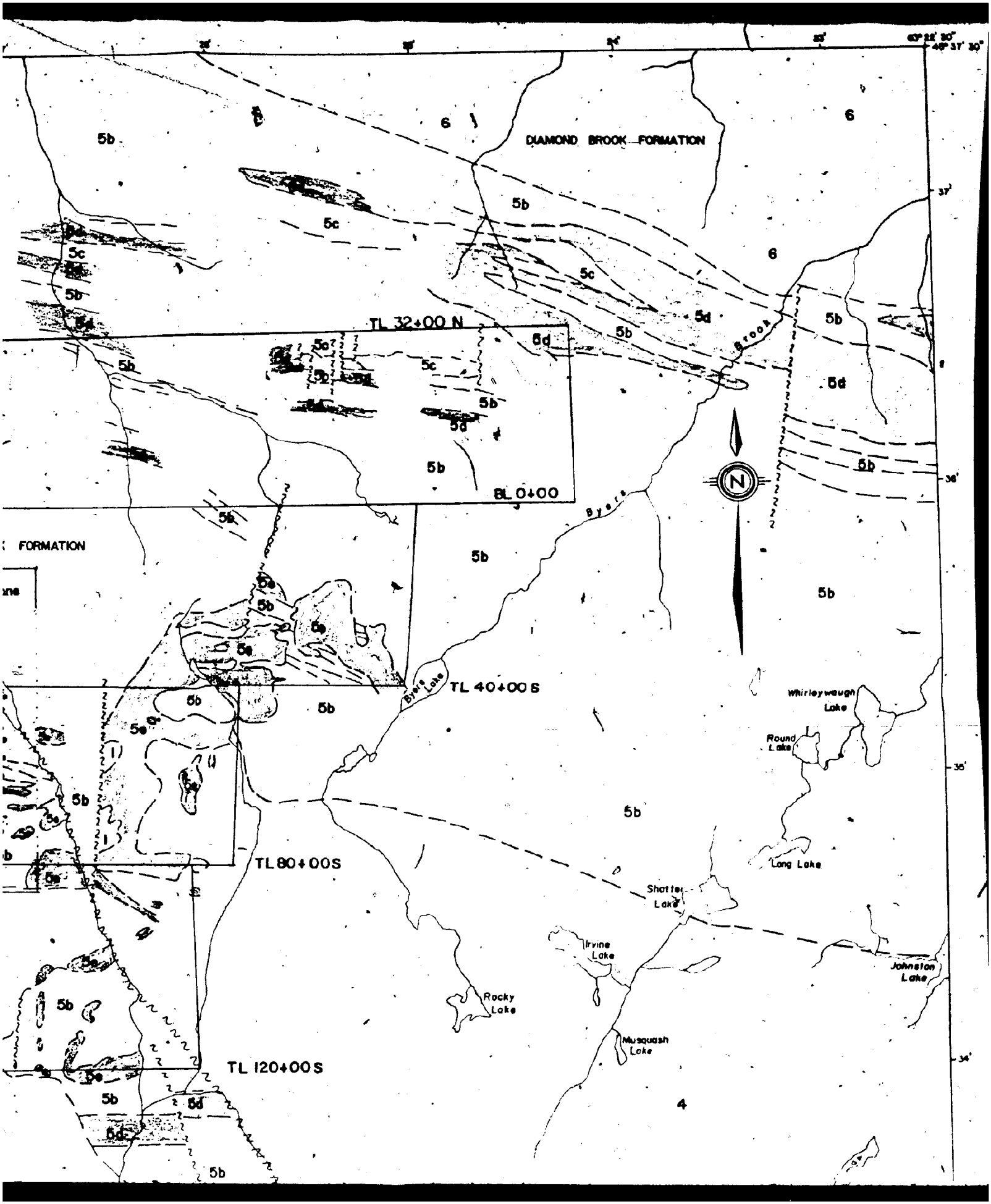
DIAMOND BROOK FORMATION
TL 32+00 N
BL 0+00
TL 40+00 S
TL 80+00 S
TL 120+00 S
Byers Lake
Whirleywaugh Lake
Round Lake
Long Lake
Shatter Lake
Irvine Lake
Johnston Lake
Rocky Lake
Musquash Lake
5b
5c
5d
6
4

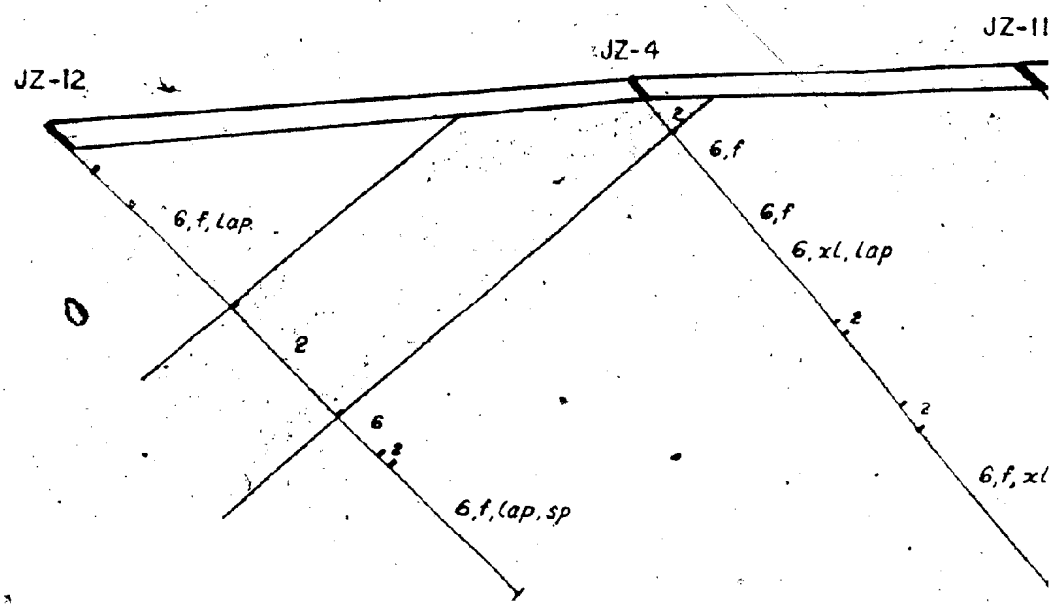

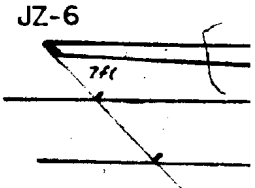

STRATIFIED ROCKS

Basalt flows

(7) Rhyolite flows, flow banded or massive

ABBREVIATIONS

xl – phenocrysts
ly – lythophysae
fl – flow banding

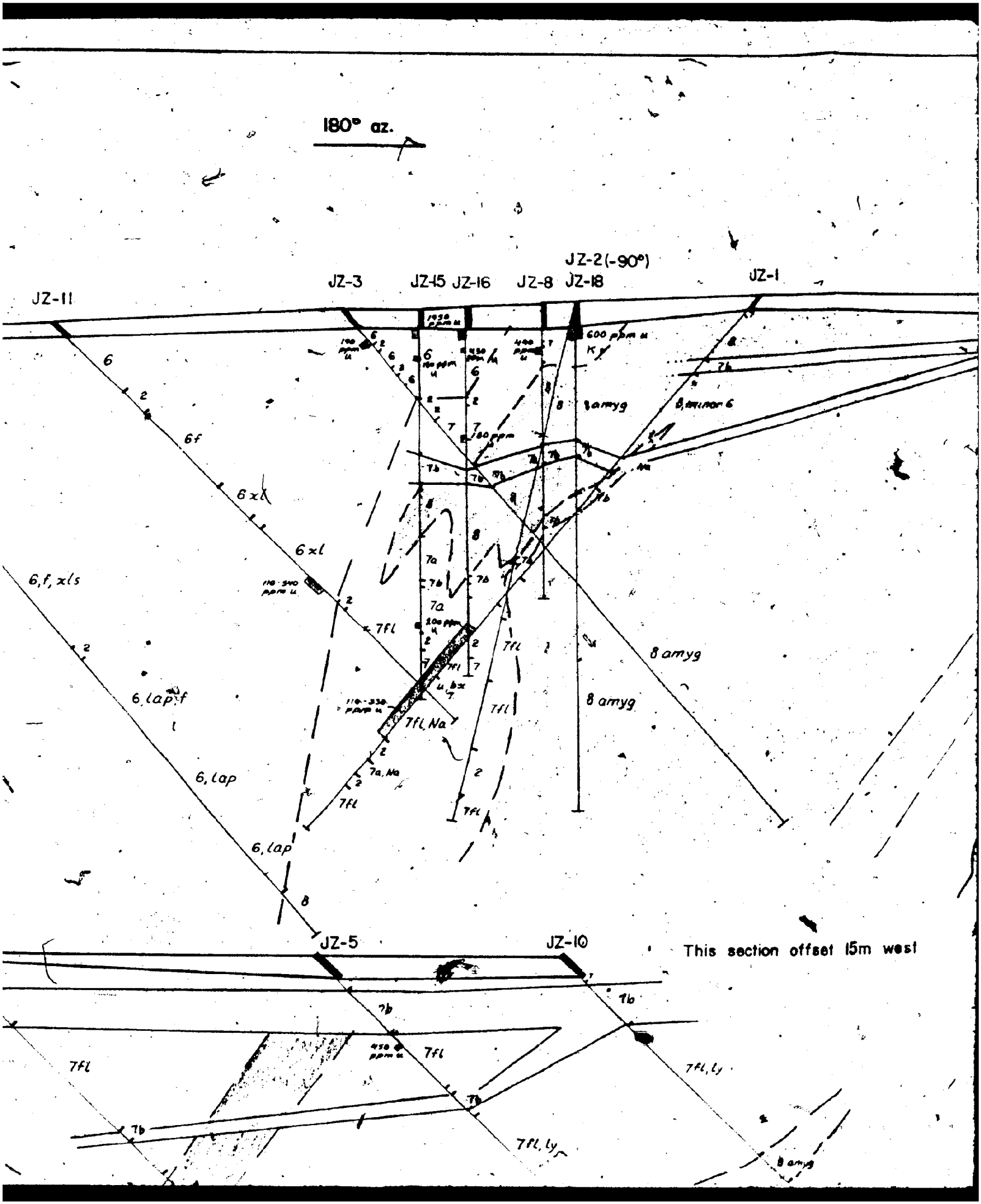
180° az.
JZ-2(-90°)
JZ-11
JZ-3
JZ-15
JZ-16
JZ-8
JZ-18
JZ-1
JZ-5
JZ-10
This section offset 15m west
6
6f
6xl
6,f,xls
6,lap,f
6,lap
8
8 amyg
7fl
7fl,Na
7a,Na
7a
7b
7fl,ly
u,bx

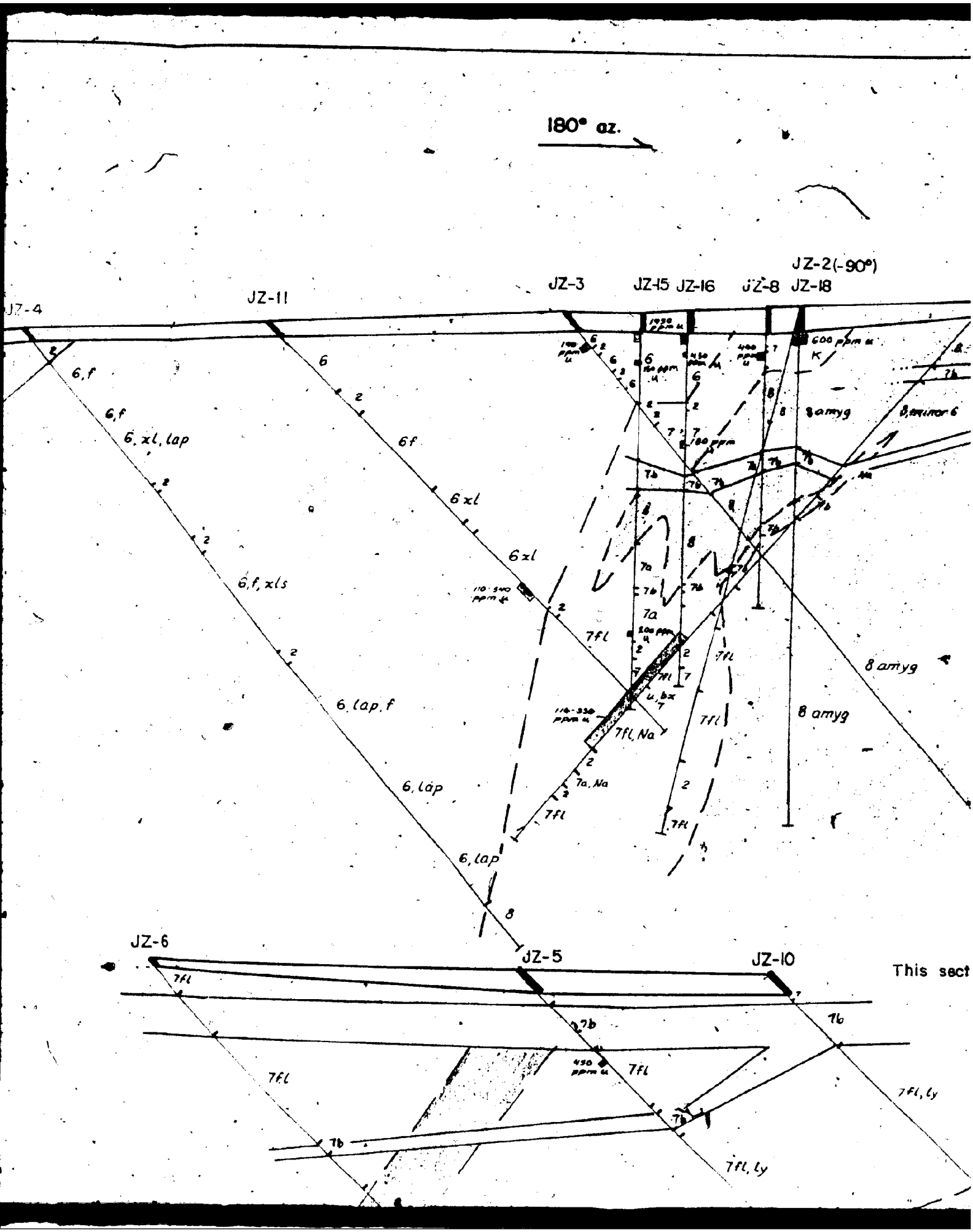
180° az.
JZ-2(-90°)
JZ-3
JZ-15
JZ-16
JZ-8
JZ-18
JZ-4
JZ-11
6, f
6, f
6, xl, lap
6
6f
6 xl
6 xl
6, f, xls
6, lap, f
6, lap
6, lap
8
8 amyg
8 amyg
8, minor 6
7fl
7fl, Na
7a, Na
7a
7b
7fl, ly
7fl, ly
JZ-6
JZ-5
JZ-10
This sect

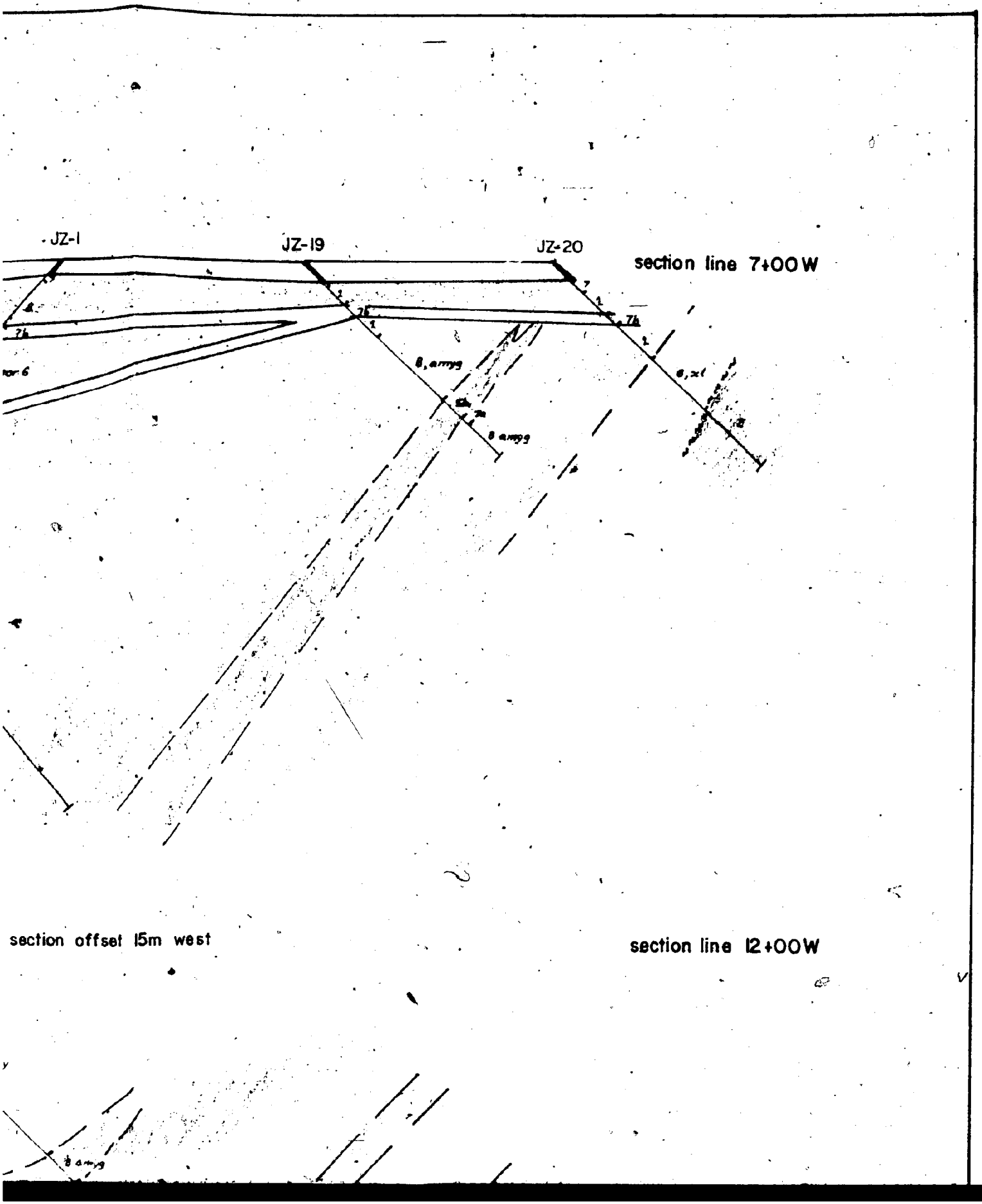
JZ-1
JZ-19
JZ-20
section line 7+00W
section offset 15m west
section line 12+00W

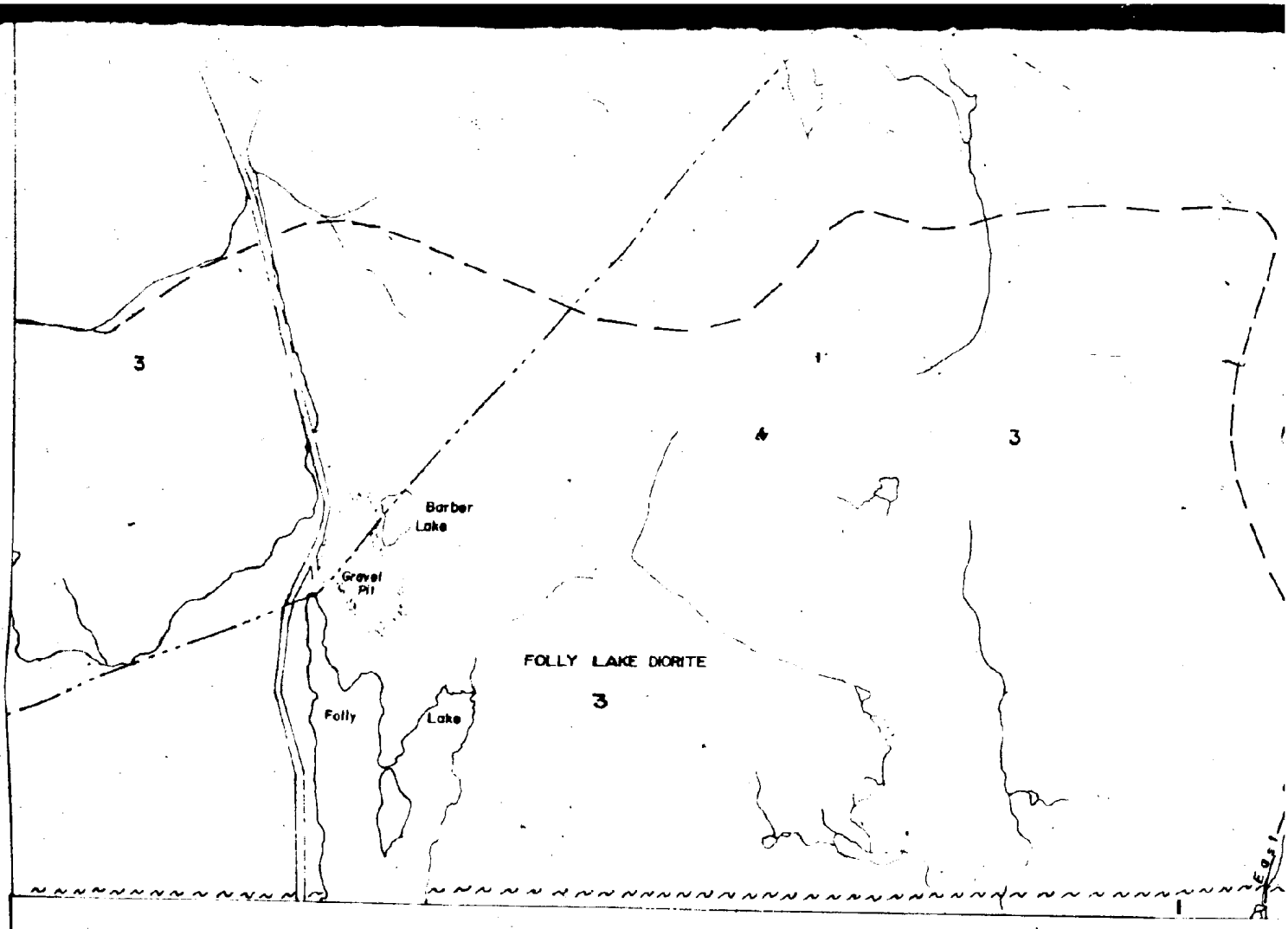

GE(

STRATIFIED ROCKS

7	Boss Point Formation Carboniferous sandstone
6 5d	Fountain Lake Group (Diamond Brook and Byers Brook Formations) Basalt Flows; 5d - Byers Brook Formation; 6 - Diamond Brook Formation
5c	Rhyolite Flows and Domes
5b	Undivided Byers Brook Formation, dominantly ash flows and tuffs with minor lahar and sedimentary horizons
5a	Polymictic Conglomerate - Lacustrine Sediments (marker horizon)
2	Wilson Brook Formation Silurian Siltstone, shale, felsic volcanic rocks
1	Boss River Complex (Folly River Schist) Pre - Hadrynian

Devono - Carboniferous

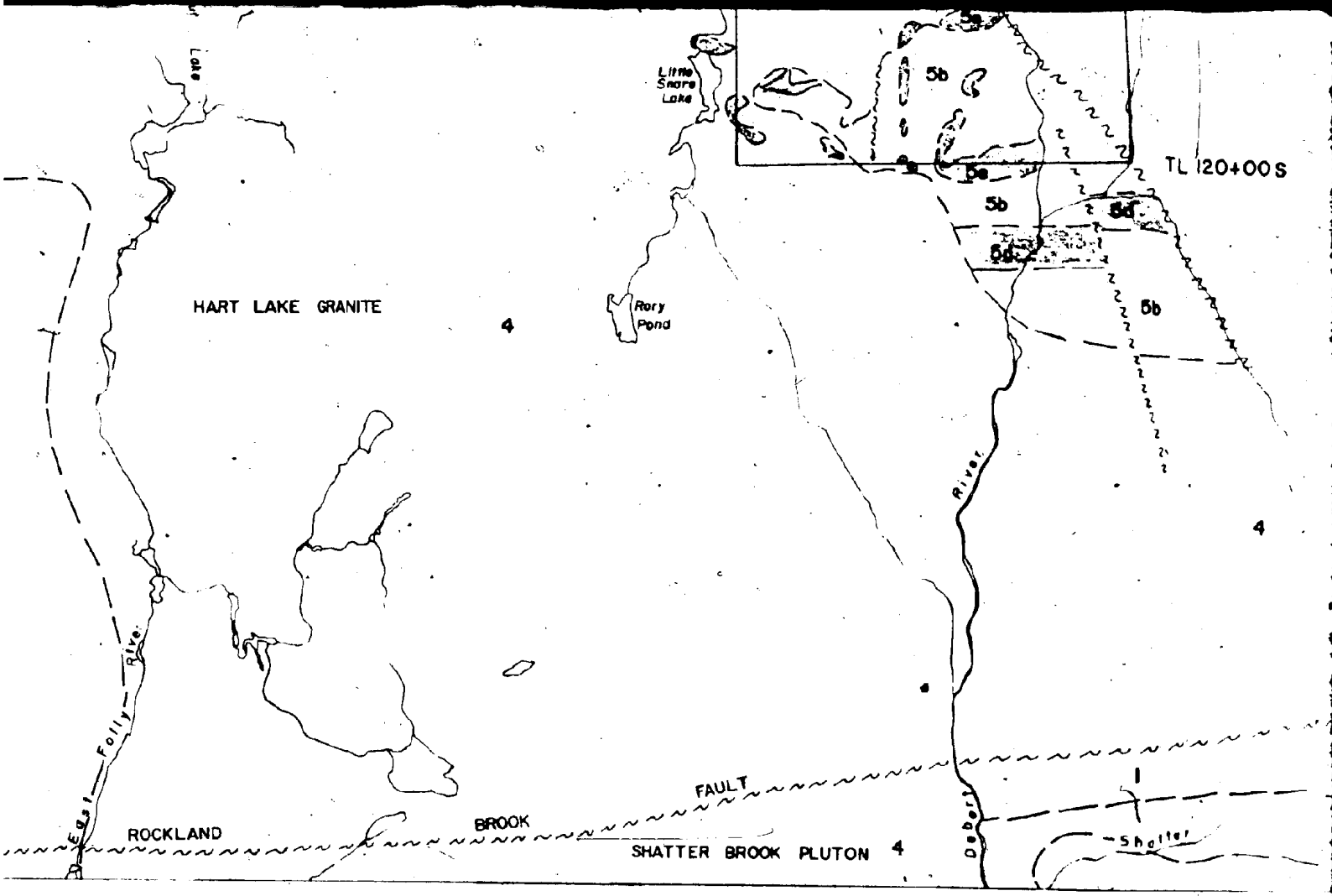

GEOLOGICAL COMPILATION, COBEQUID HIGHLANDS, WENTWORTH AREA, NOVA SCOTIA

PLUTONIC ROCKS

Carboniferous	5a	Fountain Lake Group Fine Grain Mafic Dikes, Sills, Feeders
	4	Hart Lake Granite, Shatter Brook and Gain Brook Plutons
	3	Folly Lake Diorite

Scale - 1:25000

0 0.5 1.0

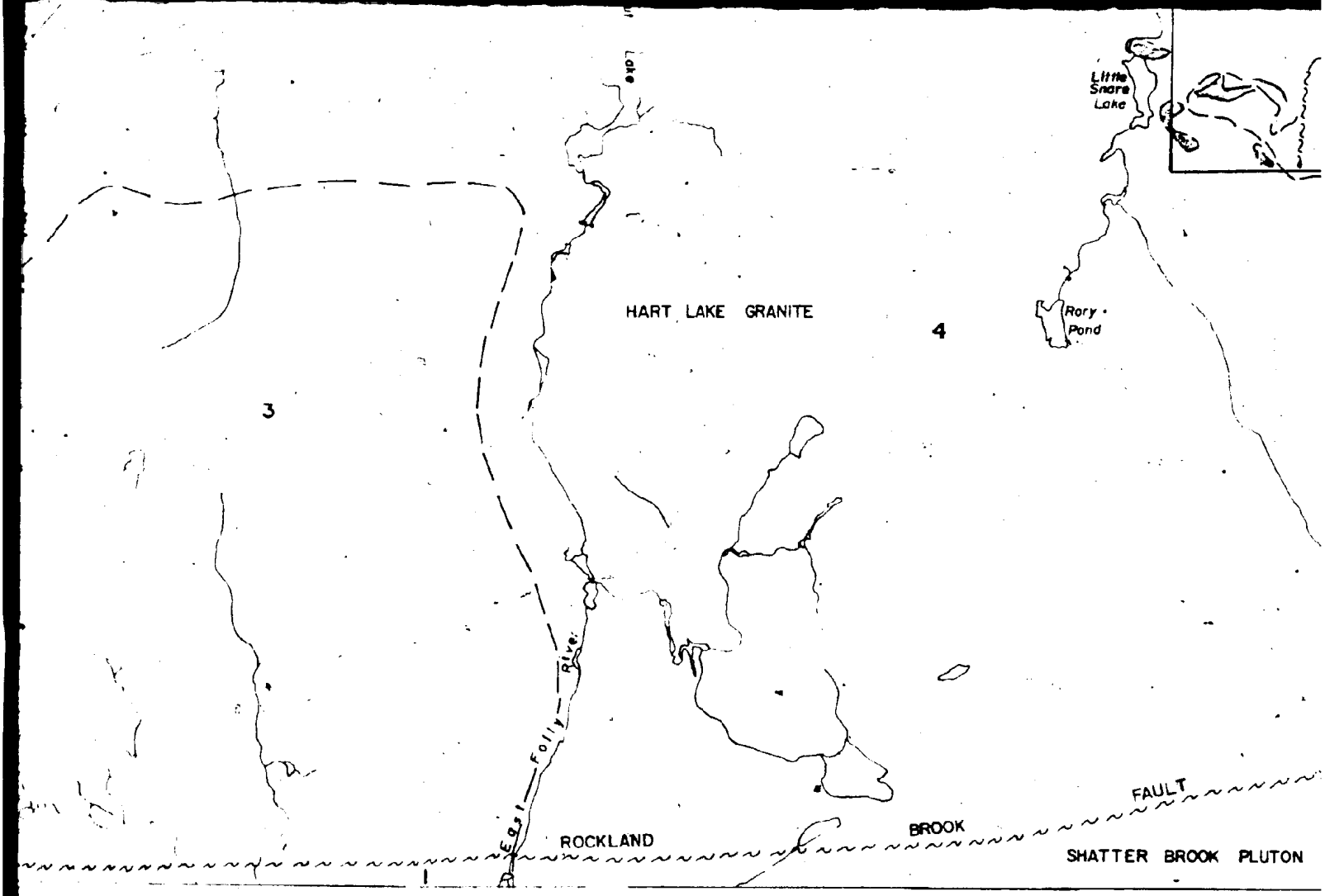

GEOLOGICAL COMPILATION, COBEQUID HIGHLANDS, WENT

PLUTONIC ROCKS

d Byers Brook Formations)
tion'; 6- Diamond Brook

nantly ash flows and tuffs
zons

Sediments (marker horizon)

c rocks

t)

Devono-Carboniferous

5e	Fountain Lake Group Fine Grain Mafic Dikes, Sills, Feeders
4	Hart Lake Granite, Shatter Brook and Gain Brook Pluton
3	Folly Lake Diorite

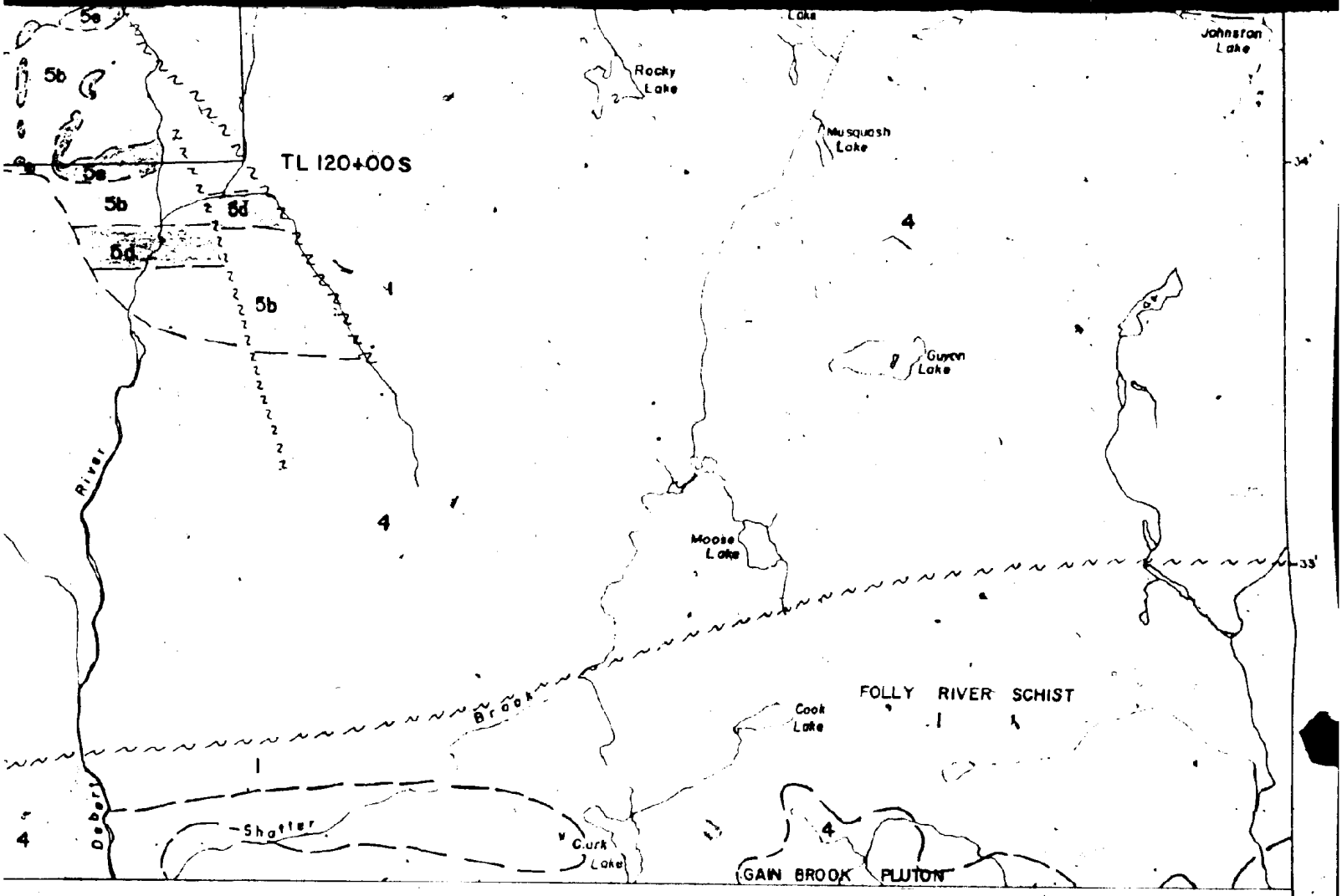

'WORTH AREA, NOVA SCOTIA

Geological Contact

Fault

Diamond Drill Hole

Scale- 1:25000

0 0.5 1.0 1.5 2.0 km.

FIGURE 4

6, f, lap, sp

JZ-6

7fl

STRATIFIED ROCKS

- Basalt flows
- (7) Rhyolite flows, flow banded or massive, commonly with spherulites and lithophysae
  (7b) Porphyritic rhyolite, >25% phenocrysts
- 6 — Rhyolite ash flows and tuffs
- (5a) Laminated siltstone, reworked ash (lacustrine)
  (5b) Conglomerate

INTRUSIVE ROCKS

- 4 — High-Zr rhyolite dikes
- High-Zr composite dikes
- Diabase dikes
- f — Granite

ABBREVIATIONS

xl – phenocrysts
ly – lythophysae
fl – flow banding
sp – spherulitic
bx – brecciated
lap – lapilli
f – fiamme
amyg – amygduloidal
lam – laminar bedding
agglom – agglomerate
f.g. – fine grained

F – fluorite
ep – epidote
Ca – calcite veins
Q – quartz veins
Mt – magnetite veins
U – uranium
ga – galena
Sn – cassiterite
REE – rare earth elements
W – tungsten
Th – thorium

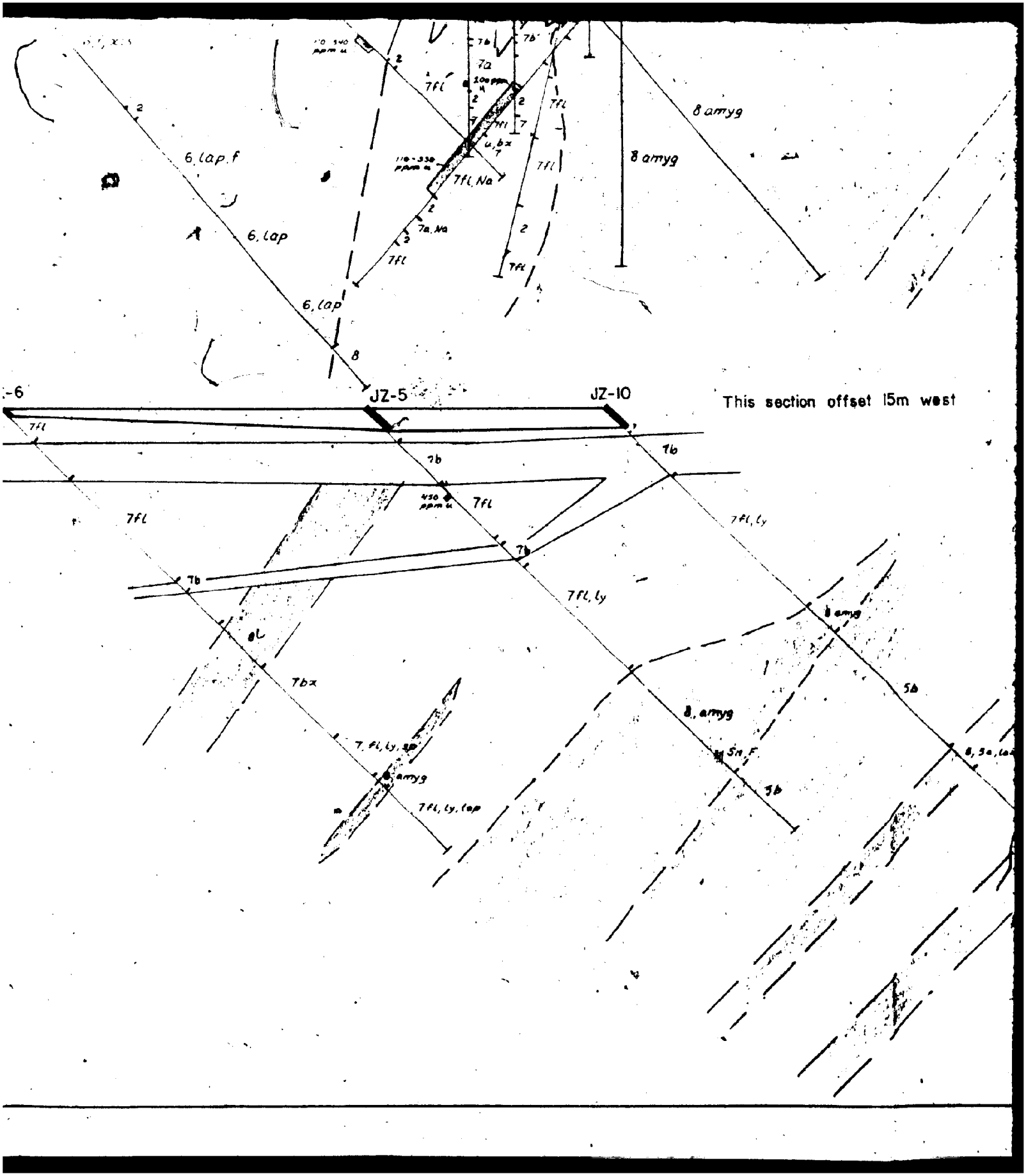
JZ-5
JZ-10
This section offset 15m west
6, lap, f
6, lap
8 amyg
7fl, Na
7a, Na
7fl
7b
7a
7fl, ly
7b x
8, amyg
5b
5n, F
7, fl, ly, lap
7fl, ly, lap

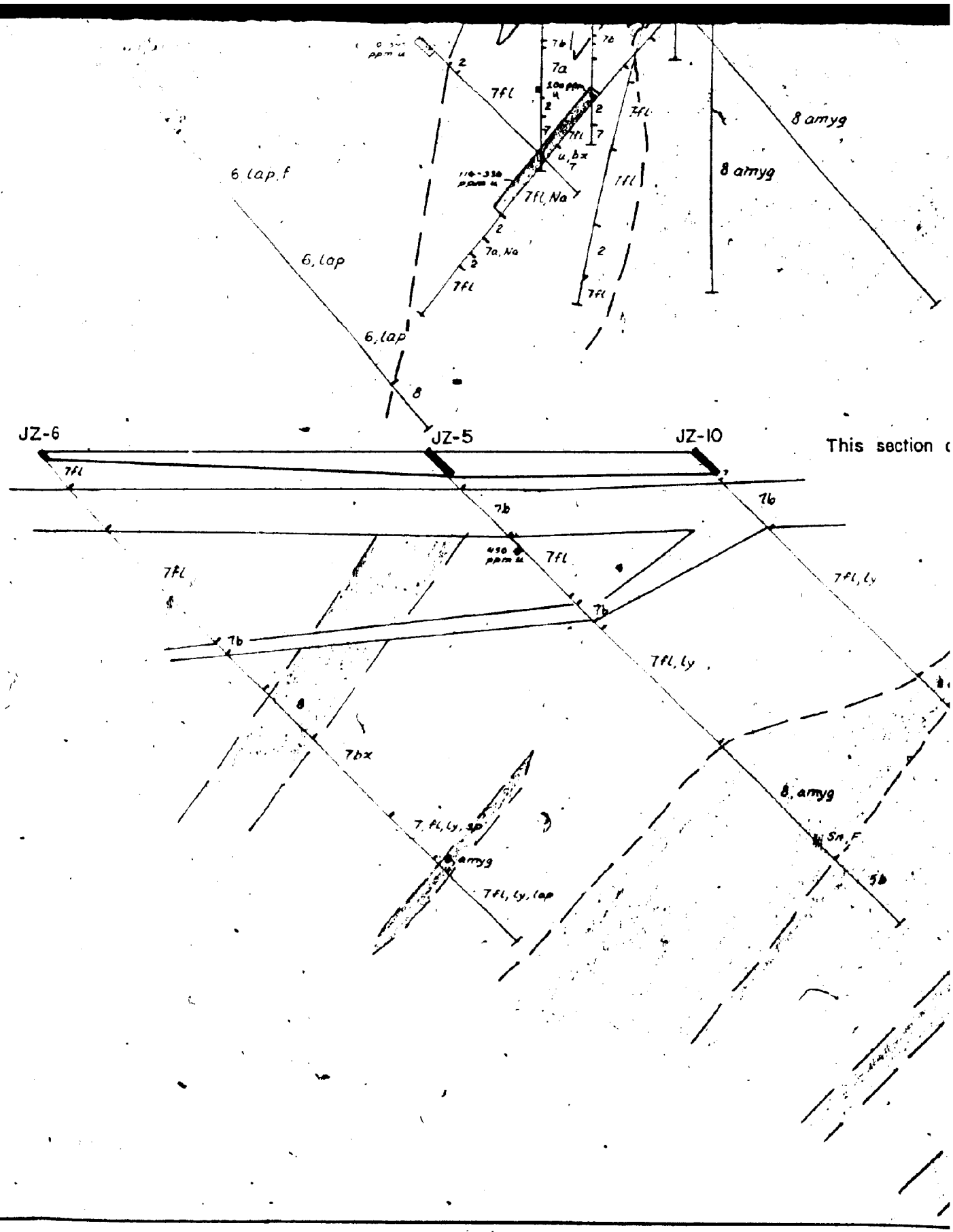

This section

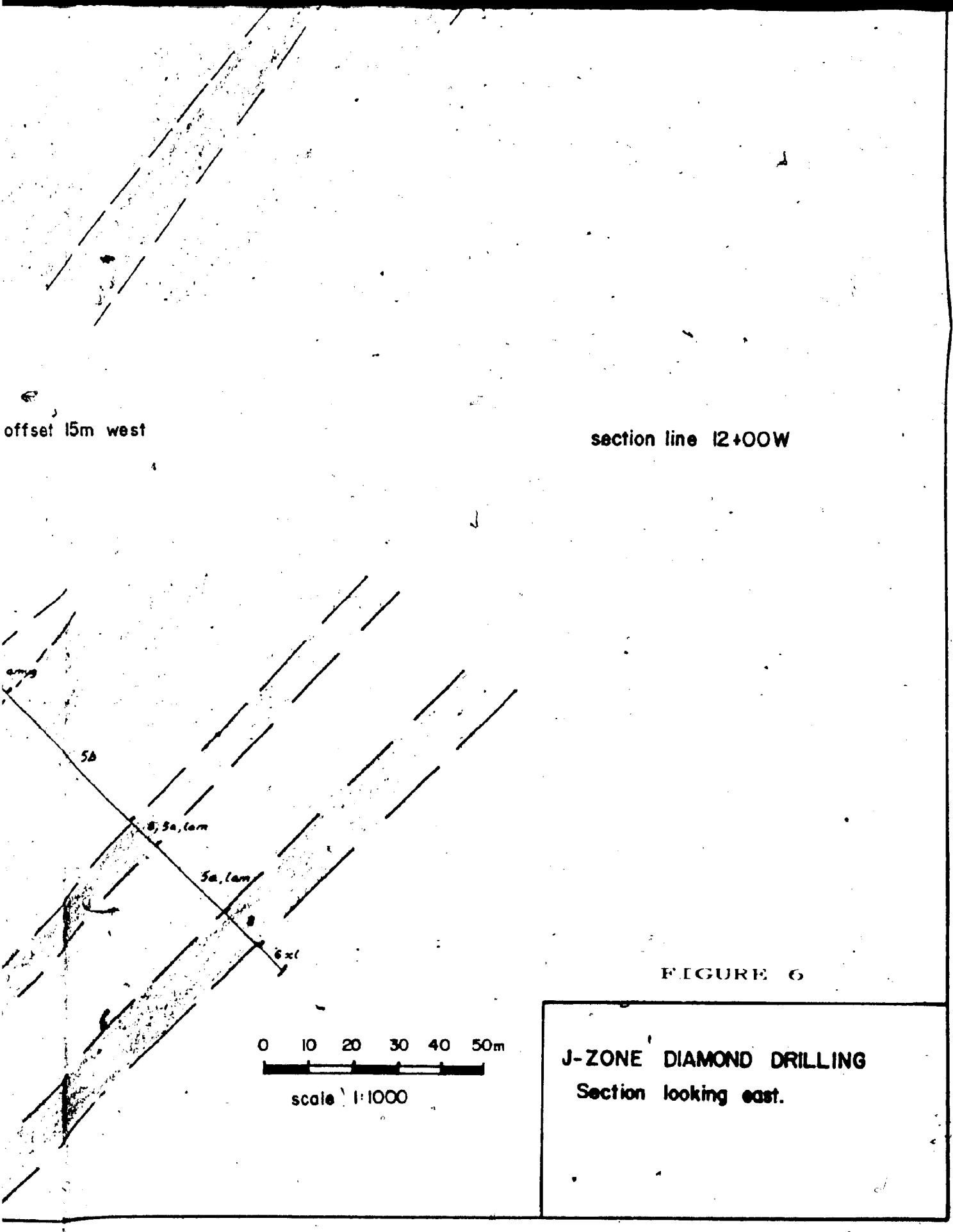

FIGURE 6

J-ZONE DIAMOND DRILLING
Section looking east.

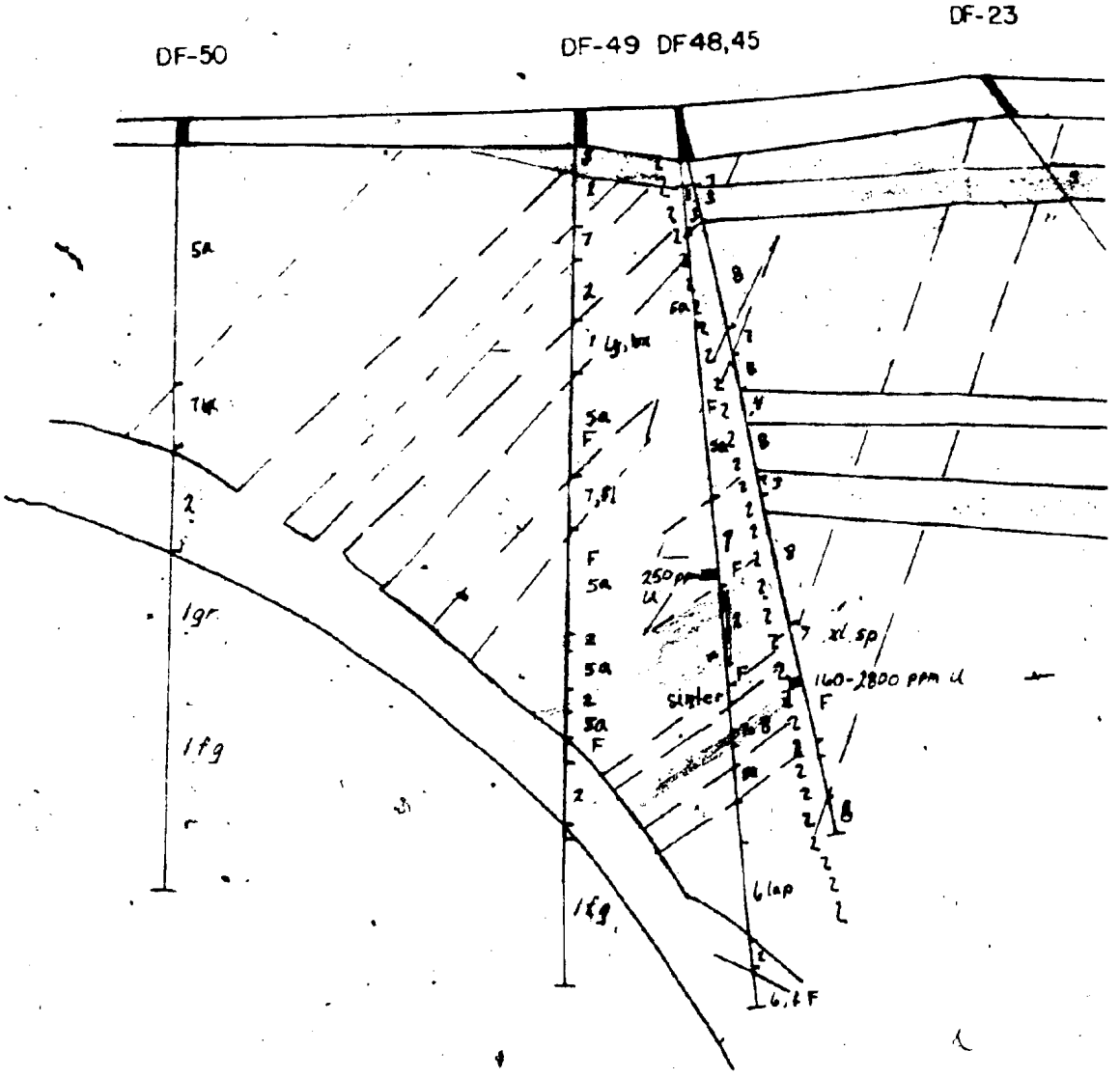
DF-50
DF-49 DF48,45
DF-23
5a
Tgl
1gr
1fg
1 Ly, lm
5a
F
7,8l
F
5a
250 ppm
U
2
5a
2
5a
F
2
1fg
sitter
xl sp
160-2800 ppm U
F
6lap
6,8 F

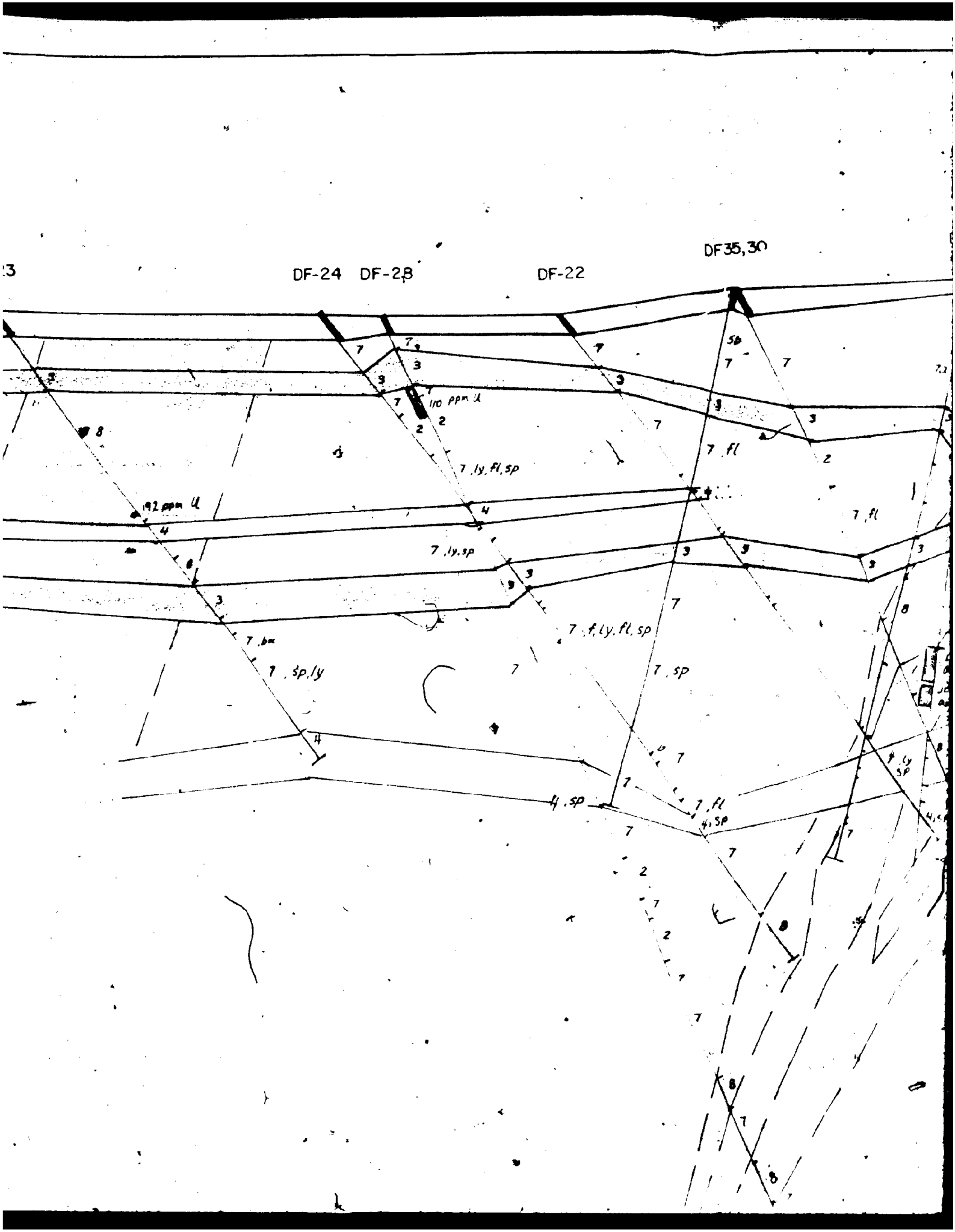
:3
DF-24
DF-28
DF-22
DF35,30
110 ppm U
192 ppm U
7, ly, fl, sp
7, ly, sp
7, f, ly, fl, sp
7, sp, ly
7, sp
4, sp
7, fl
7, fl
7, bm

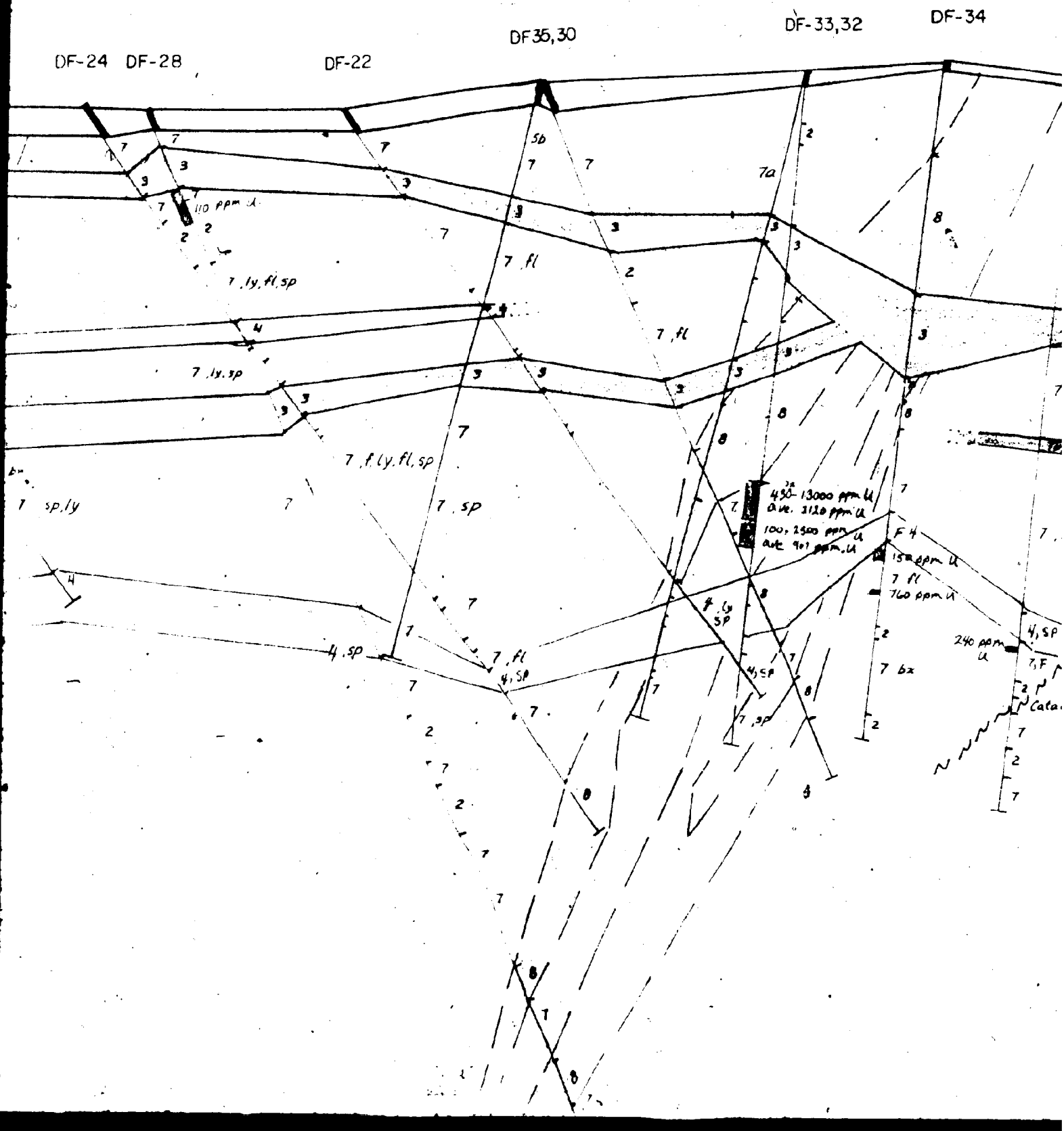
DF-24
DF-28
DF-22
DF35,30
DF-33,32
DF-34
110 ppm U
7, ly, fl, sp
7, ly, sp
7, fl
7, fl, ly, fl, sp
7, sp, ly
7, sp
4, sp
7, fl
4, SP
4, ly SP
4, SP
7, sp
450-13000 ppm U
Ave. 3120 ppm U
100, 2500 ppm U
Ave. 901 ppm U
150 ppm U
7 fl
760 ppm U
240 ppm U
4, SP
7, F
7 bx
Cata

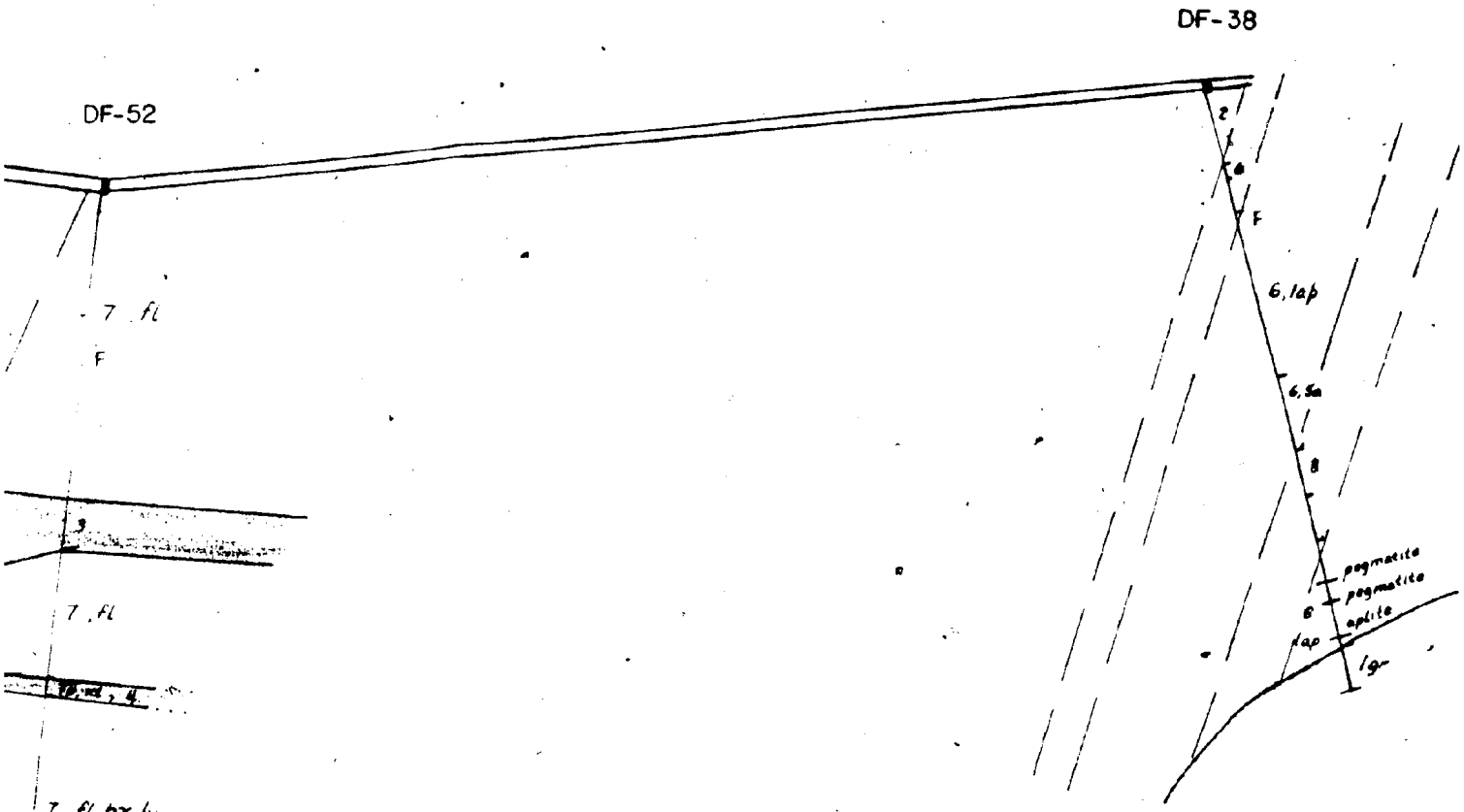
DF-38
DF-52
2
F
6, lap
6, Sa
8
pegmatite
pegmatite
aplite
lap
lgr
7, fl
F
3
7, fl
7, fl, bx, ly
4, SP
7, F
2
Cataclastite
7
2
7

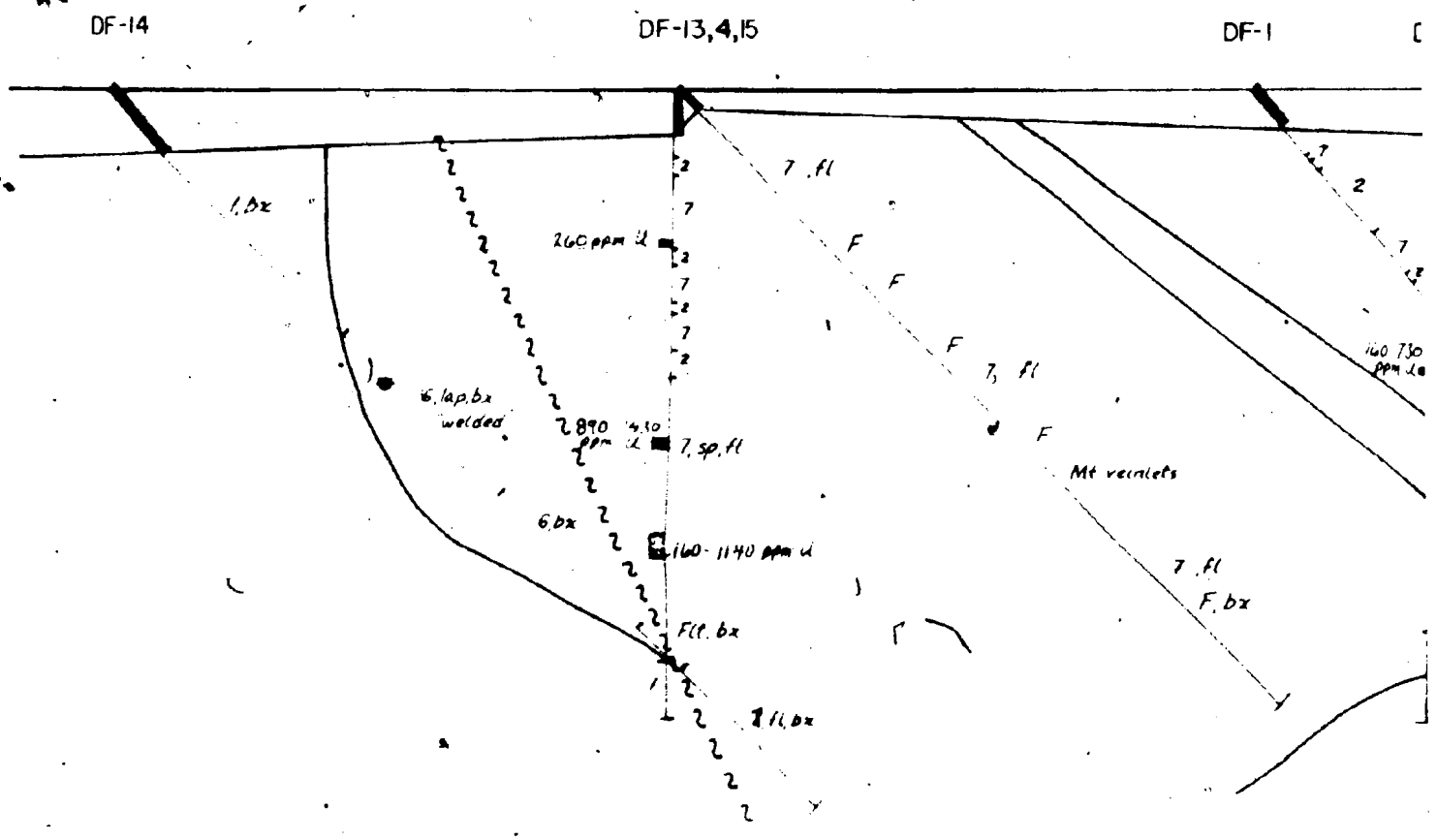
DF-14
DF-13,4,15
DF-1
1, bx
260 ppm U
6, lap, bx welded
2,890 ppm U
7, sp, fl
6, bx
160 - 1140 ppm U
Flt. bx
7 fl, bx
7 . fl
F
F
F
7, fl
Mt veinlets
7 . fl
F, bx
160 730 ppm U

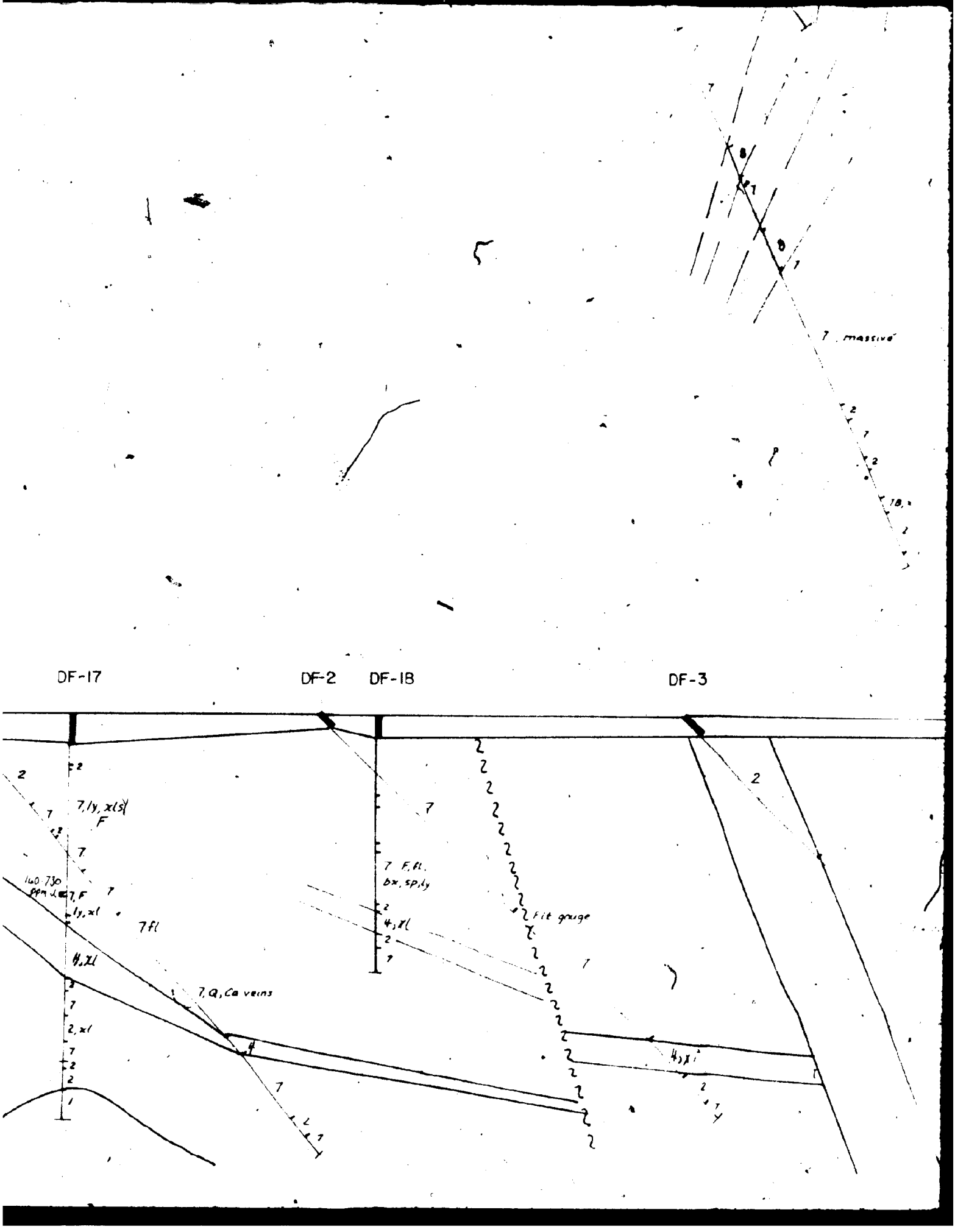
7, massive
DF-17
DF-2
DF-18
DF-3
7, ly, xl(s)
F
160-730
ppm
7, F
ly, xl
7fl
4, Xl
7, Q, Ca veins
2, xl
7, F, fl,
bx, sp, ly
4, Xl
Fit gauge
4, Xl

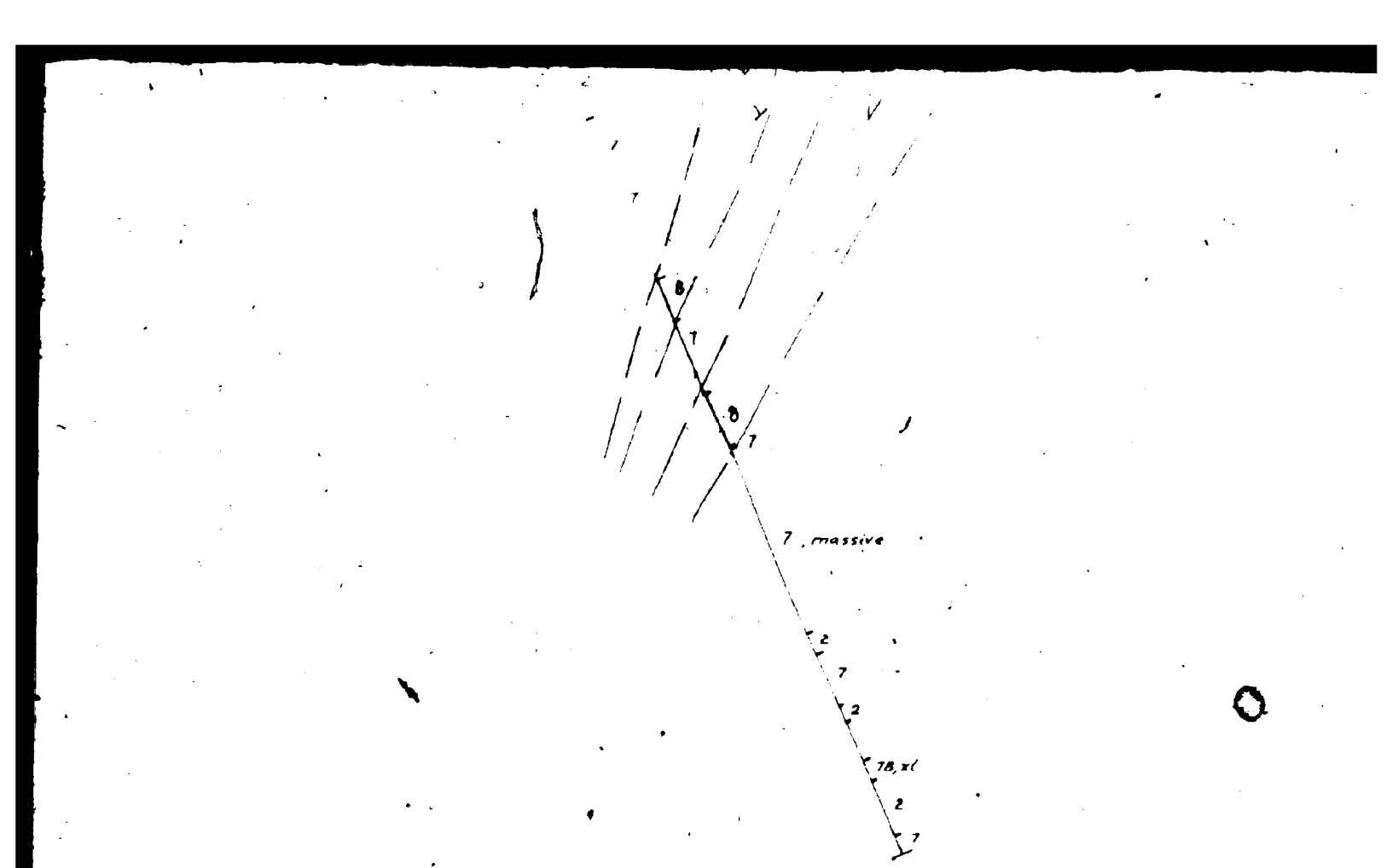

DF-2 DF-18 DF-3 DF-12

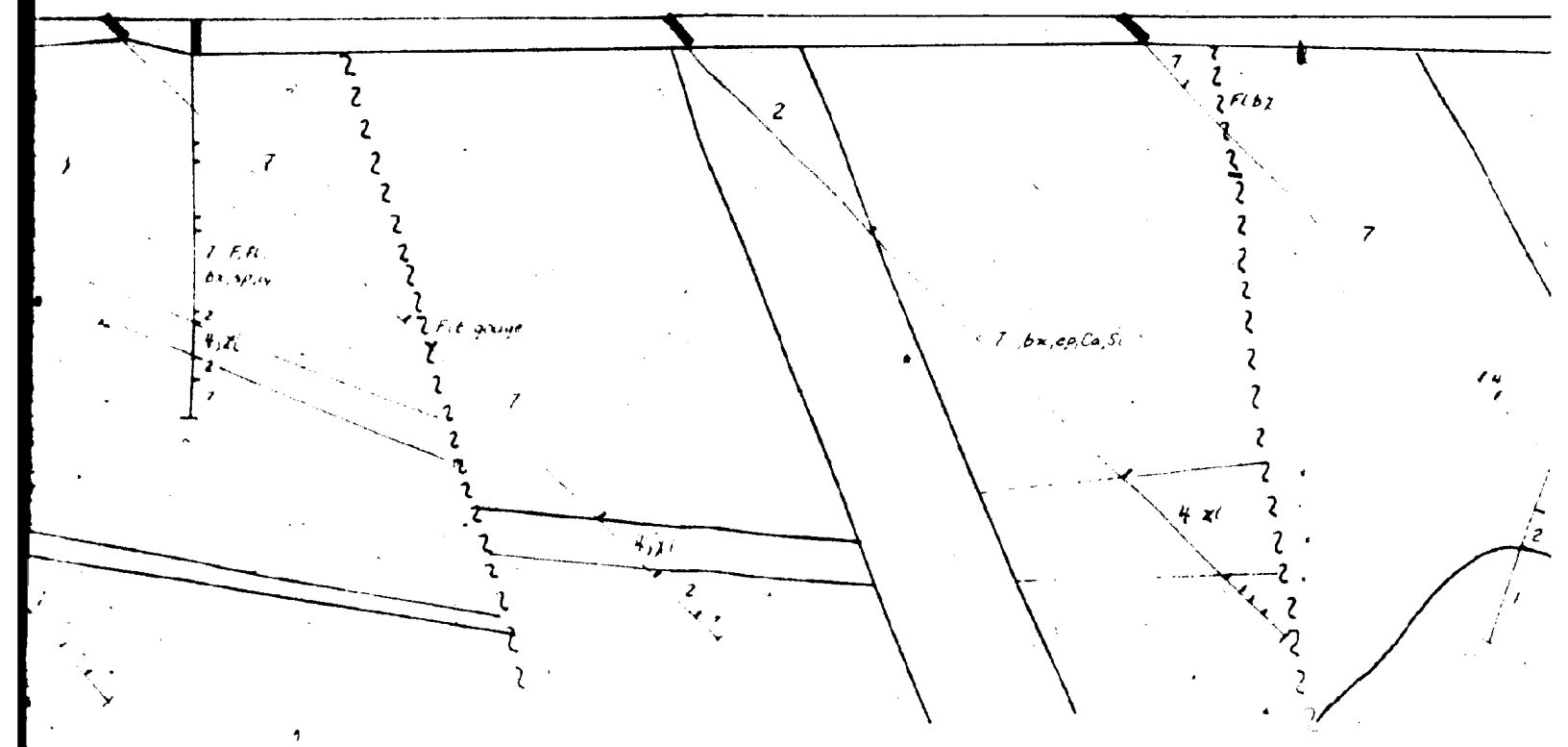

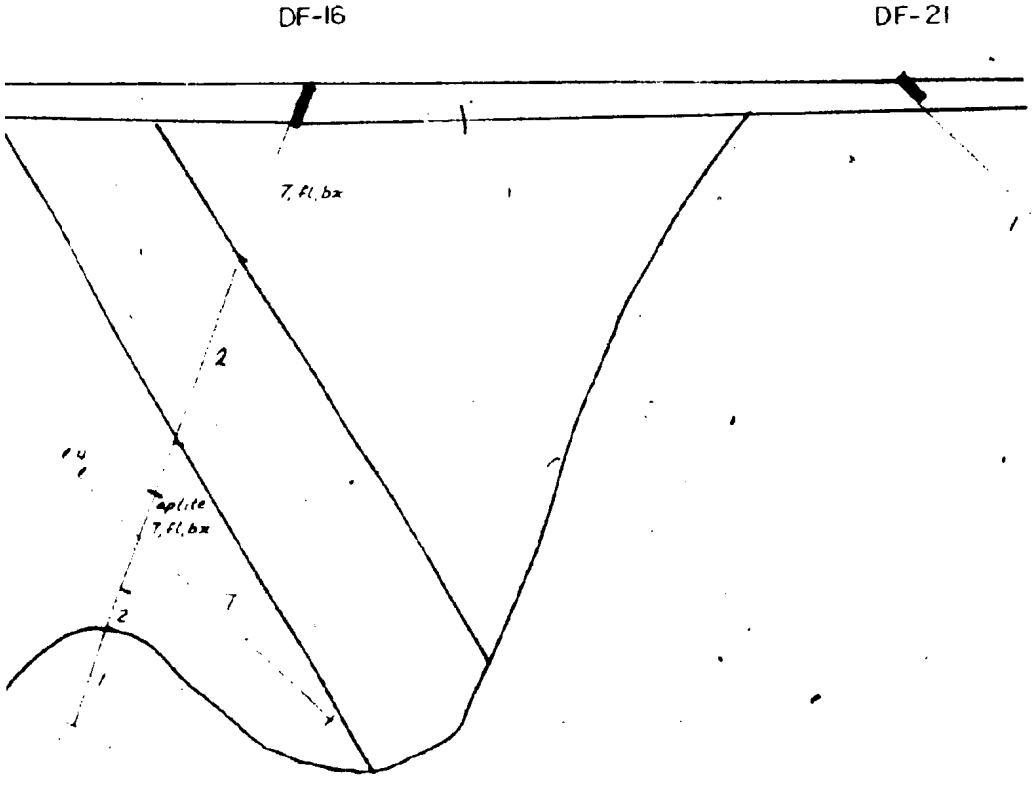
DF-16
DF-21
T, Fl, bx
2
aplite
T, Fl, bx
T
2
1

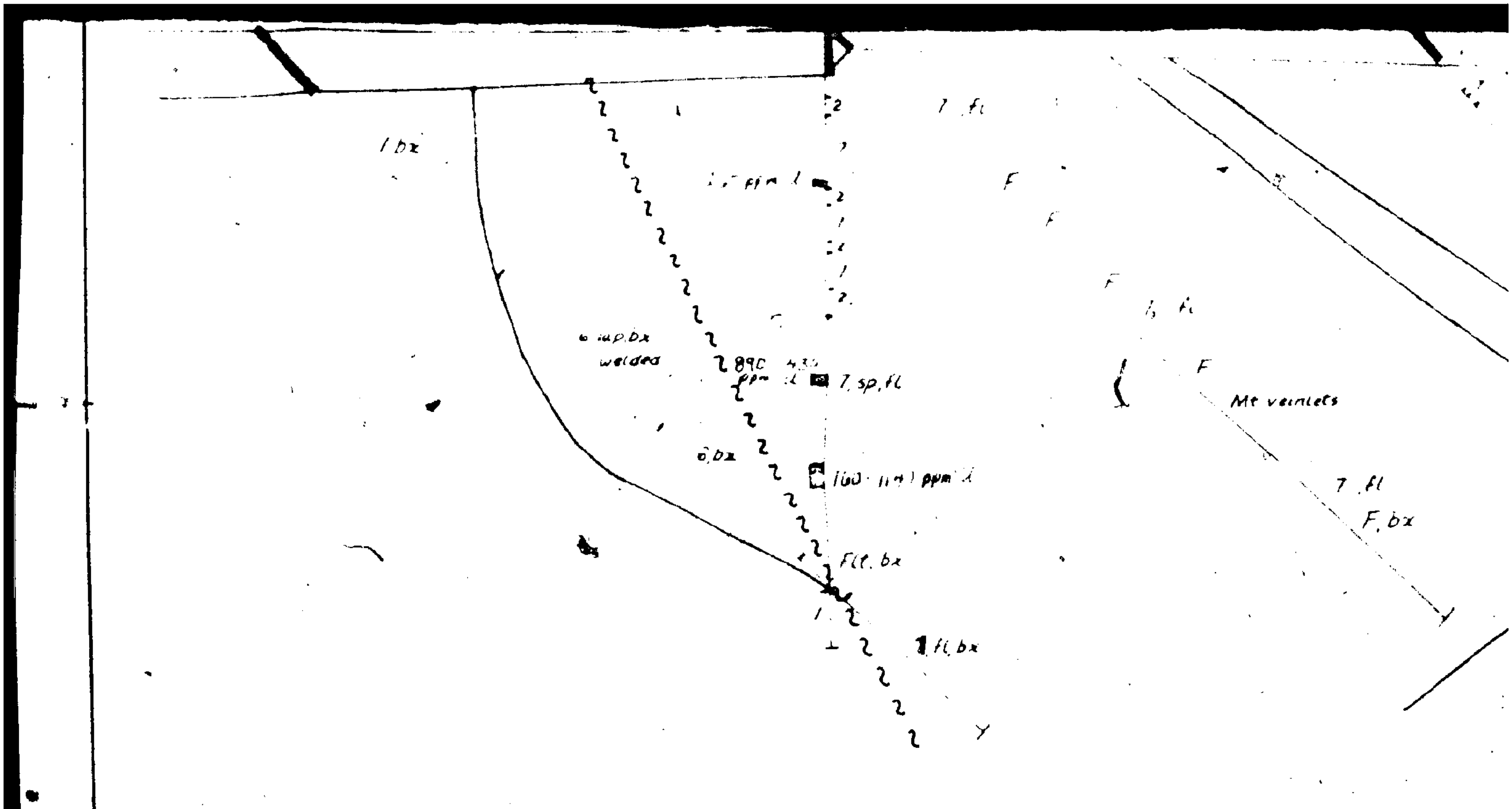

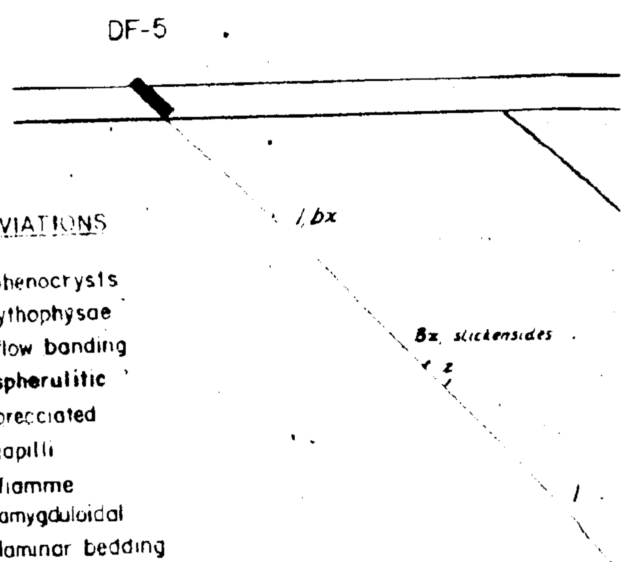

STRATIFIED ROCKS

8	Basalt flows
7 7b	(7) Rhyolite flows, flow banded or massive, commonly with spherulites and lithophysae (7b) Porphyritic rhyolite, > 25% phenocrysts
6	Rhyolite ash flows and tuffs
5a 5b	(5a) Laminated siltstone, reworked ash (lacustrine) (5b) Conglomerate

INTRUSIVE ROCKS

4	High-Zr rhyolite dikes
3	High-Zr composite dikes
2	Diabase dikes
1	Granite

ABBREVIATIONS

xl - phenocrysts
ly - lythophysae
fl - flow banding
sp - spherulitic
bx - brecciated
lap - lapilli
f - fiamme
amyg - amygduloidal
lam - laminar bedding
agglom - agglomerate
f.g. - fine grained

F - fluorite
ep - epidote
Ca - calcite veins
Q - quartz veins
Mt - magnetite veins
U - uranium
ga - galena
Sn - cassiterite
REE - rare earth elements
W - tungsten
Th - thorium

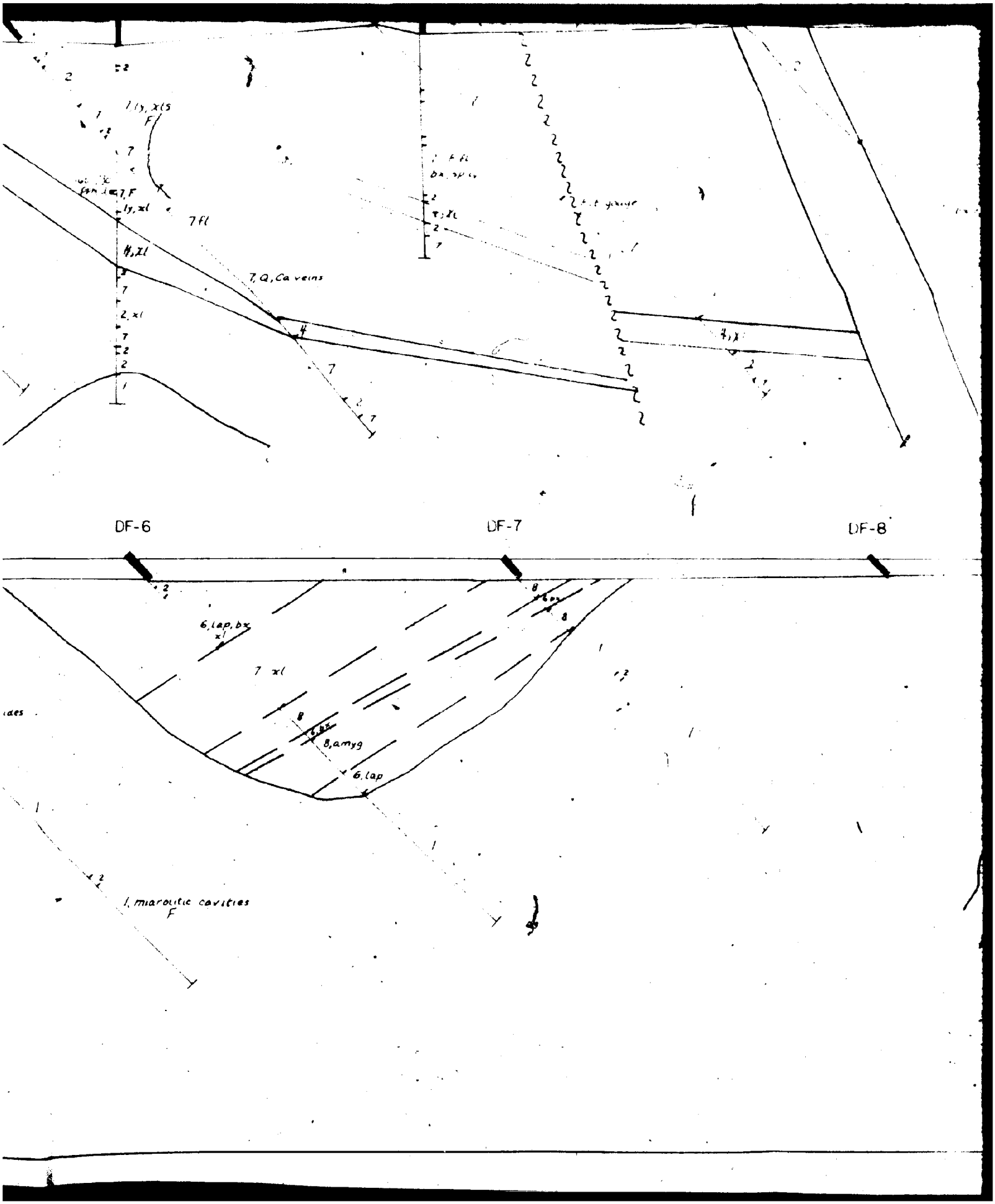
DF-6
DF-7
DF-8
7, Q, Ca veins
6, lap, bx
7 xl
8, amyg
6, lap
1, miarolitic cavities

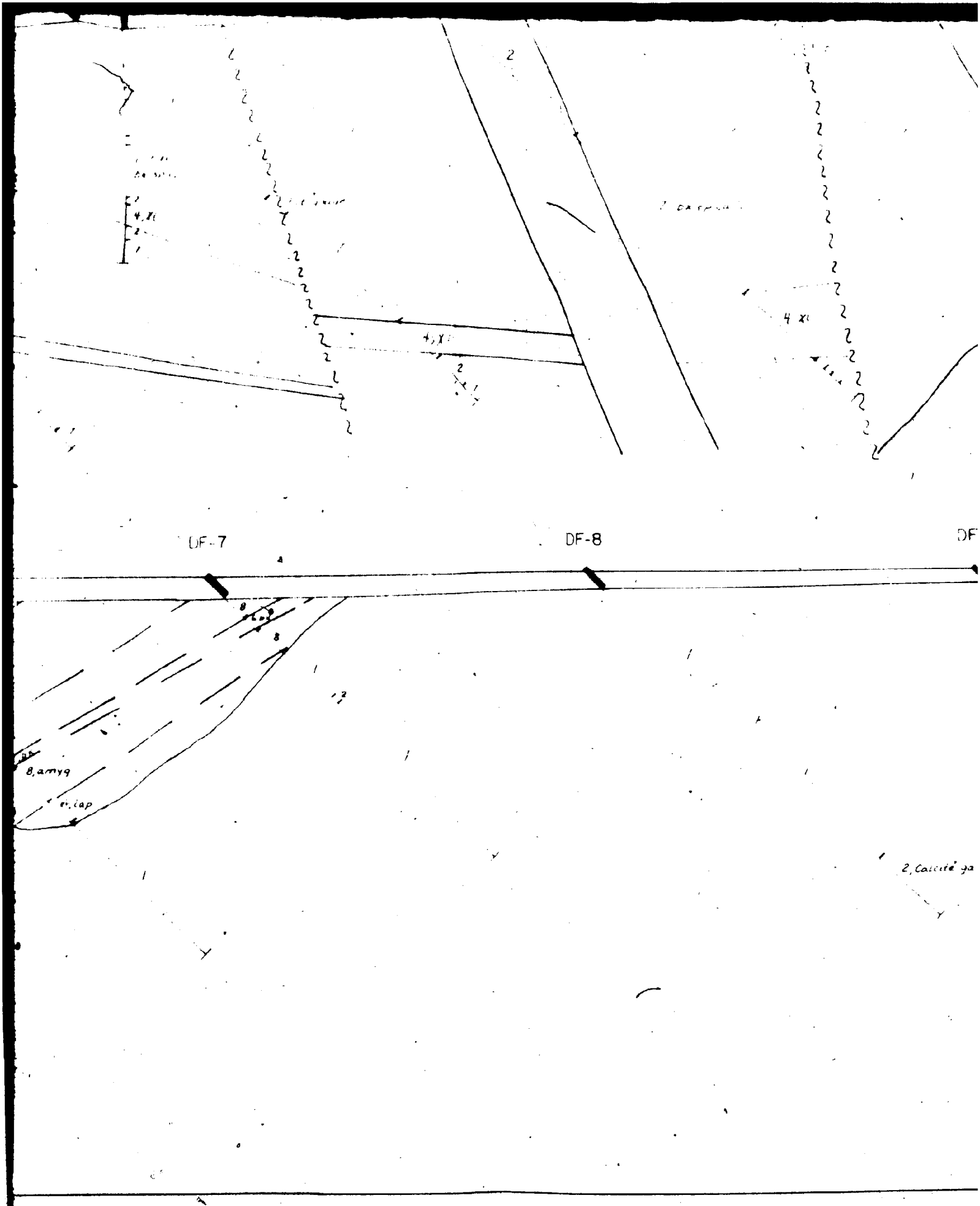
DF-7
DF-8
DF
8, amyg
2, Calcite ga

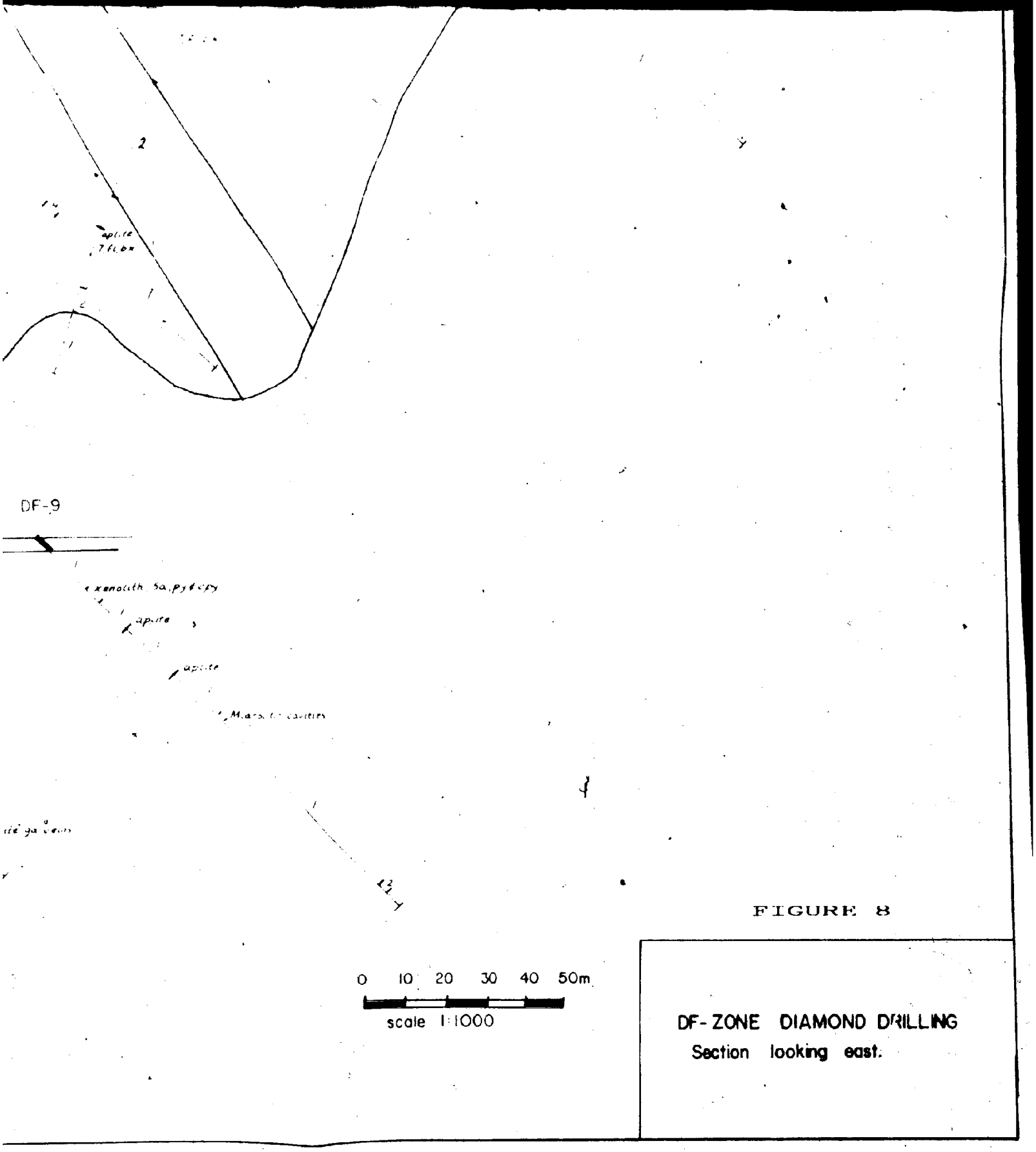

FIGURE 8

DF-ZONE DIAMOND DRILLING
Section looking east.

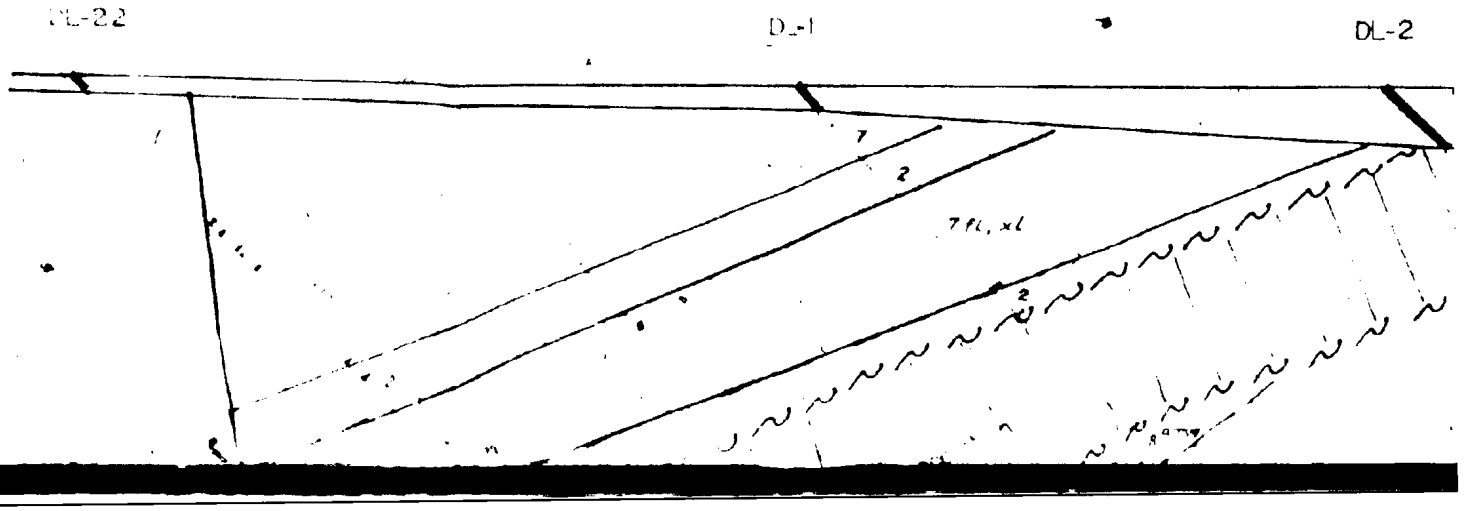
DL-1
DL-2

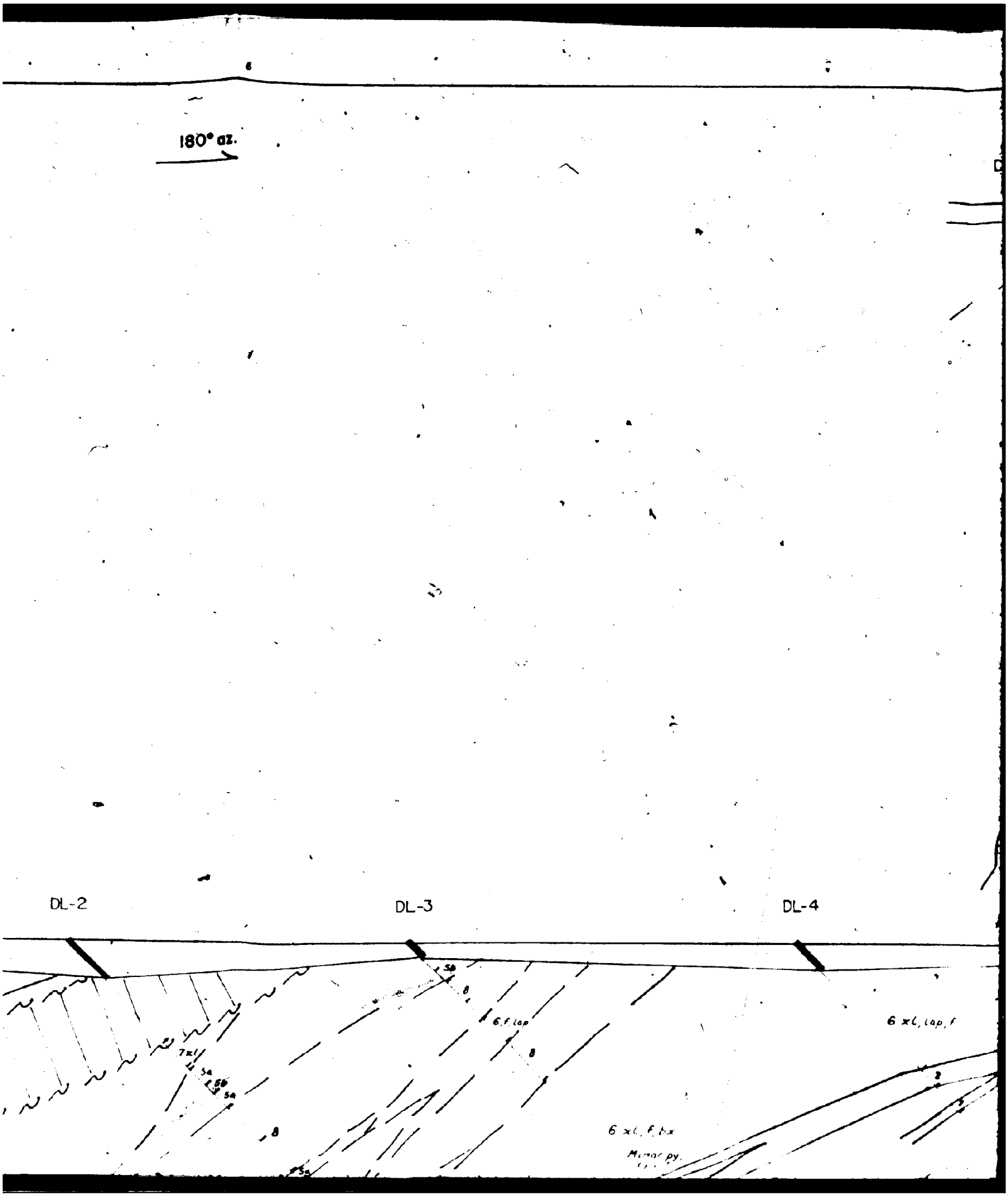
180° az.
DL-2
DL-3
DL-4
6 xl, lap, f
6 xl, f, bx

180° az.

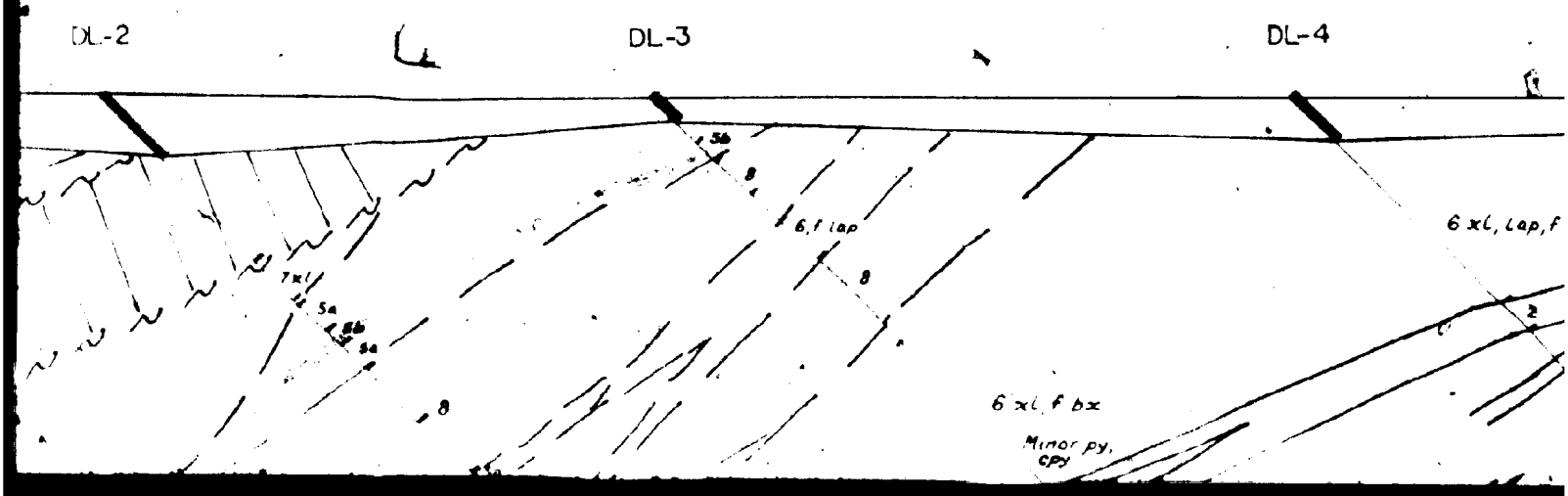

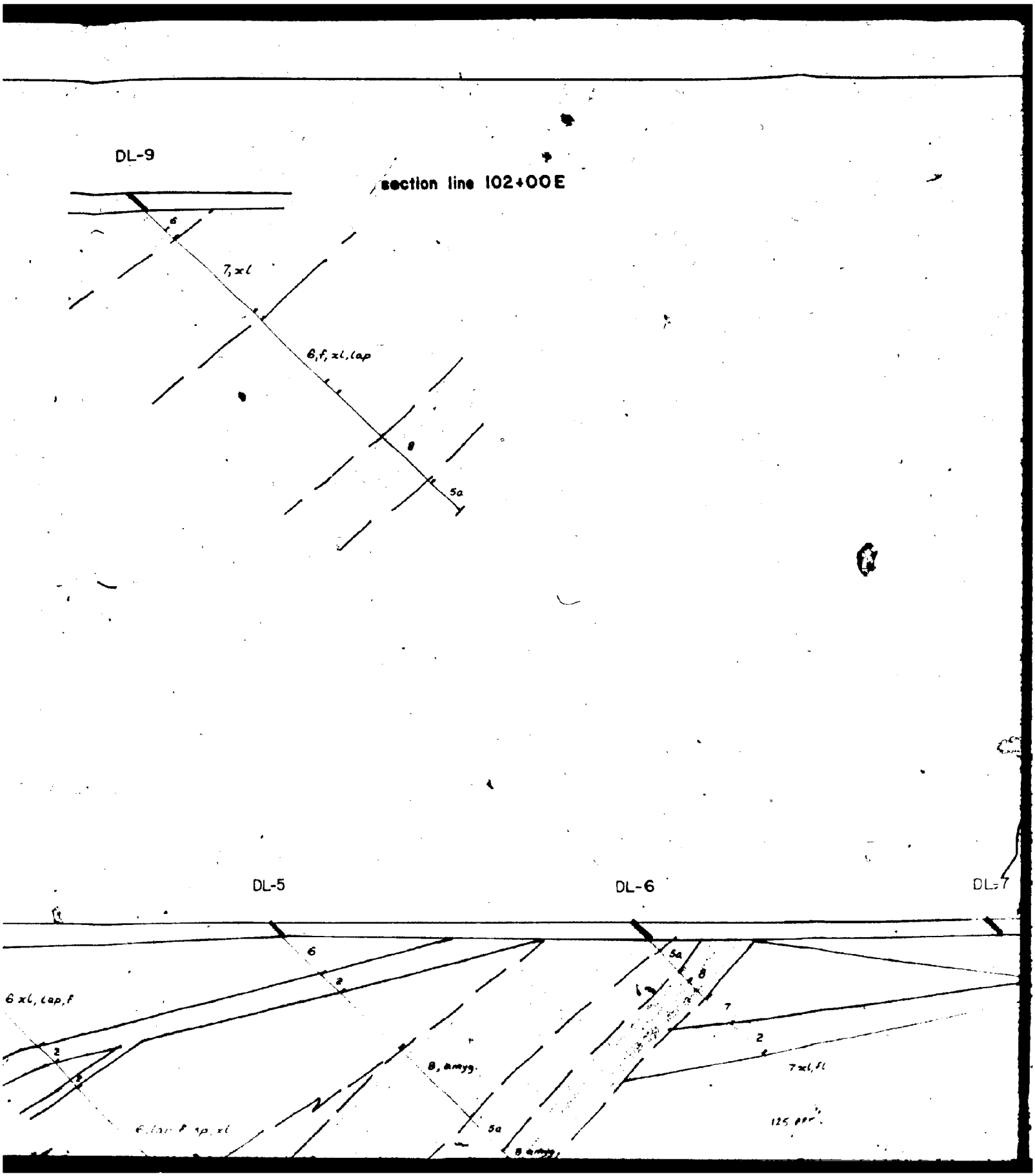
DL-9
section line 102+00E
6
7, xl
6, f, xl, cap
8
5a
DL-5
DL-6
DL-7
6
2
6 xl, cap, f
3
4
8, amyg.
5a
7
8
7 xl, sl
125 ppm

section line 102+00E

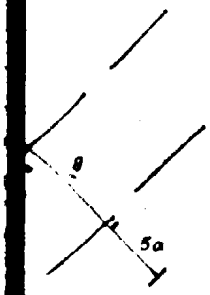

DL-6

DL-7

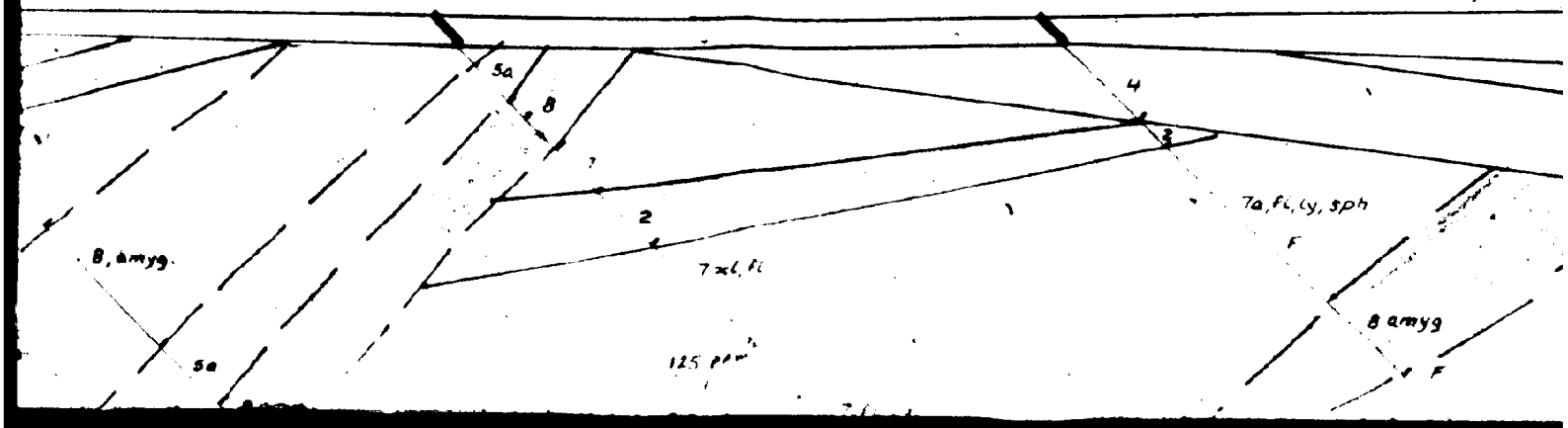

STRATIFIED ROCKS

- Basalt flows
- (7) Rhyolite flows, flow banded or massive, commonly with spherulites and lithophysae
  (7b) Porphyritic rhyolite, >25% phenocrysts
- 6 — Rhyolite ash flows and tuffs
- (5a) Laminated siltstone, reworked ash (lacustrine)
  (5b) Conglomerate

INTRUSIVE ROCKS

- 4 — High-Zr rhyolite dikes
- 3 — High-Zr composite dikes
- 2 — Diabase dikes
- 1 — Granite

ABBREVIATIONS

xl – phenocrysts
ly – lythophysae
fl – flow banding
sp – spherulitic
bx – brecciated
lap – lapilli
f – fiamme
amyg – amygduloidal
lam – laminar bedding
agglom – agglomerate
f.g. – fine grained

F – fluorite
ep – epidote
Ca – calcite veins
Q – quartz veins
Mt – magnetite veins
U – uranium
ga – galena
Sn – cassiterite
REE – rare earth elements
W – tungsten
Th – thorium

section line 96+00E

DL-8 DL-10 DL-12

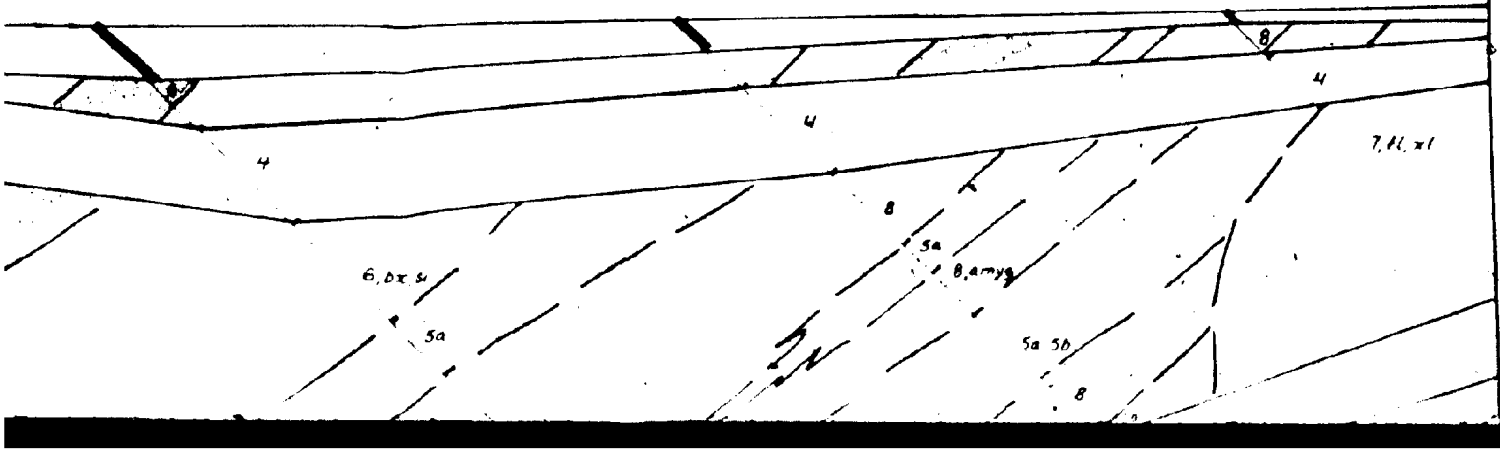

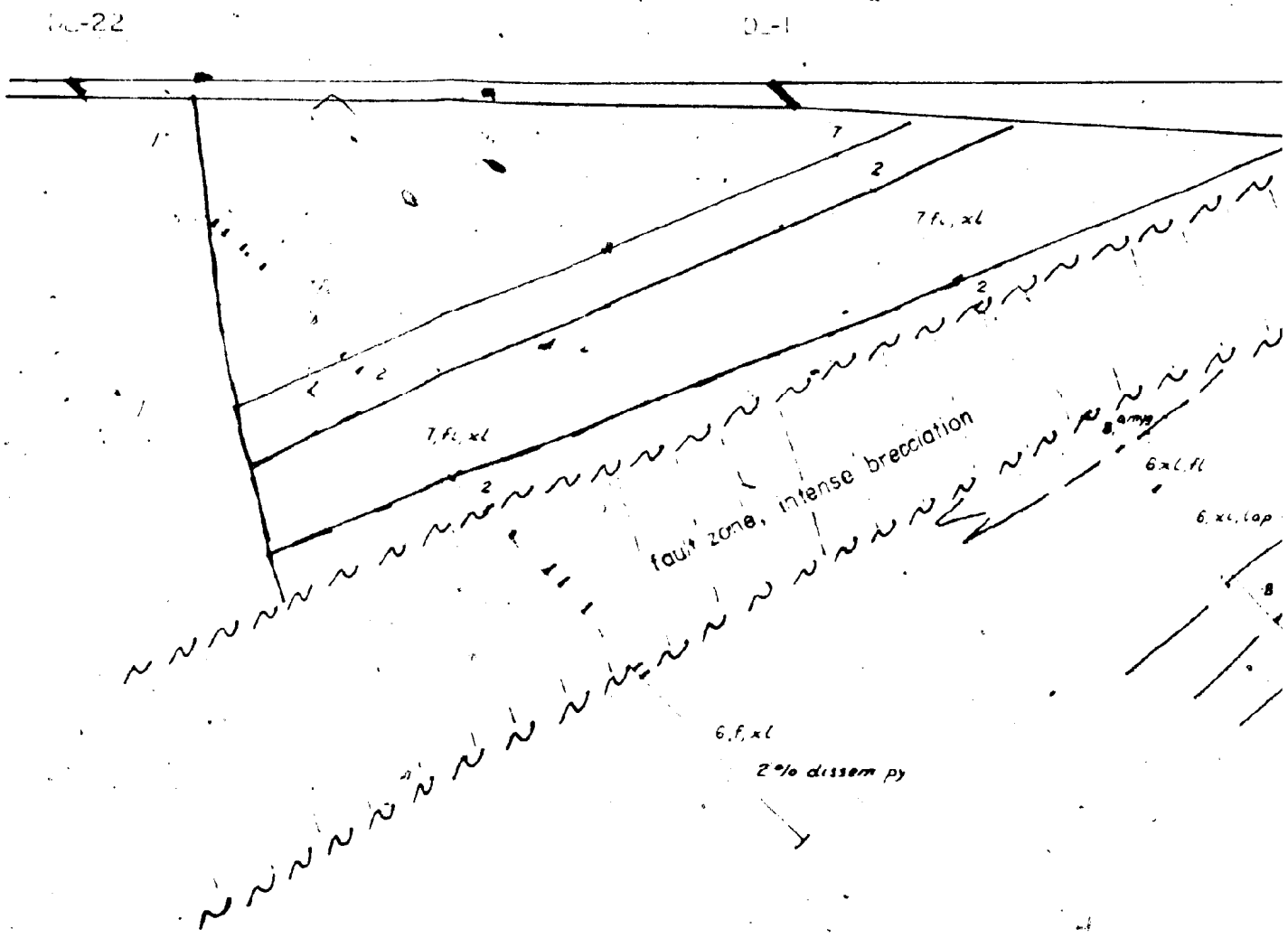
DC-22
DC-1
1
2
7, f, xl
7, f, xl
2
2
2
fault zone, intense brecciation
6, f, xl
2% dissem py
6, xl, f
6, xl, lap
8

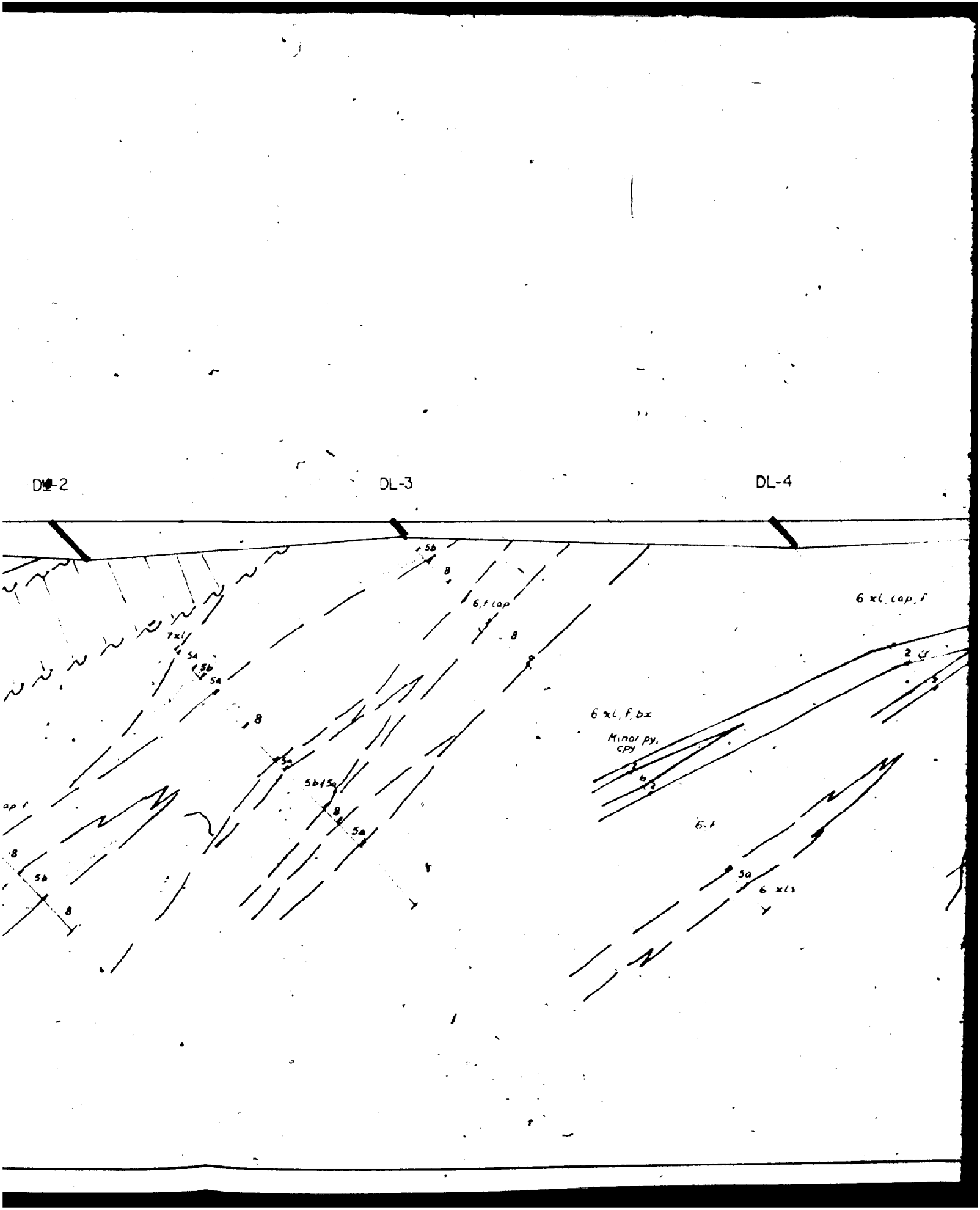
DL-2
DL-3
DL-4
5b
8
6, f cap
6 xl, cap, f
7 xl
5a
5b
5a
8
2 cr
6 xl, f, bx
Minor py, cpy
5a
5b/5a
8
5a
6 f
8
5b
8
5a
6 xls

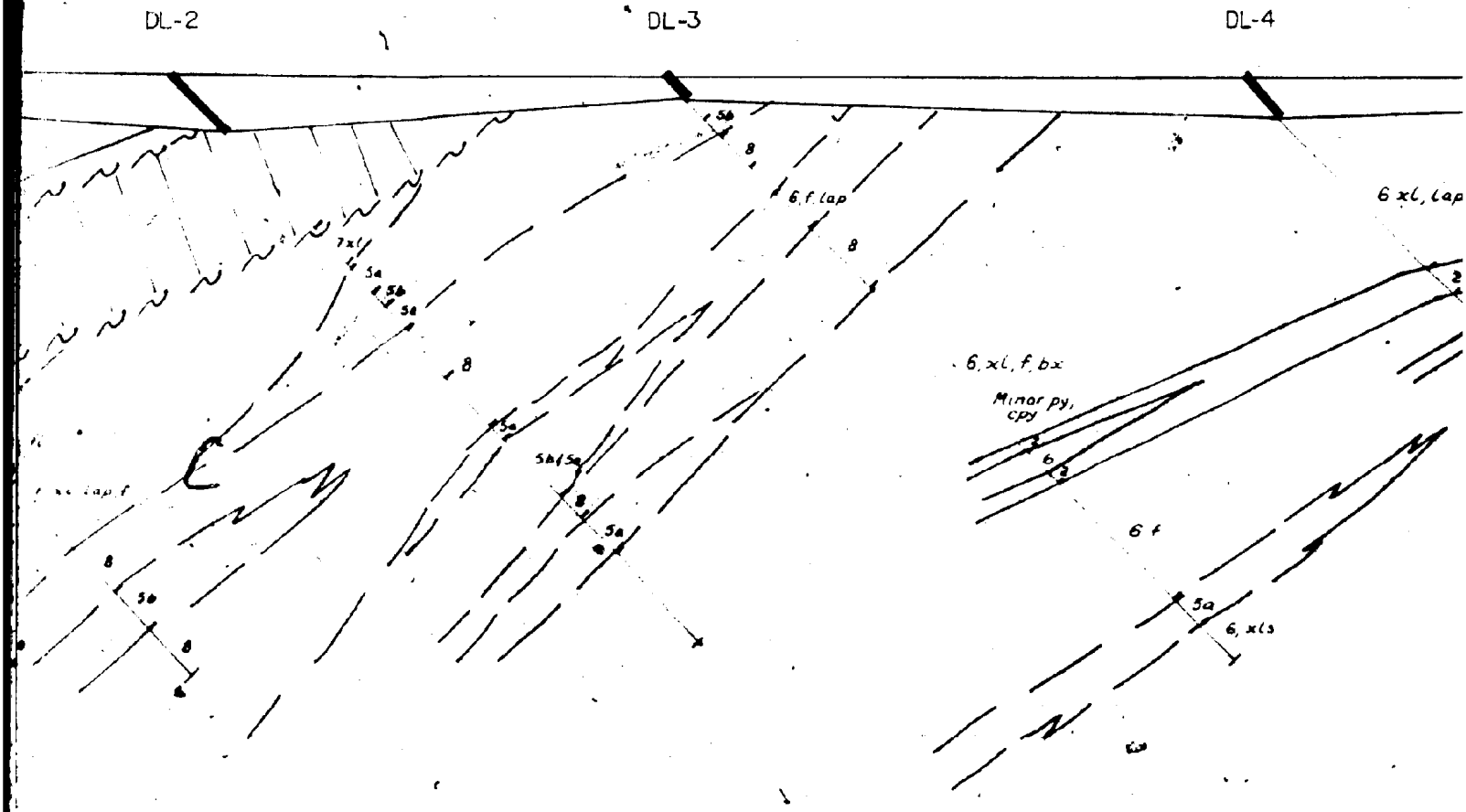
DL-2
DL-3
DL-4
6, f, lap
6 xl, lap
6, xl, f, bx
Minor py, cpy
6 f
6, xls

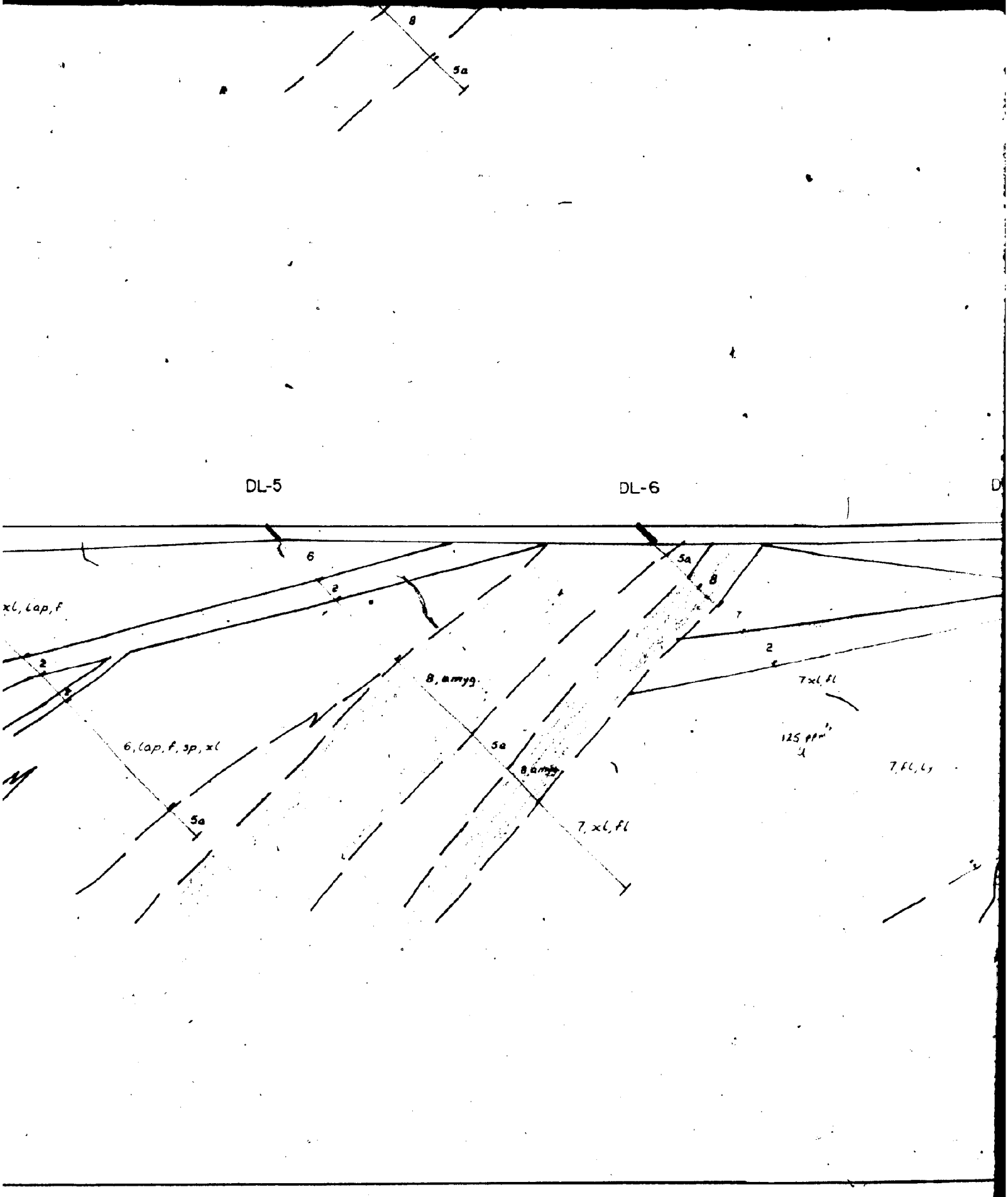
DL-5
DL-6
8
5a
6
2
xl, cap, f
2
6, cap, f, sp, xl
5a
8, amyg.
5a
8, amyg.
7, xl, fl
5a
8
7
2
7xl, fl
125 ppm
7, fl, l,

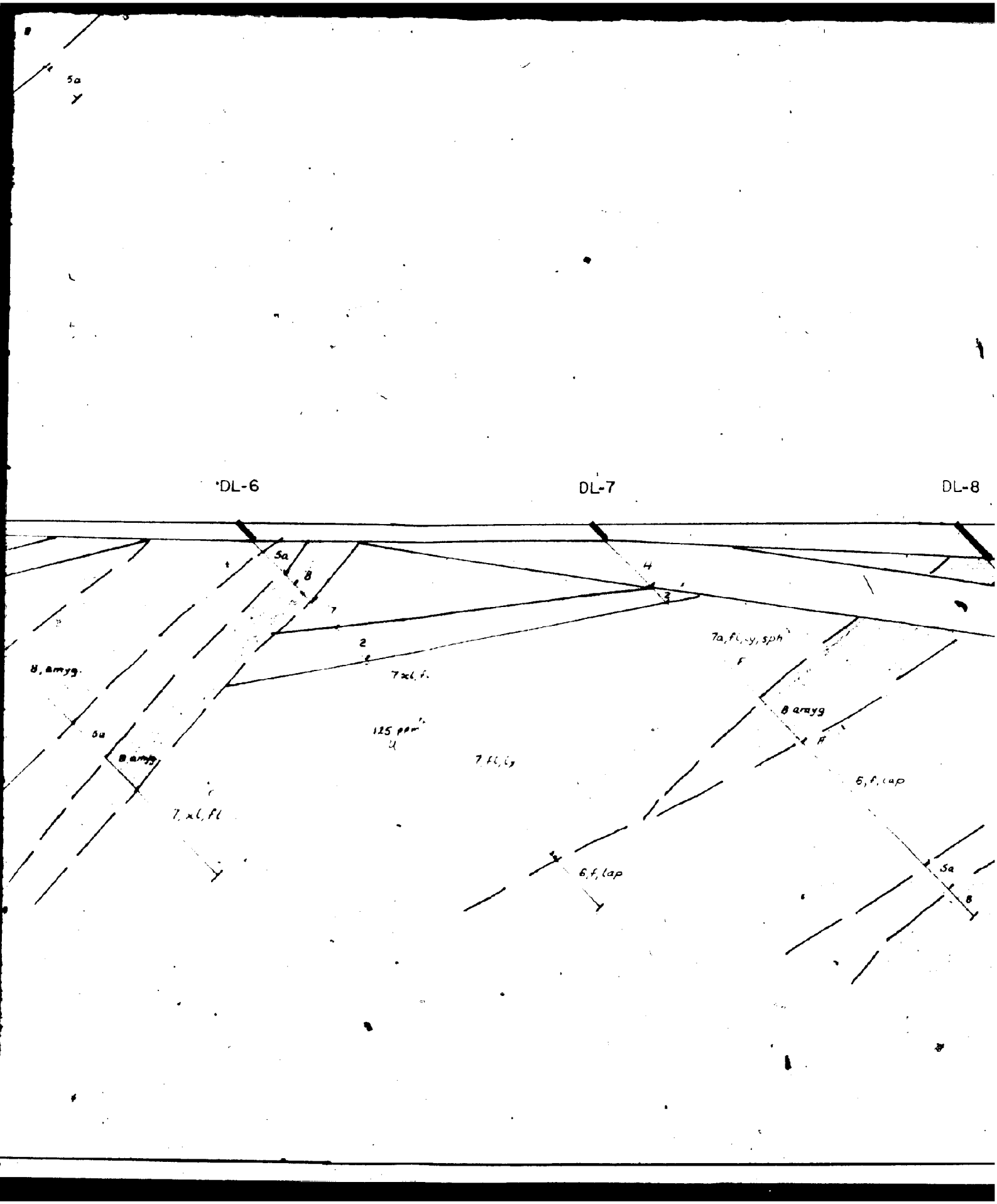
DL-6
DL-7
DL-8
5a
8
7
2
4
3
8, amyg.
7xcl, f.
125 ppm
7, fl, cy
7a, fl, cy, sph
8 amyg
6, f, lap
7, xcl, fl
6, f, lap
5a
8

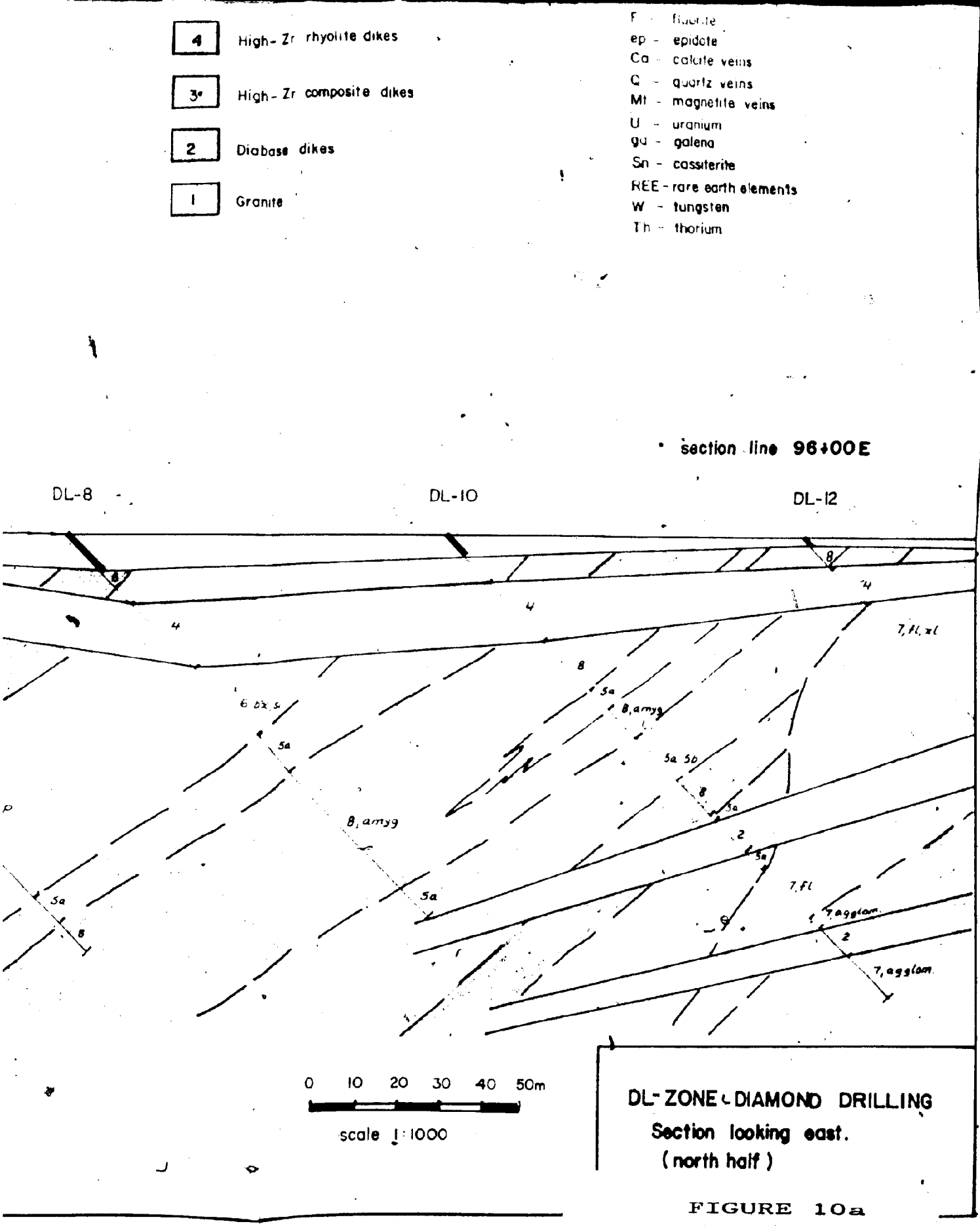
4 High-Zr rhyolite dikes
3e High-Zr composite dikes
2 Diabase dikes
1 Granite
F - fluorite
ep - epidote
Ca - calcite veins
Q - quartz veins
Mt - magnetite veins
U - uranium
ga - galena
Sn - cassiterite
REE - rare earth elements
W - tungsten
Th - thorium
section line 96+00E
DL-8
DL-10
DL-12
4
8
5a
8, amyg
5a, 5b
7, Fl, xl
7, Fl
7, agglom
0 10 20 30 40 50m
scale 1:1000
DL-ZONE - DIAMOND DRILLING
Section looking east.
(north half)

FIGURE 10a

DL-10 DL-12 DL-14

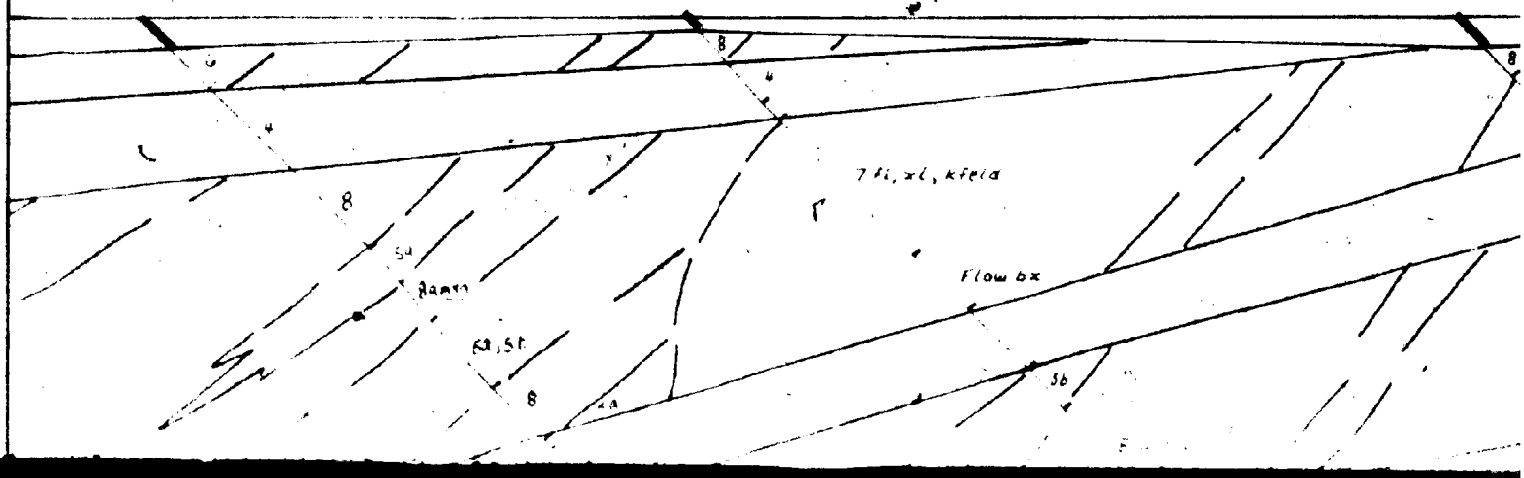

180° az.

section

DL-14

DL-15

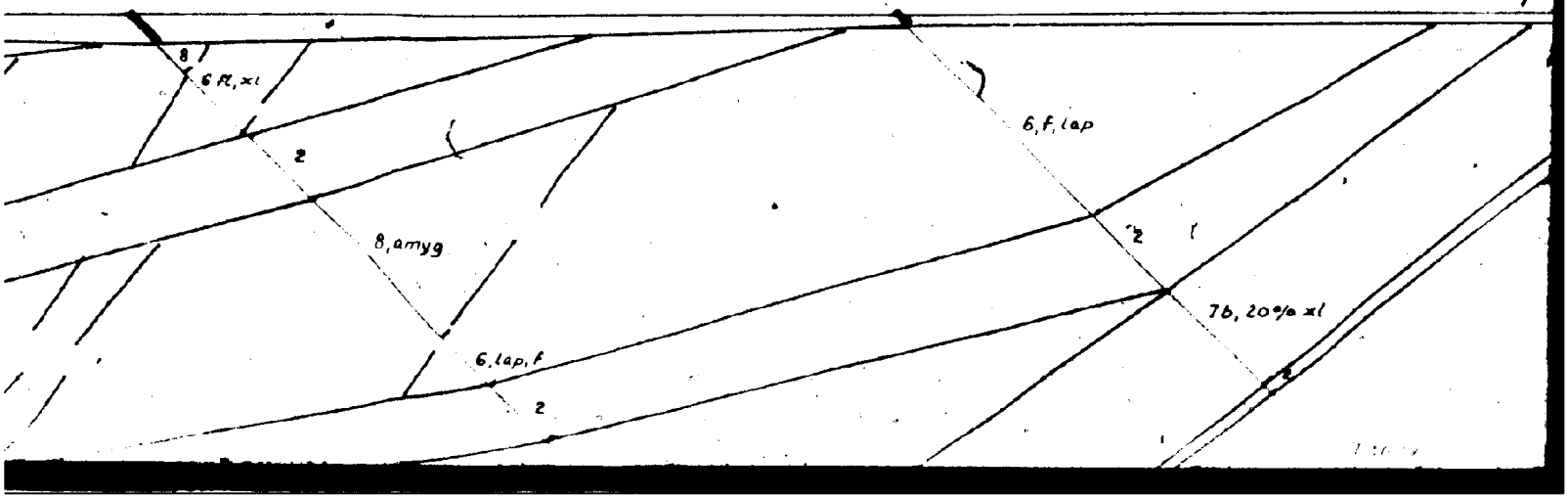

180° az.

section line

DL-14

DL-15

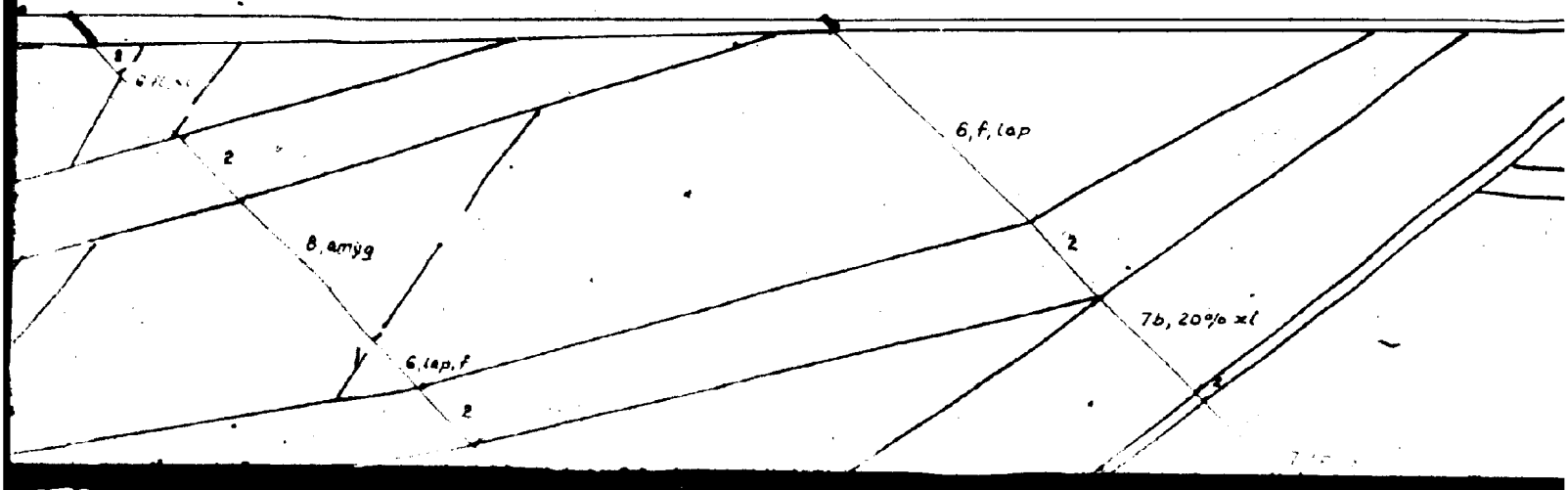

DL-11 DL-13 DL-18

n line 103+00 E

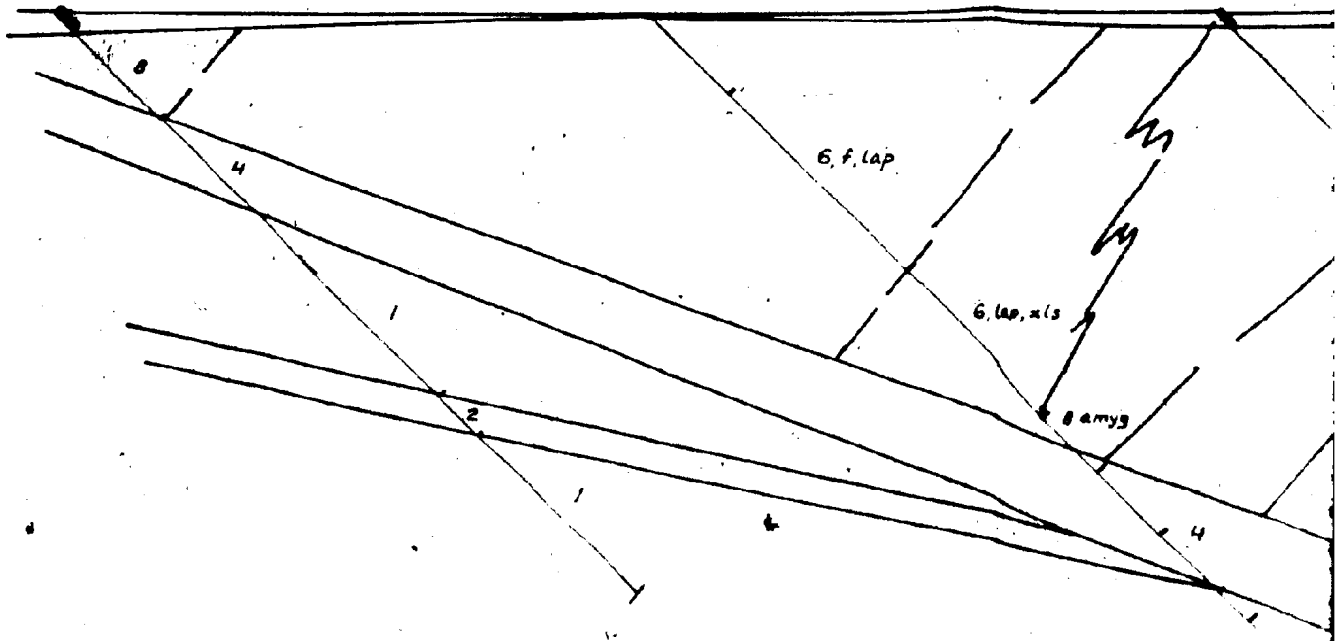

DL-16
DL-19 (-70°)

DL-17

section line 96+00 E

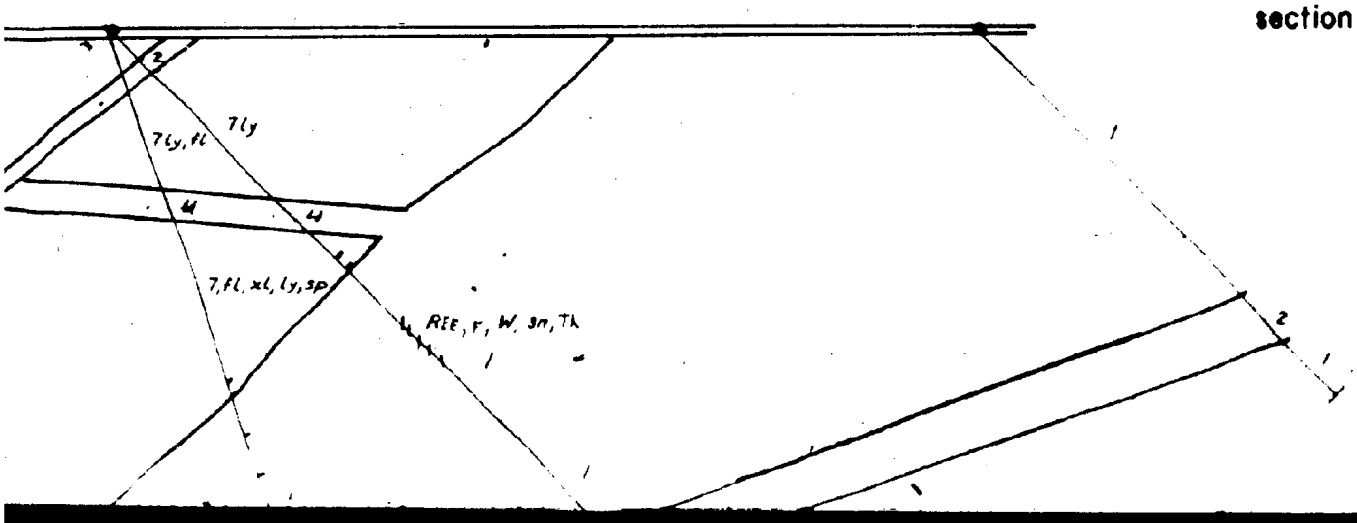

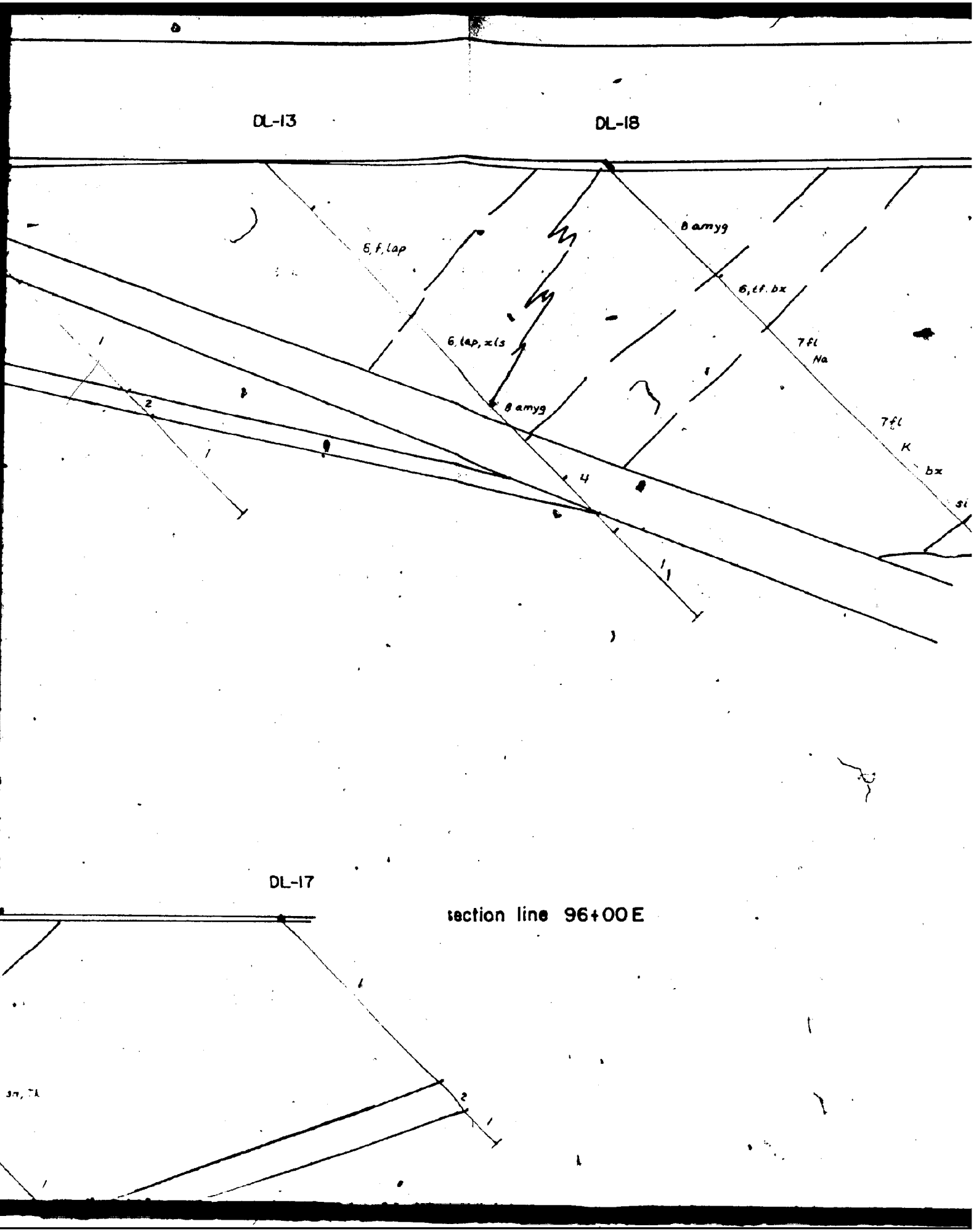
DL-13
DL-18
6, f, lap
6, lap, xls
8 amyg
8 amyg
6, lf. bx
7fl
Na
7fl
K
bx
DL-17
section line 96+00E

DL-20

DL-21

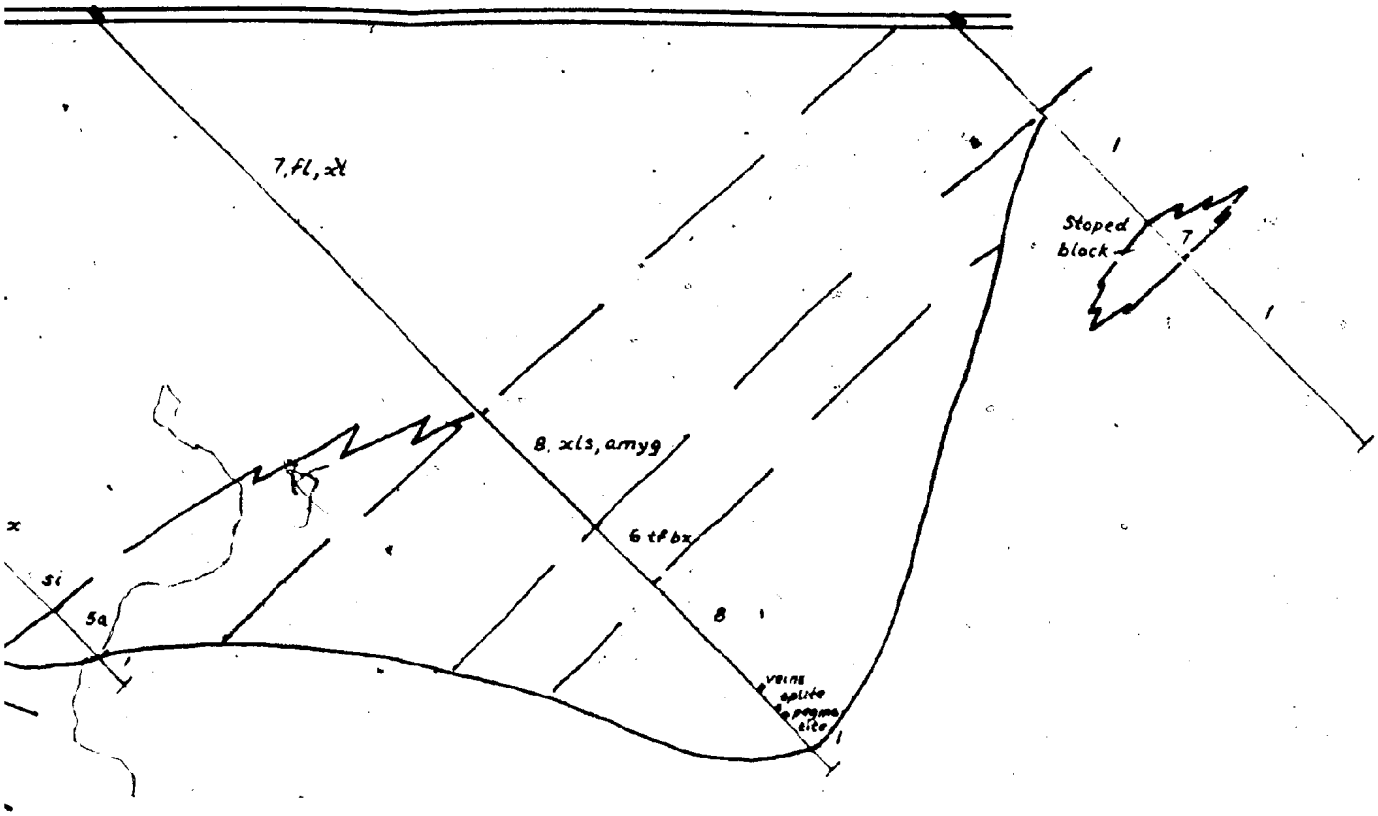

STRATIFIED ROCKS

Basalt flows

(7) Rhyolite flows, flow banded or massive, commonly with spherulites and lithophysae
(7b) Porphyritic rhyolite, >25% phenocrysts

Rhyolite ash flows and tuffs

(5a) Laminated siltstone, reworked ash (lacustrine)
(5b) Conglomerate

INTRUSIVE ROCKS

High-Zr rhyolite dikes

High-Zr composite dikes

ABBREVIATIONS

xl - phenocrysts
ly - lythophysae
fl - flow banding
sp - spherulitic
bx - brecciated
lap - lapilli
f - fiamme
amyg - amygdaloidal
lam - laminar bedding
agglom - agglomerate
fg - fine grained

F - fluorite
ep - epidote
Ca - calcite veins
q - quartz veins
M - magnetite veins

DL-10 DL-12 DL-14

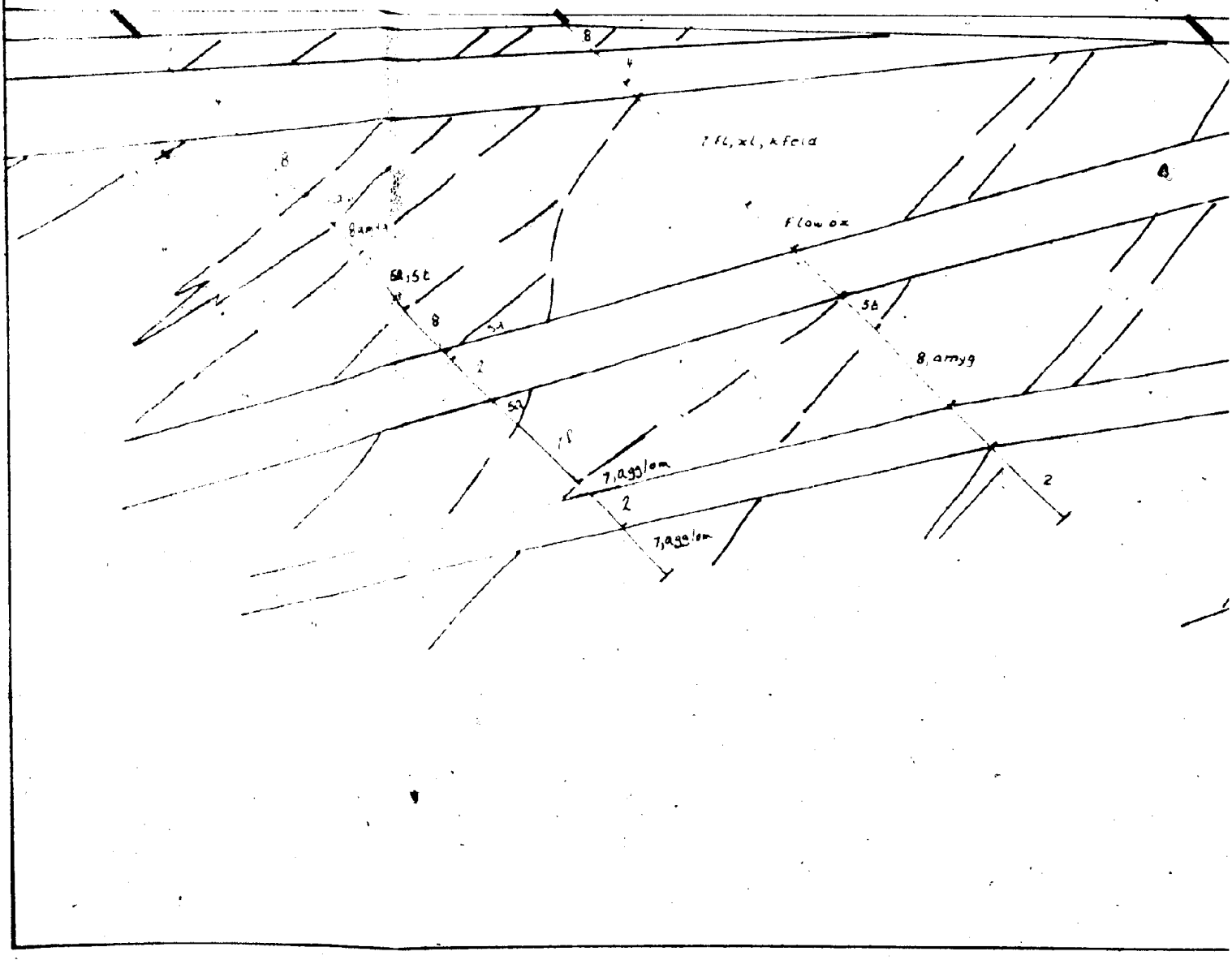

DL-14

DL-15

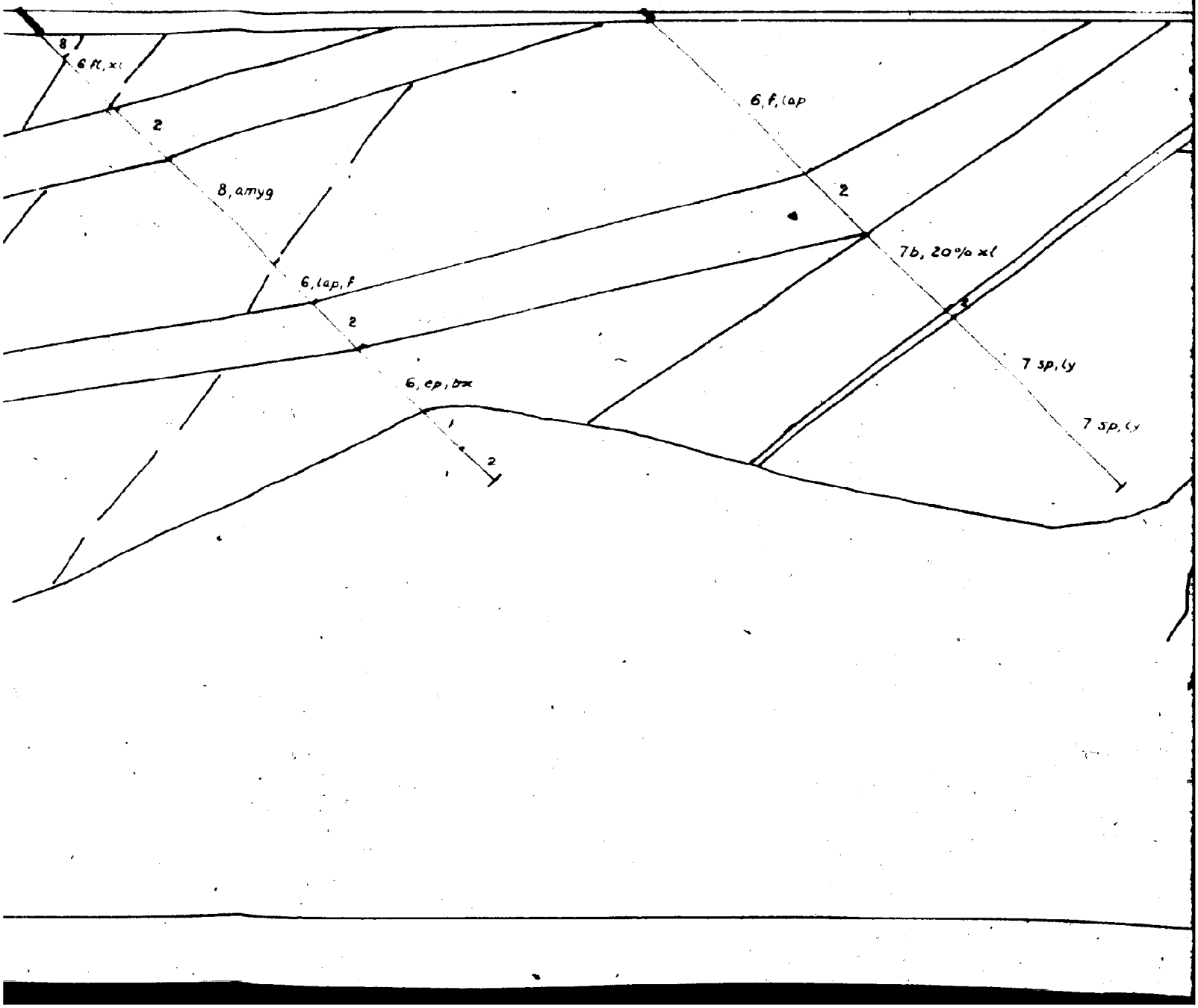

DL-14

DL-15

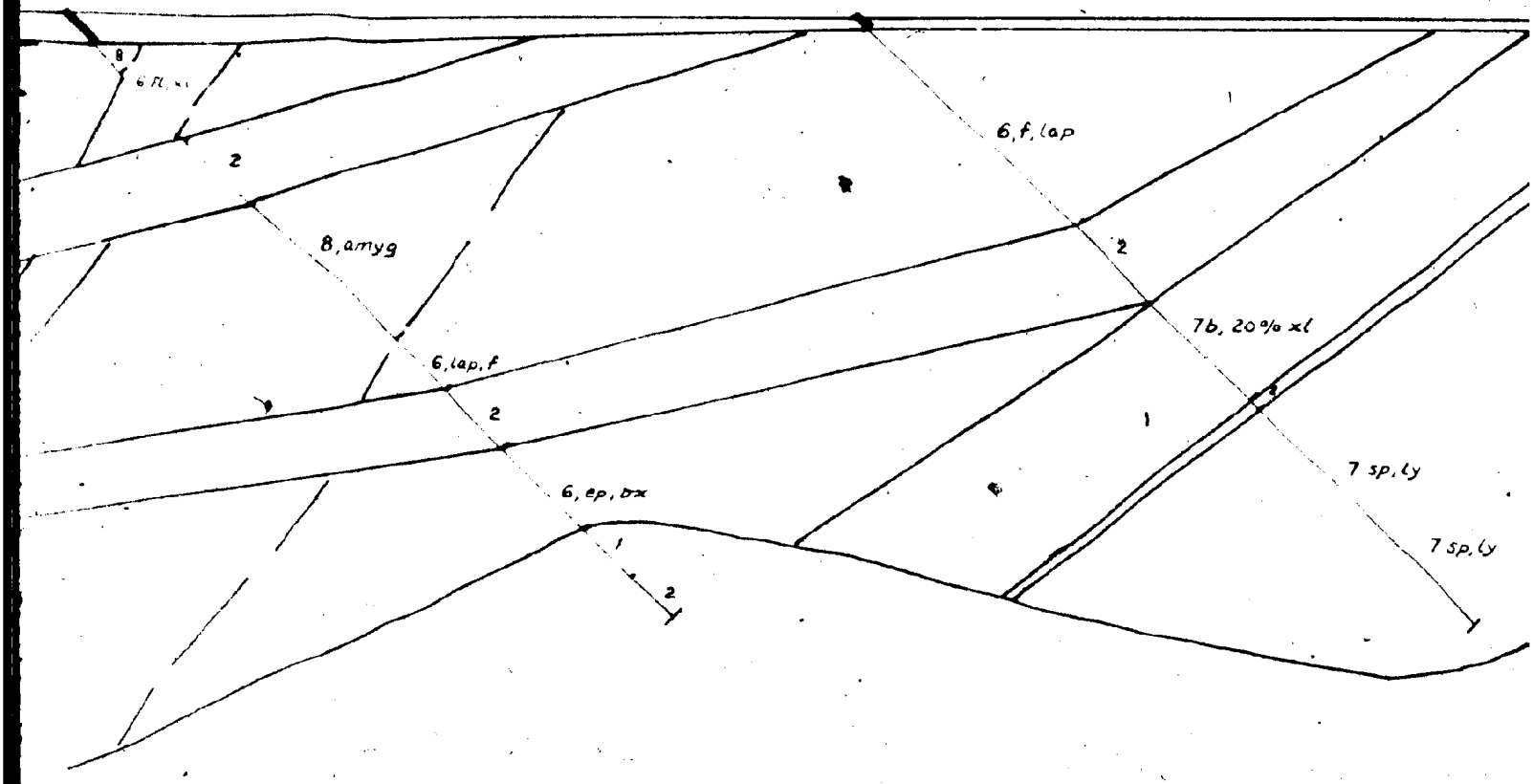

DL-16
DL-19 (-70°)

DL-17

section line 96+00 E

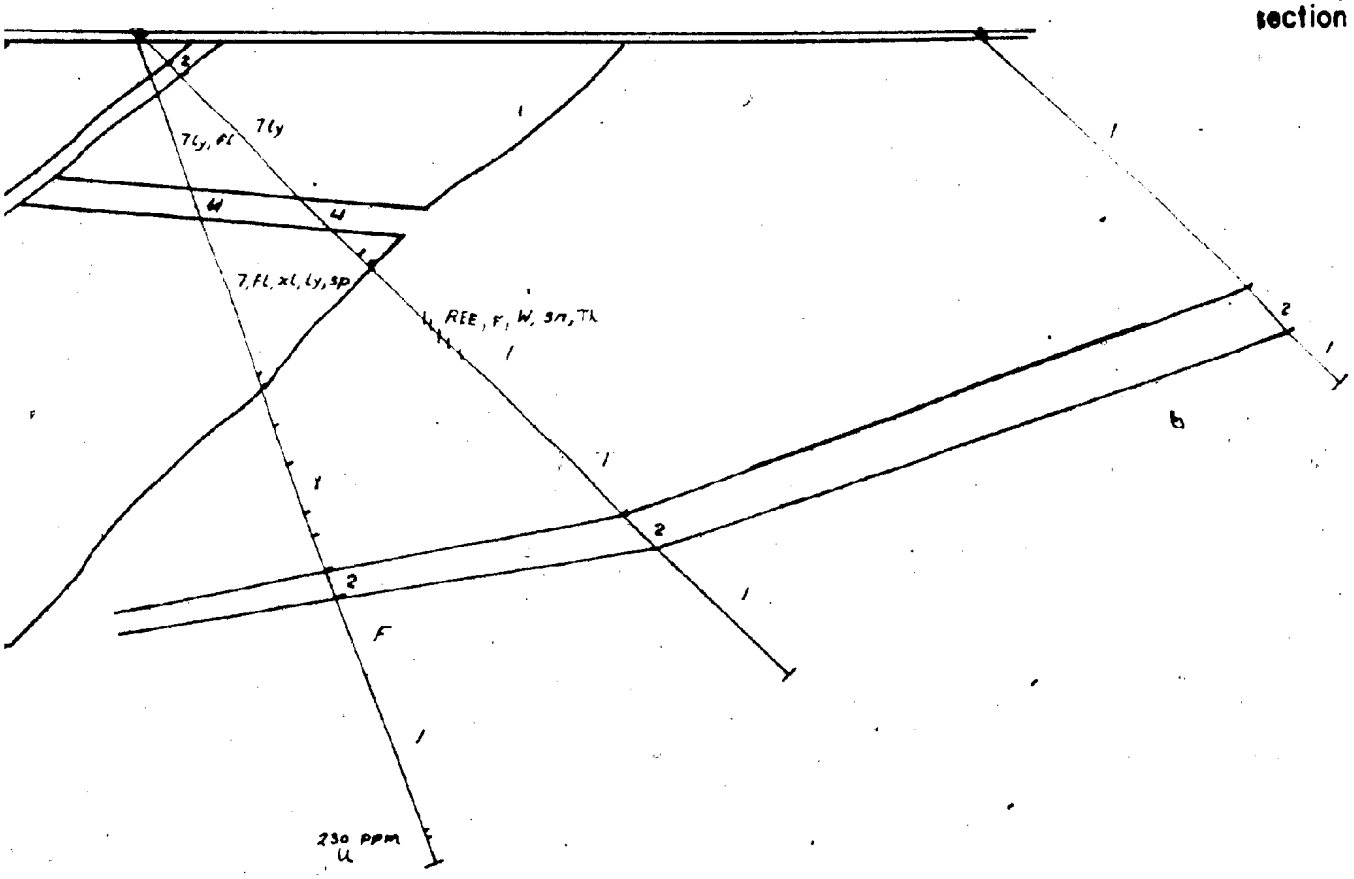

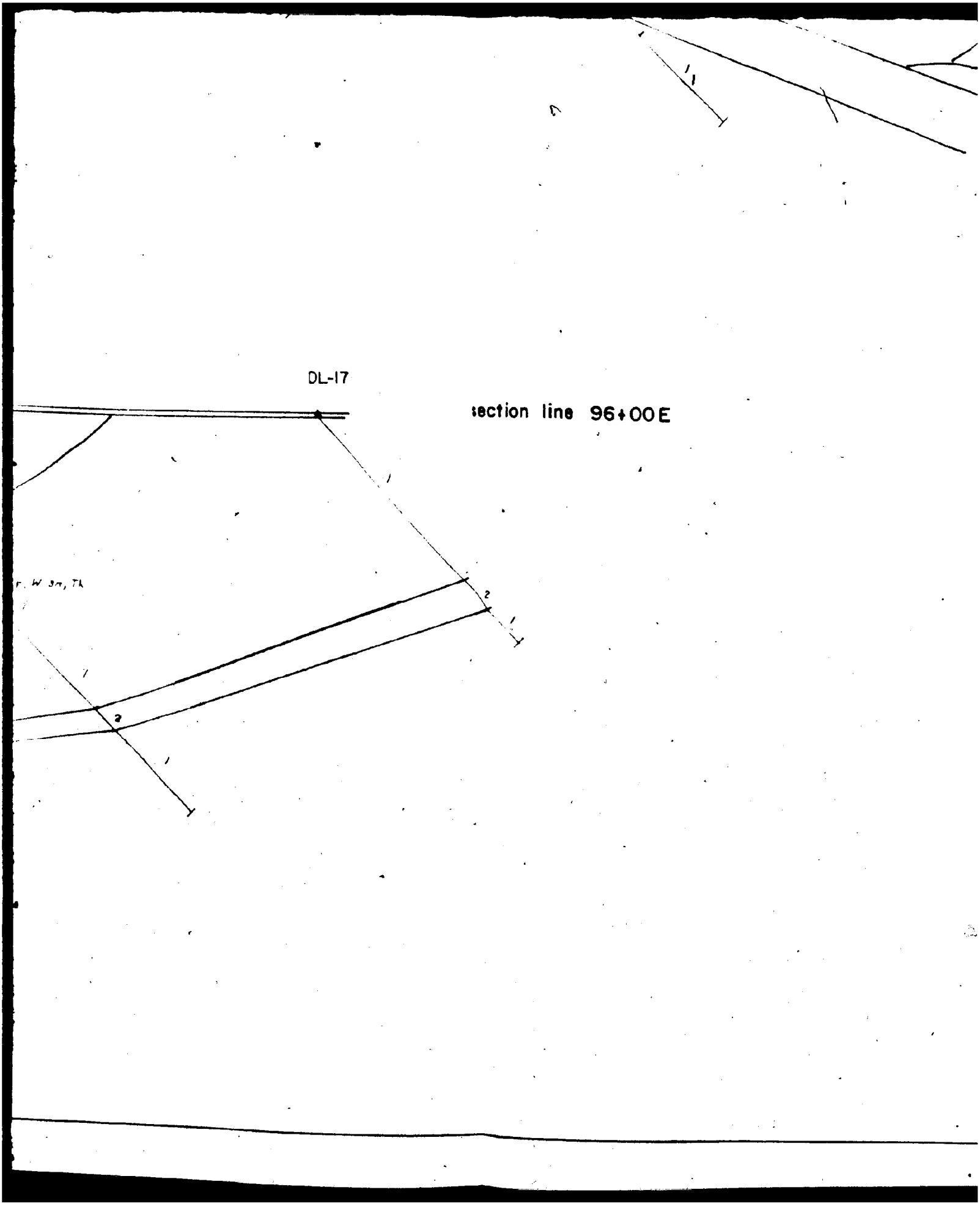
DL-17
section line 96+00E

STRATIFIED ROCKS

Basalt flows

(7) Rhyolite flows, flow banded or massive, commonly with spherulites and lithophysae
(7b) Porphyritic rhyolite, >25% phenocrysts

6 Rhyolite ash flows and tuffs

(5a) Laminated siltstone, reworked ash (lacustrine)
(5b) Conglomerate

INTRUSIVE ROCKS

4 High-Zr rhyolite dikes

3 High-Zr composite dikes

2 Diabase dikes

1 Granite

ABBREVIATIONS

xl - phenocrysts
ly - lythophysae
fl - flow banding
sp - spherulitic
bx - brecciated
lap - lapilli
f - fiamme
amyg - amygdaloidal
lam - laminar bedding
agglom - agglomerate
f.g. - fine grained

F - fluorite
ep - epidote
Ca - calcite veins
Q - quartz veins
Mt - magnetite veins
U - uranium
ga - galena
Sn - cassiterite
REE - rare earth elements
W - tungsten
Th - thorium

0 10 20 30 40 50

scale 1:1000

DL-ZONE DIAMOND DRILLING
Section looking east.
(south half)

FIGURE 10b